U.S. Department
of Transportation
Federal Railroad
Administration

Office of Research,
Development and Technology
Washington, DC 20590

Risk Analysis Methodology for Unit and Manifest Trains Transporting Hazardous Material

DOT/FRA/ORD-24/24

Final Report | July 2024

REPORT DOCUMENTATION PAGE

Form Approved
OMB No. 0704-0188

1. REPORT DATE *(05/15/2022)*	**2. REPORT TYPE**	**3. DATES COVERED** *(From - To)*
	Technical Report	August 2019 – May 2022

4. TITLE AND SUBTITLE
Risk Analysis Methodology for Hazardous Material Unit and Manifest Trains

5a. CONTRACT NUMBER
693JJ619C000017

5b. GRANT NUMBER

5c. PROGRAM ELEMENT NUMBER

6. AUTHOR(S)
Xiang Liu[1] ORCID: 0000-0002-4348-7432
Di Kang[1] ORCID: 0000-0003-3337-2815
Tyler C. Dick[2] ORCID: 0000-0002-2527-1320
Jiaxi Zhao[2] ORCID: 0000-0002-8706-970X
Zheyong Bian[4] ORCID: 0000-0001-9094-3333
Zhipeng Zhang[1] ORCID: 0000-0002-5127-0284
Steve Kirkpatrick[3] ORCID: 0000-0001-9590-7980
Chen-Yu Lin[2] ORCID: 0000-0003-0337-5230

5d. PROJECT NUMBER

5e. TASK NUMBER

5f. WORK UNIT NUMBER

7. PERFORMING ORGANIZATION NAME(S) AND ADDRESS(ES)
1. Rutgers, The State University of New Jersey, Piscataway, NJ
2. University of Illinois at Urbana Champaign, Urbana, IL
3. Applied Research Associates, Inc., Los Altos, CA
4. University of Houston, Houston, TX

8. PERFORMING ORGANIZATION REPORT NUMBER

9. SPONSORING/MONITORING AGENCY NAME(S) AND ADDRESS(ES)
U.S. Department of Transportation
Federal Railroad Administration
Office of Railroad Policy and Development
Office of Research, Development and Technology
Washington, DC 20590

10. SPONSOR/MONITOR'S ACRONYM(S)

11. SPONSOR/MONITOR'S REPORT NUMBER(S)
DOT/FRA/ORD-24/24

12. DISTRIBUTION/AVAILABILITY STATEMENT
This document is available to the public through the FRA website.

13. SUPPLEMENTARY NOTES
COR: Francisco González, III

14. ABSTRACT
Between August 2019 and May 2022, the Federal Railroad Administration sponsored researchers from Rutgers University, the University of Illinois at Urbana Champaign, Applied Research Associates, and the University of Houston to develop a risk analysis methodology for railroad transportation of hazardous materials (hazmat) given specific parameters (e.g., configuration, train length, placement of hazmat cars in a train, speed, yard type, yard switching approach, traffic exposure, and other operational factors). The methodology accounts for transportation risks on both mainlines and in yards and terminals. The methodology integrates train derailment probability, derailment severity, probability of a hazmat car derailing and releasing, amount of hazmat releasing quantity, and the release consequence (in terms of casualties). The risk analysis methodology can be used to quantify the overall transportation risk (including mainline and yard/terminal) given specific train configurations and operational characteristics, thereby comparing alternative service options for hazardous materials transportation.

15. SUBJECT TERMS
Risk analysis; unit train; manifest train; hazardous material; mainlines; yard; terminal.

16. SECURITY CLASSIFICATION OF:			**17. LIMITATION OF ABSTRACT**	**18. NUMBER OF PAGES**	**19a. NAME OF RESPONSIBLE PERSON**
a. REPORT	**b. ABSTRACT**	**c. THIS PAGE**			**19b. TELEPHONE NUMBER** *(Include area code)*
				292	

Standard Form 298 (Rev. 8/98)
Prescribed by ANSI Std. Z39.18

METRIC/ENGLISH CONVERSION FACTORS

ENGLISH TO METRIC	METRIC TO ENGLISH
LENGTH (APPROXIMATE)	**LENGTH (APPROXIMATE)**
1 inch (in) = 2.5 centimeters (cm)	1 millimeter (mm) = 0.04 inch (in)
1 foot (ft) = 30 centimeters (cm)	1 centimeter (cm) = 0.4 inch (in)
1 yard (yd) = 0.9 meter (m)	1 meter (m) = 3.3 feet (ft)
1 mile (mi) = 1.6 kilometers (km)	1 meter (m) = 1.1 yards (yd)
	1 kilometer (km) = 0.6 mile (mi)
AREA (APPROXIMATE)	**AREA (APPROXIMATE)**
1 square inch (sq in, in^2) = 6.5 square centimeters (cm^2)	1 square centimeter (cm^2) = 0.16 square inch (sq in, in^2)
1 square foot (sq ft, ft^2) = 0.09 square meter (m^2)	1 square meter (m^2) = 1.2 square yards (sq yd, yd^2)
1 square yard (sq yd, yd^2) = 0.8 square meter (m^2)	1 square kilometer (km^2) = 0.4 square mile (sq mi, mi^2)
1 square mile (sq mi, mi^2) = 2.6 square kilometers (km^2)	10,000 square meters (m^2) = 1 hectare (ha) = 2.5 acres
1 acre = 0.4 hectare (he) = 4,000 square meters (m^2)	
MASS - WEIGHT (APPROXIMATE)	**MASS - WEIGHT (APPROXIMATE)**
1 ounce (oz) = 28 grams (gm)	1 gram (gm) = 0.036 ounce (oz)
1 pound (lb) = 0.45 kilogram (kg)	1 kilogram (kg) = 2.2 pounds (lb)
1 short ton = 2,000 pounds (lb) = 0.9 tonne (t)	1 tonne (t) = 1,000 kilograms (kg)
	= 1.1 short tons
VOLUME (APPROXIMATE)	**VOLUME (APPROXIMATE)**
1 teaspoon (tsp) = 5 milliliters (ml)	1 milliliter (ml) = 0.03 fluid ounce (fl oz)
1 tablespoon (tbsp) = 15 milliliters (ml)	1 liter (l) = 2.1 pints (pt)
1 fluid ounce (fl oz) = 30 milliliters (ml)	1 liter (l) = 1.06 quarts (qt)
1 cup (c) = 0.24 liter (l)	1 liter (l) = 0.26 gallon (gal)
1 pint (pt) = 0.47 liter (l)	
1 quart (qt) = 0.96 liter (l)	
1 gallon (gal) = 3.8 liters (l)	
1 cubic foot (cu ft, ft^3) = 0.03 cubic meter (m^3)	1 cubic meter (m^3) = 36 cubic feet (cu ft, ft^3)
1 cubic yard (cu yd, yd^3) = 0.76 cubic meter (m^3)	1 cubic meter (m^3) = 1.3 cubic yards (cu yd, yd^3)
TEMPERATURE (EXACT)	**TEMPERATURE (EXACT)**
[(x-32)(5/9)] °F = y °C	[(9/5) y + 32] °C = x °F

QUICK INCH - CENTIMETER LENGTH CONVERSION

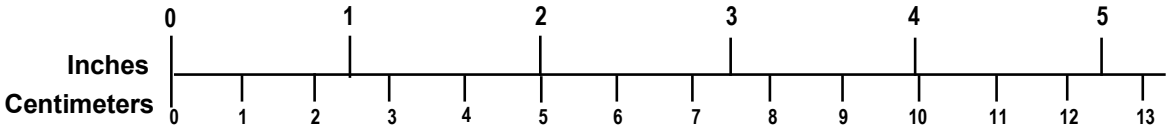

QUICK FAHRENHEIT - CELSIUS TEMPERATURE CONVERSIO

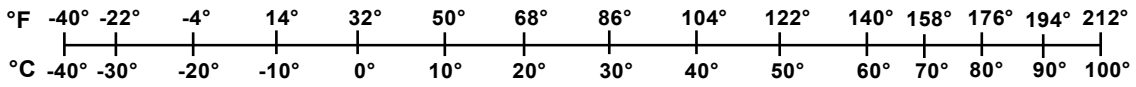

For more exact and or other conversion factors, see NIST Miscellaneous Publication 286, Units of Weights and Measures. Price $2.50 SD Catalog No. C13 10286

Updated 6/17/98

Acknowledgements

The authors acknowledge Francisco González, III and Dr. Phani Raj from the Federal Railroad Administration for their advice and guidance during this research project. The authors also thank Zezhou Wang, Xin Wang, Junyan Dai, and Noelle Darling from Rutgers University, and Xi Zhang from the University of Houston for their assistance on this report.

Contents

Illustrations

Tables

Executive Summary

Freight trains safely and efficiently transport large amounts of hazardous materials (hazmat) over long distances. Despite the low probability of occurrence, a hazmat train release incident could result in significant consequences. Train type could affect hazmat transport risk; unit trains experience hazmat release risk on mainlines and when arriving at or departing from terminals, whereas manifest trains (i.e., mixed trains) experience additional switching risks in classification yards.

This research was conducted between August 2019 and May 2022 by a team from Rutgers University, the University of Illinois at Urbana Champaign, Applied Research Associates, and the University of Houston. Based on prior literature and using various data sources from 1996 to 2018, the team analyzed the risk of railroad hazmat transportation considering train type, train length, the placement of hazmat cars in a train, speed, yard type, yard switching approach, traffic exposure, and several other operational factors. Researchers developed a risk analysis methodology to estimate the overall transportation risk on both mainlines and in yards or terminals. The research methodology accounted for train derailment probability, derailment severity, probability of a hazmat car derailing and releasing, amount of hazmat released, and release consequences. The team developed a risk profile that is a probabilistic distribution of release quantities and/or consequences (e.g., total release quantity or estimated casualties) given a specific transportation demand (e.g., total number of hazmat cars to transport).

Researchers applied the risk analysis methodology in a case study including eight operational scenarios categorized by train type, hazmat car position, yard switching approach, and yard type. The team concluded that placing all tank cars at the positions with the lowest probabilities of derailing could provide the lowest risk given equal transportation demand. Based on the data and parameters used in the case study, researchers also found that the risks associated with arrival/departure events in terminals and yard switching events could be comparable to the risk on mainlines under certain circumstances. Since there are many factors that affect risk in hazmat rail transport, the risk calculation should be performed for each type of train arrangement, as the risk analysis methodology can be tailored to fit various operational characteristics.

1. Introduction

Between August 2019 and May 2022, the Federal Railroad Administration (FRA) sponsored researchers from Rutgers University, the University of Illinois at Urbana Champaign, Applied Research Associates, and the University of Houston to develop a risk analysis methodology for railroad transportation of hazardous materials (hazmat) given specific parameters (e.g., configuration, train length, placement of hazmat cars in a train, speed, yard type, yard switching approach, traffic exposure, and other operational factors). The methodology accounts for transportation risks on both mainlines and in yards and terminals.

1.1 Background

Rail is a safe and efficient mode for transporting hazmat. In the past decade, traffic from hazmat transportation by unit trains has significantly increased in the United States. Despite the very low rate of occurrence per traffic exposure, accidents still happen, and their potentially severe consequences remain a major concern in the U.S. For example, in January 2005, a train collision occurred in Graniteville, South Carolina, that led to the release of 60 tons of chlorine gas, nine fatalities, more than 600 injuries, an evacuation of about 5,400 people, and an economic loss exceeding $6.9 million (NTSB, 2005). In February 2015, a unit train transporting 3.1 million gallons of Bakken crude oil derailed 27 loaded tank cars in Mount Carbon, West Virginia. As a result, one nearby house and an adjacent garage were destroyed by fire, about 378,000 gallons of crude oil were released from tank cars, the released crude oil was discharged into the Kanawha River and contaminated soil around the derailment location, about 300 people were evacuated from within a one-half mile radius of the accident scene, and the total economic loss was estimated to be $2.5 million (NTSB, 2015).

Railroads achieve operational efficiencies and economies of scale by transporting bulk commodities in unit trains that cycle between a pair of loading and unloading terminals while bypassing intermediate classification yards. The railcars in a unit train are often of a uniform design and dedicated to a specific operation, making multiple trips as a train set. This contrasts with manifest trains which comprise railcars with different sizes and types designed for various commodities. It has been hypothesized that a unit train with loaded railcars of uniform design may be more susceptible to relevant in-train forces than a manifest train. However, it is also theorized that unit trains may reduce train-handling challenges associated with the mixture of loaded, empty, long, and short railcars in manifest trains. To better evaluate the operational safety risks of unit trains and manifest trains transporting hazmat, research is needed to understand whether important safety parameters (i.e., tank car derailment, release likelihood, and consequences) significantly differ between manifest and unit trains.

1.2 Objective

This research analyzes the risks of railroad hazmat transportation, given specific train configurations and railroad operational information. For example, to transport 100 tank cars every 10 days, a railroad may hold the railcars and place them into one 100-railcar unit train that departs every 10 days or, alternatively, put them into a total of 10 manifest trains (1 departing each day) with each train comprised of 10 tank cars in certain positions on the same railroad corridor. The research team's proposed risk analysis methodology can be used to identify and quantify possible differences in the risks posed by these different train configurations and

shipment strategies for transporting hazmat on mainlines and in yards, respectively. The methodology accounts for train derailment probability, derailment severity, probability of a hazmat car derailing and releasing, quantity of hazmat releasing, and release consequences. The risk model creates a risk profile that is a probabilistic distribution of a certain release consequence (e.g., total release quantity or estimated casualties) given traffic demand.

1.3 Overall Approach

This study investigated the multiple-car derailment and hazmat release risk differences between unit and manifest trains in three stages. First, an integrated, probabilistic, multiple-car release risk assessment methodology with track and operational characteristics was proposed which considered unit train and manifest train configurations in its risk evaluation. Low-probability hazmat release incidents were divided into categories using the following parameters: 1) train derailment; 2) derailment severity (e.g., number of cars derailed); 3) number of tank cars derailed; 4) number of tank cars releasing contents; 5) amount released; and 6) hazmat-specific release consequence. Second, researchers analyzed whether unit train and manifest train configurations have different effects on each risk parameter using statistical analysis and physics-based modeling approaches. Third, the resulting risk parameters were implemented into a risk analysis methodology and a comprehensive case study was conducted.

1.4 Scope

This project focuses on analyzing the impact of train configuration (i.e., unit train versus manifest train) on the risk of hazmat transportation. It studies the differences in derailment rates, derailment severities, tank car derailment probabilities, release probabilities, and release consequences, comparing unit trains and manifest trains transporting the same amount of hazmat.

1.5 Organization of the Report

This technical report is organized as follows:

- Section 2 summarizes existing literature pertaining to state-of-the-art research on railroad hazmat transportation and identifies knowledge gaps.
- Section 3 develops the overall methodologies to estimate the risk of railroad hazmat transportation on mainlines and in yards, respectively.
- Section 4 presents the mainline derailment rate analysis based on traffic data from the Surface Transportation Board (STB) "R-1" Annual Report Financial Data, Public Use Carload Waybill Sample Data, and mainline derailment data from the FRA Rail Equipment Accident (REA) database.
- Section 5 proposes a statistical model, or Truncated Geometric (TG) model, and a physical model (i.e., one-dimensional derailment kinematics model) to estimate mainline derailment severity.
- Section 6 introduces key parameters in yard safety and risk analysis.
- Section 7 develops a model to estimate the conditional probability of a derailed tank car releasing its contents.
- Section 8 proposes a release consequence model.
- Section 9 uses a case study to interpret the point-to-point risk model that integrates both mainline risk and yard risk.

- Section 10 draws conclusions and proposes managerial implications based on the research findings.

2. Literature Review

2.1 Introduction

This section provides a literature review of risk analysis for rail transport of hazmat release, including the event chain leading to hazmat release, possible risk factors, and existing state-of-the-art risk analysis methodologies. Prior research related to train derailment risk has included wheel-rail interaction (Ling et al., 2017), derailment causal analysis (Britton et al., 2017; Liu, 2017b), and hazmat transportation risk (Branscomb et al., 2010; Liu, 2016b, 2017a, 2017c; Liu et al., 2014b, 2018; Liu, Saat, & Barkan, 2013a, 2013b; Liu & Schlake, 2016; Nayak et al., 1983; Verma & Verter, 2007). These studies have focused on various risk mitigation strategies related to infrastructure (Liu, Saat, & Barkan, 2013a, 2013b), rolling stock (Schlake et al., 2011), tank car safety enhancement (Barkan, 2008; PHMSA, 2015; Saat & Barkan, 2011; Schlake et al., 2011), train makeup (Bagheri et al., 2012, 2014), and mitigation of release consequence (Yoon et al., 2009). Each of these risk reduction strategies focuses on at least one event in the causal chain of an accident-caused release incident.

The hazmat release risk on mainline was analyzed based on the event sequence (i.e., train accident occurrence, number of cars derailed, number of hazmat cars derailed, number of hazmat cars releasing, and release consequence). To analyze the hazmat release risk in a yard, relevant references were reviewed to identify the possible factors that cause release risk, the level of the risk in yards, and the difference of yard risk from mainline risk when adopting different risk reduction strategies (e.g., rerouting, optimal placement of hazmat cars, etc.).

2.2 Mainline Hazmat Release Risk Analysis

Railroad hazmat transportation on mainline can be synthetically structured as a multi-event, multifactor risk management problem. Figure 1 shows that a release incident involves five factors: 1) train accident occurrence, 2) number of cars derailed, 3) number of hazmat cars derailed, 4) number of hazmat cars releasing, and 5) release consequences (Liu et al., 2014b).

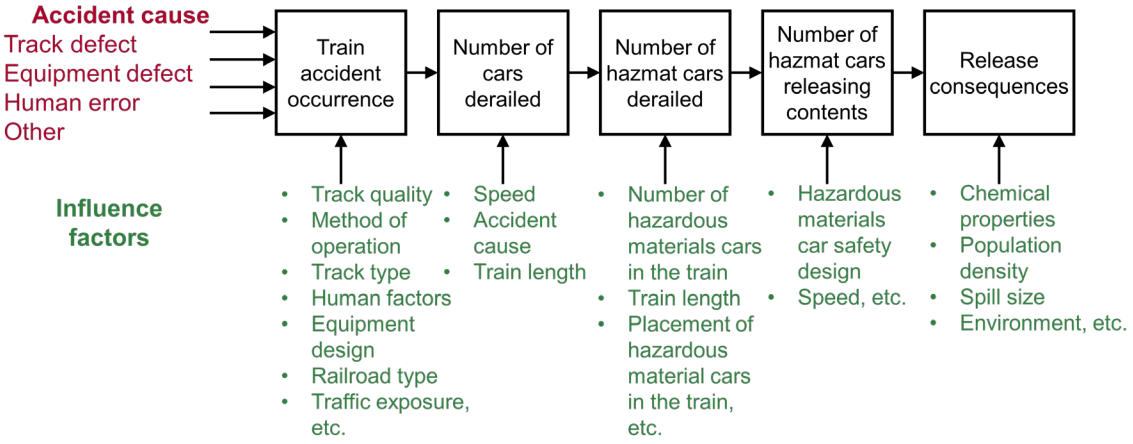

Figure 1. Event chain leading to hazardous materials release and consequences

As shown in this figure, train accidents may be directly caused by any of several factors (e.g., track defects, equipment defects, human error, etc.) and influenced by many potential factors (e.g., track quality, method of operation, track type, human factors, equipment design, railroad

type, traffic exposure, etc.). If a derailment occurs, the number of cars derailed can be used to measure the severity of the incident. The number of cars derailed can be influenced by several factors (e.g., train speeds, accident causes, and train lengths), but if the derailed cars are loaded with hazmat, the incident may be much more severe. Risk factors for this type of severe incident include the number of hazmat cars in the train, the nature of the hazmat in the consist, train length, placement of hazmat cars, etc. If the hazmat releases to the environment, consequences related to chemical properties and types of hazards posed by the released chemical, population density in nearby areas, spill size, and environment must be considered. Much of the prior research has focused on the different stages of events that ultimately lead to a hazmat release.

Several researchers have already considered rail transport of hazmat risk analysis based on the event chain. Liu & Schlake (2016) modeled the probability of a liquefied natural gas (LNG) tender car release incident due to a freight train derailment on a mainline. The authors estimated the probability based on the event sequence. First, they proposed a train accident probability estimation model. Second, they built the conditional probability model of an LNG tender derailment, which was conditional on the event of a train derailment. Finally, they estimated the conditional probability of a derailed LNG tender car releasing. The researchers used data provided by FRA to estimate the parameters of the probability model accounting for a number of factors, including FRA track class, method of operation, annual traffic density level, train length, the point of derailment, accident speed, the position of the LNG tender in a train (there is one LNG tender car behind the locomotive), and LNG tender car design.

Similarly, Liu et al. (2014b) built a model to estimate the probability distribution of the number of tank cars releasing after a train derailment occurs. They considered the probability distributions of points of derailment (e.g., the position of the first car derailed), number of cars derailed (e.g., both tank cars and other types of railcars and locomotives), number of hazmat tank cars derailed given the total number of cars derailed, and the number of tank cars releasing given the total number of hazmat tank cars derailed. Liu (2016b) built a practical probabilistic risk analysis model to estimate the in-transit risk of transporting crude oil by rail in unit trains on mainlines. The model accounts for track-segment-specific characteristics including segment length, FRA track class, method of operation, and annual traffic density; train-specific characteristics such as train length, train speed, and tank car safety design; and population density along each segment. The risk model estimated segment-specific risks that were measured by the expected number of affected persons based on the event chain, considering the probabilities or probability distributions of a train accident on a specific segment per train shipment, number of tank cars derailed, number of cars releasing, and number of persons affected.

Kawprasert & Barkan (2010) also modeled the rail transport of hazardous material risk based on the occurrence of the event chain. Similar to Liu (2016b), their research considered the consequences of tank car hazmat releasing. They measured the annual risk by the number of people affected per year. In addition, they also considered the effect of train speed on railroad hazmat transportation risk, and thus estimated the speed-dependent conditional probability of release. The effects of track-class upgrades on risk were also considered. Tracks with higher FRA classes have lower accident rates, but higher permissible speeds increase the conditional probability of release if a tank car is derailed in an accident. For the route analyzed in the case study, use of the speed-dependent conditional probability of release resulted in a slight increase in the overall risk estimate, and upgrading to Class 3 track provided the greatest reduction in risk.

Bagheri et al. (2014) developed a comprehensive assessment methodology to evaluate rail transport risk, one that incorporates the sequence of events leading to hazmat release from the derailed railcars and the resulting consequence. They estimated different parameters to quantify the model, including probability of train derailment, probability of derailment by position, number of railcars derailed, number of derailed railcars releasing, and population exposure based on FRA train accident data.

Verma (2011) developed a risk assessment methodology which takes into consideration the differentiating features of trains (e.g., train-length, train-decile position of hazmat railcar) and the characteristics of train accidents (i.e., the sequence of events leading to hazmat release and the associated consequence from ruptured railcars). Their empirical analysis based on the FRA accident dataset revealed that the front of the train is riskiest and that the 7–9th train-deciles are most appropriate for moving hazmat railcars for freight-trains of any length. Furthermore, it was concluded that rail-track risk can be reduced by strategically distributing hazmat railcars in the train-consist. Liu et al. (2018) developed an integrated, generalized risk analysis methodology that can estimate accident-cause-specific hazmat transportation risk, accounting for various train and track characteristics, including train length, speed, point of derailment, the number and placement of tank cars in a train, tank car safety design, and population density along rail lines. Using the two major causes of accidents on freight railroads – broken rails and track geometry defects – as an example, they demonstrated a step-by-step analytical procedure and decision support tool to assess how accident frequency, severity, and hazmat transportation risk vary by accident causes.

2.2.1 Train Accident Occurrence

Many severe hazmat release incidents are caused by train accidents, particularly train derailments. Derailments account for over 72 percent of all types of accidents on freight railroads (Liu, 2016a). FRA identified around 389 distinct accident causes (FRA, 2011) related to infrastructure, rolling stock, human factors, and other factors (Liu et al., 2012). Prior research has found that over 70 percent of freight train mainline derailments were caused by either infrastructure defects or rolling stock failures (Liu et al., 2012).

Liu et al. (2012) analyzed train derailment data from FRA's rail equipment accident database for the period between 2001 and 2010 for each track type, accounting for frequency of occurrence by cause and number of cars derailed. Statistical analyses were conducted to examine the effects of accident cause, type of track, and derailment speed. The analysis showed that broken rails or welds were the leading derailment cause on main, yard, and siding tracks. Bing et al. (2015) identified the chain of events that lead to a hazmat release, defined the corresponding risk metrics and how they vary with equipment and operational factors, and described estimates of selected risk metrics. One notable finding from their study is that broken rails, welds, and other rail defects are the most frequent causes of hazmat release accidents. Liu (2015) used a negative binomial regression model to present a statistical analysis of U.S. Class I railroad freight train derailment rates on main tracks by year from 2000 to 2012 based on FRA accident and traffic data. The analysis showed a significant temporal decline in the rate of freight train derailment (−5.9 percent per year) and that the rate of change in accident rate varied by accident cause. Lui found that rates of freight train derailment caused by broken rails or welds and track geometry defects declined by 6 and 5 percent annually, respectively, the rate of derailment caused by bearing failure decreased by 11 percent annually, and the rate of derailment caused by train

handling errors fell by 7 percent annually. Liu (2017b) developed a log-linear statistical model that can estimate the number of freight-train derailments accounting for railroad, accident cause, season, and traffic volume. The analysis showed that broken rails and track geometry defects are the two leading freight-train derailment causes for four major U.S. freight railroads. Fall and winter seasons appear to have higher likelihoods of a broken-rail-caused derailment, given the same railroad and traffic level throughout the year. By contrast, track-geometry-defect-caused derailments occur more frequently in spring and summer. Liu (2016a) developed a statistical methodology for risk analysis of freight train collisions in the United States occurring between 2000 and 2014. Negative binomial regression models were developed to estimate the frequency of freight train collisions as a function of year and traffic volume, both by track type and accident cause. The analysis showed a temporal decline in collision rate on mainline during the study period. Further, the relationship between annual collision frequency and traffic exposure may vary with the type of track and accident cause. Xiao et al. (2008) and Morales-Ivorra et al. (2016) found that a curved track may have a higher derailment rate compared with a tangent track, all else being equal.

Hazmat risk reduction strategies include the prevention of track defects (Liu, Saat, & Barkan, 2013a), equipment condition monitoring to reduce in-service failures (Schlake et al., 2011), and the use of more advanced train control technologies to reduce human error (Martland et al., 2001). Researchers have proposed different risk reduction strategies and evaluated their effectiveness.

Liu et al. (2011) found that upgrading track class is likely to prevent certain track-related derailments; however, this upgrade may also increase the risk of certain types of equipment failure which are more likely to occur at higher speeds. A general method was developed to assess derailment risk by accident cause and FRA track class. The safety benefits of track class upgrades in reducing the risks from certain accident causes were quantitatively evaluated. Liu et al. (2013a) developed an analytical framework to evaluate risk reduction by implementing three risk reduction strategies, including broken rail prevention, tank car fleet upgrade, and train speed reduction. Prevention of broken rails represents an accident prevention strategy to reduce the probability of a tank car derailment, whereas tank car upgrade and speed reduction affect the probability of a derailed-car release. Liu (2017c) quantified the relationship between ultrasonic rail defect inspection frequency and railroad hazmat transportation risk. He applied a Pareto optimization model to determine optimal annual inspection frequencies on different track segments with different risk levels. The model provided an evaluation of segment-specific hazmat transportation risk due to rail failures, as well as an assessment of risk-based prioritization of rail defect inspection. Schlake et al. (2011) found that improvement in monitoring railcar conditions could substantially reduce in-service failures and derailments, operational waste, and variability in rail operations and could enhance network productivity, capacity, and reliability. Bing et al. (2015) examined three safety initiatives that are designed to reduce the number of train accidents that could lead to hazmat releases: application of Positive Train Control (PTC), implementation of a new Rail Integrity Rule developed through the Railroad Safety Advisory Committee (RSAC), and implementation of Electronically Controlled Pneumatic (ECP) brakes. They found that positive train control, improved rail integrity, and implementation of electronically controlled pneumatic brakes can reduce car derailment by 3.7 - 5.0 percent, 4.7 - 8.1 percent, and 2.5 - 4.8 percent, respectively.

2.2.2 Number of Cars Derailed

The total number of cars derailed depends on accident cause, speed, train length, and point of derailment (Saccomanno & El-Hage, 1991b; 1989). The number of cars derailed (a proxy indicator of accident severity) is an important consideration.

Saccomonno and El-Hage (1991b; 1989) developed a model to minimize the number of derailed cars carrying dangerous goods, considering different marshalling strategies and rail corridor conditions. The authors applied the model in the Sarnia–Toronto rail corridor derailment analysis. The results demonstrated that marshalling strategies for cars carrying dangerous goods should be sensitive to corridor conditions that affect the causes of train derailments. Effective marshalling strategies can substitute for speed controls on the shipment of dangerous goods, resulting in similar or improved derailment profiles and lower operating costs. In Liu's (2016a) research, the total number of cars derailed is used to measure the train collision risk. The author proposed a probability model developed from the statistical analysis to predict the number of cars derailed in the future. The model can be used to project the risk of freight train collisions and enable a data-driven assessment of the safety effectiveness of certain accident prevention strategies. In research by Liu et al. (2017), the number of cars derailed per derailment was measured as the derailment severity. They compared the derailment rates and severities for different FRA track classes, method of operations (e.g., non-signaled and signaled), and annual traffic densities. The analysis showed that signaled track with a higher FRA track class and higher traffic density is associated with a lower derailment rate. Liu et al. (2013) estimated derailment severity by the number of cars derailed after a train derailment occurs, accounting for residual train length, derailment speed, and loading factor (i.e., proportion of loaded cars in a train). They developed a zero-truncated negative binomial (ZTNB) regression model to estimate the conditional mean of train derailment severity. Recognizing that the mean is not the only statistic describing data distribution, a quantile regression (QR) model was also developed to estimate derailment severity at different quantiles.

2.2.3 Number of Hazmat Cars Derailed

The total number of hazmat cars derailed is related to train length, number of hazmat and non-hazmat cars in a train, and their placements (Verma, 2011). Possible strategies for reducing the probability of a hazmat tank car derailment include reducing the speed of the train to reduce the total number of vehicles derailed (Kawprasert & Barkan, 2010) and the placement of hazmat tank cars in positions that are less likely to derail (Bagheri et al., 2012, 2014).

Liu (2017a) compared hazmat transportation risk in unit trains with mixed trains. The analysis found that a unit train has a higher probability of a release incident per train derailment because the large number of tank cars in a unit train increases tank car derailment probability and thus risk. However, use of a unit train would also reduce the number of shipments compared with the scenario where the same number of hazmat cars were shipped in multiple mixed trains. Overall, unless tank cars are in the positions least likely to derail, unit trains may have a lower total risk; however, if all tank cars are placed in the lowest-probability derailment positions, distributing tank cars to multiple mixed trains would result in a lower risk level. Bagheri et al. (2012) estimated the hazmat transportation risk as the expected number of hazmat cars derailed. They studied the problem of where to place hazardous material cars in the train assembly process to minimize the overall hazmat car derailment risk. The model considered both the probability of railway cars derailing en route by position as well as the risk associated with additional

operations in the rail yard. The results suggested that a more than 57 percent reduction in risk can be achieved if individual hazmat cars within each block are positioned to minimize in-transit risk. Bagheri et al. (2014) found that the third quarter of the train has the lowest derailment probability. Therefore, the risk of the number of hazmat cars derailed will be reduced when hazmat cars are placed in the third quarter of the train. Additionally, based on the FRA accident dataset, another empirical analysis conducted by Verma (2011) revealed that the front of the train is riskier, and that the 7–9th train-deciles are most appropriate for moving hazmat railcars for freight trains of any length. They concluded that the risk can be reduced by strategically distributing hazmat railcars in the train. Due to different analytical methods and data used, the conclusions from the literature may not necessarily be identical, which highlights the need for further study using more recent data.

2.2.4 Number of Hazmat Cars Releasing Contents

Not all derailed or damaged tank cars release their contents. Data from the Tank Car Accident Database (TCAD) developed by the Railway Supply Institute (RSI) and the Association of American Railroads (AAR) show that tank car release probability can be reduced by using more robust tank car designs (Barkan, 2008; PHMSA, 2015; Saat & Barkan, 2011). In addition, reducing train speed can reduce the accident impact on the tank car, therefore decreasing release probability (Kawprasert & Barkan, 2010).

Liu et al. (2014b) used "number of tank cars releasing per train derailment" to estimate the railroad hazmat transportation risk, considering principal operational characteristics such as train length, derailment speed, accident cause, position of the first car derailed, number and placement of tank cars in a train, and tank car safety design. The effects of train speed, tank car safety design, and tank car positions in a train were evaluated by the number of cars that release their contents in a derailment. The analysis showed that reducing train speed, improving tank car safety design (various tank car types affect the conditional probability of releasing), and changing tank car placement all have the potential to reduce the number of tank cars releasing per derailment. In addition, there are interactive effects among different risk reduction strategies. Barkan (2008) analyzed car safety design features or "risk reduction options" (RROs), including top fitting protection, head protection, and tank thickness regarding their effect on the conditional probability of release in an accident and their incremental effect on tank car weight. He considered all possible combinations of these RROs and measured their effectiveness in terms of the reduced release probability per unit of weight increase and the identified Pareto optimal set of options, including the combinations of RROs that provided the greatest improvement in safety (i.e., the least amount of additional weight for any desired level of tank car weight increase). The results of this analysis were used by AAR's Tank Car Committee to develop new specifications for higher capacity non-insulated and insulated non-pressure tank cars, resulting in an estimated 32 and 24 percent respective improvement in safety. Saat and Barkan (2011) developed a model to estimate the probability of hazardous material releasing, given the condition of tank car RROs, including increasing tank head thickness, increasing tank shell thickness, adding an 11-gage steel jacket and insulation, adding either half- or full-height head shields to the tank head, adding top fittings protection, removing bottom fittings, and any combination of options. They also presented an optimization model by identifying a set of Pareto-optimal solutions for a baseline tank car design in a bi-criteria decision problem. This model provided a quantitative framework for a rational decision-making process involving tank car safety design enhancements to reduce the risk of hazmat release. Kawprasert and Barkan

(2010) proposed a model to estimate the conditional probability of tank car release based on four events: 1) the contents were lost because of head damage; 2) the contents were lost because of shell damage; 3) the contents were lost because of top fitting damage; and 4) the contents were lost because of bottom fitting damage. They determined the conditional probability of tank car release based on the occurrence probabilities of the four events multiplied by speed adjustment factors. Prabhakaran and Booth (2018) proposed a novel methodology for quantifying and characterizing how changes to tank car design or the tank car operating environment lead to reductions in puncture probabilities. They considered several parameters that are relevant to tank car performance under derailment conditions, including multiple derailment scenarios, derailment dynamics, impact load distributions, impactor sizes, operating conditions, tank car designs, etc.

2.2.5 Release Consequences

The consequences of a release can be measured by different metrics, such as property damage, environmental impact, traffic delay, or the size of affected population. Geographical information systems (GIS) can be used for consequence analysis when integrated with other databases such as census and rail network data (Verma & Verter, 2007). The use of a lower-hazard chemical, rerouting of hazmat traffic to avoid populated areas, or improved emergency response and evacuation have been identified as potential strategies to mitigate release consequences, thereby reducing the risk (Branscomb et al., 2010).

In Liu's (2016b) research, the risk associated with rail transport of crude oil was measured by the number of persons affected due to hazmat release. His research showed that annual crude oil release risk on the studied route in 2015 was equal to approximately one incident every 84 years. Similarly, Glickman et al. (2007) measured the expected consequence of a major hazmat release by the expected number of residents in the critical area of exposure. Their research aimed to optimize the train routing strategy at the network level considering this risk. They developed a model to quantify the risk and then used a weighted combination of cost and risk to generate alternate routes. The alternate routes achieved significantly lower risk than the practical routes with a small increase in cost. The authors also noted a tradeoff that minimizes the transport of hazmat risk (measured by the consequence) and the cost.

Kawprasert and Barkan (2010) also modeled hazmat rail transport risk by the number of people affected per year while simultaneously considering the effects of train speed and track class. Bagheri et al. (2014) used population exposure to estimate the consequence of hazmat release. They concluded that rail is the preferred option for hazmat transportation when compared to truck transportation because the probability of release from multiple railcars would be extremely small. They also found that using a unit train to transport hazardous material presented the lowest risk. Verma (2011) also used population exposure as the consequence of hazmat release. They calculated the population exposure as a function of the volume of hazmat released from multiple sources and the population density of the accident centers. They used a circle, with the accident location as the center, to represent the impact area. The hazmat transport activity can be visualized as the movement of this circle along the railroad, which carves out a band as the region of possible impacts. The number of people living in the band is the population exposure.

Yoon et al. (2009) studied the consequences to soil and groundwater from railroad-tank-car spills of light, non-aqueous phase liquids. The authors presented the development and application of an environmental screening model to assess infiltration and redistribution of non-aqueous phase

liquid in soils and groundwater, and to assess groundwater cleanup time using a pumping system. They developed a hydrocarbon spill screening model (HSSM) to consider the unique characteristics of railroad-tank-car spill sites. First, the HSSM model was used to simulate non-aqueous phase liquids' infiltration and redistribution. Then they used a non-aqueous phase liquid dissolution and ground water transport module and a pumping system module to simulate the effects of properties, excavation, and removal on non-aqueous phase liquid redistribution and cleanup time.

Raj (1988) proposed a risk assessment model to evaluate the consequence to the public from the transportation of hazmat. The model considers the various operational and hazmat property parameters, including the make-up of the freight trains, annual volumes of hazmat transport, train accident statistics both on main line and in yards, the effects of leak prevention devices such as head shields and shelf couplers, population density distribution, and the behavior of the chemicals in the environment after release.

Adams et al. (2011) performed a study to support the U.S. Nuclear Regulatory Commission (NRC) in determining the types and frequency of railway accidents involving severe, long duration fires that could affect rail transport of spent nuclear fuel (SNF). That study used train accident data from both the FRA and U.S. Department of Transportation Pipeline and Hazardous Materials Safety Administration (PHMSA) databases, and focused on accidents where hazmat was released from multiple train cars. The study estimated the frequency of a severe fire at 6.2 $\times 10^{-4}$ accidents per million freight train-km (1 x 10^{-3} per million freight train-mi).

The estimation of the potentially affected area around a derailment requires an assessment of the evacuation area. PHMSA, Transport Canada (TC), and Secretaría de Infraestructura, Comunicaciones y Transportes (SICT) published the Emergency Response Guidebook (ERG) (U.S. DOT et al., 2016), which is a common resource used by emergency responders to establish evacuation area sizes for various derailment events with different hazmat commodities. Other industry resources on emergency preparedness and response, such as the CN Railroad Emergency Preparedness Guide (Dangerous Goods Awareness Level) (Canadian National Railway, 2019), will often refer to the ERG as a primary resource for responders in hazmat derailments.

The International Association of Fire Chiefs (IAFC) (2015) performed a Unit Train Derailment Site Case Study looking at emergency response tactics. They examined five recent unit train derailments and fires and evaluated the emergency response for each case. They observed that (1) none of the fire departments surveyed had a pre-plan for railway emergencies; (2) no fire department surveyed, whether career, combination, or volunteer, had enough AR-AFFF foam for ethanol incidents or AFFF foam for crude oil incidents; and (3) four of the five surveyed departments used the ERG at some point in their incidents, and the evacuation section proved to be especially helpful.

2.3 Yard Hazmat Release Risk Analysis

Railroads in North America transported more than two million carloads of hazmat in 2018 (AAR, 2019b). While hazmat transportation accounts for only 6 percent of rail traffic in the United States and more than 99 percent of shipments reached their destinations safely, this traffic is responsible for a major share of railroad liability and insurance risk (AAR, 2019b). Most hazmat shipments by rail involve more than one train movement due to the long distances

traveled and the need to move railcars between sidings, branch lines, and major mainline routes which may be owned by different rail carriers (TRB et al., 1994). Typically, railcars carrying hazmat shipments pass through numerous yards and are switched between trains several times over the course of each trip.

Economic transportation of these single-car shipments is facilitated by a network of carload (i.e., manifest) freight trains operating between major classification yards. Railroad classification yards serve as hubs where loaded and empty railcars from various origins are grouped together into blocks of railcars with common destinations. These blocks of railcars are then further aggregated to form trains destined to different classification yards on other parts of the network or for local delivery to nearby shippers. The railcar sorting process requires numerous coupling and uncoupling events as groups of railcars are moved between multiple parallel tracks. In the highest-volume classification yards, sorting is accomplished by pushing railcars over small hills, or "humps" (Figure 2). Once uncoupled, the railcars freely roll downhill under the force of gravity as they are sorted into different tracks and coupled to other railcars. The speed of railcars rolling down the hump and the final speed when they couple with other railcars in the designated tracks is controlled at discrete locations (as shown in Figure 2) by track mounted "retarder" brakes activated by an automated control system. The control system decides the amount of braking force each retarder brake will apply to the railcars based on the railcars' characteristics and the distance to the other cars on the designated tracks. This allows for efficient railcar sorting and ensures that the railcars rolling down the hump do not couple with other railcars in the classification tracks at an excessive speed.

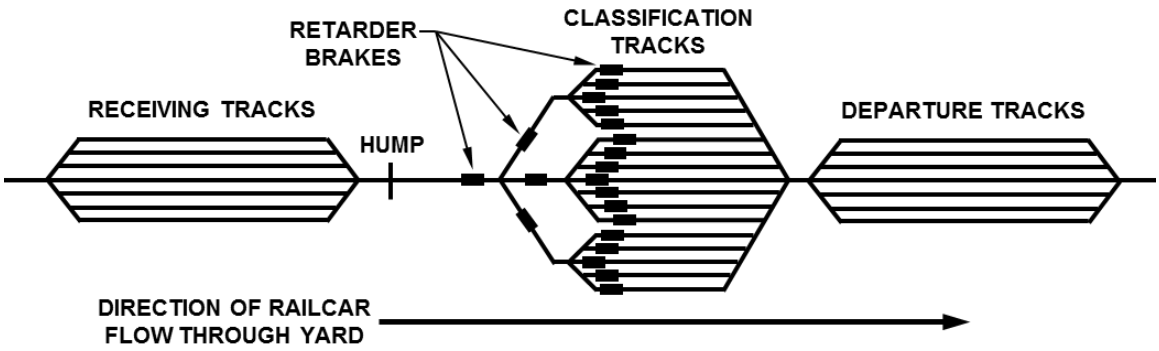

Figure 2. Schematic representation of hump classification yard for sorting railcars

Processing railcars through hump classification facilities requires considerable time. A railcar moving a single shipment in carload service spends, on average, 62 percent of its time in classification yards and only 14 percent of its time in actual line-haul mainline movement (Kumar, 2011). The remaining 24 percent of time is spent at the shipper origin and receiver destination spurs.

Despite the amount of time spent in classification yards, these facilities tend to be deemphasized in or excluded from railway hazmat transportation risk assessments (AICE, 1995). Of the three aspects of the rail transportation process (line-haul, intermediate yards, and loading/unloading), line-haul movement along mainline routes captures most of the attention when evaluating risk (Purdy et al., 1988). Glickman and Erkut (2007) argued that while the risk of movement through rail yards cannot be ignored, yard risk receives little attention due to the perception that it presents a minor risk compared to the mainline and a lack of data to support analysis.

Barkan et al. (2003) calculated railcar derailment rates for both mainlines and yards but concentrated on mainline accidents for subsequent research. Yard accidents were deemphasized since they occurred at low speeds and were less likely to lead to a hazmat release (Anderson & Barkan, 2005). Since the risk of railroad hazmat transport is the product of the likelihood of a release event and its consequence (Saat et al., 2014), Barkan et al. (2003) focused on mainline train accidents, only considering the likelihood half of the risk equation. They did not fully consider the consequence of population exposure, implicitly assuming that it is identical along mainline routes and surrounding yards and terminals. However, while many mainline route-miles are in remote, sparsely populated rural areas, most classification yards are located in urban areas that are moderately to densely populated, increasing human exposure to potential releases (Christou, 1999; DHS, 2004). FRA (2005) acknowledged the potential risk of yards by stating, "historically, some of the most catastrophic rail accidents involving hazardous materials have been in classification yards, with effects into the adjacent or nearby neighborhoods." For example, three recent yard incidents have resulted in long duration fires and evacuation of surrounding populations (Adams et al., 2011). In addition to impacting surrounding populations and the environment, yard incidents of this type pose a risk to the large numbers of other railcars concentrated in the yard, many carrying hazmat, and can cause severe rail network disruption until the facility is returned to service at full capacity (DHS, 2004).

With less focus on railroad yard accident risk, there has been a lack of research analyzing major accident causes leading to yard derailments or collisions. Qualitatively, the same track and mechanical-caused derailments that occur on the mainline can also occur in yards, albeit at low speeds. However, compared to mainline line-haul train operations, the practice of switching, sorting, and classifying hazmat railcars in yards requires additional handling processes that introduce the risk of overspeed coupling events, side-swipe collisions, and derailments due to improper use of switches. These events may arise from various human factor causes and/or failure of hump yard speed control systems, and may lead to derailed or damaged railcars and the possibility of a hazmat release.

Understanding risk in railway classification yards is also important for the analysis of strategies such as railcar placement and rerouting, which are intended to reduce the line-haul risk of railway hazmat transportation (Liu, Saat, & Barkan, 2013b). Railcar placement reduces risk by moving railcars carrying hazmat into the portion of the train with the lowest probability of release (FRA, 2005). Achieving optimal car placement for safety requires deviating from conventional operating practices in classification yards which minimize the amount of railcar handling, introducing the risk associated with additional car coupling events (Branscomb et al., 2010). Increased switching activity also increases risk of railway employee injury (An et al., 2007). Previous study of this approach has either ignored the risk in classification yards while focusing on the line-haul route risk or only acknowledged a potential increase in risk associated with the classification yard train assembly process in a cursory manner as a subject for future research (Bagheri et al., 2010, 2011, 2012; FRA, 2005).

Cozzani et al. (2007) developed a quantitative risk analysis methodology for hazardous material releases in railroad yards due to three types of accidents: derailments and collisions, switching movements, and non-accident releases (NAR). The authors derived the accident rate for all three types of accidents from specific rail yards in Italy. Using FRA REA data from 1992 to 2012, they found that the US logged a total of 7,524 incidents where at least one railcar derailed in hump classification yards (FRA, 2019). In these incidents, 24,047 railcars were derailed for an

average of 3.3 railcars derailed per incident. Based on the approximate annual number of railcars processed in hump yards during this period, the estimated US yard derailment rate was 4.3×10^{-5} railcars derailed per railcar processed. This calculated rate is very close to the rate of 4.7×10^{-5} railcars derailed per railcar processed found in the Cozzani et al. (2007) study. This derailment rate is also similar to previous estimates made using data from the late 1970s and early 1980s when there were more active hump yards processing more cars each year (Nayak et al., 1983; Raj, 1988).

Rerouting reduces mainline risk of release by shifting railcar hazmat shipments to routes with combinations of lower exposure and lower likelihood of an accident (Liu, Saat, & Barkan, 2013b). However, deviation from the most direct or lowest-cost route established by the railroad may also alter both the number and specific combination of classification yards involved in the movement, potentially introducing new risks from increased switching activity and different population exposures associated with each yard (Branscomb et al., 2010). Despite this sensitivity, several studies of the hazmat rail routing problem have ignored risk at classification yards (Azad et al., 2016; Fang et al., 2017; Glickman et al., 2007; Kawprasert & Barkan, 2008; Lai et al., 2011). Glickman and Erkut (2007) derived quantitative risk estimates of hazmat releases in specific railroad yards considering several major chemicals carried by tank cars. Verma (2009) acknowledged that, given the non-uniform population distribution around each mainline leg and classification yard, population exposure and consequence needed to be calculated for each link and node traversed by a railcar in the hazmat routing problem. Although Verma included yards in the rerouting analysis, a lack of data on yards required the assumption that the mainline derailment rate and conditional probabilities of hazmat railcar release also applied to movements within classifications yards. Verma (2011) developed a risk assessment methodology for rail hazmat transportation considering release risk in rail yards. The accident and release rates developed in this study were later used in the Value-at-risk (VAR) methodology to optimize the routing of hazmat transportation (Hosseini & Verma, 2017, 2018) and a risk assessment methodology to analyze the impact of train configuration on hazmat release risk (Cheng et al., 2017).

Kawprasert and Barkan (2010) developed a method for estimating the number of persons affected by a hazmat release based upon evacuation distances in the ERG and GIS data on railway location and population density. In this approach, the consequence is the minimum evacuation area for a given hazardous material multiplied by the population density of the affected area. Models were developed to analyze the risk of population exposure from toxic inhalation hazard (TIH) release (Thompson, 2015; Verma & Verter, 2007) and flammable liquids (Iranitalab et al., 2019; Serrano & Saat, 2014). The authors were not aware of research specifically addressing the consequence of hazmat releases in railroad yards.

The rapid increase in crude oil transportation by rail in North America in recent years has led to more hazmat being moved in dedicated unit trains of 80 to 100 railcars that transport a single commodity in a continuous movement from origin to destination (Dick & Brown, 2014). Moving large amounts of hazmat in a single unit train may increase the risk of multiple-car releases and the disproportionately large consequences of large-release events (Liu, 2017a; Liu et al., 2014b). However, these unit trains bypass intermediate classification yards and eliminate the risk associated with sorting railcars in these facilities. On the other hand, if rail cars are placed in the lowest-probability derailment positions, as suggested in previous research (Bagheri et al., 2010, 2011), distributing them to multiple mixed trains would result in a lower risk level (Liu, 2017a).

Fully quantifying this risk trade-off requires a better understanding of the risk of handling hazmat railcars in hump classification yards.

In summary, hazmat release risk in railroad yards should be considered in an integrated rail hazmat transportation risk assessment because classification yards play a pivotal role in handling hazmat cars in manifest trains, and the potential consequence of a hazmat release in a railroad yard is non-trivial. Research on railroad yard risk does not appear to be as abundant as research on the risk of mainline train accidents. Accident rate, release rate, and severity of hazmat releases in railroad yards were estimated at a preliminary level with low resolution. However, causal and other factors affecting the risk of hazmat releases in railroad yards have not been systematically analyzed. In the context of unit train and manifest train risk assessment, understanding the hazmat release risk in railroad classification yards allows for a more detailed and holistic comparison of risk. This is because by quantitatively addressing yard risk, one can evaluate the tradeoff between the two types of operation, due to their differences in the use and frequency of yard movements. Both mainline risk and yard risk can now be considered in the integrated route risk assessment for both types of trains. Developing a more detailed and sophisticated yard hazmat risk estimation will also enhance rail hazmat transportation routing optimization by providing a more accurate risk estimation for hazmat shipments routed through different yards in a railroad network, leading to better cost-benefit analysis and transportation planning. Therefore, to analyze the overall risk of hazmat transportation by rail more completely, there is a need for a more thorough investigation of the causes, likelihoods, and consequences of railroad yard accidents involving hazardous materials.

2.4 Physics-Based Modeling

A wide variety of potential modeling methodologies apply to the derailment risk and hazard consequence studied in this research. The team proposed using physics-based modeling designed to address the specific factors identified as potential causes for the differences in the train derailment rates between unit and revenue trains. For example, train-dynamics models can simulate all traction and braking behaviors to effectively determine the in-train longitudinal loads and examine differences in various train makeups (e.g., unit trains with all cars fully loaded or all empty revenue cars). Since the modeling methodologies that may be required were not known until the risk data was fully developed and analyzed, only a brief review of models is provided in this section.

2.4.1 Train Dynamics Modeling

There are two types of train dynamics models for railway applications: 1) models for simulation of the longitudinal train dynamics, including traction, braking, and longitudinal forces of the coupled cars in the train; and 2) three-dimensional (3D) models of the individual vehicle dynamics, including additional mechanics such as the wheel-rail interaction forces, suspension dynamics, etc.

The Train Operations and Energy Simulator (TOES™) model developed for and licensed to AAR-member railroads (Andersen et al., 1991, 1992) is a longitudinal train dynamics simulator used in North America. TOES has been in use for nearly 30 years, has been validated many times over, and is considered an industry standard for longitudinal train dynamics modeling.

The Train Energy and Dynamics Simulator (TEDS) model (Andersen et al., 2012; Sharma & Associates, Inc., 2015) is a similar one-dimensional longitudinal dynamics model. TEDS is a

more recently developed tool that calculates the in-line train forces and motions under specified track, traction, and braking conditions. Additional studies that have developed similar longitudinal dynamics models include Mokkapati et al. (2011) and Wu et al. (2014).

3D vehicle dynamics models are required for more complex vehicle motions. These models, also known as multi-body simulation (MBS) models, can simulate rail and vehicle characteristics and predict the lateral and vertical forces in the vehicle, including wheel-rail forces, that can be used to detect the conditions for the initiation of a derailment. There are a wide range of these MBS models for rail vehicle simulation, including NUCARS™ developed by AAR/TTCI; ADAMS Rail, built on the MSC Software Corporation Automatic Dynamic Analysis of Mechanical Systems (ADAMS) MBS platform; and a series of similar codes developed internationally, such as GENSYS in Sweden or VAMPIRE by British Rail. A summary of the applications of these MBS models is beyond the scope of the current literature review. However, this type of model would be appropriate for investigating potential effects such as harmonic sloshing in a train, e.g., Vera et al. (2005); Hazrati et al. (2015).

2.4.2 Derailment Modeling

The dynamics of a train after the initiation of a derailment are complex and difficult to simulate accurately with analytical models. As a result, more recent derailment models have relied on computational solvers to simulate the response. Below are examples of modeling methodologies that have been applied to freight train derailments.

Toma (1998) developed a detailed two-dimensional (2D) MBS train derailment model for his Ph.D. thesis project. He includes a good description of the previous analytical models for derailments but ultimately develops a model with significant improvements that reduces the relevance of those earlier efforts. Toma's model includes significant features from a longitudinal model such as the traction, braking, and coupler forces for the cars on the track. Once derailed, the cars are subject to 2D motions with a velocity-dependent ground friction model, impact forces, and uncoupling of cars based on strength and displacement limits. The primary limitations of Toma's model are the simplifications necessary in an MBS model for calculating impact behaviors and the constraint that the model is only 2D.

Paetsch et al. (2006) developed a 2D rigid-body model to examine the gross motions of rail cars in derailments using ADAMS. The results of the ADAMS model were used to investigate various modes of motion of the derailed cars and to conduct sensitivity studies. The model correlated well to a similar purpose-built model based on the railcar 2D equations of motion (Jeong et al., 2007).

Kirkpatrick et al. (2006) developed a 3D model for simulating train derailments using the LS-DYNA finite element solver. The fully 3D finite element model allows for the addition of many complex derailment mechanics, such as tanks rolling over or lifting over other tanks, deformation and failure of components and connections (e.g., truck separations and breakup, coupler failures), realistic impact scenarios between derailed cars, and derailment conditions on slopes, elevated rail berms, etc. However, the model used more simplified analyses of the longitudinal train forces for cars on the rail (i.e., constant braking friction).

Sharma & Associates (2015) similarly used the LS-DYNA solver to simulate train derailments as part of an analytical methodology to assess the effectiveness of tank design modifications, train speed operational restrictions, and various train braking systems. Sharma's study constrained the

motions of the derailed cars to 2D motions. The study claimed to include the appropriate braking forces in the cars that did not derail, but the methodology is not described in the report.

2.4.3 Hazmat Release Consequence Modeling

A wide variety of physical mechanisms are involved in hazmat consequence analyses. These include thermal effects of fires, blast effects from rapid gas deflagrations or explosions, rapid venting or other release mechanisms from punctures in pressurized tanks, and gas cloud dispersion for various toxic commodities under different atmospheric conditions. Advanced simulation methodologies can be applied to all these mechanisms. However, detailed simulation of these consequence mechanisms is beyond the scope of this effort and only simplified consequence models or algorithms were applied.

The current methodology for analyzing the effects of fire on rail tank cars and BLEVE uses the Analysis of Fire Effects on Tank Cars (AFFTAC) computer model (Birk, 2000; Runnels, 2016). AFFTAC is used by Transport Canada, U.S. DOT, and tank car manufacturers for evaluating and qualifying thermal protection systems for rail tank cars subjected to pool fire exposures.

Additional information on the effects of railroad tank cars exposed to fire can be found in a separate literature search published by Lam et al. (2015). The literature search was performed for the National Research Council Canada and focuses on crude oil, condensate, and ethanol behavior.

Raj and Turner (1993) described models to assess the consequences of chemical hazard for: 1) vapor inhalation toxicity; 2) pool fire burning (i.e., injury due to thermal radiation); 3) vapor cloud explosion (i.e., blast effects and injury); 4) vapor cloud burning (i.e., burn injury due to fire engulfment); and 5) corrosivity (i.e., skin burn injury due to physical contact). They developed a risk model considering the characteristics of tank cars, the puncture probability, properties of the hazmat released and its behavior in the environment, the occurrence of the accident in different population density areas under different types of weather conditions at the time of the accident, and other scenarios. Toxicity, fire, and explosion behavior of the chemicals were considered. The model's applications focused on the transportation of poison-by-inhalation (PIH) and flammable materials.

Raj (1995) provided a good summary of potential consequence models that can be applied to the dispersion of toxic vapors generated from: 1) a pool of low vapor pressure liquid; 2) the polymerization or self-reaction of chemicals; and 3) the consequences of a thermal explosion in a tank car. He evaluated the overall risks to the population from the rail transport of certain chemicals. Most of the studied chemicals have hazards, such as inhalation toxicity (i.e., vapors), flammability (i.e., fire thermal radiation hazards), and explosivity (i.e., blast wave damage hazards). A few of the chemicals pose potential hazards from the tendency to self-heat due to the initiation of a polymerization reaction caused by loss of inhibitor or exposure to an external fire. The author modeled various hazardous behaviors and evaluated the risks in terms of probabilities of hazardous event occurrence and the public's exposure to hazards. He concluded that the overall probability of occurrence of a self-heating induced thermal explosion type accident is rare ($l0^{-6}$ per year). The hazardous effects of an explosion of this type have limited range (< 200 m) and consequently the public exposure values are relatively small (1 to 50).

2.5 Knowledge Gaps

Although the rail transport of hazmat release risk has been studied extensively, little previous work has compared the risks pertaining to the use of different types of trains, particularly unit trains versus other types of trains for the same traffic demand. Most importantly, very limited research has specifically studied the hazmat release risk for unit trains in which all cars carry the same commodity and are shipped from the same origin to the same destination. A unit train transporting hazmat might have more severe consequences in a derailment accident once the hazmat releases. Future work can narrow the knowledge gap by developing integrated, generalized risk analysis methodologies, accompanied by a decision support tool, to estimate hazmat transportation risk for unit trains.

Most of the reviewed references focus on hazmat release risk on railroad mainlines. Only a few studies have considered the risk of switching hazmat railcars in classification yards (Glickman & Erkut, 2007), which could lead to hazmat release. The difference between hazmat release risk on a mainline vs. in a yard has not yet been studied. For example, to achieve optimal car placement or train rerouting for safety on mainline trains, classification yards deviate from conventional operating practices that minimize the amount of railcar handling, introducing the risk associated with additional car coupling events. Increased switching activity also increases the risk of railway employee injury. However, previous study of this approach has either ignored the risk in classification yards while focusing on the line-haul route risk or only acknowledged a potential increase in risk associated with the classification yard train assembly process in a cursory manner as a subject for future research.

2.6 Conclusions

This chapter has reviewed the literature on rail transport of hazmat release risk analysis. The team reviewed the related references in three parts, including mainline hazmat release risk analysis, yard hazmat release risk analysis, and physics-based modeling. Factors that contribute to or influence risk include infrastructure condition, equipment condition, human factors, traffic exposure, speed, accident cause, point of derailment, train length, number of hazmat cars in the train, placement of hazmat cars in the train, hazmat car safety design, chemical properties, population density, spill size, environment, etc. The literature was reviewed in terms of train types (i.e., unit train versus manifest trains), risk analysis methods (i.e., physical models & simulation versus statistical & probabilistic models), accident occurrence railroad location (i.e., mainline versus yards), and release consequences and contributing factors (i.e., other consequences and contributing factors versus population density and exposure). Knowledge gaps were identified, and future work may be planned accordingly.

3. Railroad Hazmat Transportation Risk Analysis Methodology

3.1 Mainline Risk Analysis Methodology

3.1.1 Introduction

This chapter proposes a methodology to quantify the risk of railroad hazmat transportation. This methodology is based on a chain of events: 1) the train is involved in an accident; 2) at least one rail vehicle (a locomotive or a railcar) is derailed; 3) at least one rail vehicle transporting hazmat is derailed; 4) at least one derailed hazmat car releases contents; 5) the quantity of hazmat released is based on the number of tank cars releasing; and 6) the consequences of hazmat release are determined given a releasing quantity.

Figure 3 shows the chain of events used for risk analysis of a hazmat tank car release. The key elements involved in each event in the chain are described in detail. Using train-related and track-related information (e.g., segment length, train length, number of tank cars, and speed), the risk analysis methodology can be used to quantify the probability of train derailment, the number of cars derailed, the number of hazmat cars derailed, the number of hazmat cars releasing, the amount of hazmat release, and the consequences. The following subsections includes sequential discussion of these events and their probabilities.

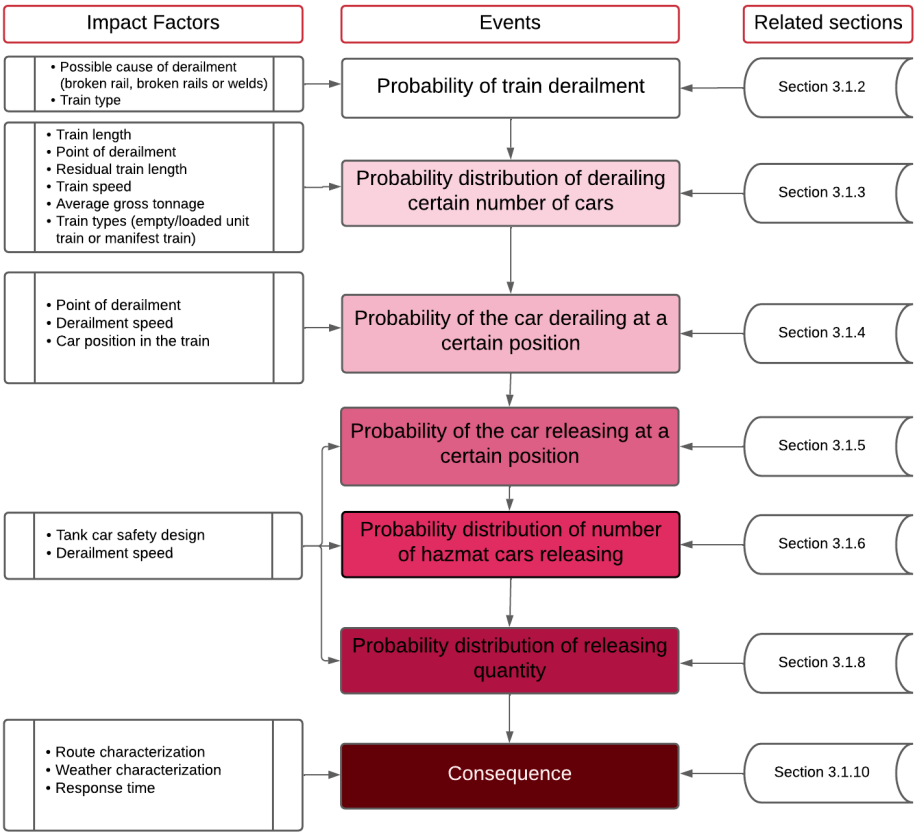

Figure 3. Train type-based tank car releasing risk analysis based on the event chain

3.1.2 Train Derailment Probability

According to Liu (2015), when traffic exposure is large and the derailment rate is relatively low, the probability of train derailment can be numerically approximated by multiplying the derailment rate by the mileage of the train shipment. Thus, the probability of train derailment can be estimated based on the train derailment rate (i.e., the number of derailments normalized by the corresponding traffic volume) using historical train derailment data and traffic data. FRA has categorized more than 300 accident causes into 5 groups based on the circumstances and conditions of each accident (FRA, 2012). The hierarchically organized cause groups are track, equipment, human factors, signal, and miscellaneous, with each cause being assigned a unique cause code. A study by Arthur D. Little, Inc (1996) grouped similar FRA accident causes together based on experts' opinions, producing a variation on the FRA subgroups. Previous studies (Liu, 2015; Liu et al., 2012; Schafer & Barkan, 2008) found that the ADL cause groups could be more fine-grained, allowing for greater resolution for certain causes. For example, FRA combines broken rails, joint bars, and rail anchors into the same subgroup, whereas the ADL grouping distinguishes between broken rail and joint bar defects. For this reason, the research team used ADL cause groups to conduct its cause-specific railroad derailment analysis.

Because the traffic volume data obtained from financial data from Class I railroad annual reports and Surface Transportation Board waybill sample data was available for the years between 1996 and 2018 at the time of this analysis, the team used the number of accidents that occurred by their cause category during the same period. In total, there were 2,462 unit train derailments and 5,514 manifest train derailments during these years, which are classified into 46 cause groups. Table 1 shows train derailment data from 1996 to 2018 by cause group and train type on Class I mainlines.

Table 1. FRA-reportable Class I mainline train derailment data, 1996-2018

(a) Unit train derailments

Cause group	Number of derailments During the period	Percent of total
Broken Rails or Welds	440	17.87
Broken Wheels (Car)	230	9.34
Bearing Failure (Car)	182	7.39
Buckled Track	152	6.17
Other Axle/Journal Defects (Car)	152	6.17
Track Geometry (excl. Wide Gauge)	141	5.73
Obstructions	98	3.98
Wide Gauge	87	3.53
Roadbed Defects	71	2.88
Other Wheel Defects (Car)	70	2.84
Turnout Defects – Switches	65	2.64
Track-Train Interaction	58	2.36
Other Miscellaneous	56	2.27
Misc. Track and Structure Defects	50	2.03
Lading Problems	46	1.87
Joint Bar Defects	46	1.87
Coupler Defects (Car)	41	1.67

Cause group	Number of derailments During the period	Percent of total
Other Rail and Joint Defects	40	1.62
Use of Switches	38	1.54
Sidebearing, Suspension Defects (Car)	36	1.46
Train Handling (excl. Brakes)	32	1.30
Non-Traffic, Weather Causes	31	1.26
Rail Defects at Bolted Joint	30	1.22
Train Speed	28	1.14
Truck Structure Defects (Car)	27	1.10
Centerplate/Carbody Defects (Car)	22	0.89
All Other Car Defects	22	0.89
Misc. Human Factors	21	0.85
Stiff Truck (Car)	15	0.61
Switching Rules	15	0.61
Failure to Obey/Display Signals	14	0.57
Other Brake Defect (Car)	14	0.57
Handbrake Operations	12	0.49
Brake Rigging Defect (Car)	12	0.49
Loco Electrical and Fires	11	0.45
Track/Train Interaction (Hunting) (Car)	10	0.41
Brake Operation (Main Line)	9	0.37
Mainline Rules	9	0.37
Signal Failures	8	0.32
Loco Trucks/Bearings/Wheels	8	0.32
Turnout Defects – Frogs	5	0.20
All Other Locomotive Defects	3	0.12
Brake Operations (Other)	2	0.08
UDE (Car or Loco)	1	0.04
Employee Physical Condition	1	0.04
Air Hose Defect (Car)	1	0.04
Total	**2,462**	**100**

(b) Manifest train derailments

Cause group	Number of derailments During the period	Percent of total
Broken Rails or Welds	639	11.59
Track Geometry (excl. Wide Gauge)	391	7.09
Bearing Failure (Car)	343	6.22
Train Handling (excl. Brakes)	324	5.88
Obstructions	243	4.41
Track-Train Interaction	212	3.84
Lading Problems	211	3.83
Wide Gauge	186	3.37
Coupler Defects (Car)	184	3.34

Cause group	Number of derailments During the period	Percent of total
Use of Switches	182	3.30
Broken Wheels (Car)	173	3.14
Sidebearing, Suspension Defects (Car)	164	2.97
Other Wheel Defects (Car)	164	2.97
Brake Operation (Main Line)	163	2.96
Centerplate/Carbody Defects (Car)	148	2.68
Buckled Track	147	2.67
Other Miscellaneous	145	2.63
Turnout Defects – Switches	142	2.58
Misc. Track and Structure Defects	98	1.78
Train Speed	94	1.70
Stiff Truck (Car)	85	1.54
Roadbed Defects	82	1.49
Joint Bar Defects	70	1.27
Other Axle/Journal Defects (Car)	64	1.16
Other Brake Defect (Car)	64	1.16
Loco Trucks/Bearings/Wheels	63	1.14
All Other Car Defects	62	1.12
Track/Train Interaction (Hunting) (Car)	58	1.05
Misc. Human Factors	58	1.05
Switching Rules	55	1.00
Other Rail and Joint Defects	51	0.92
Rail Defects at Bolted Joint	51	0.92
Handbrake Operations	49	0.89
Non-Traffic, Weather Causes	44	0.80
Failure to Obey/Display Signals	39	0.71
Brake Rigging Defect (Car)	35	0.63
All Other Locomotive Defects	35	0.63
Signal Failures	35	0.63
Air Hose Defect (Car)	33	0.60
Truck Structure Defects (Car)	25	0.45
Loco Electrical and Fires	23	0.42
Mainline Rules	23	0.42
Turnout Defects – Frogs	20	0.36
Radio Communications Error	12	0.22
UDE (Car or Loco)	10	0.18
Brake Operations (Other)	6	0.11
TOFC/COFC Defects	5	0.09
Employee Physical Condition	2	0.04
Handbrake Defects (Car)	2	0.04
Total	**5,514**	**100**

In this study, the team developed a cause-based train derailment probability model. First, train derailment causes were classified into three categories based on the most suitable traffic exposure data for derailment rate calculation: train miles, ton miles, and car miles (including locomotives and railcars), respectively. For example, "broken wheels" could be associated with car miles traveled, and thus the probability of derailment caused by "broken wheels" should be calculated based on the traffic metric "car miles." In contrast, obstruction-caused accidents may be associated more with the number of trains regardless of number of rail vehicles, and thus the probability of derailment caused by "obstruction" could be calculated based on the traffic metric "train miles."

Let TRM denote the set of train-mile-based derailment causes, TOM be the set of ton-mile-based derailment causes, and CM be the set of car-mile-based derailment causes. If a train has L cars (including locomotives and railcars), its gross tonnage is denoted as GW, and it travels on a track with the length of L_t (in miles). The probability of train derailment due to the cth cause can be calculated by:

$$P_{c|c\in TRM} \approx d_{TRM}/1{,}000{,}000 \times L_t \times p_c \quad (3\text{-}1)$$

$$P_{c|c\in TOM} \approx d_{TOM}\ /1{,}000{,}000{,}000 \times GW \times L_t \times p_c \quad (3\text{-}2)$$

$$P_{c|c\in CM} \approx d_{CM}/1{,}000{,}000{,}000 \times L \times L_t \times p_c \quad (3\text{-}3)$$

where:

$P_{c|c\in TRM}$ = the probability that this train derails and the derailment is caused by a train-mile-based cause

$P_{c|c\in TOM}$ = the probability that this train derails and the derailment is caused by a ton-mile-based cause

$P_{c|c\in CM}$ = the probability that this train derails and the derailment is caused by a car-mile-based cause

d_{TRM} = number of train derailments per million train-miles (see Table 2)

d_{TOM} = number of train derailments per billion gross ton-miles (see Table 2)

d_{CM} = number of train derailments per billion car-miles (see Table 2)

p_c = fraction of train derailments due to cth cause in the total number of derailments (see Table 1)

L = train length, i.e., number of cars (including locomotives and railcars) in the train

L_t = the length (in miles) of the track segment where the train will travel from origin to destination

GW = gross tonnage (in tons) of the train (including lightweight and lading, as well as locomotive tonnages)

Table 2. Derailment rate by traffic metric (see Section 4)

(a) Unit train

Metric	Derailment Rate
Derailments per million train-miles	0.85
Derailments per billion gross ton-miles	0.10
Derailments per billion car-miles	8.14

(b) Manifest train

Metric	Derailment Rate
Derailments per million train-miles	0.67
Derailments per billion gross ton-miles	0.14
Derailments per billion car-miles	11.39

The derailment rate by traffic metric data shown in Table 2 is calculated in Section 4 using FRA-reportable Class I mainline train derailment data for the years 1996-2018. The derailments per billion car miles metric only considers railcars. Since derailment can happen on locomotives or railcars, the team approximated the car miles that include both locomotives and railcars due to data limitations. Since the train derailment probability per train shipment is very minimal, the probability of a train derailment on segment i (PTD_i) can be estimated by Equation (3-4) by setting the track length L_t in Equations (3-1) to (3-3) to the track length of segment i.

$$PTD_i \approx \sum_{c \in TRM} P_{c|c \in TRM} + \sum_{c \in TOM} P_{c|c \in TOM} + \sum_{c \in CM} P_{c|c \in CM} \tag{3-4}$$

with the constraint $1 = \sum_c p_c$.

Consider a train with five locomotives (assuming each has a weight of 212.5 tons) and 115 loaded cars (assuming each has a weight of 143 tons) running on a 1-mile rail segment. The probability of a derailment incident on this 1-mile rail segment for a single train is calculated and shown in Table 3. As an example, the derailment probability for a manifest train due to broken rails or welds is calculated below. This cause group is based on car-miles (railcars only), which has derailments d_{CM} of 11.39 per billion car-miles, according to Table 2b. From Table 1b, the percentage of derailments due to broken rails or welds within all causes is around 11.59 percent. Using Equation (3-3), the probability that this manifest train would be derailed due to broken rails or welds can be calculated as follows:

$$\begin{aligned} P_{broken\ rails\ or\ welds} &= \frac{d_{CM}}{1{,}000{,}000{,}000} \times L \times L_t \times p_i \\ &= \frac{11.39}{1{,}000{,}000{,}000} \times 120 \times 1 \times 11.59\% = 1.58E-07 \end{aligned} \tag{3-5}$$

This result is the same as the number in Table 3b. Note that the probability calculation results in Table 3 are specific to a given train configuration.

Table 3. Train derailment probability by cause and train type

(a) Unit train

Derailment cause	Traffic metric used	Derailment probability (one train shipment on a 1-mile segment)
Broken Rails or Welds	Car mile	1.75E-07
Broken Wheels (Car)	Car mile	9.13E-08
Bearing Failure (Car)	Car mile	7.22E-08
Buckled Track	Train mile	5.25E-08
Other Axle/Journal Defects (Car)	Car mile	6.03E-08
Track Geometry (excl. Wide Gauge)	Train mile	4.87E-08
Obstructions	Train mile	3.38E-08
Wide Gauge	Train mile	3.00E-08
Roadbed Defects	Train mile	2.45E-08
Other Wheel Defects (Car)	Car mile	2.78E-08
Turnout Defects – Switches	Car mile	2.58E-08
Track-Train Interaction	Car mile	2.30E-08
Other Miscellaneous	Train mile	1.93E-08
Misc. Track and Structure Defects	Train mile	1.73E-08
Lading Problems	Car mile	1.83E-08
Joint Bar Defects	Car mile	1.83E-08
Coupler Defects (Car)	Car mile	1.63E-08
Other Rail and Joint Defects	Car mile	1.59E-08
Use of Switches	Train mile	1.31E-08
Sidebearing, Suspension Defects (Car)	Car mile	1.43E-08
Train Handling (excl. Brakes)	Train mile	1.10E-08
Non-Traffic, Weather Causes	Train mile	1.07E-08
Rail Defects at Bolted Joint	Car mile	1.19E-08
Train Speed	Train mile	9.67E-09
Truck Structure Defects (Car)	Car mile	1.07E-08
Centerplate/Carbody Defects (Car)	Car mile	8.73E-09
All Other Car Defects	Train mile	7.60E-09
Misc. Human Factors	Train mile	7.25E-09
Stiff Truck (Car)	Train mile	5.18E-09
Switching Rules	Train mile	5.18E-09
Failure to Obey/Display Signals	Train mile	4.83E-09
Other Brake Defect (Car)	Car mile	5.55E-09
Handbrake Operations	Train mile	4.14E-09
Brake Rigging Defect (Car)	Car mile	4.76E-09
Loco Electrical and Fires	Train mile	3.80E-09
Track/Train Interaction (Hunting) (Car)	Car mile	3.97E-09
Brake Operation (Main Line)	Car mile	3.57E-09
Mainline Rules	Train mile	3.11E-09
Signal Failures	Car mile	3.17E-09
Loco Trucks/Bearings/Wheels	Car mile	3.17E-09
Turnout Defects - Frogs	Car mile	1.98E-09
All Other Locomotive Defects	Train mile	1.04E-09
Brake Operations (Other)	Train mile	6.90E-10
UDE (Car or Loco)	Car mile	3.97E-10
Employee Physical Condition	Train mile	3.45E-10
Air Hose Defect (Car)	Car mile	3.97E-10
Total derailment probability		9.30E-07

(b) Manifest train

Derailment cause	Traffic metric used	Derailment probability (one train shipment on a 1-mile segment)
Broken Rails or Welds	Car mile	1.58E-07
Track Geometry (excl. Wide Gauge)	Train mile	4.75E-08
Bearing Failure (Car)	Car mile	8.50E-08
Train Handling (excl. Brakes)	Train mile	3.94E-08
Obstructions	Train mile	2.95E-08
Track-Train Interaction	Car mile	5.26E-08
Lading Problems	Car mile	5.23E-08
Wide Gauge	Train mile	2.26E-08
Coupler Defects (Car)	Car mile	4.56E-08
Use of Switches	Train mile	2.21E-08
Broken Wheels (Car)	Car mile	4.29E-08
Sidebearing, Suspension Defects (Car)	Car mile	4.07E-08
Other Wheel Defects (Car)	Car mile	4.07E-08
Brake Operation (Main Line)	Car mile	4.04E-08
Centerplate/Carbody Defects (Car)	Car mile	3.67E-08
Buckled Track	Train mile	1.79E-08
Other Miscellaneous	Train mile	1.76E-08
Turnout Defects - Switches	Train mile	1.73E-08
Misc. Track and Structure Defects	Train mile	1.19E-08
Train Speed	Train mile	1.14E-08
Stiff Truck (Car)	Train mile	1.03E-08
Roadbed Defects	Train mile	9.96E-09
Joint Bar Defects	Car mile	1.74E-08
Other Axle/Journal Defects (Car)	Car mile	1.59E-08
Other Brake Defect (Car)	Car mile	1.59E-08
Loco Trucks/Bearings/Wheels	Car mile	1.56E-08
All Other Car Defects	Train mile	7.53E-09
Track/Train Interaction (Hunting) (Car)	Car mile	1.44E-08
Misc. Human Factors	Train mile	7.05E-09
Switching Rules	Train mile	6.68E-09
Other Rail and Joint Defects	Car mile	1.26E-08
Rail Defects at Bolted Joint	Car mile	1.26E-08
Handbrake Operations	Train mile	5.95E-09
Non-Traffic, Weather Causes	Train mile	5.35E-09
Failure to Obey/Display Signals	Train mile	4.74E-09
Brake Rigging Defect (Car)	Car mile	8.68E-09
All Other Locomotive Defects	Train mile	4.25E-09
Signal Failures	Car mile	8.68E-09
Air Hose Defect (Car)	Car mile	8.18E-09
Truck Structure Defects (Car)	Car mile	6.20E-09
Loco Electrical and Fires	Train mile	2.79E-09
Mainline Rules	Train mile	2.79E-09
Turnout Defects – Frogs	Car mile	4.96E-09
Radio Communications Error	Train mile	1.46E-09
UDE (Car or Loco)	Car mile	2.48E-09
Brake Operations (Other)	Train mile	7.29E-10
TOFC/COFC Defects	Train mile	6.08E-10
Employee Physical Condition	Train mile	2.43E-10
Handbrake Defects (Car)	Train mile	2.43E-10
Total derailment probability		1.05E-06

3.1.3 Probability of the Total Number of Cars Derailed

Section 5 will detail the methodology used to estimate derailment severity, which is defined as the total number of cars (i.e., locomotives and railcars) derailed per train derailment. Derailment severity is related to derailment speed, gross tonnage per car, and residual train length, defined as the number of locomotives and railcars behind the point of derailment (POD), or the position of the first car derailed in a train. The normalized POD (NPOD) is calculated by dividing the POD by the train length.

Using FRA-reportable train derailment data from 1996 to 2018, the "best fits" for the NPOD distributions (i.e., all accident causes combined) for both manifest and unit trains are Beta distributions based on the maximum likelihood estimation method using a statistical tool called R. The Beta distribution fits are consistent with findings from prior research using older datasets (Saccomanno & El-Hage, 1989, Saccomanno & El-Hage, 1991, and Liu et al., 2014). Figure 4 shows comparisons between the fitted NPOD distributions for unit trains and manifest trains for all causes combined. The normalized position of derailment on mainlines might be affected by train type, operation speed, and train length (i.e., the number of locomotives and railcars). Section 3.3 includes the comparison of the Beta distribution fits for all data combined, data that has derailment speed above or below the average speed, and data that has train length above or below the average train length for unit trains and manifest trains using FRA-reportable train derailment data from 1996 to 2018. Although derailment speed and train length slightly affect the Beta distribution fits of NPOD, the differences are not significant.

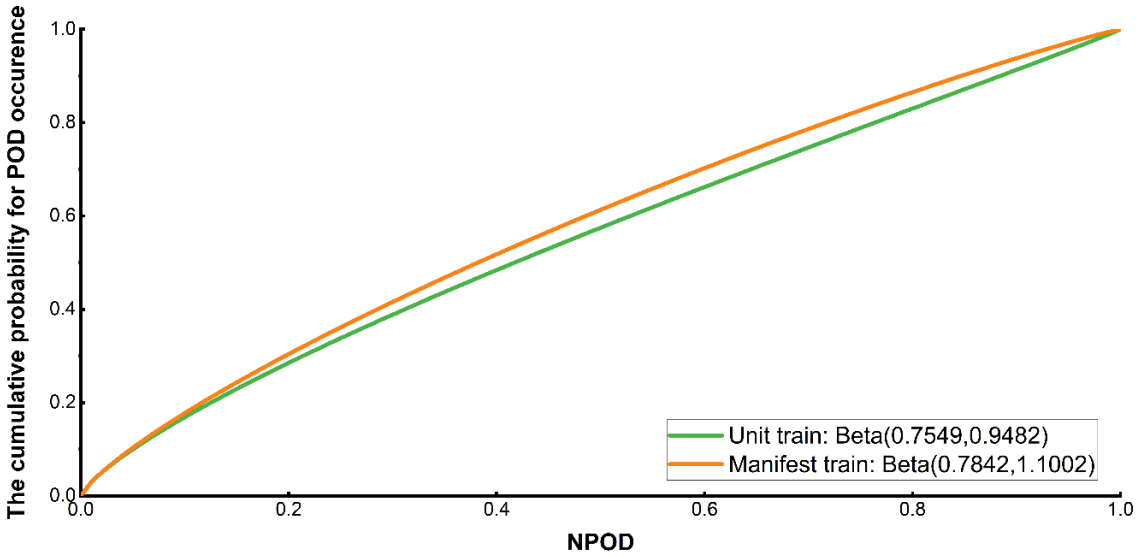

Figure 4. Comparison of fitted NPOD distributions for unit train and manifest train for all causes combined

The probability that the POD is at the k^{th} position is defined in the equation (Liu et al., 2014b):

$$Pod(k) = F\left(\frac{k}{L}\right) - F\left(\frac{k-1}{L}\right) \quad (3\text{-}6)$$

where:

$Pod(k)$ = the probability that POD is at the k^{th} position of a train

$F(x)$ = cumulative density distribution of the fitted NPOD distribution (i.e., Beta distributions shown in Figure 4)

$L =$ train length, i.e., number of cars (including locomotives and railcars) in the train

Define $P_i(x|k)$ as the conditional probability of x vehicles derailing given that the POD is at k^{th} position on segment i and given that a derailment has occurred. The statistical model (i.e., the TG model) for estimating train derailment severity can be found in prior research (Anderson, 2005; Bagheri et al., 2011; Saccomanno & El-Hage, 1989b, 1991b). For a train derailment incident, the number of cars derailed is greater than or equal to one, and less than or equal to the residual train length (defined as $L_r = L - POD + 1$, including locomotives and railcars). The TG model can shorten the number of derailed cars beyond the range $[1, L_r]$. Bagheri (2010) has used this model to estimate the number of cars derailed per train derailment. Given train length L and the POD, the probability of x cars derailing can be estimated as follows, using the TG model:

$$P_i(x|k) = \frac{\frac{\exp(z)}{1+\exp(z)}\left[\frac{1}{[1+\exp(z)]^{x-1}}\right]}{1-\left[\frac{1}{1+\exp(z)}\right]^{L_r}} \tag{3-7}$$

where z is a function given by,

$$z = -0.952 - 0.0306 \times DS - 0.0018 \times L_r - 0.00239 \times GT + 0.119 \times EUT - 0.339 \times LUT \tag{3-8}$$

$$L_r = L - POD + 1 \tag{3-9}$$

where:

$P_i(x|k)$ = the conditional probability of x vehicles derailing given that the POD is at k^{th} position on segment i and given that a derailment has occurred

DS = train derailment speed (miles per hour)

k = the position (in car number) at which the derailment is initiated

L_r = number of residual cars (including locomotives and railcars) after POD

L = train length, i.e., number of cars (including locomotives and railcars) in the train

GT = average gross tonnage per car

EUT = if the train is an empty unit train, EUT = 1, otherwise EUT = 0

LUT = if the train is a loaded unit train, LUT = 1, otherwise LUT = 0

$Pod(k)$ = the probability that POD is at the k^{th} position of a train

x = the number of cars that derail behind the point of derailment

The parameters used in Equation (3-8) will be explained in detail in Section 5. When building this model, a manifest train is used as a reference. Thus, for manifest trains, variables EUT and LUT in Equation (3-8) are set to 0.

3.1.4 Position-based Car Derailment Probability

It is assumed that if a train derailment occurs, cars will derail sequentially after the POD. For example, if there are three vehicles derailed, they are POD, POD+1, and POD+2. Using the model introduced in Section 3.1.3, the probability distribution of the total number of cars derailed can be calculated. According to previous work by Liu et al. (2018), the probability that the car at j^{th}position of the train derails on segment i, given a train derailment, can be calculated as:

$$PD_i(j) = \sum_{k=1}^{j} \left[Pod_i(k) \times \sum_{x=j-k+1}^{L_r} P_i(x|k) \right] \tag{3-10}$$

$\sum_{x=j-k+1}^{L_r} P_i(x|k)$ is the sum of the probability that a locomotive or railcar at the j^{th} position is derailed, given that the POD is at k^{th} position.

3.1.5 Position-based Tank Car Releasing Probability

In the next step, the position-dependent derailment probability is extended to the position-dependent tank car releasing probability given a train derailment. Let $I_t(j)$ be the 0-1 indicator, which equals 1 if the car at j^{th}position of a train is a t^{th} type tank car of certain designs, and 0 otherwise. Assume that there are m types of tank cars on a train. Assume that the conditional probability of releasing (CPR) a derailed tank car is the same given the same design and accident speed. In other words, for a t^{th}design type tank car at a given speed, regardless of where it is located on a train, its CPR is assumed to be the same (denoted as r_t). This assumption is made due to limited information regarding the relationship between the release probability of a derailed tank car and its position in a train.

For a car at j^{th}position of a train, the position-based tank car releasing probability on segment i given a train derailment, which is denoted as $R_i(j)$, can be calculated as:

$$R_i(j) = PD_i(j) \times \sum_{t=1}^{m} [I_t(j) \times r_t] \tag{3-11}$$

where:

$I_t(j)$ = the 0-1 indicator, which equals 1 if the car at j^{th} position of a train is a t^{th} type designed tank car, and 0 otherwise

m = number of tank car types on a train

$R_i(j)$ = the position-based tank car releasing probability of j^{th} position in a train at segment i given a train derailment

r_t = the CPR of a derailed tank car of type t

$PD_i(j)$ = the probability of derailment at j^{th} position of a train on segment i

3.1.6 Probability Distribution of the Number of Tank Cars Releasing

Based on the position-based tank car releasing probability given a train derailment, the probability distribution of the number of tank cars releasing contents can be calculated. Let y_j represent whether the tank car at j^{th} position releases content, which is a 0-1 variable. For each car in a train, whether a tank car at j^{th} position would release is a Bernoulli variable with releasing probability of $R_i(j)$, and the probability of releasing could vary by position in a train (due to the position-dependent car derailment probability):

$$y_j \sim Bernoulli\big(R_i(j)\big) \tag{3-12}$$

For the entire train, the total number of tank cars releasing contents follows a Poisson Binomial distribution, which is the sum of independent Bernoulli random variables that are not necessarily identically distributed (Chen & Liu, 1997).

The Poisson Binomial distribution is used to estimate the probability associated with a certain number of releasing tank cars in a group of derailed tank cars. Let x_R be the total number of tank cars releasing contents and L be the train length expressed as number of cars in the consist. For each tank car, whether it will release is a binary event (release or no release) with release probability $R_i(j)$, $\forall j$: $y_j = 1$. x_R can be mathematically expressed as Equation (3-13). It follows the Poisson Binomial distribution with the mean of $\sum_{j=1}^{L} R_i(j)$ and the variance of $\sum_{j=1}^{L} R_i(j) \times \big(1 - R_i(j)\big)$.

$$x_R = \sum_{j=1}^{L} y_j \sim Possion\ Binomial\ Distribution \tag{3-13}$$

A hypothetical example with seven cars, as shown in Figure 5, is used to explain the process of calculating the total number of tank cars derailed. The train in this example has two locomotives ($L1^{st}$ and $L2^{nd}$), three non-tank cars (the, 3^{rd}, 5^{th}, and 7^{th} vehicles), and two tank cars (the 4^{th} and 6^{th} vehicles). The two tank cars both conform to DOT-117 design specifications. Based on Equation (3-6), if the derailment speed is assumed to be 25 mph, the probability of POD at k^{th} position is shown in Table 4.

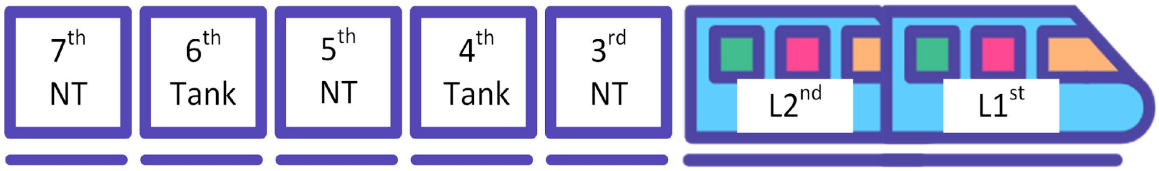

Figure 5. Example where the manifest train consists of seven cars (two locomotives, three non-tank cars, and two tank cars); NT represents a non-tank car in this figure

Table 4. The probability that POD is at the k^{th} position of a train, for the example with seven cars

k	1	2	3	4	5	6	7	Total
$POD(k)$	0.2342	0.1662	0.1454	0.1317	0.1205	0.1095	0.0924	1

The probability of x cars derailing can also be obtained, given that the POD is at k^{th}position, based on Equation (3-7). The results are shown in Table 5.

Table 5. The conditional probability of x cars derailing given that the POD is at the k^{th} position per derailment, for the example with seven cars

	$P_i(x\|k)$							
k	x = 1	x = 2	x = 3	x = 4	x = 5	x = 6	x = 7	Total
1	1.98E-01	1.76E-01	1.56E-01	1.39E-01	1.23E-01	1.10E-01	9.73E-02	1
2	2.20E-01	1.95E-01	1.73E-01	1.54E-01	1.37E-01	1.21E-01	0.00E+00	1
3	2.50E-01	2.22E-01	1.97E-01	1.75E-01	1.55E-01	0.00E+00	0.00E+00	1
4	2.96E-01	2.63E-01	2.33E-01	2.07E-01	0.00E+00	0.00E+00	0.00E+00	1
5	3.74E-01	3.32E-01	2.94E-01	0.00E+00	0.00E+00	0.00E+00	0.00E+00	1
6	5.30E-01	4.70E-01	0.00E+00	0.00E+00	0.00E+00	0.00E+00	0.00E+00	1
7	1.00E+00	0.00E+00	0.00E+00	0.00E+00	0.00E+00	0.00E+00	0.00E+00	1

Following Equation (3-10), the probability that the car at the j^{th} position of a train derails on segment i is shown in Table 6.

Table 6. The conditional probability that the car at the j^{th}position of a train derails on segment i per train derailment, for the example with seven cars

Position j	1	2	3	4	5	6	7
$PD_i(j)$	0.2342	0.3539	0.4216	0.4478	0.4357	0.3824	0.2722

According to Equation (3-11), the position-based tank car releasing probabilities are calculated as shown in Table 7. The "NA" in the table represents that the car at that position is not a tank car.

Table 7. Position-based tank car releasing probability per derailment, for the example with seven cars

Position j	1	2	3	4	5	6	7
$R_i(j)$	NA	NA	NA	0.0193	NA	0.0165	NA

Only the 4^{th} and 6^{th} cars are tank cars. The position-based tank car releasing probability of the 4^{th} and 6^{th} positions at segment i is used, which can be mathematically represented by $R_i(4)$ and $R_i(6)$, as the input to calculate the probability distribution of the total number of tank cars releasing (Table 8). As mentioned above, given the probability of a tank car releasing at each position, the number of tank cars releasing (x_R) follows a Poisson Binomial distribution. In this seven-car example, the possible values for x_R can be zero (no tank car release), one (exactly one tank car releasing contents), and two (two tank cars releasing contents). The conditional probability of release for a single DOT 117 tank car is 0.043 (Treichel et al., 2019a) and the derailment speed is assumed to be 25 mph. This value is used to calculate $R_i(j)$ and X_R. The CPR of a tank car is affected by accident characteristics such as speed and tank car features (e.g., tank thickness and top fitting protection). The conditional probabilities of releasing vary for different types of tank cars, and the CPR can be within the range of 0.041 to 0.134 for various tank car types (Treichel et al., 2019a). Due to data confidentiality, this report is not allowed to

show tank-car-specific CPR without AAR permission. Instead, the range of CPR values is provided.

Table 8. Probability distribution of releasing x_R tank cars per derailment, for the example with seven cars

	x_R=0	x_R=1	x_R=2	Total
$P(x_R)$	0.9645	0.0352	0.0003	1

3.1.7 Summary of Derailment and Releasing Risk Analysis

Given all probability distributions described above, the probability of multiple tank cars releasing on segment i per shipment can be calculated as follows:

$$P_i(x_R) \approx PTD_i \times P\left(\sum_{j=1}^{L} y_j = x_R\right) \quad (3\text{-}14)$$

where:

$P_i(x_R)$ = probability of x_R tank cars releasing contents on segment i per train shipment

PTD_i: = probability of a train derailment occurring on segment i, defined by Equation (3-4).

x_R = total number of tank cars releasing hazmat content

y_j = the 0-1 indicator, which equals 1 if the car at j^{th} position is releasing content, and 0 otherwise

L = train length, i.e., number of cars (including locomotives and railcars) in the train

3.1.8 Probability Distribution of the Releasing Quantity

In Section 3.1.7, the probability distribution of releasing x_R tank cars on each segment per shipment was derived. In this subsection, the probability distribution for the quantity released is calculated. Based on historical data from the TCAD, previous research conducted by the RSI-AAR Railroad Tank Car Safety Research and Test Project (AAR, 2014) developed the probability distribution of release quantity from a single tank car. Because most of the non-pressure tank cars (e.g., DOT-111 and DOT-117) have a volume capacity of around 30,000 gallons, an example distribution for volumes of liquids released from a non-pressurized, 30,000-gallon tank car was developed for general and representative use (Figure 6). In this research, the amount released is represented in terms of percentage of car capacity loss based on a prior study (Treichel et al., 2019a). The y-axis in Figure 6 is the fraction of the incidents of release in which the specified total volume content of the tank car (shown on x-axis) was released into the environment. This distribution is used to generate the release amount given the number of tank cars releasing contents. The input is the number of cars releasing and the output is the probability distribution of the amount released.

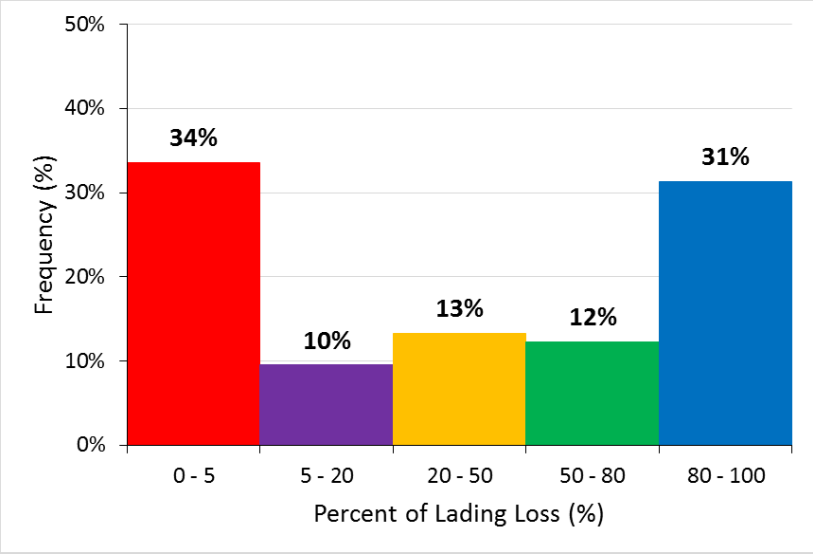

Figure 6. Probability distribution of release quantity for one non-pressurized tank car

Table 9 depicts the lading loss per car and probability distribution for the five levels of releasing quantity for a non-pressurized 30,000-gallon tank car. The TCAD data are quite detailed, but the limitation in the quantity of loss makes it difficult to break them down by speed because of the asymmetry of data, so that distributions of quantity of loss in a certain speed range may be skewed or unreliable due to a few data points. Therefore, the team used the aggregated probability distribution of release quantity. Due to information constraints, it is assumed that the release quantity of a tank car is independent of other tank cars. For multiple tank cars releasing contents, the total release quantity is an aggregation of the release quantity from multiple tank car releases. To be more specific, the potential release quantity for a release incident (with a specific number of releasing tank cars) is the combination of the five levels in Table 9.

Table 9. Probability of quantity released for five levels of release

Quantity of Release (QR)	Average Quantity of Release	Lading Loss per Car (in gallons)	Probability
0%-5%	2.50%	750	0.336
5%-20%	12.50%	3,750	0.095
20%-50%	35.00%	10,500	0.133
50%-80%	65.00%	19,500	0.123
80%-100%	90.00%	27,000	0.313

Each incident with a particular number of tank cars releasing contents has a probability distribution of release quantity. Take, for example, a situation where it is known that 20 tank cars are released. In such a case, there are 5^{20} possible combinations of release amount, which leads to a probability distribution of the total amount of hazmat release given 20 releasing tank cars. Summing up the probability distributions of the release quantity for all possible values for "the number of tank cars releasing contents," the probability distribution of the total amount released can be obtained. For example, assume that there are 20 tank cars on a manifest train, and the probability of releasing 1, 2, 3, …, 20 tank cars are all identical and equal to 0.05. There are two possible cases which might result from releasing 4,500 gallons: 1) there are six tank cars

releasing contents and each of them releases 750 gallons; or 2) there are two tank cars releasing contents: one of them releases 750 gallons and the other tank car releases 3,750 gallons (note: there is a factor "2" reflecting that there are two ways to designate which car is releasing 750 or 3,750 gallons). Thus, according to Table 9, the probability of releasing 4,500 gallons can be calculated by:

$$\begin{aligned} &P(releasing\ 4{,}500\ gallons\ hazmat) \\ &\quad = P(there\ are\ six\ tank\ cars\ releasing\ contents) \\ &\quad \times P(a\ tank\ car\ releasing\ 750\ gallons)^6 \\ &\quad + P(there\ are\ two\ tank\ cars\ releasing\ contents) \\ &\quad \times P(one\ tank\ car\ releasing\ 750\ gallons) \\ &\quad \times P(one\ tank\ car\ releasing\ 3{,}750\ gallons) \times 2 \\ &\quad = 0.05 \times 0.336^6 + 0.05 \times 0.336 \times 0.095 \times 2 = 0.0032 \end{aligned} \tag{3-15}$$

3.1.9 Case Study for 65 Cars (Including Locomotives and Railcars)

The research team conducted a more complex case study with a 65-car manifest train (as shown in Figure 7) on a 1-mile track segment: 5 head-end locomotives (212.5 tons each), followed by 20 tank cars and 40 non-tank cars (143 tons each). The derailment speed is 25 mph, and the tank car type is DOT-117 (non-pressurized) for all tank cars. The lading capacity for DOT-117s varies by detailed specifications, but generally it ranges from 28,000 - 32,000 gallons. Therefore, the probability distribution of release quantity for one non-pressurized tank car, developed in Section 3.1.8, is applicable.

Using the methods presented in Section 3.1.2, the probability of at least one car in the train derailing on a 1-mile segment can be calculated as 7.08E-07. Figure 8 and Figure 9 show the position-based derailment probability and probability distribution of the number of cars releasing per train derailment, respectively. Figure 10 depicts the reverse cumulative distribution of release quantity per train derailment and per train shipment, respectively.

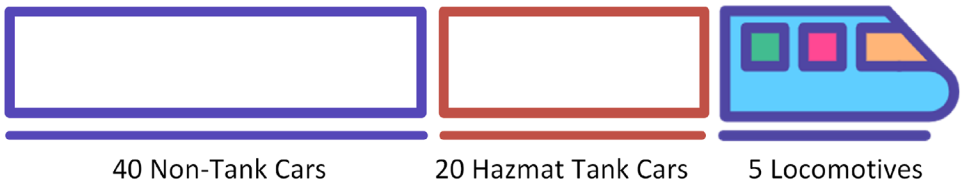

Figure 7. Train consist used in the case study (5 locomotives, 20 tank cars in one block, 40 non-tank cars)

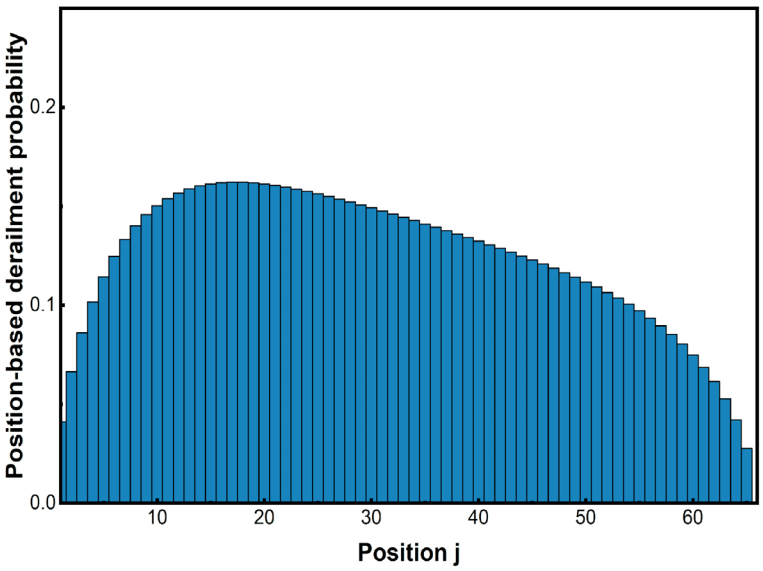

Figure 8. Position-based derailment probability distribution for the example with 65 cars per train derailment (5 head-end locomotives, followed by 20 tank cars in a block and 40 non-tank cars)

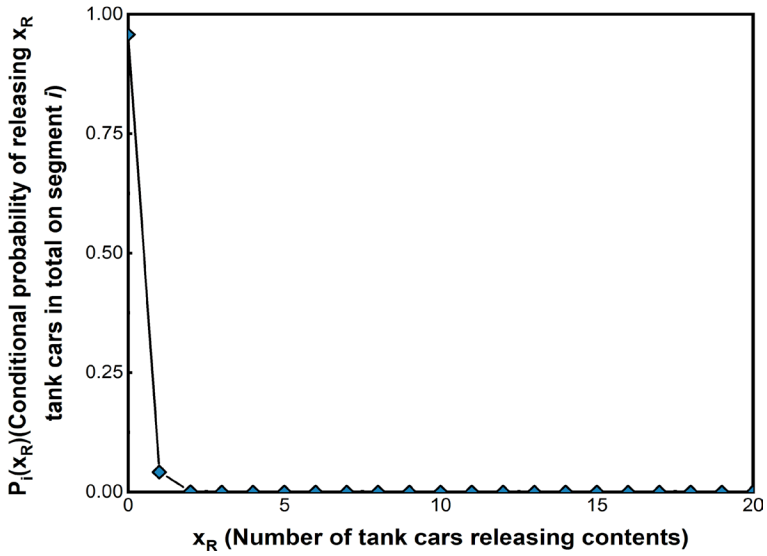

Figure 9. Position-based probability distribution of the number of cars releasing per train derailment

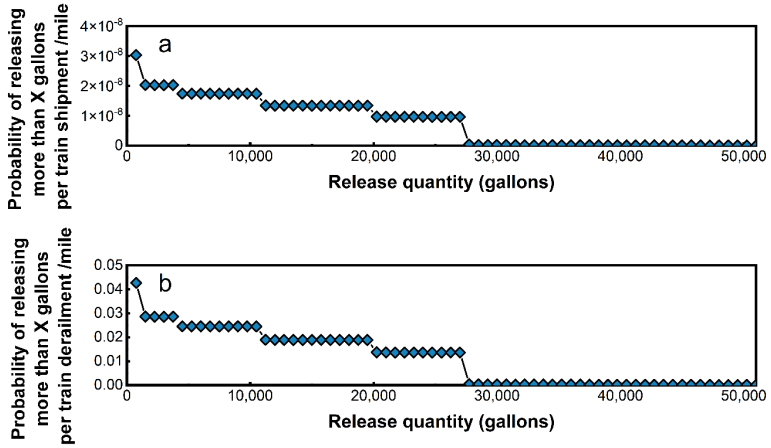

Figure 10. Reverse cumulative distribution of release quantity (a) per train shipment, and (b) per train derailment

3.1.10 Consequence of Release

Section 8 builds the consequence model of tank car release based on the route characterization, weather characterizations, time after the derailment of interest, evacuation time, etc. The output from Section 3.1.8 gives the probability distribution of release quantity. Looking at the distribution, the research team found that the probability of releasing more than 150,000 gallons of content in total is almost zero. Thus, for the consequence model in Section 8, the research team focused only on casualties resulting from exposure to fire and evaluated the total casualties caused by one, three, or five tank cars releasing contents, which represent small, medium, and large sizes of tank car release incidents, respectively. Since the casualties caused by one tank car (30,000 gallons), three tank cars (90,000 gallons), and five tank cars (150,000 gallons) is known from Section 8, while no casualty is assumed when no tank car releases, it is possible to piecewise linearly interpolate casualties when release quantity is between 0-30,000 gallons, 30,000-90,000 gallons, and 90,000-150,000 gallons. Equation (3-16) is the formula to calculate expected total casualties.

$$TC(t) = \sum_{0<x\leq 150{,}000} P_{re}(x) \times C(x,t) \times f \tag{3-16}$$

where:

$TC(t)$ = total casualties after t minutes caused by a releasing incident

$P_{re}(x)$ = the probability of releasing x gallons of contents from all releasing tank cars in total per traffic demand (calculated by the conditional probability of releasing x gallons from Section 3.1.8 times the train derailment probability from Section 3.1.2, and then times the number of train shipments)

$C(x,t)$ = the expected total casualties per fire event caused by releasing x gallons of content at response time t, and $t \in [0,120]$ in minutes (from Section 8)

f = a factor reflecting the percentage of release accidents involving fires

3.2 Methodology of Yard Risk Analysis

3.2.1 Introduction

In addition to the mainline risks described in previous sections, railroad yards and terminals impose additional risks to railway transportation for both unit trains and manifest trains (Figure 11). Two major types of risk exist over the course of a unit train shipment as compared with three for a manifest train shipment, due to the additional classification yard switching risk. The operations of unit trains and manifest trains both involve additional non-mainline risks while arriving at and departing from terminals and yards, and manifest trains encounter additional risks while being disassembled, sorted, and reassembled into new trains at classification yards. However, compared to mainline operations, less research has been conducted analyzing the risk associated with terminals and yards, despite their distinct operational activities that differ from those on the mainline.

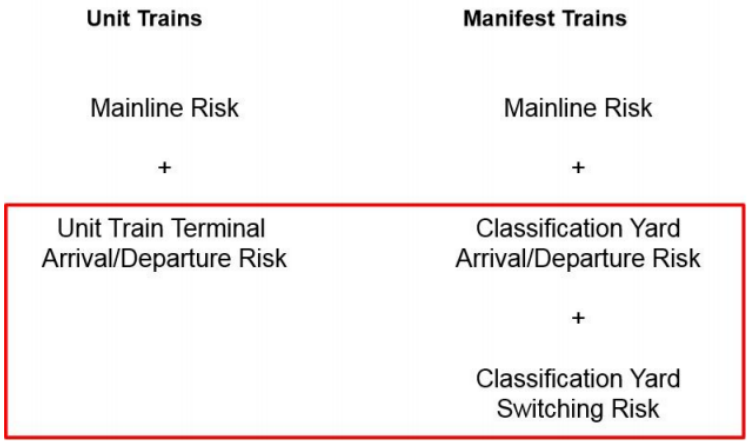

Figure 11. Risk composition comparison of unit and manifest trains

Within this research, events associated with unit train arrivals and departures from terminal facilities and manifest train arrivals and departure from classification yards are referred to as freight consist events (also referred to as arrival/departure (A/D) events in the following sections) to be consistent with how they are labeled and categorized in FRA's Incident/Accident Database. Events associated with the actual railcar classification, sorting, switching, and train assembly process in classification yards are referred to as yard switching consist events (or simply yard switching events) to similarly be consistent with the incident/accident database (Figure 11). As will be discussed in Section 6, these two types of yard and terminal events are distinct in terms of their underlying causes and characteristics, such as the resulting number of cars derailed.

Since A/D (i.e., freight consist) incidents typically involve a mainline freight train operating on non-mainline loading/unloading terminal tracks or entering a receiving yard or leaving a departure yard at a classification yard facility (Figure 12), the overall risk analysis approach is similar to that used for the mainline. However, the yard switching consist type of event typically involves the movement of a single railcar, a cut of cars, or a portion of a train (potentially moving in reverse or as a shoving movement), where the traditional mainline definitions of a train consist, point of derailment, and position-based accident probability are not readily applicable. Therefore, a new risk analysis methodology for yards and terminals is needed.

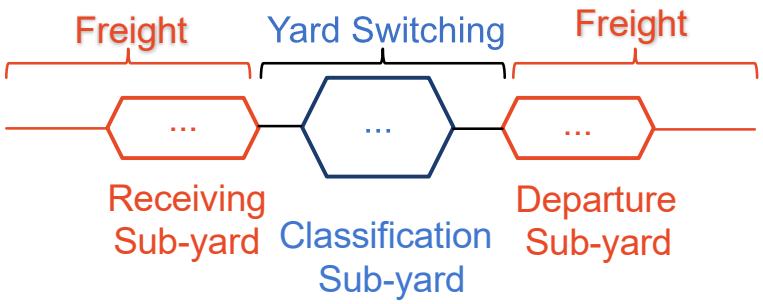

Figure 12. Yard and terminal accident location and train consist type

This section outlines a proposed methodology to quantify the risk of railroad hazmat transportation at yards and terminals for both unit and manifest train A/D events, and manifest train yard switching events. The overall approach, documented in complete detail in Section 6, is formulated based on a chain of events: 1) the train (or block of hazmat cars being shipped) is involved in a terminal or yard-related accident; 2) there is at least one car (locomotive or railcar) derailed; 3) there is at least one car transporting hazmat derailed; (4) of the hazmat cars derailed, there is at least one car releasing contents; 5) a quantity of hazmat is released based on the number of tank cars releasing; and 6) consequences of the hazmat release result from a given release quantity.

Similar to those presented earlier for the mainline analysis, flow charts (Figure 13) illustrate this chain of events and are used to analyze the risk of a hazmat railcar releasing during a yard/terminal A/D "freight consist" event (Figure 13a) or yard switching "yard consist" event (Figure 13b). If specific information on the train and yard routing, such as mainline segment length or number and type of yard/terminal facilities visited by the shipment, train type, train length, number of tank cars, etc., is available, the risk analysis methodology can quantify the probability of train derailment, number of cars derailed, number of hazmat cars derailed, hazmat cars releasing, and quantity of release. The following subsections will sequentially discuss these events and the proposed methodology for quantifying their probabilities. The risk analysis procedures for the yard/terminal arrival and departure "freight consist" events are analogous to those for the mainline, given the similarity in train consist characteristics between mainline and A/D events. The A/D analysis follows a sequence of calculating the derailment probability, derailment severity based on the position of hazmat cars in the train, and release consequences based on derailment severity. In contrast, the analysis of yard switching "yard consist" events uses a novel process to calculate derailment severity (i.e., railcars derailed) because the overall manifest train length and the specific position of the group of hazmat cars of interest both become less clear while trains are being classified in a yard. Also, as described in the following paragraphs, the yard and terminal approach must consider yard-specific traffic metrics that differ from the train-miles, car-miles, and ton-miles used on the mainline.

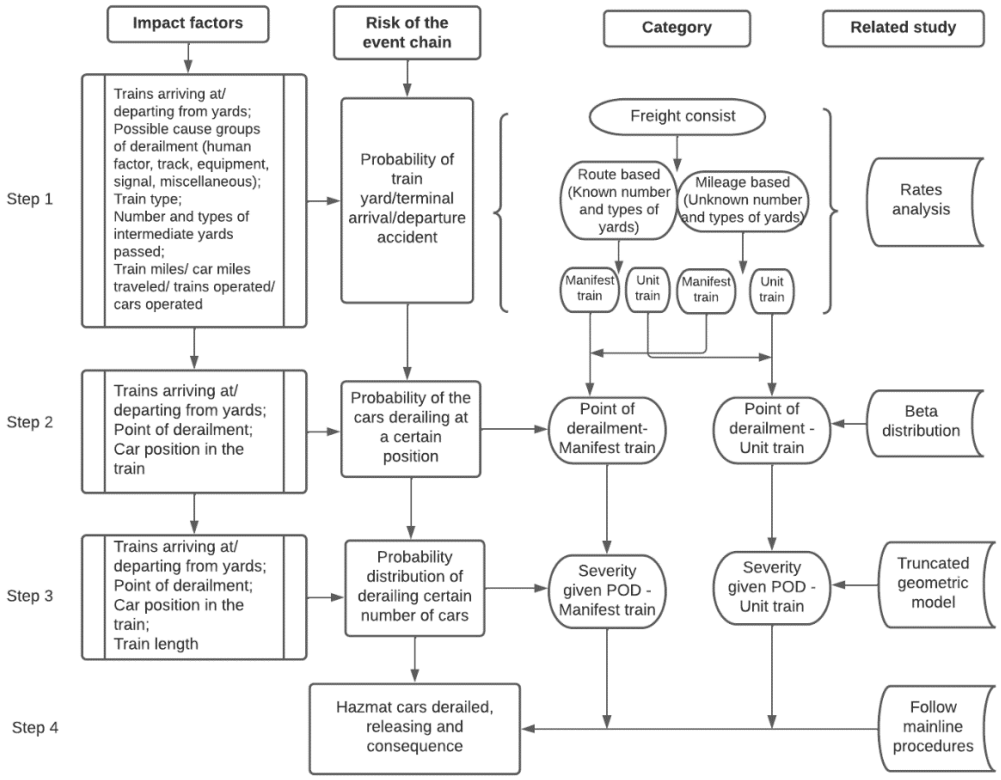

(a)

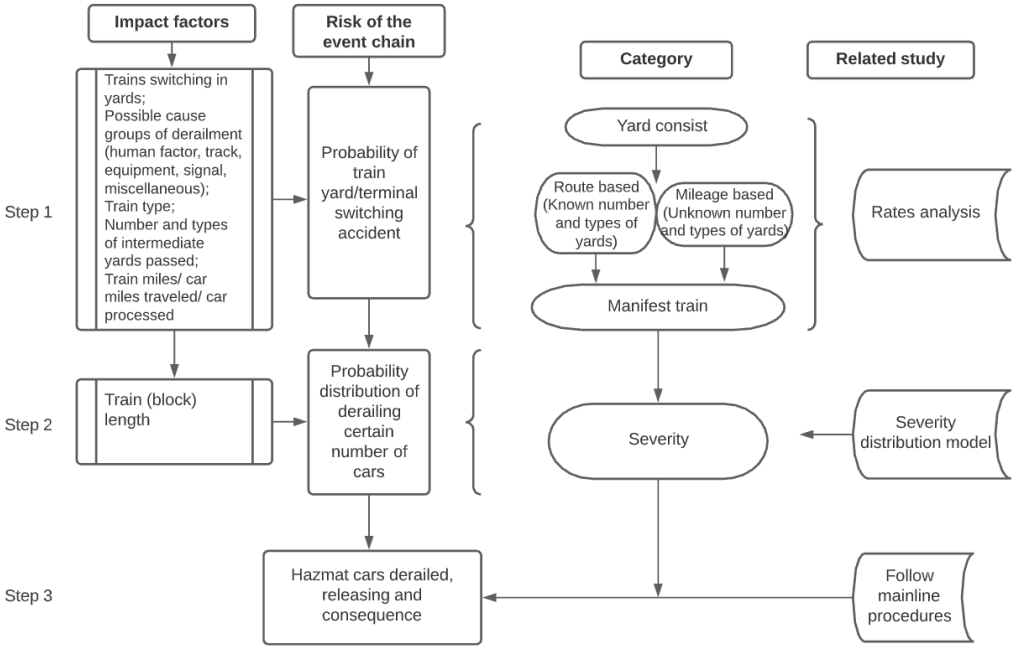

(b)

Figure 13. Train type-based tank car release risk analysis event chains for a) freight consist yard/terminal A/Ds, and b) yard switching consist

Although the mainline travel distance between origin and destination can be estimated when planning or analyzing a non-unit train shipment, information on the exact sequence of manifest trains and number and type of classification yards involved in the movement may not be known. Thus, two approaches to quantify yard risk are needed for manifest trains:

- **Generic Mileage-Based Approach** is used if the number and type of intermediate classification yards is not known. This approach looks at the average rate of yard A/D and switching events as a function of mainline traffic metrics. The underlying assumption is that the number of intermediate yards (and the associated expected number of yard derailments) is linearly proportional to the overall mainline distance travelled from origin to destination.
- **Detailed Route-Based Approach** is used if the exact number and type of intermediate classification yards is known. This approach develops specific rates of occurrence for yard A/D and yard switching events as a function of actual yard traffic metrics, such as the number of train arrivals and departures or number of railcars processed. Different rates are developed for hump and flat switching classification yards. Because it is more specific to actual yard operating metrics and the exact yards involved in the shipment, the detailed route-based approach should produce more accurate estimates than the generic mileage-based approach when specific yard details are known.

3.2.2 Train Derailment Probability

Similar to that of the mainline, the probability of trains derailing in yards and terminals can be estimated by the train derailment rate (i.e., the number of derailments normalized by the total traffic) calculated from historical train derailment data and traffic data. When collecting and summarizing detailed Surface Transportation Board Class I Railroad R-1 annual report financial data for the years 1996 through 2018, the denominator traffic data (e.g., annual mainline train-miles, mainline car-miles, mainline ton-miles, number of trains and railcars operated, and number of railcars switched in classification yards) is calculated separately for unit trains and manifest trains, as is appropriate.

The accident data is extracted from FRA's Incident/Accident database over the same 23-year period. The number of yard accidents can be categorized by train type (i.e., unit or manifest train), consist type (i.e., freight or yard switching consist) and yard type (i.e., hump or flat switching) to calculate corresponding accident rates. As an example, for each ADL cause group, the total number of A/D incidents occurring during the study period and the percentage of total number of incidents for each group are listed for unit trains at terminals (Table 10a) and manifest trains at classification yards (Table 10b). Derailment rates can then be computed as the relevant accident data divided by the corresponding traffic data for each train type and event type.

Table 10. FRA-reportable Class I yard train A/D event derailment data, 1996-2018

(a) Unit train derailments

Cause group	Frequency	Percent of total
Broken rails or welds	224	26.79
Wide gauge	106	12.68
Turnout defects: switches	105	12.56
Use of switches	79	9.45
Switching rules	42	5.02

Cause group	Frequency	Percent of total
Miscellaneous track and structure defects	29	3.47
Track geometry (excluding wide gauge)	27	3.23
Other miscellaneous	26	3.11
Other wheel defects (car)	19	2.27
Roadbed defects	18	2.15
Rail defects at bolted joint	13	1.56
Train handling (excluding brakes)	13	1.56
Train speed	12	1.44
Stiff truck (car)	12	1.44
Lading problems	11	1.32
Other rail and joint defects	10	1.20
Track–train interaction	9	1.08
Side bearing and suspension defects (car)	8	0.96
Miscellaneous human factors	8	0.96
Handbrake operations	7	0.84
Joint bar defects	7	0.84
Buckled track	6	0.72
Signal failures	5	0.60
Nontraffic, weather causes	5	0.60
Brake rigging defect (car)	4	0.48
Failure to obey or display signals	3	0.36
Locomotive trucks, bearings, and wheels	3	0.36
All other locomotive defects	3	0.36
All other car defects	3	0.36
Brake operation (main line)	2	0.24
Centerplate or car body defects (car)	2	0.24
Extreme weather	2	0.24
Bearing failure (car)	2	0.24
Turnout defects: frogs	2	0.24
Broken wheels (car)	2	0.24
Locomotive electrical and fires	2	0.24
Handbrake defects (car)	1	0.12
Brake operations (other)	1	0.12
UDE (car or locomotive)	1	0.12
Other brake defect (car)	1	0.12
Mainline rules	1	0.12
Total	**836**	**100**

(b) Manifest train derailments

Cause group	Frequency	Percent of total
Switching rules	908	15.45
Use of switches	766	13.03
Broken rails or welds	685	11.66
Wide gauge	625	10.63
Turnout defects: switches	486	8.27
Train handling (excluding brakes)	407	6.93
Other miscellaneous	206	3.51
Handbrake operations	195	3.32

Cause group	Frequency	Percent of total
Train speed	183	3.11
Miscellaneous track and structure defects	155	2.64
Track–train interaction	150	2.55
Track geometry (excluding wide gauge)	141	2.40
Brake operation (main line)	136	2.31
Lading problems	79	1.34
Other wheel defects (car)	70	1.19
Signal failures	63	1.07
Side bearing and suspension defects (car)	59	1.00
Coupler defects (car)	56	0.95
Stiff truck (car)	54	0.92
Roadbed defects	51	0.87
Radio communications error	48	0.82
Rail defects at bolted joint	37	0.63
Miscellaneous human factors	37	0.63
Centerplate or car body defects (car)	28	0.48
Turnout defects: frogs	28	0.48
Mainline rules	26	0.44
Nontraffic, weather causes	22	0.37
All other car defects	18	0.31
Other rail and joint defects	16	0.27
Brake operations (other)	15	0.26
Other brake defect (car)	15	0.26
Brake rigging defect (car)	14	0.24
Extreme weather	13	0.22
Locomotive trucks, bearings, and wheels	12	0.20
All other locomotive defects	12	0.20
Buckled track	11	0.19
Failure to obey or display signals	10	0.17
Joint bar defects	10	0.17
Broken wheels (car)	8	0.14
Obstructions	4	0.07
Handbrake defects (car)	4	0.07
Employee physical condition	4	0.07
Truck structure defects (car)	4	0.07
Air hose defect (car)	2	0.03
UDE (car or locomotive)	1	0.02
Bearing failure (car)	1	0.02
Locomotive electrical and fires	1	0.02
Track–train interaction (hunting) (car)	1	0.02
Total	**5,877**	**100**

3.2.2.1 Generic Mileage-based Approach

The generic mileage-based approach is designed for instances when the number and type of intermediate classification yards involved in a manifest train shipment are not known. In these cases, it is assumed that the number of intermediate yards (and associated expected number of yard derailments) is linearly proportional to the overall mainline distance travelled from origin to destination. Thus, the average rate of yard A/D and yard switching events is assumed to be a function of mainline traffic metrics (i.e., train-miles, car-miles, and ton-miles). As detailed in Section 6, yard derailments from the FRA REA database for the years 1996-2018 were classified

by train type and yard process and normalized by appropriate STB R-1 mainline traffic metrics (train-miles and car-miles) to produce corresponding derailment rates (Table 11). The rates calculated over this entire 23-year period are shown here for purposes of illustrating the overall methodology. Section 6 further explores trends in these yard/terminal derailment rates over time and their sensitivity to the exact duration of the study period.

Table 11. Generic freight and yard consist derailment rates (1996-2018) for various train types and mainline traffic metrics (see Section 6)

	Arrival/Departure (Freight Consist)		Yard Switching (Yard Consist)	
Group	Derailments per Million Mainline Train-Miles	Derailments per Billion Mainline Car-Miles	Derailments per Million Mainline Manifest Train Train-Miles	Derailments per Billion Mainline Manifest Train Car-Miles
Manifest Trains	0.70	11.88	1.57	26.86
Unit Trains	0.29	2.81	N/A	N/A
Empty Unit	0.10	1.00	N/A	N/A
Loaded Unit	0.48	4.63	N/A	N/A

Like the mainline approach, all yard and terminal A/D (i.e., freight consist) derailment causes are classified into two categories based on denominator traffic metrics: mainline train-miles and mainline car-miles (including locomotives and railcars). Therefore, the respective rate contributions of the two cause categories (i.e., train-mile-based causes and car-mile-based causes) are observed. Comparably, manifest train yard-switching-type accidents can also be inferred from the train-miles and car-miles traveled on the mainline, resulting in two denominator metrics: train-miles and car-miles.

Let $FTRM$ denote the set of freight consist train-mile-based derailment causes, and FCM be the set of freight consist car-mile-based causes. For yard consist, let $YTRM$ be the set of train-mile-based causes, and let YCM be the set of car-mile-based causes. If a train has L_l cars (locomotives and railcars) and it travels a total length of L_t on mainline, then the probability of train derailment due to the ith cause can be calculated by Equations (3-17) to (3-20):

Freight Consist Arrival/Departure:

$$P_{i|i\in FTRM} \approx d_{FTRM}/1{,}000{,}000 \times L_t \times p_i \quad (3\text{-}17)$$

$$P_{i|i\in FCM} \approx d_{FCM}/1{,}000{,}000{,}000 \times L_l \times L_t \times p_i \quad (3\text{-}18)$$

Yard Switching:

$$P_{i|i\in YTRM} \approx d_{YTRM}/1{,}000{,}000 \times L_t \times p_i \quad (3\text{-}19)$$

$$P_{i|i\in YCM} \approx d_{YCM}/1{,}000{,}000{,}000 \times L_l \times L_t \times p_i \quad (3\text{-}20)$$

where:

$P_{i|i\in FTRM}$ = probability that this freight consist train derails while arriving at or departing from a yard and the derailment is caused by a train-mile-based cause

$P_{i|i\in FCM}$ = probability that this freight consist train derails while arriving at or departing from a yard and the derailment is caused by a car-mile-based cause

$P_{i|i\in YTRM}$ = probability that this yard consist train derails while switching in a yard and the derailment is inferred from the mainline train-miles traveled

$P_{i|i\in YCM}$ = probability that this yard consist train derails while switching in a yard and the derailment is inferred from the mainline car-miles traveled

d_{FTRM} = freight consist train derailments per million mainline train-miles (Table 11)

d_{FCM} = freight consist train derailments per billion mainline car-miles (Table 11)

d_{YTRM} = yard consist train derailments per million mainline train-miles (Table 11)

d_{YCM} = yard consist train derailments per billion mainline car-miles (Table 11)

p_i = percentage of derailments of ith cause in the total number of derailments

L_l = train length, i.e., number of cars in the train including locomotives

L_t = the total length (in miles) of the track segment traversed by the train from origin to destination

As mentioned, different causes are more closely associated with different traffic metrics when calculating derailment rates. The probability of a train derailment during a shipment due to any cause (PTD) can be approximately estimated by Equation (3-4) for unit trains and manifest trains respectively (detailed calculation in Section 6).

Unit trains:
$$PTD_{unit} \approx \sum_{i\in FTRM} P_{i|i\in FTRM} + \sum_{i\in FCM} P_{i|i\in FCM} \quad (3\text{-}21)$$

Manifest trains:
$$PTD_{manifest} \approx \sum_{i\in FTRM} P_{i|i\in FTRM} + \sum_{i\in FCM} P_{i|i\in FCM} + \sum_{i\in YTRM} P_{i|i\in YTRM} + \sum_{i\in YCM} P_{i|i\in YCM} \quad (3\text{-}22)$$

3.2.2.2 Generic Mileage-based Example

To better illustrate the generic mileage-based yard and terminal derailment rates, consider an example 100-railcar manifest train shipment that travels 2,000 miles between origin and destination classification yards, and a comparable 100-railcar unit train shipment that travels 2,000 direct miles from origin to destination (Figure 14). Assume that the number of intermediate yards is unknown for the manifest train shipment, requiring the mileage-based yard and terminal derailment rates to be applied.

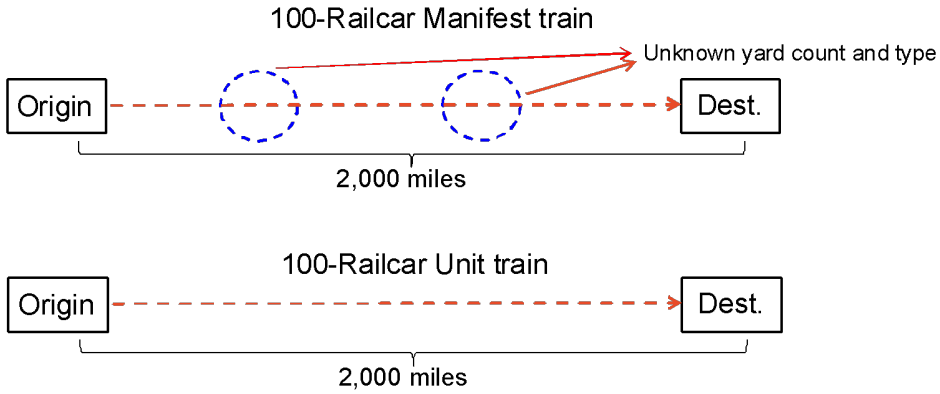

Figure 14. Example shipment schematic diagram with unknown yard routing

Considering the number of train-miles and car-miles accumulated from origin to destination by each train type and the average derailment rates as shown in Table 11, the expected number of derailments during each shipment can be estimated (Table 12). Note the difference in the relative derailment likelihood as calculated using the train-mile and car-mile traffic metrics. This difference highlights the need to apply an approach that considers both traffic metrics and the proportion of accident causes related to each metric (Equations (3-21) and (3-22)). A more detailed example of this approach is included in later sections.

Table 12. Train type derailment likelihood comparison for example shipment using generic mileage-based rates

Traffic Metric	Expected Manifest Train Yard Derailments per Shipment		Expected Unit Train Terminal Derailments per Shipment	
	Calculation Process	Result	Calculation Process	Result
Train-mile	(Manifest Freight Derailments per Train-Mile Running) × (2,000 Train-miles) + (Yard Switching Derailments per Train-Mile Running) × (2,000 Train-miles)	4.55E-03	(Unit Freight Derailments per Train-Mile Running) × (2,000 Train-miles)	5.78E-04
Car-mile	(Manifest Freight Derailments per Car-Miles Running) × (2,000 × 100) Car-miles + (Yard Switching Derailments per Car-Miles Running) × (2,000 × 100) Car-miles	7.75E-03	(Unit Freight Derailments per Car-Mile Running) × (2,000 × 100) Car-miles	5.62E-04

3.2.2.3 Detailed Route-based Approach

In addition to generic mileage-based rate analysis, another more detailed route-based approach considers the exact number and types of terminals and yards that a shipment traverses from origin to destination. To support this more detailed approach, the occurrence of yard/terminal arrival and departure derailments must be linked to appropriate yard traffic metrics describing the frequency of train and railcar arrivals and departures at classification yards and unit train terminals. Similarly, the occurrence of yard switching derailments must be linked to the number of railcars processed through a given yard. As detailed in Section 6, yard derailments from the FRA REA database for the years 1996-2018 were classified by train type and yard process, and normalized by appropriate STB R-1 yard traffic metrics over the same period to produce corresponding derailment rates (Table 13).

Table 13. Detailed freight and yard consist derailment rates (1996-2018) for various train types, yard types and yard traffic metrics (see Section 6)

	Arrival/Departure (Freight Consist)		Yard Switching (Yard Consist)
Group	Derailments per Million Train Arrival/Departures	Derailments per Million Car Arrival/Departures	Derailments per Million Cars Processed in Classification Yards
Manifest Train	61.52	1.04	6.43
Flat Yard	118.92	2.02	6.38
Hump Yard	36.53	0.62	6.49
Unit Train	76.95	0.74	N/A
Empty Unit	27.59	0.27	N/A
Loaded Unit	126.31	1.22	N/A

Yard and terminal train A/D (i.e., freight consist) accidents can be categorized as train-A/D-based or car-A/D-based, corresponding to two categories of causes: train-process-based and car-process-based (corresponding to train-mile-based and car-mile-based on the mainline). Therefore, the yard and terminal derailment rate calculation must consider the relative contribution of each traffic metric to the likelihood of A/D derailments. For yard switching consist accidents, regardless of the category of causes, the rate calculation is based on the number of railcars processed in a specific yard.

Let $FTRP$ denote the set of freight consist train-processed-based derailment causes, and FCP be the set of freight consist car-processed-based causes. For yard consist, let YCS be the set of any cause.

If a manifest train has L_l cars (locomotives and railcars), passes m intermediate yards with n arrival and departure events (one at origin yard, 2×m at m intermediate classification yards and one at destination yard), it has $(m+1) \times L_l$ car switching movements (each car is switched once at the origin yard and once at each intermediate yard). Similarly, a unit train with L_l cars (locomotives and railcars) will have two A/D events (one at the origin yard and one at the destination yard). The probability of train derailment due to the ith cause can be calculated by Equations (3-23) to (3-25):

Freight Consist Arrival/Departure:

$$P_{i|i\in FTRP} \approx d_{FTRP}/1{,}000{,}000 \times n \times p_i \quad (3\text{-}23)$$

$$P_{i|i\in FCP} \approx d_{FCP}/1{,}000{,}000{,}000 \times L_l \times n \times p_i \quad (3\text{-}24)$$

Yard Switching:

$$P_{i|i\in YCS} \approx d_{YCS}/1{,}000{,}000 \times L_l \times (m+1) \times p_i \quad (3\text{-}25)$$

where:

$P_{i|i\in FTRP}$ = probability that this freight consist train derails while arriving at or departing from a yard and the derailment is caused by a train-processed-based cause

$P_{i|i\in FCP}$ = probability that this freight consist train derails while arriving at or departing from a yard and the derailment is caused by a car-processed-based cause

$P_{i|i\in YCS}$ = probability that this yard consist train derails while switching in a yard

d_{FTRP} = train derailments per million train A/D events (Table 13)

d_{FCP} = train derailments per billion car A/D events (Table 13)

d_{YCS} = train derailments per million cars processed in the yard (Table 13)

p_i = percentage of derailments of ith cause in the total number of derailments

L_l = train length, i.e., number of cars in the train including locomotives

n = number of A/D events that a shipment involves

m = number of intermediate yards that a manifest train shipment involves

Considering all causes, the probability of a train derailment in a yard or terminal during a shipment due to any cause (PTD) can be approximately estimated by Equation (3-4) for unit trains and manifest trains, respectively (detailed calculation in Section 6).

Unit trains:
$$PTD_{unit} \approx \sum_{i \in FTRP} P_{i|i \in FTRP} + \sum_{i \in FCP} P_{i|i \in FCP} \quad (3\text{-}26)$$

Manifest trains:
$$PTD_{manifest} \approx \sum_{i \in FTRP} P_{i|i \in FTRP} + \sum_{i \in FCP} P_{i|i \in FCP} + \sum_{i \in YCS} P_{i|i \in YCS} \quad (3\text{-}27)$$

3.2.2.4 Detailed Mileage-based Example

Considering the same example presented earlier, a hypothetical 100-railcar manifest train shipment travels 2,000 miles between origin and destination classification yards, and a comparable 100-railcar unit train shipment travels 2,000 miles direct from origin to destination (Figure 15). Unlike the previous example where the details of the manifest train route were not known, in this case the manifest train shipment is assumed to be composed of two separate legs, with the shipment connecting between trains at one intermediate classification yard. In this scenario, the manifest train shipment involves a total of four yard A/D events compared with two terminal A/D events for the unit train. Additionally, a total of 200 railcar switching events is required for the manifest train shipment (100 railcars switched at the origin yard and 100 railcars switched at the intermediate yard).

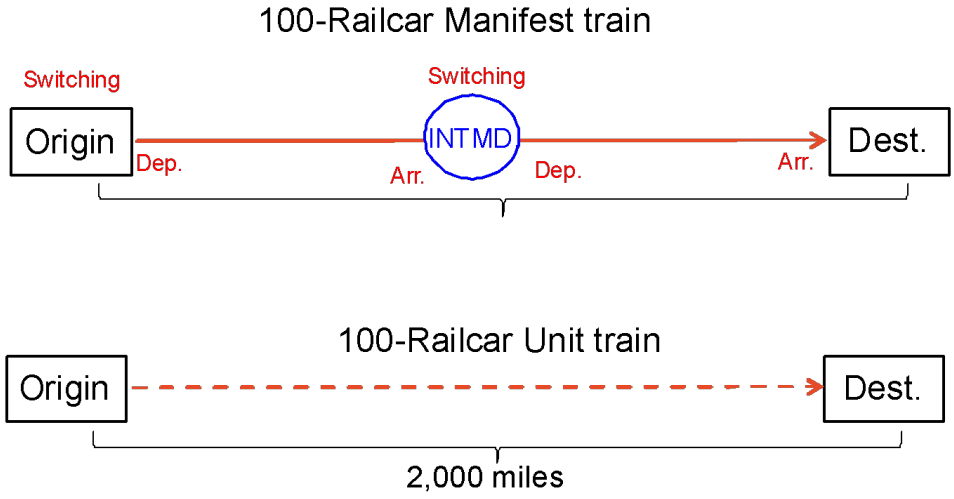

Figure 15. Example shipment schematic diagram with known yard routing

Considering the number of train and railcar A/D events and railcar switching events accumulated from origin to destination by each train type, and the average derailment rates in Table 13, the expected number of derailments during each shipment can be estimated (Table 14).

Like in the previous example, there is a difference in the relative derailment likelihoods as calculated using the train A/Ds (i.e., trains processed) and railcar A/Ds (i.e., railcars processed) traffic metrics. Again, this difference highlights the need to apply the approach that considers both traffic metrics and the proportion of accident causes related to each metric (Equations (3-26) and (3-27)).

Table 14. Train type derailment likelihood comparison for example shipment using detailed route-based rates

Traffic Metric	Expected Manifest Train Yard Derailments per Shipment		Expected Unit Train Terminal Derailments per Shipment	
	Calculation Process	Result	Calculation Process	Result
Trains processed	(Manifest Freight Derailments per Train A/D Event) × (4 A/D Events) + (Manifest Yard Switching Derailments per Car Processed) × (200 Cars Switched)	1.53E-03	(Unit Freight Derailments per Train A/D event) × (2 A/D Events)	1.54E-04
Cars processed	(Manifest Freight Derailments per Car A/D Event) × (4 A/D Events × 100 Cars) + (Manifest Yard Switching Derailments per Car Processed) × (200 Cars Switched)	1.70E-03	(Unit Freight Derailments per Car A/D Event) × (2 A/D Events × 100 Cars)	1.49E-04

Compared to the results in Table 12 that were calculated using the generic mileage-based approach, the derailment likelihood is far lower when calculated using the detailed approach (Table 14). In this example, the detailed approach better captures the yard and terminal derailment likelihood for a relatively long mainline trip with only one intermediate yard for the manifest train shipment. Many manifest and unit train trips are far shorter than 2,000 miles, and thus the generic mileage-based approach that uses mainline train-miles and car-miles over-estimates the amount of yard and terminal operations involved in a trip. If the example shipment were shortened from 2,000 to 500 miles, the mileage-based values in Table 12 would decrease by a factor of four, while the detailed route-based values in Table 14 would remain the same, since the exact pattern of yards and terminals encountered by each train remains the same. Given this tendency, the detailed route-based approach should be used whenever information on intermediate yards and terminals involved in the shipment is available. The mileage-based approach should only be used as a rough approximation when no specific yard or terminal routing information is available.

3.2.3 Derailment Severity

Section 6 details the methodology used to estimate derailment severity for yard and terminal accidents, including both freight consist and yard switching consist events. In the context of this research, derailment severity is defined as the total number of cars (i.e., locomotives and railcars) derailed per train derailment. Unlike mainline accidents, yard and terminal accidents usually involve a smaller range of derailment speeds. Additionally, yard switching consist events lack the required definition of residual train length while individual railcars or cuts of cars are being switched in classification yards. Therefore, distinct approaches are required to estimate the severity of yard and terminal accidents for both freight consists and yard switching consists.

3.2.3.1 A/D Accident (Freight Consist) Severity

The NPOD distribution for FRA train derailment data between 1996 and 2018 should follow a Beta distribution for both manifest trains and unit trains. Considering the comparable train operations between mainline and yard A/D activities, a similar position-based severity method

can be used for yard (i.e., manifest train) and terminal (i.e., unit train) freight consist A/D derailments.

The normalized point of derailment was calculated by dividing POD by train length. To identify the differences between manifest and unit trains, train-type-based POD distributions were developed for unit train terminal A/D accidents (Figure 16a) and manifest train yard A/D accidents (Figure 16b) using yard accident/incident data from 1996 to 2018.

After an initial peak at the front of the train, the NPODs of the unit train distribution are more evenly distributed throughout the remainder of the train, while the manifest train is more consistently skewed to the front of the train with continually diminishing probability toward the end of the train. In the manifest train derailment distribution, 70 percent of derailment events fall in the first half of the train (i.e., in the interval [0,0.5]), while in the unit train derailment distribution, approximately one half of derailment events fall in this same interval covering the first half of the train. These results suggest a difference in NPOD distributions between the manifest train and the unit train, justifying the need to develop train-type-based yard/terminal NPOD models. The detailed fitting performance is introduced in Section 6.

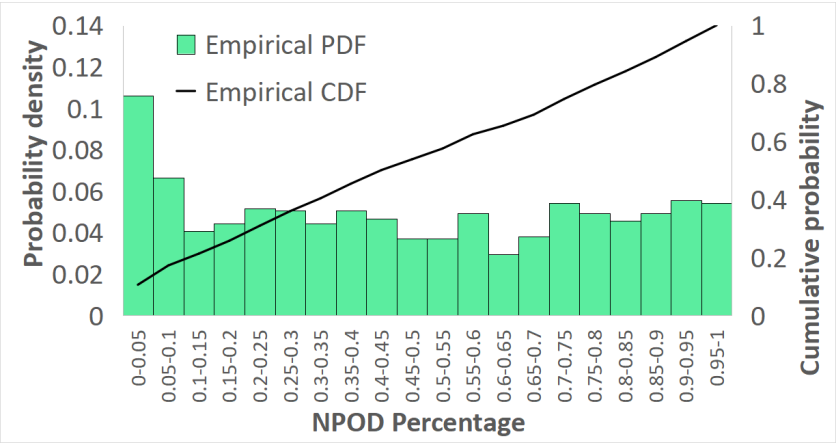

(a)

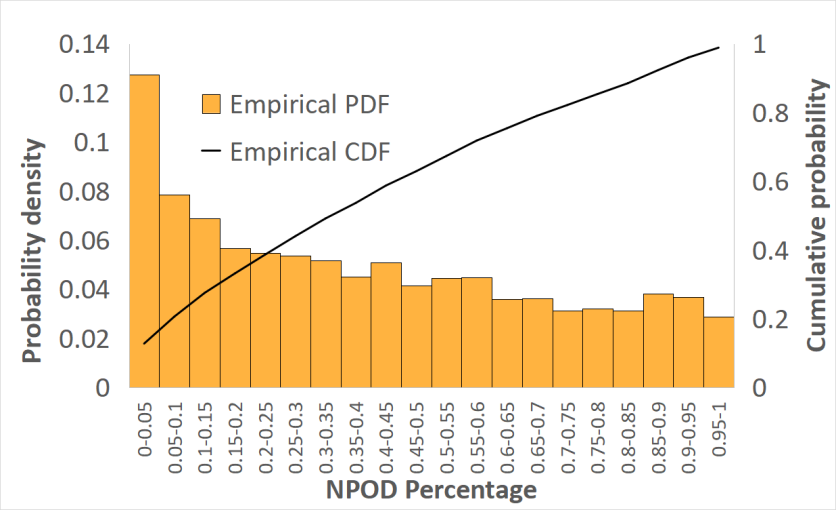

(b)

Figure 16. Empirical NPOD distributions for (a) unit train, and (b) manifest train yard/terminal A/D derailments (1996-2018)

The probability that POD is at the k^{th} position is defined as follows:

$$POD(k) = F\left(\frac{k}{L}\right) - F\left(\frac{k-1}{L}\right) \tag{3-28}$$

where:

$Pod(k)$ = the probability that POD is at the k^{th} position of a train

$F(x)$ = cumulative density distribution of the fitted NPOD distribution
L = train length

Similarly, define $P_i(x|k)$ as the probability of x vehicles derailing given that the POD is at k^{th} position on segment i. The probability of x cars derailing can be estimated with the TG model:

$$P_i(x|k) = \frac{\frac{\exp(z)}{1+\exp(z)}\left[\frac{1}{[1+\exp(z)]^{x-1}}\right]}{1-\left[\frac{1}{1+\exp(z)}\right]^{L_r}} \tag{3-29}$$

$$z_{yard} = -a - b \times L_r\ (L) \tag{3-30}$$

$$\text{or } z_{yard} = -a \tag{3-31}$$

$$L_r = L - POD + 1 \tag{3-32}$$

where:

$P_i(x|k)$ = the probability of x vehicles derailing given that the POD is at k^{th} position on segment i

L_r = number of cars after POD

L = total train length

a and b = coefficients for each parameter

For manifest trains and loaded unit trains, Equation (3-30) should be applied to Equation (3-29) to predict the derailment severity given the POD. For empty unit trains, Equation (3-31) should be substituted into Equation (3-29) instead. The detailed fitting performance and selection of explanatory variables influencing the number of cars derailed is explained in Section 6.

It is assumed that if a train derailment occurs, cars will derail sequentially after the POD. After calculating the probability distribution of the total number of cars derailed, the probability that the car at the j^{th} position of the train derails on segment i can be expressed as follows (defined as $PD_i(j)$):

$$PD_i(j) = \sum_{k=1}^{j}\left[POD_i(k) \times \sum_{x=j-k+1}^{L_r} P_i(k)\right] \tag{3-33}$$

$\sum_{x=j-k+1}^{L_r} P_i(k)$ is the sum of the probability that the derailment has spread to j^{th} position given the POD at k^{th} position.

Using the same process introduced earlier for mainline derailments, each combination of possible POD and number of cars derailed is examined to determine the railcar position numbers

that will derail in each scenario. These positions are compared to the known (or assumed) positions of the hazmat railcars in the manifest or unit train to determine the number of hazmat railcars derailed in that scenario. The probability of that scenario (conditional on a derailment having occurred) is determined from the combined probability of the POD being at that position (Equation (3-28)), and the probability of a given number of railcars derailed (Equation (3-29)). Combining all possible POD and derailment size combinations yielding the same number of hazmat cars derailed yields the probability distribution of the number of hazmat cars derailed given that a yard or terminal A/D derailment has occurred.

3.2.3.2 Yard Switching Accident (Yard Switching Consist) Severity

Unlike yard A/D (i.e., freight consist) accidents, yard switching accidents usually involve a cut of cars or single railcars where the definition of residual train length does not apply or cannot be estimated during the various stages of the switching process. Therefore, an alternate approach is needed to estimate derailment severity for yard switching consist derailments in different types of classification yards.

The probability density distribution of each number of cars derailed for all FRA REA yard switching consist accidents (1996-2018) is compiled (Figure 17) to determine the best fitting distribution to predict derailment severity. Overall, the probability distribution of derailment severity (i.e., number of cars derailed) suggests a generalized exponential distribution. Developing individual fitted distributions for hump yards and flat yards further distinguishes between these facilities and more accurately captures the derailment severity corresponding to their distinct operating strategies, devices, and infrastructures. The detailed functions and fitting performance is described in Section 6. The probability of x vehicles derailing on segment i during the yard switching process can be represented by $P_i(x)$.

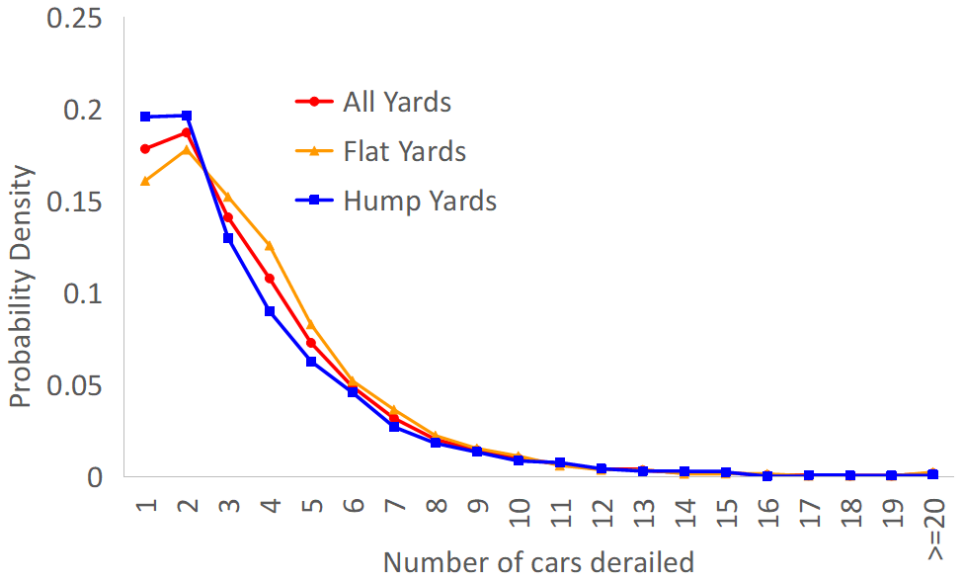

Figure 17. Empirical distribution of number of cars derailed for yard switching derailments for different types of yards

The probability of y number of tank (i.e., hazmat) cars involved in the derailment given x vehicles derailed $P_i(x)$ can be derived using probability theory. Overall, the probability of y number of tank cars derailing during the yard switching process can be calculated by:

$$P_i(y) = \sum_{x=1}^{l} [P_i(x) \times P_i(x)] \quad (3\text{-}34)$$

To explain the process of calculating the total number of tank cars derailed during the yard switching process, consider a hypothetical example with seven railcars being switched (Figure 18). During the yard switching process, the specific order of railcars, especially the position of tank cars, is usually unknown. However, since the objective of yard switching is to sort and group railcars by common destination, a simplifying assumption can be made that all tank cars remain grouped together during railcar shunting. The train in this example has four non-tank cars ($1^{st} - 3^{rd}$ Non-Tank, and 7^{th} Non-Tank) and three tank cars ($4^{th} - 6^{th}$ Tank).

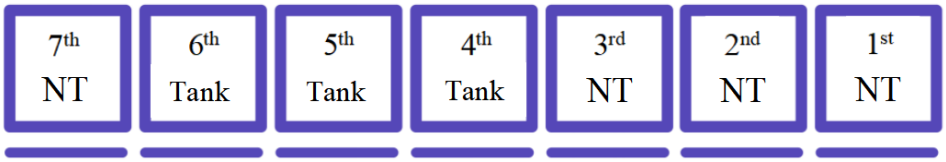

Figure 18. Example yard switching consist with seven railcars composed of three tank cars and four non-tank (NT) cars

The number of tank cars derailed in a yard switching derailment is determined by the position of the POD and the total number of railcars derailed, as shown by the matrix for the example railcar composition (Table 15).

Table 15. Example number of hazmat cars derailed given POD and total number of cars derailed

	POD	Total Number of Cars Derailed						
		1	**2**	**3**	**4**	**5**	**6**	**7**
Non-tank	**1**	0	0	0	1	2	3	3
Non-tank	**2**	0	0	1	2	3	3	
Non-tank	**3**	0	1	2	3	3		
Tank Car	**4**	1	2	3	3			
Tank Car	**5**	1	2	2				
Tank Car	**6**	1	1					
Non-tank	**7**	0						

Based on the number of cars derailed distribution described previously (Figure 17), the probability of x number of cars derailed given that a yard switching derailment has occurred can be determined (Table 16) based on the fitted generalized exponential distribution of derailment severity. The distribution includes the possibilities of derailing from 1 to 20 or more railcars, with an overall probability summing to one. For circumstances when the cut of cars is shorter than 20 railcars in length, the maximum number of cars that can derail is constrained by the

length of the cut. Therefore, the possibility of derailing all railcars in the block is truncated. The value Pi'(x_{max}) is defined as the truncated probability of derailing x railcars when x_{max} is the maximum number of cars that can derail due to the length of the car group. Hence, if the cut of cars is only one car long, given that at least one railcar derailed, the probability of derailing one car under this condition is 1 (P_i'(1)=1).

A key difference between the yard switching methodology and that used for mainline and train A/D events is that these same derailment size probabilities are applied to any railcar regardless of its position within the group of railcars being switched. This assumption is made because the probability of a yard switching derailment occurring is calculated per railcar processed. Given that railcar positions are either unknown or change during the switching process, there is no basis to adjust either the per-railcar probability of causing a derailment or the probability distribution of the number of railcars derailed based on railcar position. However, the point of derailment influences the maximum possible number of cars derailed and when the truncated probability should be applied. In the example, if the derailment starts at the 6th railcar, a maximum of two railcars can derail (the 6th and 7th). The complete probability of the number of cars derailed given POD (Table 17) is derived by truncating the distribution in Table 16 when appropriate. In addition, as explained previously, the probability of the point of derailment occurring at any specific railcar position is assumed to be equal for all possible positions and is therefore equal to 1/7 (0.143) in the example.

Table 16. Probability of derailing x railcars in yard switching incident

x	1	2	3	4	5	6	7
CDF(x)	3.11E-01	5.25E-01	6.73E-01	7.75E-01	8.45E-01	8.93E-01	9.26E-01
$P_i(x)$	3.11E-01	2.14E-01	1.48E-01	1.02E-01	7.01E-02	4.83E-02	3.32E-02
$P_i'(x_{max})$	1.00E+00	6.89E-01	4.75E-01	3.27E-01	2.25E-01	1.55E-01	1.07E-01
x	**8**	**9**	**10**	**11**	**12**	**13**	**14**
CDF(x)	9.49E-01	9.65E-01	9.76E-01	9.83E-01	9.89E-01	9.92E-01	9.95E-01
$P_i(x)$	2.29E-02	1.58E-02	1.09E-02	7.49E-03	5.16E-03	3.55E-03	2.45E-03
$P_i'(x_{max})$	7.36E-02	5.07E-02	3.49E-02	2.41E-02	1.66E-02	1.14E-02	7.86E-03
x	**15**	**16**	**17**	**18**	**19**	**20**	**>20**
CDF(x)	9.96E-01	9.97E-01	9.98E-01	9.99E-01	9.99E-01	9.99E-01	1.00E+00
$P_i(x)$	1.69E-03	1.16E-03	8.00E-04	5.51E-04	3.80E-04	2.61E-04	5.79E-04
$P_i'(x_{max})$	5.42E-03	3.73E-03	2.57E-03	1.77E-03	1.22E-03	8.40E-04	5.79E-04

Table 17. Probability of number of cars derailed given POD

POD Prob.	POD	Cars Derailed							
		1	2	3	4	5	6	7	Sum
0.143	**1**	0.311	0.214	0.148	0.102	0.070	0.048	0.107	1.000
0.143	**2**	0.311	0.214	0.148	0.102	0.070	0.155		1.000
0.143	**3**	0.311	0.214	0.148	0.102	0.225			1.000
0.143	**4**	0.311	0.214	0.148	0.327				1.000
0.143	**5**	0.311	0.214	0.475					1.000
0.143	**6**	0.311	0.689						1.000
0.143	**7**	1.000							1.000

Combining the probability distribution of severity given POD and the probability of each POD from Table 17, the probability of x number of cars derailed given that a yard switching derailment occurs is shown in Table 18. Using data from Table 15, the number of hazmat cars involved in each derailment scenario is indicated in Table 18 by various colors of shading: red for three, orange for two, yellow for one, and green for zero hazmat cars derailed, respectively.

Table 18. Probability of total number of cars derailed categorized by resulting number of tank cars derailed

	Cars Derailed							
POD	**1**	**2**	**3**	**4**	**5**	**6**	**7**	**Sum**
1	0.044	0.031	0.021	0.015	0.010	0.007	0.015	0.143
2	0.044	0.031	0.021	0.015	0.010	0.022		0.143
3	0.044	0.031	0.021	0.015	0.032			0.143
4	0.044	0.031	0.021	0.047				0.143
5	0.044	0.031	0.068					0.143
6	0.044	0.098						0.143
7	0.143							0.143

Shading color code: Red = 3 cars derailed, Orange = 2, Yellow =1, Green = 0

After grouping and summing each probability in Table 18 by the number of hazmat cars derailed, the conditional probability of y number of tank cars derailed given that a derailment occurs for this example cut of cars is summarized in Table 19.

Table 19. Conditional probability of y tank cars derailed given yard switching derailment occurs for the example group of railcars

Hazmat Cars Derailed (y)	Probability
0	0.358
1	0.298
2	0.175
3	0.169
Sum	1

3.2.4 Tank Car Releasing Probability and Consequences

Once the yard-specific derailment rates, the number of cars derailed, and the distribution of tank cars derailed are determined, the probability distribution of the number of tank cars releasing content described in Section 6 is applicable to the remainder of the yard and terminal derailment risk analysis for both A/D events (i.e., unit and manifest trains) and yard switching events (i.e., manifest trains only). The same methodology is used except the CPR is reduced by multiplying by a factor of 0.35 to reflect the fact that most yard accidents have lower severity and chance of release than mainline accidents in general, due to lower yard operating speeds relative to mainline speeds, for which the base CPR factors are developed (Treichel et al., 2019a). The details of this exercise are described in Section 9.

3.3 Additional Considerations

The normalized position of derailment on mainlines might be affected by train type, operation speed, and train length (i.e., locomotives and railcars). The research team conducted a comparison of the Beta distribution fits for all data combined, using data with derailment speeds above or below the average speed, and using data with train lengths above or below the average for unit trains and manifest trains (drawn from FRA train derailment data from 1996 to 2018). The average train length is 110 cars for unit trains and 83 cars for manifest trains, including locomotives and railcars. The average derailment speed is 25 mph for both unit and manifest trains. The best Beta distribution fits of NPOD, considering different impacting factors, are summarized in Table 20. Figure 19 shows the similarity of the fitted NPOD distributions among different datasets considering derailment speed and train length. Although derailment speed and train length slightly affect the Beta distribution fits of NPOD, the differences are not significant.

Table 20. Parameters of best fitted Beta distribution using various datasets considering different factors

(a) Considering derailment speed for unit trains

Unit train	Data that has derailment speed greater than or equal to 25 mph	Data that has derailment speed less than 25 mph
α	0.81	0.70
β	1.01	0.89

(b) Considering train length for unit trains

Unit train	Data that has train length (the number of locomotives and railcars) greater than or equal to 110	Data that has train length (the number of locomotives and railcars) less than 110
α	0.77	0.74
β	0.94	0.96

(c) Considering derailment speed for manifest trains

Manifest train	Data that has derailment speed greater than or equal to 25 mph	Data that has derailment speed less than 25 mph
α	0.78	0.79
β	1.06	1.13

(d) Considering train length for manifest trains

Manifest train	Data that has train length (the number of locomotives and railcars) greater than or equal to 83	Data that has train length (the number of locomotives and railcars) less than 83
α	0.79	0.78
β	1.08	1.13

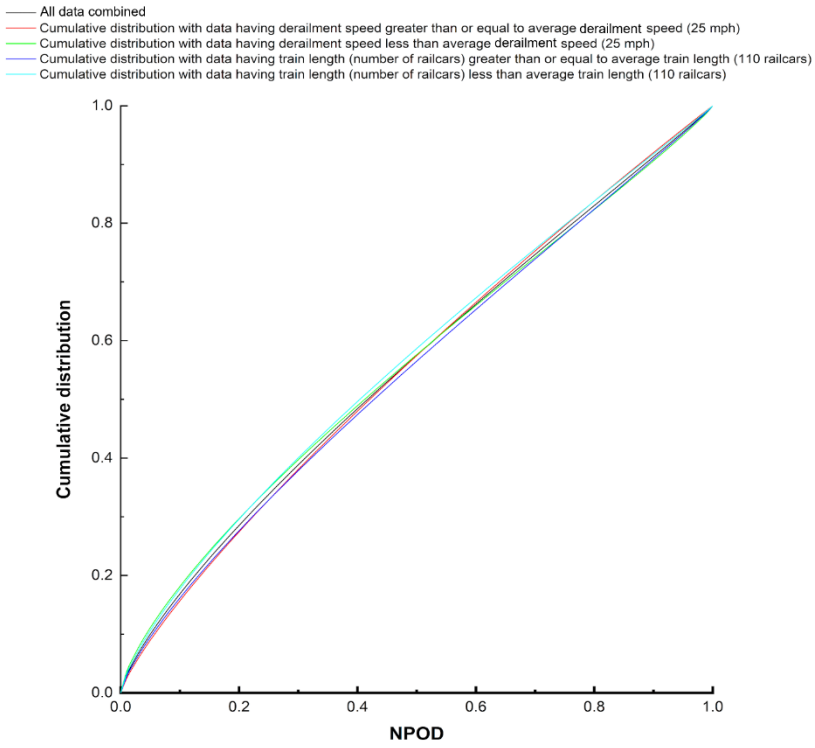

(a) Unit train

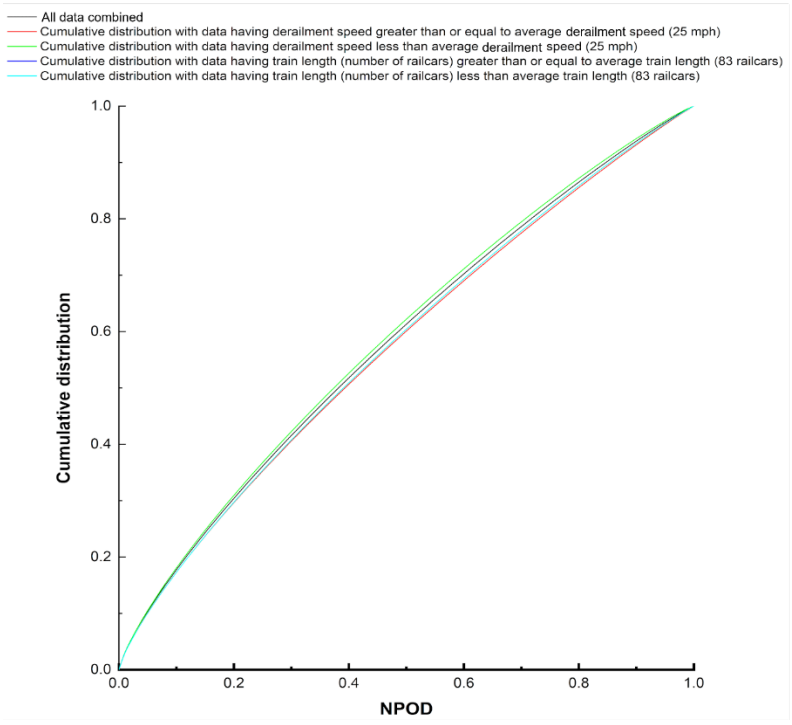

(b) Manifest train

Figure 19. Comparison of best fitted NPOD distributions for (a) unit train and (b) manifest train considering derailment speed and average train length

4. Mainline Derailment Rate Analysis

4.1 Quantifying Recent Trends in Class I Freight Railroad Train Length and Weight by Train Type

Railroads have a strong economic incentive to maximize the length and weight of freight trains. Since the mid-1990s, various technological innovations have facilitated the operation of longer and heavier trains, and railroads have since made infrastructure investments to accommodate them. Recent shifts in railway operating and management strategies have increasingly emphasized long trains but have also drawn public and agency scrutiny. The advantages and disadvantages of increased train size are difficult to analyze because public data on train length and weight over time is limited. Articulated intermodal railcars, artificially short local trains, and light empty unit trains skew industry averages across all train types and mask trends over time. To provide greater insight on the average and distribution of train length and weight for different train types over time, the research team conducted a detailed analysis of Class I railroad annual report financial data and STB waybill sample data collected for the years 1996 through 2018. Dividing traffic statistics by train type allows for a specific focus on loaded unit train length and weight distributions, which isolates many of the factors responsible for skewing overall averages. Over the past 23 years, the average length and weight of loaded, non-hazmat unit trains have steadily increased. Train size distributions indicate that unit trains exceeding 140 railcars in length have become more frequent over the past ten years while hazmat unit trains are typically smaller in size. This information can aid researchers and industry practitioners in assessing the benefits and disadvantages of operating longer trains.

4.1.1 Introduction

In the United States, Class I freight railroads transport approximately 1.7 billion tons of freight each year (AAR, 2019a). Freight railroads seek to obtain economies of scale by hauling many loaded railcars with a single crew and a small number of locomotives. Certain train operating costs are independent of train length, making longer and heavier freight trains more economically viable. For example, labor costs for the train crew, which comprise one of the largest components of the total operating cost (Lovett et al., 2015), are fixed per train start and thus distributed over more revenue tons of freight as train length and weight increase. Longer and heavier trains also can reduce costs through improved fuel efficiency, partly because aerodynamic drag is greatest at the front of a train and partly because heavier railcars typically have less aerodynamic drag area per revenue ton of freight. Other factors such as train speed and route terrain also have a large effect on fuel efficiency (Fullerton et al., 2015).

From a capacity perspective, longer trains allow fewer trains to move the same volume of freight across a mainline corridor (Barrington & Peltz, 2009; C. Martland, 2013; Moore Ede et al., 2007). However, long trains spend more time traversing speed restrictions and impose higher individual meet delays on opposing traffic (Diaz de Rivera et al., 2020). Long trains also can increase mainline train delay and reduce capacity if they exceed the length of most passing sidings on single-track lines (Atanassov & Dick, 2015; Dick et al., 2019)/ this is a key consideration in North America, where approximately 70 percent of principal mainlines are single track with passing sidings (Richards, 2006). At yards, long trains with a greater number of blocks are more complicated to assemble and prepare for departure, decreasing yard efficiency (Dick, 2019). From a service perspective, longer trains may require customers to ship greater

quantities of freight in a single batch, and railroads may hold trains until more railcars for a common destination are ready to depart on the same train (Dong, 1997). These actions provide railroads with greater economies of scale, but they also run counter to the preferences of many shippers for faster, more reliable railcar transit times across the rail network.

From a safety perspective, statistical analysis of derailments on U.S. Class I railroads from 2006 to 2015 suggests that dispatching a fixed number of railcars in fewer, longer trains can decrease the expected number of derailments (Wang, 2019). However, perceived operational safety issues associated with longer trains, such as crew fatigue, train handling, braking reliability, and lengthened blockages of highway-rail grade crossings, have drawn the attention of the U.S. federal government (Government Accountability Office (GAO), 2019).

The cost, capacity, service, and safety advantages and disadvantages of increased train size are difficult to analyze because there is relatively little public data available on train length and weight over time. Since most freight railroad operating data is proprietary, published statistics are typically aggregated at the industry level across all commodities and train types, making them difficult to interpret. To better identify and quantify recent trends in increasing train length and weight by train type, the research team conducted a more detailed analysis of public rail traffic data.

4.1.1.1 Past and Present Emphasis on Train Size

The economies of scale that drive railroads to operate longer and heavier freight trains have been present for decades and are a fundamental feature of rail transportation. Outside of closed-loop mine-to-port operations, specialized shipments of single commodities in bulk "unit trains" comprising approximately 100 railcars began operating in the United States during the 1960s (Starr, 1976). In 1967, the Norfolk & Western Railroad (now part of Norfolk Southern) set the current North American record for the longest and heaviest freight train by testing a loaded coal train with 500 railcars stretching over 21,000 feet in length and weighing over 48,000 tons. Prior to the deregulation of U.S. railroads in 1980, various regulations on crew size and rates for multiple-car shipments limited the economic benefits associated with longer trains. The mechanical strength of couplers, locomotive adhesion, and train braking capability also limited practical train lengths. But the advent of distributed power in the 1980s, and alternating current traction locomotives with higher adhesion and improved low-speed tractive effort capabilities in the 1990s, allowed bulk unit train lengths to exceed 120 railcars (Beck et al., 2003). By 2010, railroads operated 150-railcar trains on certain corridors (AAR, 2019a). Today, longer trains are not limited to bulk commodities, as railroads have implemented 14,000-foot intermodal trains on transcontinental corridors (Bell, 2013).

Railroads also boost economies of scale by using heavier trains to increase the payload capacity of individual railcars so that larger weights can be carried. In 1991, U.S. Class I freight railroads began to accept railcars with 286,000 lb (286k) gross railcar weight in interchange service (Martland, 2013). With a nominal payload capacity of 110 tons, these new railcars offered a 10-percent increase in tons of freight per railcar, compared to the previous maximum of 100 tons carried by a railcar with a gross weight of 263,000 pounds (Newman et al., 1991). Analyzing the impact of this new railway technology on grain transportation in Western Canada, Dick and Clayton (2001) described how improved railcar manufacturing technology allowed new 286k covered hoppers for grain service to be shorter and have a lower empty tare weight than the 263k railcars they replaced (Dick & Clayton, 2001). The shorter but heavier railcars allowed railroads

to further increase train weight and freight transportation productivity by fitting a larger number of railcars into the same linear length of train. By 2010 and 2011, respectively, nearly all U.S. coal traffic (Martland, 2013) and nearly 70 percent of U.S. grain traffic (Prater & O'Neil Jr, 2013) was converted to 286k railcars (grain traffic conversion lags because many branchlines and shortlines that serve agricultural areas have insufficient traffic density to economically upgrade bridges and track structure to handle 286k railcars).

With the removal of technological and regulatory barriers, the main impediments to even longer and heavier freight trains, which would further minimize operating costs, are railroad policy, freight shipment demand patterns, and the length of passing sidings (Grimes, 1981; Keaton, 1991). Martland (2008) noted the inability of existing passing sidings to support the operation of long trains and estimated that two-thirds of unit trains in operation are "length-limited" by passing sidings. The length of a typical existing passing siding on single track in North America ranges from 6,000 to 7,500 feet to accommodate trains of 100 to 120 railcars (Blaine et al., 1981). Railroads have invested capital to extend the length of these existing passing sidings (Welch & Gussow, 1986) to accommodate trains exceeding this length, and have constructed new sidings of 9,000 to 10,000 feet to support trains with 150 railcars and 7 distributed power locomotives. Recently, Class I railroads have increased their standard siding length to 12,000 feet to support even longer trains (Barton & McWha, 2012). In the early 1990s, the Illinois Central Railroad (now operated by Canadian National) converted its mainline from double track to single track with 15,000-foot passing sidings every 12 miles (Blaszak, 1992). These extended passing sidings allowed the railroad's management to develop a long train operating strategy that became a key component of the Precision Scheduled Railroading (PSR) concepts promoted by former CEO E. Hunter Harrison (Harrison, 2005). With the widespread implementation of business strategies incorporating PSR and its focus on asset utilization and cost control, several Class I railroads are pursuing ever longer trains (Barrow, 2019; Government Accountability Office (GAO), 2019; Stagl, 2018).

Public and government agency scrutiny of train length and weight has heightened in recent years due to an increase in the number of trains transporting large quantities of petroleum crude oil and ethanol. A series of derailments involving these trains resulted in the release of large quantities of hazmat and caused subsequent fires, which prompted federal action to address the safe transportation of flammable liquids by rail (PHMSA, 2015). To properly assess the safety of petroleum crude oil and ethanol unit trains, these incidents must be placed in proper context given trends in railway traffic, train length, and train weight by train type over time. This reinforces the importance of conducting a more detailed analysis of public rail traffic data to identify and quantify recent trends in increasing train length and weight by train type.

4.1.1.2 Train Size Metrics

This report primarily examines train size in terms of length and weight. Common metrics to quantify train length are the total number of railcars in the train and the total linear length of the train in feet. Although the linear length of each train is a critical operating parameter and is documented on each train manifest, it is not reported or documented directly in any public datasets. While the number of railcars per train is more readily available and can be derived from other railroad operating statistics, it is not an ideal metric for general comparisons of train length across all train types. Individual railcars come in a variety of shapes and sizes, optimized to the density of a particular lading or otherwise customized to a certain type of service. Conventional

single-unit four-axle railcars with two trucks (i.e., bogies) can range in length from 29 to 89 feet. Articulated, twin-unit autoracks used to transport motor vehicles are approximately 145 feet long. Intermodal railcars used to transport highway trailers and shipping containers are much longer than conventional railcars – twin-unit drawbar-connected flatcars are approximately 190 feet long while five-unit articulated or drawbar-connected well cars in double-stack container service can exceed 300 feet in length for a single railcar. Articulated railcars for transporting coal, grain, and potash have only seen prototype or limited experimental use, making railcar lengths much more consistent for unit trains transporting a particular commodity. When measured in linear feet, a 25-railcar intermodal train composed of five-unit articulated railcars may exceed the length of a unit train composed of 125 railcars where each railcar is 55 feet long.

Common metrics to quantify train weight are gross tons, gross trailing tons, and revenue tons of freight. Gross tons refer to the total weight of the train including the operating weight of the locomotives, tare (i.e., empty) weight of the railcars, and the weight of lading (i.e., the freight being shipped). Gross trailing tons is the total weight of the train excluding all locomotives (i.e., the weight of all railcars and lading). Revenue tons refers only to the weight of the freight being transported and excludes the weight of the locomotives and tare weight of the railcars. While all three types of weight metrics are generally proportional to train length in feet and number of railcars, railcar weight can vary greatly between commodity, type of service, and empty and loaded condition. For example, a mixed freight train (i.e., manifest train) typically includes a mixture of empty and loaded railcars that often do not use a 286k maximum gross railcar weight. A unit train of equal linear length and number of railcars where every railcar is loaded to 286k or 263k gross weight will be much heavier than the manifest train. Further, an intermodal train of the same linear length but with fewer longer railcars and carrying trailers and containers of lightweight, high-value consumer goods will likely be lighter than both the manifest and the unit train.

4.1.1.3 Published Data and Previous Research

AAR publishes the most readily available public data on train size over time in their annual "Railroad Facts" publication (AAR, 2019a). The AAR data includes average railcars and average revenue tons per freight train combined across all U.S Class I railroads for each year dating back to 1929. In 2018, the average freight train consisted of 73.5 railcars and transported 3,661 tons of freight. Both metrics show long-term trends of increasing average train length and weight over time. However, as an average overall train type, the data does not fully capture changes in the distribution of train length and weight over time and provides little information about the magnitude and frequency of the heaviest and longest trains. The calculation of average train length and weight includes local trains (i.e., way freights) that distribute and collect railcars from individual rail shippers. In fulfilling this role, local trains naturally have fewer railcars and weigh less than long-distance trains operating between major terminals, skewing both averages toward lower values.

The average railcars per train metric published by AAR appears to show the effect of articulated intermodal railcars developed in the 1980s. According to the data, despite industry efforts to accommodate and operate longer trains over the past few decades, the average train length in 2018 was only 3.5 railcars longer than in 1970, 1.7 railcars longer than in 1985, and 1.2 railcars shorter than in 2010. This same period saw unprecedented growth in intermodal traffic and the adoption of long, multi-unit, articulated railcars allowing railroads to transport trailers and

containers using fewer railcars. Intermodal trains have grown longer as measured by linear feet per train while becoming substantially shorter as measured by the number of railcars per train. Separately calculating average train length by type of train or service can help isolate the influences of intermodal and local trains.

Although the number of railcars per train published by the AAR has not increased substantially over the past few decades, the revenue tons per train have seen a much larger increase. In 2018, the average train carried approximately twice as many revenue tons as in 1970, 42 percent more tons than in 1985, and 2 percent more tons than in 2010. These increases are more consistent with industry efforts to operate longer and heavier trains. However, as with train length, the average revenue tons per train includes local trains that naturally carry fewer tons of freight. The average also includes empty railcars that count as zero revenue tons toward the average, further skewing the absolute magnitude of the average revenue tons per train away from the heaviest trains. Separately calculating the weight of empty and loaded unit trains could provide a better metric for the average weight of the heaviest trains.

Few published distributions of train length and/or weight exist to supplement the AAR averages. Wang (2019) presented distributions of train-miles and railcar-miles for two Class I railroads. One railroad provided a distribution of operating train-mile traffic for the years 2011 to 2015, grouped by train length in linear feet, where approximately 15 percent of train-miles were accumulated by trains longer than 8,000 feet or 129 railcars (assuming an average length of 62 feet per railcar). The second railroad provided more detailed operating data for the years 2014 to 2016, which were used to construct a similar distribution showing approximately 24 percent of train-miles were accumulated by trains with 120 or more railcars, including 5 percent of train-miles accumulated by trains with 150 or more railcars. Although these distributions provide greater insight into the magnitude and frequency of long train operations, they represent a single snapshot that does not show trends over time. Also, since the distributions consider all types of traffic, railcar counts are subject to the same influences from local and intermodal trains described earlier.

4.1.1.4 Research Questions

The previous sections have described the limitations of available data on train length and weight that are essential to assess the safety of operating longer and heavier trains. To provide a better understanding of how train length and weight have changed in recent decades, the research team conducted a more detailed analysis of public rail traffic data to identify and quantify recent trends by train type and commodity.

The team investigated the following research questions for the period 1996 to 2018:

- How has the share of rail traffic by train type changed over time?
- What are the trends in average train length and weight by train type over time?
- What is the distribution of loaded unit train traffic by length and weight over time?
- How has the share of hazmat traffic moving in unit trains and the share of unit train traffic involving hazmat changed over time?
- What are the trends in average train length for non-hazmat unit trains and unit trains carrying various hazmat commodities over time?

4.1.2 Methodology

To address the research questions, the team analyzed two types of traffic data from the STB: "R-1" Annual Report Financial Data and Public Use Carload Waybill Sample Data. The following subsections detail each of these two data sources and the analysis performed to obtain traffic data of interest.

4.1.2.1 STB "R-1" Annual Report Financial Data

Since 1996, every U.S. Class I railroad has been required to file an annual report with the STB. These annual reports, commonly referred to as the "R-1" Annual Report Financial Data, summarize various financial, asset ownership, and operating data, as well as statistics for each calendar year (STB, 2020b). Within the report submitted by each railroad, Schedule 755 summarizes various railroad operating statistics of interest to this research. The following line items (numbers in each bullet refer to Schedule 755 line items) were collected for each Class I railroad for the period 1996-2018, inclusive (2019 R-1 data was not available at the time this work was done):

- 2-5. Train-miles running (unit, way, through, and total)
- 8-11. Locomotive unit-miles (unit, way, through, and total)
- 85-88. Car-miles (unit, way, through, and total)
- 99-101. Gross ton-miles (unit, way, and through)
- 117. Yard switching hours
- 120-122. Number of loaded freight cars (unit, way, and through)

The above statistics cover all railroad traffic transported during a given year, including hazmat and non-hazmat traffic. A useful aspect of these statistics not found in other statistical summaries of railroad transportation productivity is that they include totals by train type. The instructions for Schedule 755 define unit, way, and through trains as follows (STB, 2020b):

- Unit trains are single-commodity trains on a single waybill moving from origin to destination in specialized service.
- Way trains are "locals" operated primarily to gather and distribute cars and move them between rail shippers and intermediate stations or points.
- Through trains are those operated between two or more major concentration or distribution points (i.e., yards and terminals).

These train type divisions provide two key benefits when examining train length and weight. First, as described earlier, local (i.e., way) trains that distribute and collect railcars at a small number of shippers are naturally shorter and lighter than other long-distance trains. Isolating way train traffic into a separate train type category removes this effect from the average values calculated for through and unit trains. Secondly, because unit trains typically do not involve intermodal traffic, the effect of articulated intermodal railcars can be isolated to way and through trains. The combined effect of isolating these effects is that the average number of railcars will be a more accurate representation of the average linear length of unit trains.

A limitation of the "R-1" data is that unit train traffic does not distinguish between loaded and empty unit trains. As described earlier, the light weight of empty unit trains can heavily skew average train weight calculations away from the heaviest unit trains that are generally of greater interest. Thus, the research team devised an approach to divide the various unit train traffic statistics between loaded and empty unit trains. Unit trains typically make a loaded trip from origin to destination and then return empty to the same origin for reloading. In some cases, such as a power plant that receives coal from multiple mines, the unit train may cycle to various origins and the loaded and empty trips may not be of identical length. Directional running and various other operational and routing preferences can also cause the loaded and empty unit train trips to be of slightly different lengths. However, across all unit train operations for all Class I railroads during a given year, the research team felt it was reasonable to assume no overall net circuity between the loaded and empty portions of a unit train round trip. On this basis, reported train-miles and car-miles are evenly split into 50 percent loaded and 50 percent empty. Quantitative support for this assumption is provided by the empty and loaded car-miles by car type in Schedule 755. For two common unit train car types (i.e., open hoppers and covered hoppers), annual empty and loaded car-miles are approximately equal. A caveat of this observation is that the empty and loaded car-mile data by car type includes all train types and is not specific to unit trains.

Because of the different train weight on the loaded and empty portion of each trip, dividing gross ton-miles between empty and loaded unit trains requires additional assumptions beyond equal empty and loaded trip distance. To determine an appropriate factor, the research team calculated loaded and empty gross tons for a range of typical unit train conditions:

- two, three, or four locomotives (each weighing 205 tons), and
- 90, 100, 110, or 120 railcars, either
    - 286k with loaded weight 143 tons and empty weight 33 tons, or
    - 263k with loaded weight 131.5 tons and empty weight 31.5 tons

For each combination of number of locomotives, number of railcars, and railcar weights, the proportion of loaded gross tons was calculated by dividing the loaded train gross tons by the sum of the loaded and empty train gross tons for that configuration. The combination of two locomotives, 120 railcars and 286k weight produced the highest factor, with 80.1 percent of gross tons being loaded. The combination of four locomotives, 90 railcars and 263k weight produced the lowest factor at 77.6 percent. Averaged across all 24 possible combinations, the loaded unit train contributes 79 percent of gross ton-miles while the empty unit train contributes 21 percent of gross ton-miles. Thus, the factors of 0.79 and 0.21 were applied to derive empty and loaded gross-ton miles from the total values provided in the "R-1" data.

During data analysis, the research team noticed various inconsistencies in the data provided by Kansas City Southern (KCS). Thus, the subsequent analysis and presentation of traffic data do not include any KCS traffic. However, all other Class I railroads are included for the years 1996-2018. Due to railroad mergers and acquisitions during the study period (e.g., the division of Conrail between CSX and Norfolk Southern; CN acquiring Illinois Central, Wisconsin Central and other smaller carriers; Canadian Pacific acquiring Dakota, Minnesota & Eastern and other smaller carriers; and Union Pacific's merger with Southern Pacific) the overall scope of

operations covered by the data changes over time. These changes can help explain some of the temporal discontinuities and irregularities in various annual traffic measures.

4.1.2.2 STB Public Use Carload Waybill Sample Data

The STB "R-1" data provides measures of overall traffic levels and average train sizes by train type but does not give any insight into the distribution of train sizes by train type or the average train size associated with hazmat traffic or specific commodities. To answer these questions, the research team analyzed STB Public Use Carload Waybill Sample Data, a stratified sample of carload waybills for all U.S. rail traffic submitted by rail carriers terminating 4,500 or more revenue carloads annually (STB, 2020a). The waybill data for years 1996 to 2018, inclusive, were used for this research.

Each record in the sample data provides details on one waybill (i.e., shipment from origin to destination) and includes the following fields of interest to this research (numbers refer to the field number in the waybill sample data record layout):

- 3. Number of carloads moving on single waybill
- 12. Hazmat shipment flag
- 13. Standard Transportation Commodity Code (STCC)
- 14. Billed tons of freight
- 26. Shipment distance (rounded to the nearest 10 miles)
- 27. Sampling stratum (based on number of carloads)
- 29/30. Expansion factor
- 59. Expanded carloads
- 60. Expanded tons

The data does not contain a record for every waybill each year. As a sample, each waybill record is representative of several actual waybill movements based on a particular sampling rate. To convert the carloads and tons for a given waybill in the sample into actual traffic, the carloads and tons specified for the sample waybill must be multiplied by the appropriate expansion factor. The waybill data is a stratified sample with waybill shipments sampled at different rates depending on the number of carloads moving on a particular waybill. Four different sampling rates are specified in the creation of the sample, corresponding to shipments of 1-2 railcars, 3-15 railcars, 61-100 railcars, or 101 or more railcars. The expansion factor is the inverse of the sampling rate per year.

For example, small shipments are sampled at an approximate rate of 1 in 40. If a waybill includes two carloads with a total weight of 200 tons (100 tons/car), this rate corresponds to an expansion factor of approximately 40, making this waybill equivalent to 40 shipments, 80 carloads, and 8,000 tons. In comparison, large multi-car shipments are sampled at an approximate rate of 1 in 2. If another waybill includes 110 carloads with a total weight of 1,100 tons (100 tons/car), this rate corresponds to an expansion factor of approximately two, making this waybill equivalent to two shipments, 220 carloads, and 22,000 tons. The exact expansion factor based on the actual sampling rates is included in fields 29 and 30 of each waybill record.

There are two main limitations to the STB waybill data in the context of this study: 1) the data does not contain any information on empty car movements, and 2) the data does not contain any information on the type of train in which the railcars shipped under a particular waybill are moving. To gain information on unit and manifest train traffic from the waybill data, the research team inferred unit train traffic from the size of multi-car shipments. Waybills with 1-2, 3-15, or 15-60 carloads are likely moving in manifest trains along with other railcars shipped under their own separate waybills. Waybills with 61-100 or 101 or more carloads per waybill are large multi-car shipments that correspond to unit train movements. Thus, the research team assumed that one multi-car shipment of 60 railcars or more corresponds to one loaded unit train. Under this assumption, the research team used the expansion factors to directly total the number of shipments, carloads, and tons moving in unit trains and the amount of traffic moving in manifest trains. The carloads, revenue tons, and distance fields are used to calculate car-miles and revenue ton-miles by type of train. Similarly, the hazmat flag field identifies the proportion of shipments, carloads, car-miles, and revenue ton-miles by train type that are hazmat shipments.

Unfortunately, there is no practical approach for deducing manifest train-miles from the waybill data. The waybills are disaggregated, and individual shipments cannot be recombined into trains between specific origin and destination terminals. However, by assuming that each large multi-car shipment corresponds to a single unit train, the expanded number of shipments for each waybill and the shipment distance are used to calculate "shipment-miles" as a proxy for unit train-miles.

4.1.3 Results

The following sections present the results of STB "R-1" Annual Report Financial Data analysis and Public Use Carload Waybill Sample Data analysis conducted to address each of the research questions presented in Section 4.1.1.4.

4.1.3.1 Rail Traffic by Train Type

Compiling R-1 data across all Class I railroads (excluding KCS) for the years 1996 to 2018 reveals various trends in the distribution of traffic by train type (Figure 20-Figure 22). Approximately one quarter of train-miles are contributed by unit trains, while manifest trains contribute approximately three times as many train-miles (Figure 20). Unit trains contribute approximately 40 percent of all car-miles (Figure 21) and 37 percent of gross ton-miles (GTM) (Figure 22), with 29 percent of GTM coming from loaded unit trains alone.

Through train-miles, unit train-miles, and GTM steadily grew between 1996 and 2006. Through train traffic then declined by approximately 25 percent from 2006 to 2009, during a period of economic recession. Largely driven by intermodal traffic, through train GTM recovered between 2009 and 2018 and exceeded the previous peak in 2006. Through train-miles and car-miles have seen a less substantial increase since 2009, suggesting that the average weight of through trains has increased in recent years. Unit train traffic, driven by bulk commodities, continued to grow between 2006 and 2008 before declining approximately 15 percent in 2009. Since 2009, unit train traffic has gradually declined, except in 2014 when unit train traffic peaked to meet or exceed the previous highs from 2008. As will be shown later in this section, the unit train traffic peak in 2014 was driven by record shipments of crude oil in unit trains.

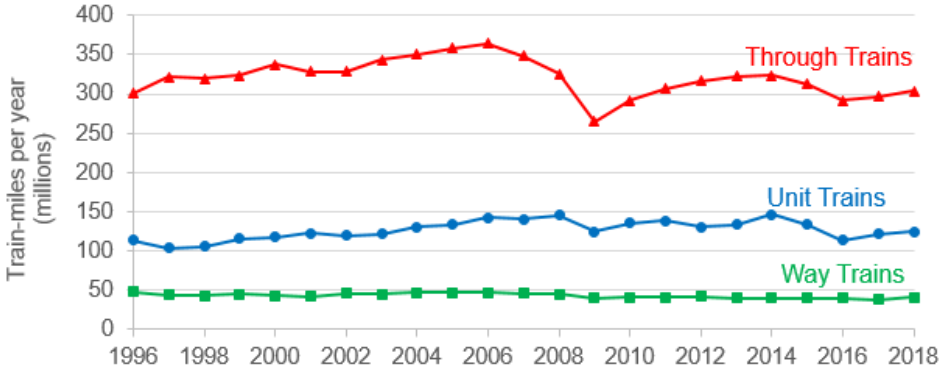

Figure 20. Annual train-miles by train type

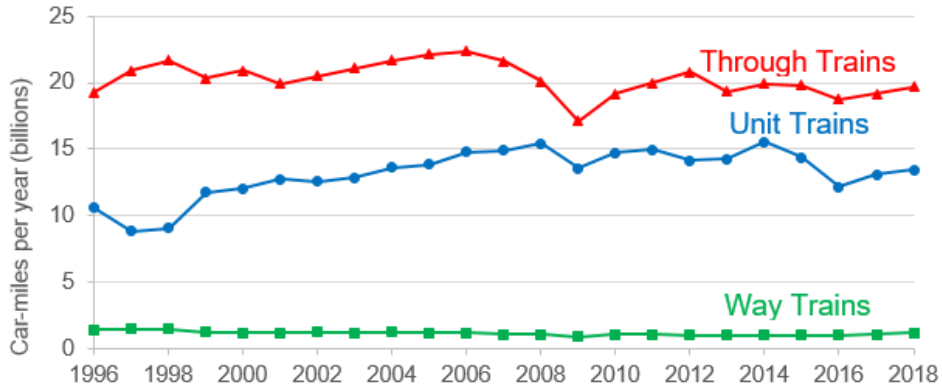

Figure 21. Annual car-miles by train type

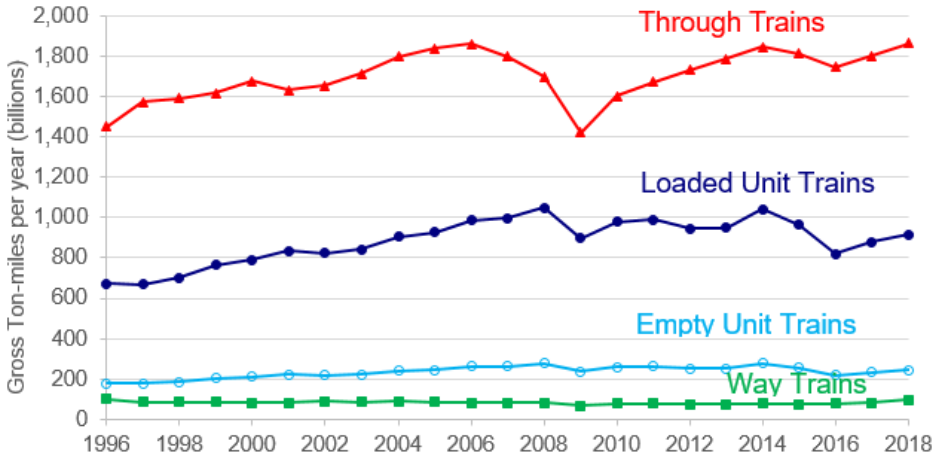

Figure 22. Annual gross ton-miles by train type

4.1.3.2 Average Train Length and Weight by Train Type

The team used the R-1 data to derive average train length and weight metrics for each type of train over time. Dividing car-miles by train-miles for each train type provides a metric of average cars per train by train type (Figure 23). In 2018, the average unit train comprised 108 railcars, the average through train had 65 railcars, and the average way train had 30 railcars. Since intermodal traffic is included under through trains, the average of 65 railcars per train and the inconsistent

trend over time are partially attributed to long, multi-unit, articulated intermodal railcars in through trains. Unit trains show a more consistent trend of increasing train length over time, peaking at 109 railcars per train in 2009. Subsequent analysis suggests that recent increases in maximum unit train sizes have been moderated by the growth of hazmat unit train traffic which tends to move in shorter and lighter unit trains.

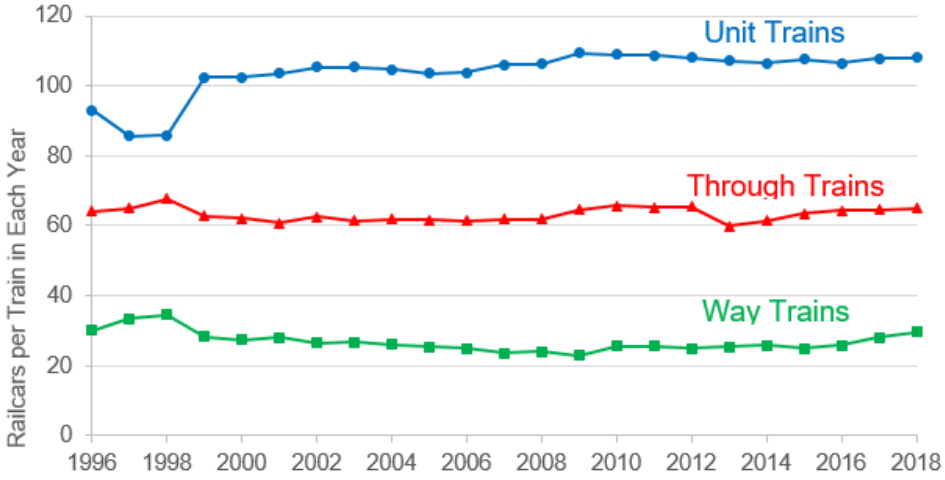

Figure 23. Annual average railcars per train by train type

Dividing gross ton-miles by train-miles for each train type provides a metric of average gross tons per train by train type (Figure 24).

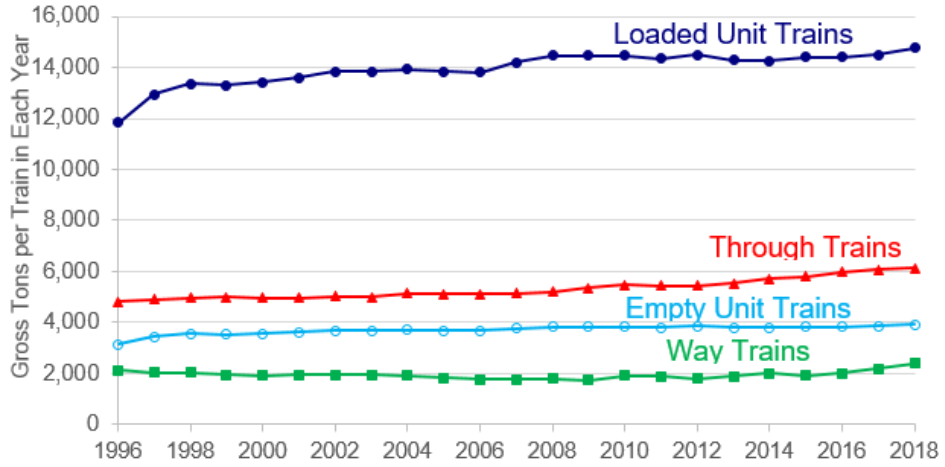

Figure 24. Annual average gross tons per train by train type

At more than 14,000 tons, the average loaded unit train in 2018 was more than twice the average through train weight (approximately 5,000 to 6,000 tons) and seven times the average way train weight (approximately 2,000 tons). Average unit train weights show a similar trend to average unit train lengths, with steady growth observed from 1996 to 2009, followed by less substantial increases. The average weight of through trains has shown a steady increase from 1996 to 2018. Through trains consistently becoming heavier while the average number of railcars per through train has remained relatively constant suggests two conclusions: 1) manifest train traffic is gradually shifting from 263k to 286k railcars, and 2) an increasing proportion of intermodal

traffic is transported on multi-unit articulated railcars with a greater gross weight per railcar (entire articulated combination) than conventional intermodal flatcars.

4.1.3.3 Distribution of Loaded Unit Train Length and Weight

While the average train lengths and weights developed from the R-1 data suggest increasing trends over time, average values do not adequately capture the magnitude and frequency of the longest and heaviest trains. To supplement these averages, the team used multi-car shipment information from the STB data to categorize each loaded unit train movement by train length (in railcars) and weight (in gross trailing tons). This analysis produced distributions of various loaded unit train traffic metrics by train length and weight.

The distribution of loaded unit train GTM by train length shows a substantial shift toward longer trains over time (Figure 25). In 1996, over 93 percent of loaded unit train GTM were accumulated by trains of 120 railcars or fewer, with two-thirds of GTM from trains with lengths between 100 and 120 railcars. From 1996 to 2006, the share of loaded unit train GTM for trains between 121 and 140 railcars in length increased tenfold, from 5 percent to 50 percent. During this same period, the share of loaded unit train GTM for trains longer than 140 railcars remained constant at approximately 1.5 percent. From 2007 to 2018, traffic from trains longer than 140 railcars grew from 1.5 to 8 percent of loaded unit train GTM.

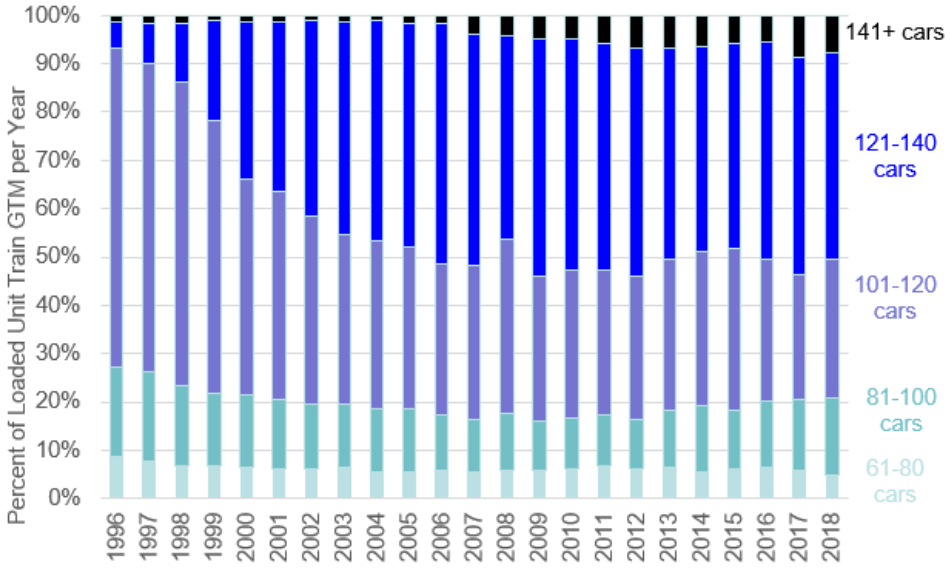

Figure 25. Distribution of annual loaded unit train gross ton-miles by train length

This analysis lends quantitative support to qualitative observations that these longest unit trains have become more common in recent years. After reaching a low of 10 percent of loaded unit train GTM in 2009, trains with lengths between 81 and 100 railcars have seen a resurgence, comprising up to 16 percent of loaded unit train GTM in 2018. It is hypothesized that this increase is largely due to increasing shipments of hazmat in unit trains of this size.

The distribution of loaded unit train GTM by train weight (i.e., gross trailing tons) shows a similar shift to heavier trains over time (Figure 26). As with train length, the most prominent changes are observed between 1996 and 2009, with a resurgence of lighter unit trains in more recent years.

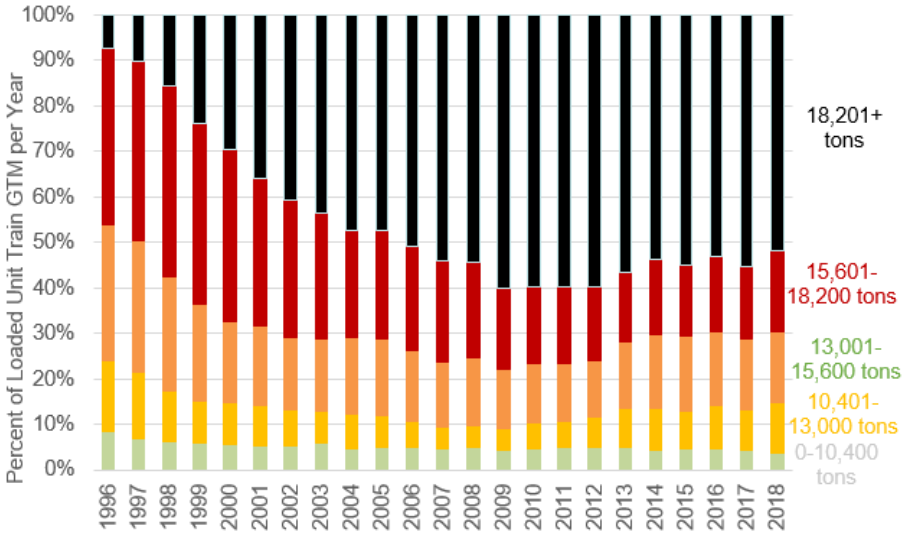

Figure 26. Distribution of annual loaded unit train gross ton-miles by train weight (gross trailing tons)

4.1.3.4 Hazmat Traffic and Unit Trains Over Time

The recent growth in hazmat traffic moving in unit trains has increased scrutiny of train length and weight. To illustrate this trend and classify hazmat traffic by train type, the team sorted STB waybills for hazmat shipments by their number of carloads. Hazmat waybills with 60 or fewer carloads were assumed to move in manifest trains while all others were assumed to be unit train movements. Various traffic metrics were calculated for the hazmat unit train and hazmat manifest train shipments to determine the fraction of hazmat carloads, car-miles, and revenue ton-miles transported in unit trains (Figure 27).

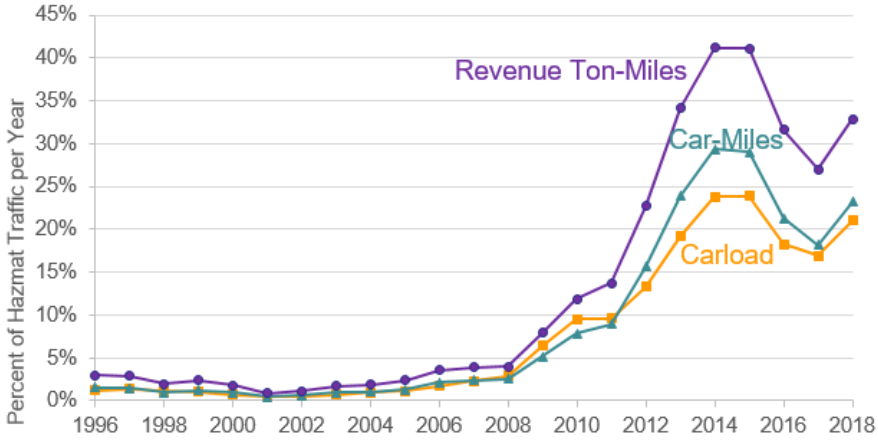

Figure 27. Annual fraction of hazmat traffic in unit trains

In 2018, 99.7 percent of hazmat shipments moved in manifest trains and 0.3 percent in unit trains. Because this small number of hazmat unit train shipments were large multi-car shipments, 21 percent of hazmat carloads moved in unit trains, generating 23 percent of hazmat car-miles and 33 percent of hazmat revenue-ton miles. This distribution of hazmat traffic by train type is quite different from the early years of the study period (1996-2005) when little hazmat traffic moved in unit trains.

A similar analysis was conducted to determine the proportion of unit train traffic involving hazmat. All waybills with 61 or more carloads (assumed to be unit trains) were divided between hazmat shipments and non-hazmat shipments. Various traffic metrics were calculated for the two groups of unit train shipments to determine the hazmat share of unit train traffic (Figure 28). In 2018, hazmat traffic comprised 13 percent of unit train-miles, 8 percent of unit train carloads, 11 percent of unit train car-miles, and 10 percent of unit train revenue ton-miles. The hazmat share of unit train traffic has increased over time, with little hazmat unit train traffic prior to 2008. Hazmat unit trains involve disproportionately fewer carloads and car-miles than predicted by their share of train-miles, indicating that hazmat unit trains are shorter on average than non-hazmat unit trains.

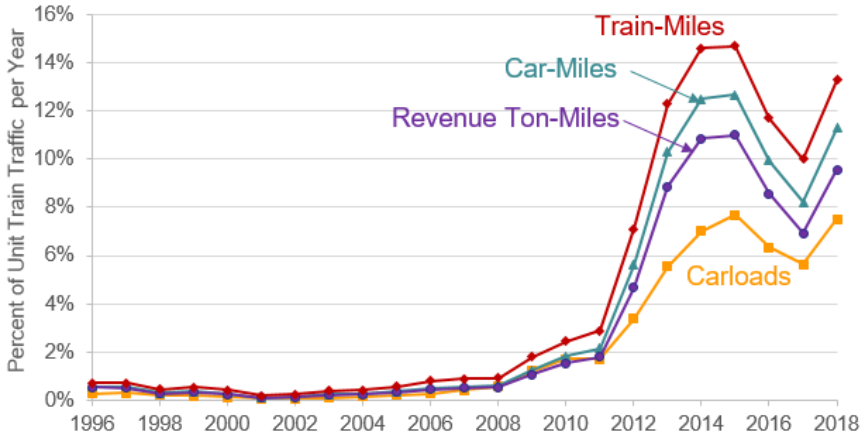

Figure 28. Annual hazmat share of unit train traffic

4.1.3.5 Non-Hazmat and Hazmat Commodity Unit Train Size

As a final step in the traffic analysis, the team used the STCC codes in the waybill data to divide the hazmat unit train traffic by commodity shipped. For 2018, hazmat unit train traffic shipments were approximately 51 percent crude oil, 38 percent ethanol, and 11 percent other commodities such as sulfur, liquefied petroleum gas (LPG), and jet fuel. The distribution of hazmat unit train traffic by commodity over time exhibits distinct trends, with ethanol rising in 2005 and crude petroleum rising in 2010 and peaking in 2014 (Figure 29). Most of the "other" hazmat unit train traffic is sulfur, which dominated hazmat unit train traffic prior to 2005.

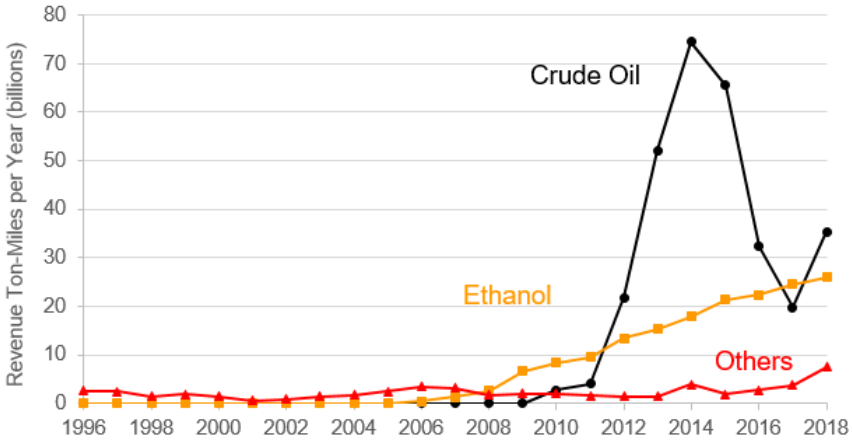

Figure 29. Annual hazmat unit train revenue ton-miles by commodity

Hazmat unit trains exhibit distinct trends in train size, with crude oil unit trains exhibiting a greater average number of railcars in length (Figure 30) and average gross tons per hazmat unit train (Figure 31) than ethanol unit trains and other hazmat unit trains.

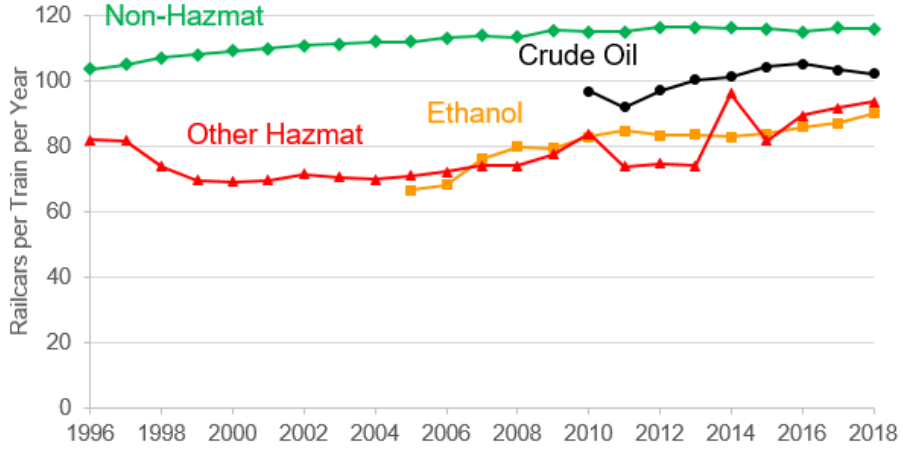

Figure 30. Annual average loaded unit train length by commodity

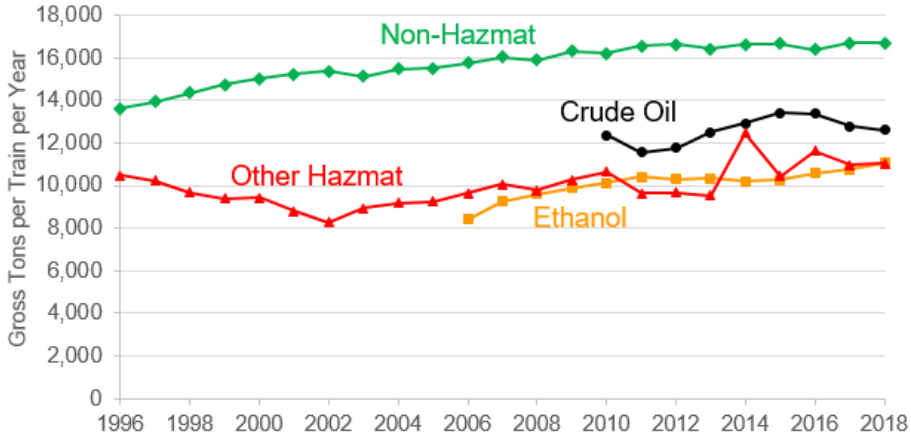

Figure 31. Annual average loaded unit train gross tons per train by commodity

Hazmat unit trains are also substantially shorter and lighter than non-hazmat unit trains. Since 1996, the average length of non-hazmat unit trains has steadily increased from 103 to 116 railcars, and gross tons from 13,600 to 16,700 tons. This difference between train types illustrates how previous average values and distributions of unit train length were influenced by shorter hazmat unit trains.

4.1.4 Conclusions and Future Work

Quantitative analysis of railroad traffic statistics reported to the STB and waybill sample data support anecdotal evidence that train sizes have increased over the past 23 years. Separating traffic data by train type can help isolate the skewing effects of artificially short trains that serve local customers and intermodal railcars that are much longer than typical railcars. Further separating hazmat and non-hazmat unit train traffic can isolate the effects of hazmat unit trains that tend to be shorter and lighter than non-hazmat unit trains. Average loaded non-hazmat unit train lengths and weights have steadily increased over the past 23 years, and distributions of train sizes indicate that trains exceeding 140 railcars in length have become more common over the

past 10 years. This information can aid researchers and industry practitioners in assessing the benefits and disadvantages of operating longer trains.

Although this analysis provides more detailed information on the distribution of unit train sizes over time, it may not exhaustively capture all the longest trains. Anecdotal evidence and published literature suggest that manifest and intermodal train lengths, measured in linear feet, are increasing. While public waybill data provides information identifying intermodal shipments, it is difficult to re-aggregate the individual shipments back into trains. Thus, future research goals include developing approaches to account for the disproportionate length of articulated intermodal railcars in public data and quantifying temporal trends in the linear length of manifest and intermodal trains. Railroad data on linear train lengths, such as those collected from dispatching systems and used by Wang (2019), is proprietary and unavailable to the public but would be a valuable resource for future study of these trends and related safety, performance, service, and asset utilization impacts.

4.2 Analysis of Freight Train Derailment Rates for Unit Trains and Manifest Trains

Rail is a safe and efficient mode of transporting hazardous materials (hazmat). In the past decade, hazmat traffic transported by unit trains has significantly increased in the United States. As a result, a comprehensive understanding of the safety and risks of hazmat unit trains is important and can contribute to the identification, evaluation, and implementation of risk mitigation strategies. Limited prior research has focused on unit train derailment risk analysis. This section develops a quantitative analysis of freight unit train derailment characteristics and compares those statistics to non-unit manifest trains (i.e., mixed trains). Mainline freight train derailment data on Class I railroads between 1996 and 2018 were analyzed for hazmat unit trains, non-hazmat unit trains, and manifest trains. Derailment rates, measured by three traffic exposure metrics (i.e., train-miles, ton-miles, and car-miles) were estimated and compared. The analyses showed that unit trains have a 30 percent lower derailment rate in terms of ton-miles and car-miles than manifest trains, while the derailment rate per million train-miles of unit trains is slightly greater than that of manifest trains. Loaded unit trains have a roughly four-fold higher derailment rate in terms of train-miles and car-miles than that of empty unit trains, and hazmat unit trains have lower derailment rates than non-hazmat unit trains. Overall, heavier and shorter loaded unit trains tend to have greater derailment rates as measured by all three traffic exposure metrics. A causal analysis was also conducted for the three train types, and infrastructure causes were the most frequent for all train types and lengths, followed by equipment-related causes. The results also showed that there were differences in major human factor causes for unit train derailments compared to manifest train derailments. These statistics provided important information for rational allocation of risk mitigation resources to improve rail hazmat transportation safety.

4.2.1 Introduction

Unit trains provide economical and efficient transportation of products by reducing operating expenses, using bulk loading, improving asset utilization, and creating economies of scale (Cook, 2015; Dick et al., 2021; Kenkel et al., 2004; Li et al., 2018; Starr, 1976). For example, Kenkel et al. (2004) conducted a profitability analysis of a 100-car unit train and showed that savings from unit-train transportation for agricultural products generally range from $0.05 to $0.15 per bushel.

Initially, unit trains were mostly used to carry coal, grain, and other forms of bulk cargo. In recent years, increasing amounts of hazmat are transported by unit trains (Li et al., 2018). Large volumes of hazmat (e.g., crude oil and ethanol) can be shipped by unit trains of 100 tank cars or more.

Based on an analysis of STB's waybill data for the years 1996-2018 (STB, 2020a), unit trains have been transporting an increasing proportion of hazmat over the past two decades (Figure 32).

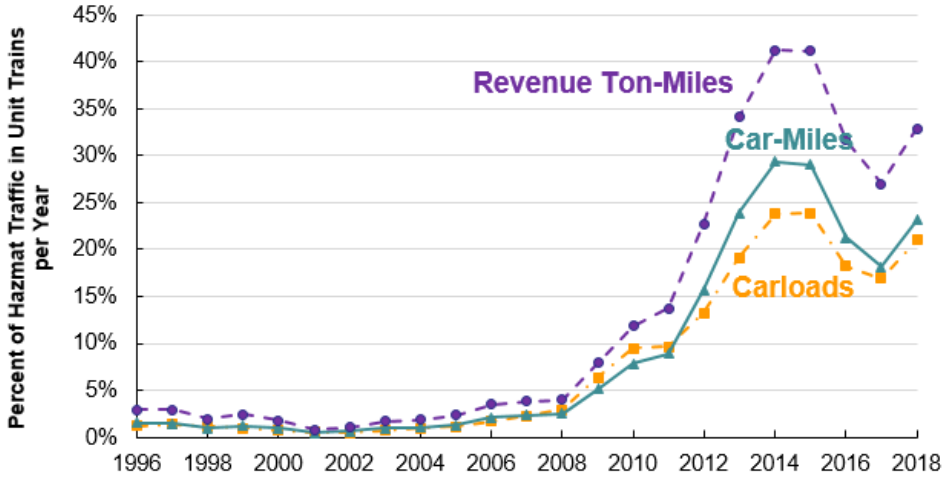

Figure 32. Fraction of hazmat traffic in unit trains based on an analysis of surface transportation board public waybill data (Dick et al., 2021)

Specifically, in 2018, approximately 21 percent of hazmat carloads moved in unit trains, generating 23 percent of hazmat car-miles and 33 percent of hazmat revenue ton-miles. This is quite different from the early years of the study period (1996-2005) when relatively little hazmat traffic moved in unit trains. Isolating unit train traffic in 2018, hazmat traffic comprised 9 percent of unit train shipments, 13 percent of unit train-miles, 8 percent of unit train carloads, 11 percent of unit train car-miles, and 10 percent of unit train revenue ton-miles; this is a substantial increase since 2008, when it comprised less than 1 percent of unit train traffic.

Despite the significant growth of unit train transportation of hazmat commodities, there has been relatively little research focusing on safety risk analyses of hazmat unit trains, including derailment, a common accident type on American freight railroads (Li et al., 2018; Liu et al., 2017). A previous study (Li et al., 2018) analyzed the derailment characteristics of loaded and empty unit trains, but it did not address train-type-specific derailment rates or accident cause distributions. The next section summarizes current research regarding train derailment analyses and rail hazmat transportation, which is relevant to the comparison of unit train and manifest train derailment frequencies and derailment rates.

4.2.2 Literature Review

Rail transports over two million carloads of hazmat in the United States annually (Liu et al., 2018) and over 99.999 percent of hazmat traffic by rail reaches its destination without a release caused by an incident (AAR, 2019b). Bagheri et al. (2014) found that rail is the preferred option for transporting large amounts of hazmat over long distances.

Unit trains increase freight railroad transportation efficiency. The rapid increase in crude oil transportation by rail in North America in recent years has led to more hazmat being moved in dedicated unit trains of 80 to 160 railcars (Dick & Brown, 2014). In addition to unit trains, manifest trains may consist of both hazmat cars and non-hazmat cars. Liu (2017a) compared hazmat transportation risk in unit trains with manifest trains and found that a unit train has a higher probability of a release incident after a train derailment occurs. Because there are generally disproportionately larger consequences in large hazmat release events, moving large amounts of hazmat in a single unit train may increase the risk of multiple-car releases compared to the use of multiple manifest trains where each train contains fewer hazmat cars (Liu et al., 2012). However, transporting hazmat in unit trains can reduce the number of accidents involving hazmat cars because fewer trains are operating to transport the same amount of hazmat (Liu, 2017a).

In terms of derailment frequency analysis, most previous studies (Li et al., 2018; Liu et al., 2012, 2017, 2018) used mainline derailment data from FRA's REA database. The statistical analysis of derailment causes and affecting factors has been widely studied in the literature (Anderson & Barkan, 2004; Barkan et al., 2003; Lin et al., 2020; Liu, 2016b; Wang et al., 2020). Liu et al. (2012; 2018) found that broken rails or welds are the most frequent causes of train derailment. Furthermore, derailment rate, which is defined as the number of derailments normalized by traffic exposure, is a critical statistic for derailment analysis. A previous study (Liu, 2015) found that there was an annual decline rate of 5.6 percent in Class I mainline freight train derailment rates from 2000 to 2014. Later, Liu et al. (2017) concluded that the freight train derailment rates on Class I railroad mainlines are affected by FRA track class (e.g., a higher track class has a higher allowable maximum speed and thus more stringent track geometry tolerances and maintenance standards), annual traffic density (e.g., below or above 20 million gross tons), and method of operation (e.g., signaled versus non-signaled). The impact of train weight on derailment rate also has been studied in the literature (Nayak et al., 1980).

4.2.3 Knowledge Gap and Research Objective

Train-type-specific derailment rate analysis is important to further understand various available options for transporting the same amount of hazmat. For example, 100 tank cars of flammable crude oil could be shipped in a single unit train, or alternatively split into multiple manifest trains. Researchers investigated which would pose a lower risk level on a given route.

The research team developed a methodology to identify unit trains and manifest trains recorded in the FRA REA database that improves upon and outperforms the method in Li et al. (2018). The team analyzed derailment frequency and cause for unit trains and manifest trains, respectively. Researchers estimated derailment rate for unit trains (particularly hazmat unit trains) and manifest trains, and explored the impact of train length and weight on derailment rate

The research provides the first analysis of train derailment rate and causes for unit trains and manifest trains. The team estimated the derailment rate and identified major derailment causes for hazmat unit trains, non-hazmat unit trains, and manifest trains using an integrated analysis of FRA REA data, STB Class I Railroad Annual Report Financial Data, and STB Public Waybill Sample data. The new methodology and information developed in this research can support further efforts in developing train-type-specific risk analysis and management solutions for transporting hazmat in unit trains and manifest trains.

4.2.4 Methodology

4.2.4.1 Data Sources

Derailment data in this study come from the FRA REA database (Form 6180.54), which records railroad accidents whose total infrastructure and rolling stock impacts exceed a monetary threshold for damage and loss to infrastructure and equipment (FRA, 2013). This reporting threshold is periodically adjusted to account for inflation, increasing from $6,300 in 1996 to $11,200 in 2021 (FRA, 2012, 2021). Detailed accident information, including operational factors, environmental factors, train characteristics, damage conditions, and other information useful for understanding the circumstances and causes of accidents are provided in the database. The team used accident data that included freight-train derailment accidents on Class I railroad mainlines from 1996 to 2018.

The traffic data analyzed in this study came from the Class I Railroad Annual Reports (Form R-1), from the STB (2020b), and from the STB Public Waybill Sample data (STB, 2020a). Three common metrics for measuring freight traffic – train-miles, car-miles, and gross ton-miles – are used in this analysis. One train-mile is the equivalent of running one train across one mile, one car-mile is the equivalent of moving one railcar across one mile, and one gross ton-mile is the equivalent of transporting one ton of railcar and freight payload across one mile. If a train consisting of 100 rail cars and carrying 10,000 gross tons (including the weight of lading, railcar, and locomotives) moves one mile, it produces one train-mile, 100 car-miles, and 10,000 gross ton-miles. Data pertaining to train-miles, car-miles, and gross ton-miles of unit trains and manifest trains were collected for each Class I railroad for the period 1996-2018. These statistics cover all railroad traffic during a given year, including hazmat and non-hazmat traffic. STB Public Waybill Sample data used in this research is representative of actual waybill movements based on a particular sampling rate and provides the number of carloads moving on a single waybill, hazmat shipping flag, billed tons of freight, expansion factors, expanded carloads, and expanded tons.

4.2.4.2 Train Type Identification

There is no data field in the FRA REA database to directly identify train type (e.g., unit train or manifest train). The team proposed a novel method to identify unit trains and manifest trains using the railroad code, train symbol ID, causing car reporting mark and number, number of empty cars, number of loaded cars, number of locomotives, and narratives recorded in the REA database.

First, the team extracted several variables from the accident database, including the number of empty cars, the number of loaded cars, the number of locomotives, the length of the train considering the total number of cars and locomotives, and the percentage of loaded or empty railcars in the train. In this research, a train is classified as loaded if 95 percent or more of its cars are loaded, and empty if 95 percent or more of its cars are empty (Figure 33). These percentages were calculated by dividing the number of loaded or empty cars by the total number of cars in the train. The threshold is set to 95 percent of loaded cars or empty cars, rather than 100 percent, because trains transporting hazmat generally have ‘‘buffer’’ cars between the locomotives and the first hazmat car, as required by federal regulation (FRA, 2015); the buffer car loading condition is independent of the loading condition of the rest of the train. This threshold was also used to identify the loading conditions (e.g., loaded trains, empty trains) of freight trains in a

previous study (Li et al., 2018). Buffer cars can either be empty or loaded with an inert material. To determine if a train is a unit train or a manifest train, further steps identify the train type when it is more than 95 percent loaded or empty, while the remaining trains with partially loaded consists are generally manifest trains.

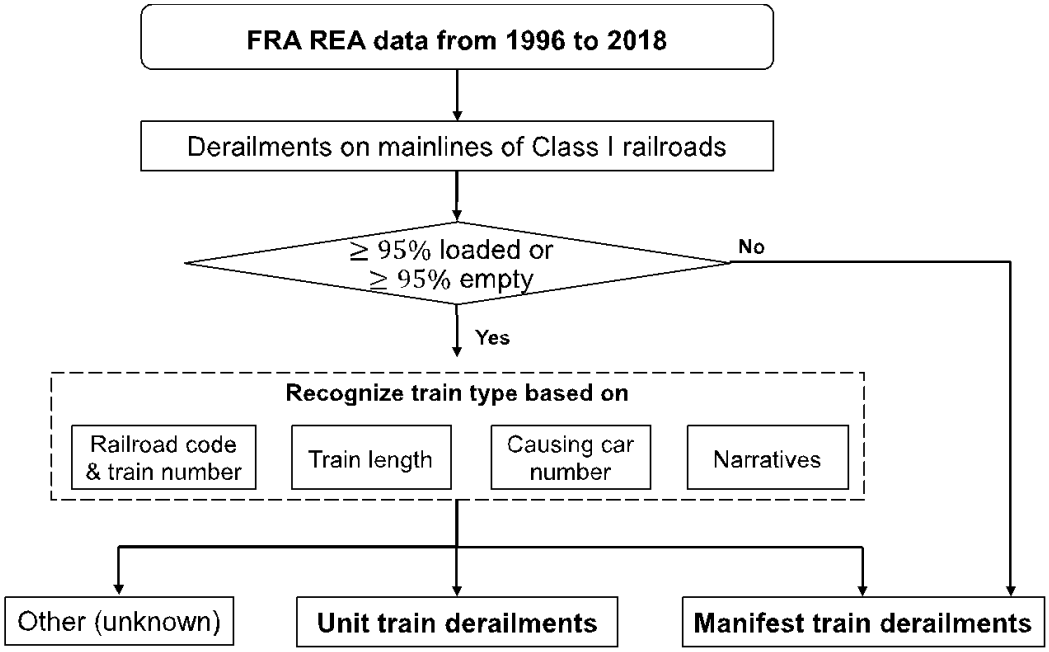

Figure 33. Methodology for classifying type of derailed trains

Next, to identify loaded or empty train derailments for unit trains and manifest trains, four criteria are considered.

1) The railroad code and train number fields in the FRA REA database are used to identify whether a derailment involved a unit train, using individual railroads' train symbol systems (anonymous, 2015; QStation, 2022; Union Pacific Historical Society, 2021). For example, based on the BNSF symbol guide (QStation, 2022), train numbers with prefixes of "C," "G," or "U" represent loaded unit coal trains, loaded unit grain trains, and unit trains other than coal or grain, respectively, while "M" signifies manifest trains.
2) Since unit trains are used for high-volume bulk commodities, the number of rail cars in unit trains is typically between 65 and 200 cars, or more (Aberdeen Carolina & Western Railway, 2022). This research classifies all trains with a smaller number of cars (e.g., a threshold of fewer than 40 cars) in length as manifest trains. For trains with lengths over 40 cars, other key variables, such as causing car number and railroad code, are used to further identify unit trains.
3) The equipment identification (i.e., reporting mark and number) for the first car involved in the derailment, as provided in the FRA REA database, can be used to assist in train type identification. For example, if the reporting mark and number for a train derailment is LW74396, using the Official Railway Equipment Registers (ORER), the rail car LW74396 was identified as a center-beam flat car. Since these cars are rarely shipped in a unit train, the corresponding derailment is highly likely to be a manifest train.

4) The FRA REA database also records narratives for reported train accidents. The narratives sometimes provide additional information, such as the incident train number, train and railcar types, and other keywords that can help distinguish between unit and manifest trains. For example, derailment records with narratives mentioning the terms "boxcar," "trailer," "container," or "local train" are likely to refer to manifest train derailments.

Note that this research focuses on the mainline derailments of six Class I railroads in the U.S.: BNSF Railway (BNSF), CSX Transportation (CSX), Grand Trunk Corporation (Canadian National's U.S. operations) (CNGT), Norfolk Southern, Soo Line Corporation (Canadian Pacific's US operations) (CP), and Union Pacific Railroad (UP). Derailments of Kansas City Southern Railway (KCS) were not included in this research, due to data limitation and some inconsistencies in historical traffic data records. From 1996 to 2018, a total of 2,462 derailed trains were classified as unit trains, 5,514 were classified as manifest trains, and 12 were classified as "other" trains of unknown type and excluded from further analysis.

4.2.5 Train Type-Specific Derailment Analysis

4.2.5.1 Train Derailment Statistics

Unit and manifest train derailment statistics are summarized and presented in this section. Train length is defined as the number of all types of railcars in the consist, including loaded cars, empty cars, and locomotives. The residual train length is the number of railcars after the position of the first derailed vehicle (FDV), while the normalized residual train length is the residual train length normalized by the total train length (see Table 21).

Table 21. Derailment statistics by train type

Group	Derailment Frequency	Average Train Length	Average Tons per Car (excl. locomotive)	Average Speed (mph)	Average Residual Train Length		Average Number of Cars Derailed
					Number of Cars	Normalized by Total Train Length	
Manifest Trains	5,514	82.6	80.7	24.3	47	57%	7.6
Empty Manifest	240	69.1	38.3	21.4	41	59%	6.8
Partially Loaded Manifest	3,925	88.9	78.3	24.3	49	55%	7.5
Loaded Manifest	1,349	66.5	98.3	24.7	41	62%	7.9
Unit Trains	2,462	110	113.8	25.1	59	54%	11.3
Empty Unit	421	110.6	29.1	24.9	70	63%	9.1
Loaded Unit	2,041	109.6	131.7	25.1	57	52%	11.7
Hazmat Loaded Unit	62	91.9	121.9	23.0	55	60%	11.5
Non-Hazmat Loaded Unit	1,979	110.1	131.9	25.2	57	52%	11.8

As shown in Table 21, the average derailment speeds of manifest trains and unit trains show minor differences (24.3 mph and 25.1 mph, respectively), as do the average normalized residual train lengths (57 and 54 percent, respectively). The significance of these two variables' differences between manifest trains and unit trains are also validated with a Pearson's chi-squared test, a commonly used statistic that evaluates the genetic association or difference between sets (Agresti & Kateri, 2011; Zhang & Liu, 2020). The test shows that the p-values of

two variables are greater than 0.05. Thus, the derailment speeds and residual train lengths of manifest trains and unit trains do not show significant differences in this study. The average weight of unit trains (12,518 tons) was nearly twice that of manifest trains (6,666 tons). Manifest trains averaged 83 cars in derailed train consists and 81 tons per railcar, while unit trains averaged 110 cars in the consist (around 33 percent more than manifest trains) and 114 tons per railcar (around 41 percent more). Manifest trains averaged 7.6 cars derailed per derailment, while unit trains derailed an average of 11.3 cars. Liu et al. (2013) indicated that derailment severity depends on the derailment speed, residual length, and loading factor. Although derailment speed did not differ significantly, a higher value of residual train length and greater train weight resulted in more cars derailed in a unit train derailment compared to a manifest train derailment. The results are consistent with the positive correlation between derailment severity, train length, and loading status identified in previous research and the associated hypothesis that the greater length and weight of unit trains indicate greater kinetic energy in the derailment compared to manifest trains, thereby causing more cars to derail, given that all else is equal.

Loaded unit trains transporting hazmat or non-hazmat bear similar characteristics in train length, train weight, residual train length, and derailment severity. Most loaded unit train derailments are non-hazmat loaded unit trains (e.g., coal trains), while only 62 of 2,041 (3 percent) derailed unit trains carried hazmat.

4.2.5.2 Causal Analysis

Train accident causes are systematically organized and categorized by FRA into five major cause groups: track, equipment, human factor, signal, and miscellaneous causes. A variation on the FRA cause groups was developed in the early 1990s by Arthur D. Little (ADL) Inc., working with AAR, based on input from railroad engineering and mechanical experts (ADL, 1996). The objective of the ADL grouping was to better link causes that could be addressed through similar or related preventative measures. For example, broken rails, joint bars, and rail anchors that are combined in the same FRA subgroup are distinguished from broken rails or welds and joint bar defects in the ADL grouping. In some cases, ADL also combined similar cause subgroups into one group (Li et al., 2018). Each FRA cause code maps onto a unique ADL cause group.

The first step in the causal analysis was to identify the ADL cause groups for both train types and rank them by the number of derailments (Table 22). Broken rails or welds was the leading cause group for both train types. Broken rails accounted for about 12 and 18 percent of manifest train derailments and unit train derailments, respectively. Each broken-rail-caused manifest train derailment had an average of 12 cars derailed, while a broken rail-caused unit train derailment had an average of 16 cars derailed. All the most frequent cause groups for unit train derailments are car-mile-related causes (i.e., related to train length), except for the obstruction. For manifest trains, although over 50 percent of derailments result from car-mile-related accident causes, some train-mile-related causes (e.g., train handling) also contribute to a greater proportion of derailments. Specifically, train handling includes accidents caused by improper train make-up at the initial terminal, improper placement of cars in the train, excessive buff or slack action in train handling, and excessive lateral drawbar force on curves. Obstruction includes snow or ice on the track, extreme weather conditions, or an object or equipment on or fouling the track. A detailed discussion of train-mile-related and car-mile-related accident causes can be found in Wang (2019).

Table 22. Distribution of cause groups by train type

(a) Unit train derailments

Rank	ADL Cause	Total Number of Derailments	Percentage (%)	Average Number of Cars Derailed
1	*Broken Rails or Welds*	440	17.87	15.8
2	*Broken Wheels (Car)*	230	9.34	9.2
3	*Bearing Failure (Car)*	182	7.39	7.5
4	*Buckled Track*	152	6.17	14.7
5	*Other Axle/Journal Defects (Car)*	152	6.17	8.3
6	*Track Geometry (excl. Wide Gauge)*	141	5.73	7.8
7	*Obstructions*	98	3.98	18.5
8	*Wide Gauge*	87	3.53	11.7
9	*Roadbed Defects*	71	2.88	12.9
10	*Other Wheel Defects (Car)*	70	2.84	6.0
11	*Turnout Defects - Switches*	65	2.64	6.2
12	*Track-Train Interaction*	58	2.36	9.3
13	*Other Miscellaneous*	56	2.27	12.7
14	*Misc. Track and Structure Defects*	50	2.03	10.8
15	*Lading Problems*	46	1.87	6.6
16	*Joint Bar Defects*	46	1.87	22.7
17	*Coupler Defects (Car)*	41	1.67	7.3
18	*Other Rail and Joint Defects*	40	1.62	25.5
19	*Use of Switches*	38	1.54	4.5
20	*Sidebearing, Suspension Defects (Car)*	36	1.46	5.8
21	*Train Handling (excl. Brakes)*	32	1.30	8.0
22	*Non-Traffic, Weather Causes*	31	1.26	8.6
23	*Rail Defects at Bolted Joint*	30	1.22	15.7
24	*Train Speed*	28	1.14	6.6
25	*Truck Structure Defects (Car)*	27	1.10	7.4
26	*Centerplate/Carbody Defects (Car)*	22	0.89	3.9
27	*All Other Car Defects*	22	0.89	4.9
28	*Misc. Human Factors*	21	0.85	14.5
29	*Stiff Truck (Car)*	15	0.61	11.5
30	*Switching Rules*	15	0.61	3.0
31	*Failure to Obey/Display Signals*	14	0.57	11.8
32	*Other Brake Defect (Car)*	14	0.57	8.5
33	*Handbrake Operations*	12	0.49	3.4
34	*Brake Rigging Defect (Car)*	12	0.49	6.4
35	*Loco Electrical and Fires*	11	0.45	14.4
36	*Track/Train Interaction (Hunting) (Car)*	10	0.41	6.3
37	*Brake Operation (Main Line)*	9	0.37	17.7
38	*Mainline Rules*	9	0.37	5.7
39	*Signal Failures*	8	0.32	6.4
40	*Loco Trucks/Bearings/Wheels*	8	0.32	13.1
41	*Turnout Defects - Frogs*	5	0.20	21.0
42	*All Other Locomotive Defects*	3	0.12	21.0
43	*Brake Operations (Other)*	2	0.08	17.5
44	*UDE (Car or Loco)*	1	0.04	29.0
45	*Employee Physical Condition*	1	0.04	11.0
46	*Air Hose Defect (Car)*	1	0.04	16.0
	TOTAL over period 1996-2018	**2462**		**11.3**

(b) Manifest train derailments

Rank	ADL Cause	Total Number of Derailments	Percentage	Average Number of Cars Derailed
1	*Broken Rails or Welds*	639	11.59	12.0
2	*Track Geometry (excl. Wide Gauge)*	391	7.09	6.0
3	*Bearing Failure (Car)*	343	6.22	5.2
4	*Train Handling (excl. Brakes)*	324	5.88	7.9
5	*Obstructions*	243	4.41	10.8
6	*Track-Train Interaction*	212	3.84	6.9
7	*Lading Problems*	211	3.83	5.5
8	*Wide Gauge*	186	3.37	9.0
9	*Coupler Defects (Car)*	184	3.34	4.6
10	*Use of Switches*	182	3.30	4.0
11	*Broken Wheels (Car)*	173	3.14	6.1
12	*Sidebearing, Suspension Defects (Car)*	164	2.97	6.2
13	*Other Wheel Defects (Car)*	164	2.97	3.8
14	*Brake Operation (Main Line)*	163	2.96	9.3
15	*Centerplate/Carbody Defects (Car)*	148	2.68	4.5
16	*Buckled Track*	147	2.67	11.7
17	*Other Miscellaneous*	145	2.63	9.8
18	*Turnout Defects - Switches*	142	2.58	5.6
19	*Misc. Track and Structure Defects*	98	1.78	9.0
20	*Train Speed*	94	1.70	5.4
21	*Stiff Truck (Car)*	85	1.54	6.8
22	*Roadbed Defects*	82	1.49	7.3
23	*Joint Bar Defects*	70	1.27	13.9
24	*Other Axle/Journal Defects (Car)*	64	1.16	5.6
25	*Other Brake Defect (Car)*	64	1.16	3.6
26	*Loco Trucks/Bearings/Wheels*	63	1.14	5.0
27	*All Other Car Defects*	62	1.12	5.0
28	*Track/Train Interaction (Hunting) (Car)*	58	1.05	9.0
29	*Misc. Human Factors*	58	1.05	6.6
30	*Switching Rules*	55	1.00	5.9
31	*Other Rail and Joint Defects*	51	0.92	15.7
32	*Rail Defects at Bolted Joint*	51	0.92	18.5
33	*Handbrake Operations*	49	0.89	4.8
34	*Non-Traffic, Weather Causes*	44	0.80	7.0
35	*Failure to Obey/Display Signals*	39	0.71	4.7
36	*Brake Rigging Defect (Car)*	35	0.63	6.0
37	*All Other Locomotive Defects*	35	0.63	6.8
38	*Signal Failures*	35	0.63	7.5
39	*Air Hose Defect (Car)*	33	0.60	7.5
40	*Truck Structure Defects (Car)*	25	0.45	6.8
41	*Loco Electrical and Fires*	23	0.42	6.2
42	*Mainline Rules*	23	0.42	5.1
43	*Turnout Defects - Frogs*	20	0.36	7.2
44	*Radio Communications Error*	12	0.22	5.5
45	*UDE (Car or Loco)*	10	0.18	7.7
46	*Brake Operations (Other)*	6	0.11	10.0
47	*TOFC/COFC Defects*	5	0.09	1.8
48	*Employee Physical Condition*	2	0.04	15.0
49	*Handbrake Defects (Car)*	2	0.04	2.0
	TOTAL over period 1996-2018	**5514**		**7.6**

The team found that a greater majority of unit train derailments resulted from track-related and equipment-related causes, which are both car-mile-related causes as classified by previous studies (ADL, 1996; Wang, 2019). Unit trains with heavier and more cars in the consist may experience more track-related and equipment-related accidents on average than manifest trains. This may be related to the features of unit train weight and length, which can cause more damage to track and rolling stock due to dynamic loading. Furthermore, unit trains have more cars derailed than manifest trains. The potential reason for this disparity in derailment severity might be the difference in train characteristics (e.g., train length, train weight) between these two train types. Meanwhile, manifest train derailments involve a relatively higher proportion of human factor-related and miscellaneous causes, which are mostly train-mile-related causes. Figure 34 focuses on the cause group distribution of derailment frequency and excludes the potential impact of traffic exposures in unit trains and manifest trains. In this figure, the blue dot "track" shows that the number of average cars derailed per accident caused by track is 14 for unit trains, and the number of unit train derailments caused by track-related factors accounts for 47 percent of unit train derailments. Additional investigations into derailment accidents normalized by traffic volumes, as well as the impact of train length and weight, are presented in Section 5.

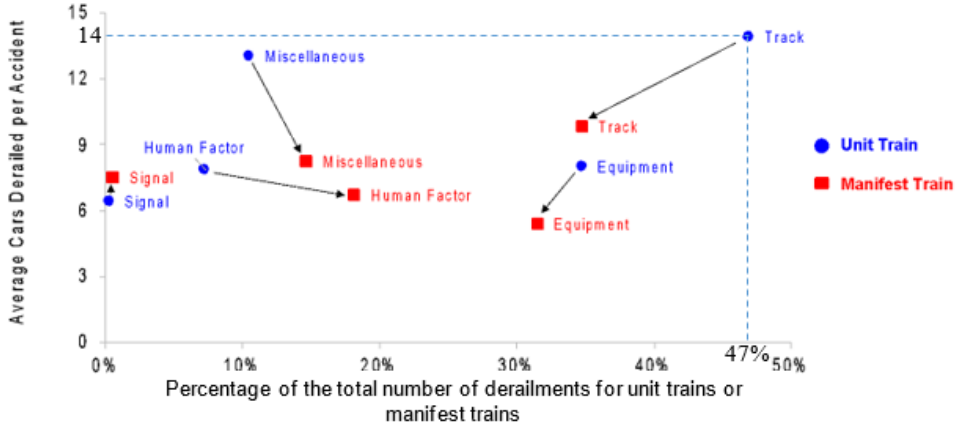

Figure 34. Distribution of cause groups in unit train derailments and manifest train derailments

4.2.6 Derailment Rate Analysis by Train Type

Derailment rate is a useful statistic to estimate the likelihood of a derailment (Anderson & Barkan, 2004; Evans, 2011; Schafer & Barkan, 2008; Zhang & Liu, 2020). An analysis of derailment rate was developed by train type using three common traffic metrics. The calculation of traffic metrics is based on Class I railroad R-1 reports and STB Public Waybill Sample data. Train-miles running, car-miles, gross ton-miles, number of loaded freight cars, and other traffic items for unit and manifest trains were collected from STB R-1 reports. The datasets cover all railroad traffic transported during a given year, including hazmat and non-hazmat traffic. STB R-1 reports include totals by train type, a practical aspect of these statistics not found in other statistical summaries of railroad transportation productivity (Dick et al., 2021). However, the Class I railroad R-1 reports lack any distribution of train sizes by train type, or the average train size associated with hazmat traffic or specific commodities. For this, the team used the STB Public Use Carload Waybill Sample data which includes hazmat shipment flag and standard transportation commodity codes (STCC). The team concluded that average loaded non-hazmat

unit train lengths and weights have steadily increased over the past 23 years. Detailed methods and results of the traffic analysis can be found in a separate study by Dick et al. (2021).

4.2.6.1 Derailment Rate Comparison

Three types of derailment rate metrics are covered in this study: per million train-miles, per billion ton-miles, and per billion car-miles (Anderson & Barkan, 2004; Evans, 2011). Equations (4-1) - (4-3) show the calculation of these rates with derailment frequency and traffic volumes.

$$Derailment\ rate\ per\ million\ train\ miles\ = \frac{Number\ of\ train\ derailments}{million\ train\ miles} \quad (4\text{-}1)$$

$$Derailment\ rate\ per\ billion\ ton\ miles = \frac{Number\ of\ train\ derailments}{Billion\ ton\ miles} \quad (4\text{-}2)$$

$$Derailment\ rate\ per\ billion\ car\ miles = \frac{Number\ of\ train\ derailments}{Billion\ car\ miles} \quad (4\text{-}3)$$

Figure 35 presents the three derailment rates by overall breakdown of train type, loading conditions within unit trains, and whether hazmat was carried within the loaded unit train. The team made the following observations:

- A unit train has a 27 percent higher average train-mile-based derailment rate than a manifest train, but it has approximately 40 percent lower average car-mile and ton-mile-based derailment rates, probably due to its greater length and weight. Unit trains transport a large amount of goods in more cars as compared to manifest trains, and therefore more prone to train-mile-based derailments. On the other hand, since more cars and goods are put on the same train for unit train operation, they experience less chance of train-mile-based derailments for individual cars or units of goods compared to those cars or goods on manifest trains, while the chance for car-mile-based derailments remains the same. Therefore, unit trains have lower car-mile or ton-mile-based derailment rates.
- Within the category of unit trains, if the derailment rate is measured per million train-miles or per billion car-miles, a loaded unit train has a four-times higher derailment rate than an empty unit train. If the derailment rate is measured by billion ton-miles, loaded unit trains still have a higher rate than empty unit trains but by a smaller margin. It is reasonable for loaded unit trains to have higher derailment rates than empty unit trains because loaded trains impose greater loads to rolling stock and track infrastructure and therefore increase the likelihood of failure (Sadeghi & Shoja, 2016). In addition, operating heavier trains requires more power and braking control, which increases the risk of derailments due to improper use or insufficient braking or power (McClanachan & Cole, 2012).
- Hazmat-loaded unit trains and non-hazmat-loaded unit trains have similar derailment rates by ton-mile. With different traffic metrics, a hazmat loaded unit train has 0.97 derailments per million train-miles and 11.06 derailments per billion car-miles, approximately 40 and 20 percent lower than loaded non-hazmat unit trains, respectively. One possible reason for this is the additional operational regulations and practices

implemented on hazmat trains as part of hazmat release risk mitigation and reduction strategies (PHMSA, 2015).

- Hazmat-loaded unit trains have lower derailments per billion ton-miles and per billion car-miles compared to manifest trains, although their derailment rate per million train-miles is slightly higher.

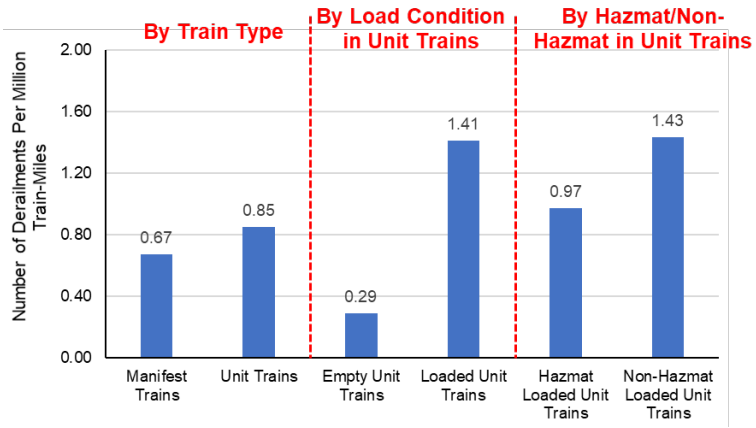

(a) Rate per Million Train-Miles

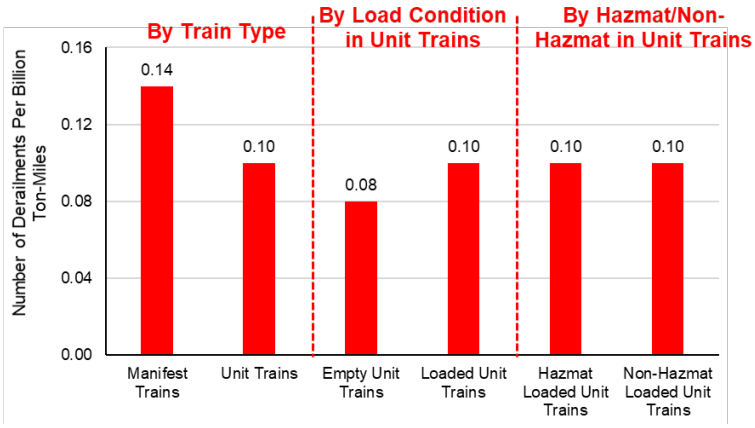

(b) Rate per Billion Ton-Miles

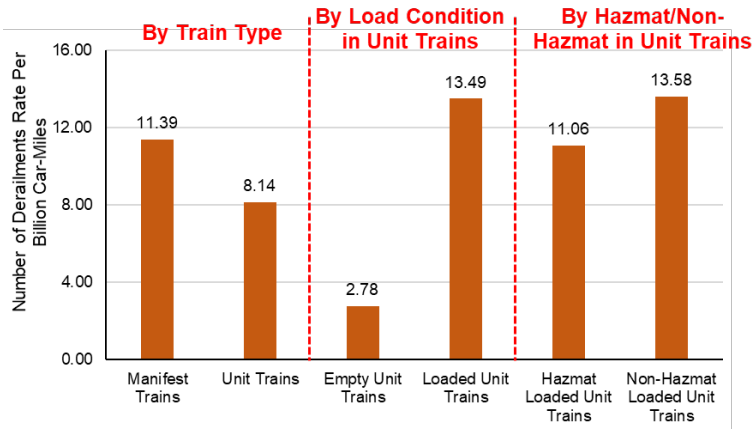

(c) Rate per Billion Car-Miles

Figure 35. Derailment rate comparison by train type

The team applied the Kolmogorov–Smirnov (KS) test to determine the difference in derailment rates between unit trains and manifest trains within the study period. The KS test is a practical, non-parametric, distribution-free test with no restrictions on sample size (Meng & Qu, 2012). Based on the P-values of derailment rate, the rates per billion ton-miles and billion car-miles for unit trains and manifest trains are statistically significantly different (P-values < 0.001) and the rates per million train-miles are slightly statistically different (P-value = 0.04). Note that a loaded unit train has the longest average train length (110 cars per train) and the highest average tonnage per car (131.7) among the studied train groups. The length and weight of non-hazmat-loaded unit trains are 20 and 9 percent greater than those of hazmat-loaded unit trains, respectively. Based on these statistics, identifying whether train weight and train length may impact derailment rates in another interesting research question.

4.2.6.2 Effect of Train Weight on Loaded Unit Train Derailment Rate

As shown in Figure 36, empty unit trains and loaded unit trains have similar derailment rates per billion ton-miles. However, the derailment rates per billion ton-miles and derailment rates per billion car-miles of loaded unit trains are considerably higher than those for empty unit trains, differing by more than a factor of four. This is consistent with previous studies that found accident rates per billion car-miles increase when using higher capacity cars (Nayak et al., 1980; Wang, 2019).

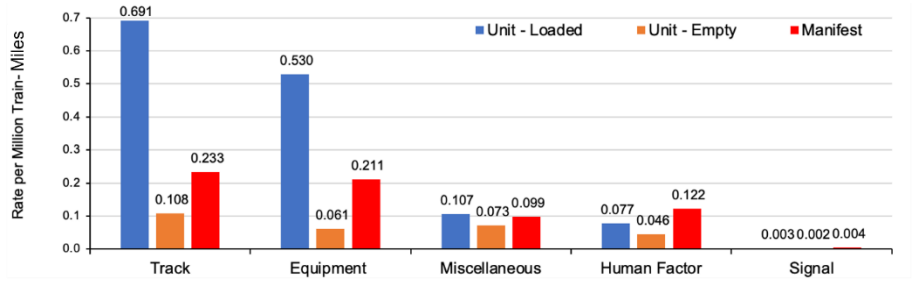

(a) Rate per million train-miles

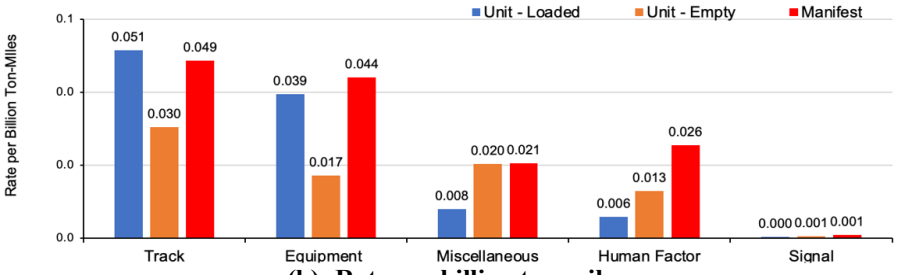

(b) Rate per billion ton-miles

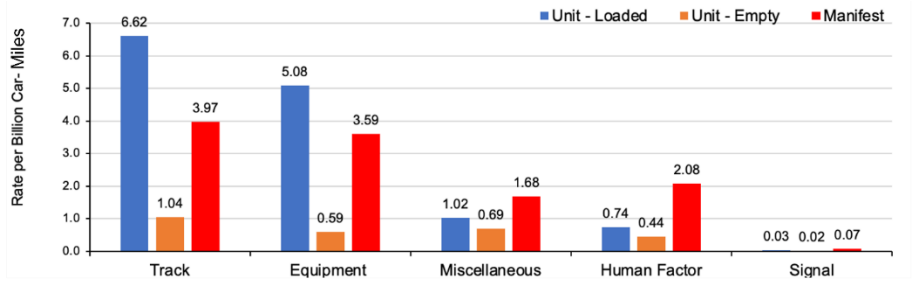

(c) Rate per billion car-miles

Figure 36. Derailment rates of loaded unit trains, empty unit trains, and manifest trains

A causal analysis was conducted to understand the potential impact of train weight on train derailment rate. Derailment causes for loaded unit trains, empty unit trains, and manifest trains are classified into five groups defined by FRA: track-related causes, equipment-related causes, miscellaneous causes, human factor-related causes, and signal-related causes.

As shown in Figure 36, the significant difference in derailment rates per million train-miles and per billion car-miles between loaded unit trains and empty unit trains can be attributed to track-related causes and equipment-related causes. Relatively minor dissimilarities exist in human factor-causes, miscellaneous causes, and signal causes, which are mostly train-mile-related. Given that one major difference between loaded unit trains and empty unit trains is train weight, a relationship between train weight and derailment rate may exist. It is presumed that heavier trains may cause more damage to track and rolling stock due to dynamic loading, which may result in a greater likelihood of track-related and equipment-related accidents, given all else is equal. This is implied in Figure 36, which compares the derailment rates for loaded unit trains and empty unit trains.

4.2.6.3 Effect of Train Length on Loaded Unit Train Derailment Rate

The distribution of derailment rates under varying loaded unit train lengths are presented in Table 23. Four train-length categories (61-80 cars, 81-100 cars, 101-120 cars, and over 120 cars) have similar derailment rates per million train-miles. However, with greater train length (particularly over 100 cars per train), derailment rates per billion car-miles and per billion ton-miles change more significantly. For example, a loaded unit train with over 121 cars has only one-third of the rate of a loaded unit train shorter than 80 cars.

Table 23. Loaded unit train derailment rates by train length

Loaded Unit Trains	Rate per Million Train-Miles	Rate per Billion Ton-Miles	Rate per Billion Car-Miles
61-80 cars	1.57	0.22	21.54
81-100 cars	1.89	0.19	20.07
101-120 cars	1.47	0.12	13.10
121+ cars	1.29	0.08	9.80

Figure 37 presents the derailment rates of different loaded unit train lengths under five causal groups (i.e., track, equipment, human factor, signal, and miscellaneous). The team found that track-related and equipment-related causes account for most loaded unit train derailments in all length categories. Furthermore, the derailment rates per billion ton-miles and rates per billion car-miles show decreasing trends associated with longer train lengths.

The decreasing trend in derailment rate in Table 23 and Figure 37 is intuitive since the longer train lengths exhibit economies of scale; longer trains require fewer train movements to transport the same number of ton-miles and car-miles. Since the occurrence of train-mile-related causes (such as those in the human factors and miscellaneous groups) are spread over a larger number of ton-miles and car-miles per train movement, the overall rate is expected to decrease with increasing train length.

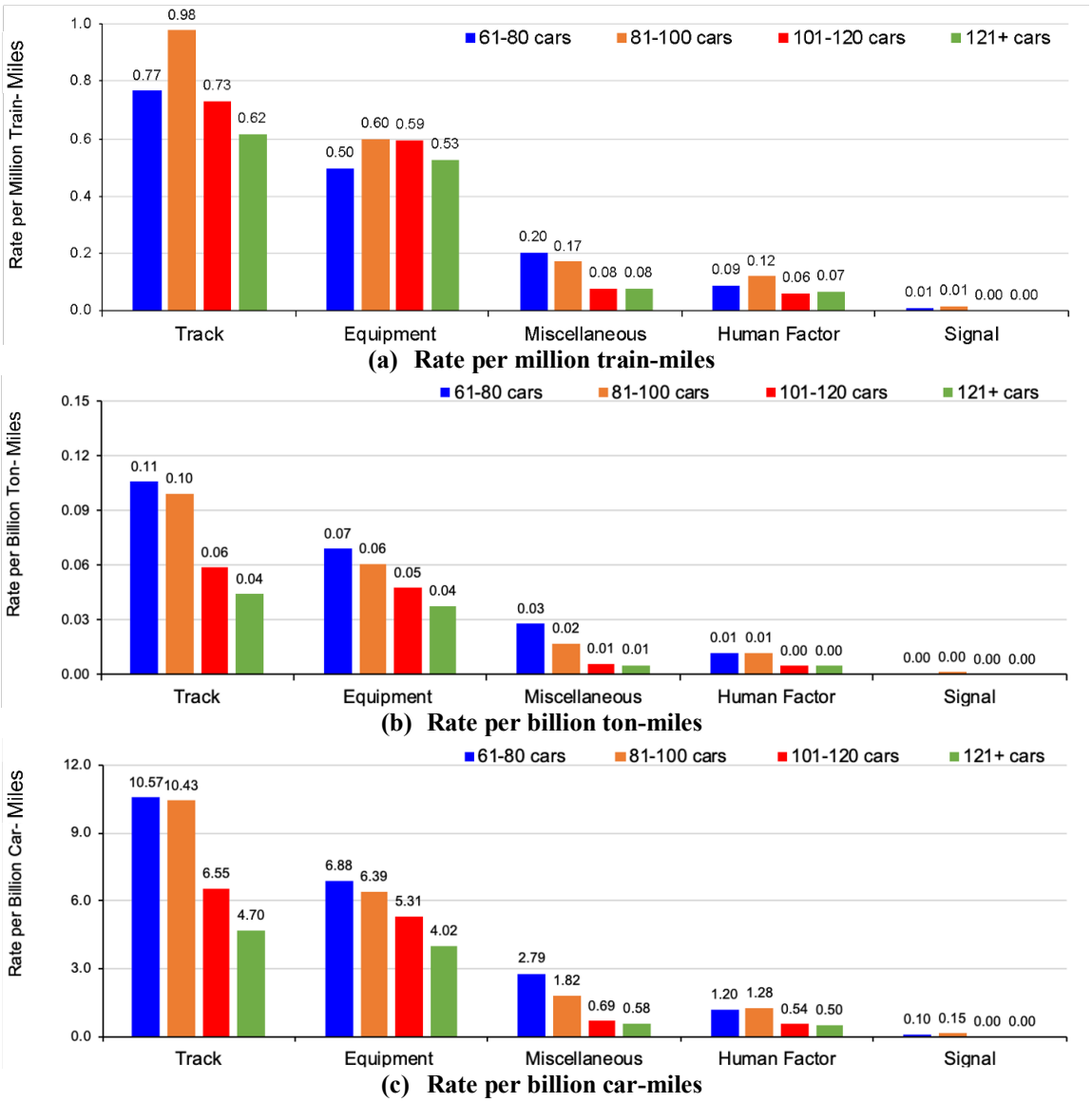

Figure 37. Derailment rates of loaded unit trains under different train lengths

The trend in train-mile rates as a function of train length in Table 23 and Figure 37 is less clear. The expectation would be that as loaded unit trains become longer and heavier, each train would impart more damage to the track infrastructure and pose a greater train handling challenge, with the rate per train-mile increasing with train length. However, this trend was not observed. It is possible that the derailment rates among the four train length groups have a confounding relationship with other factors. One example is FRA track class. Trains of longer lengths may be more prevalent on certain higher track class routes because higher track classes indicate better track maintenance standards (Liu et al., 2018) and therefore can bear more traffic loads in general. Further support for this hypothesis is provided by the loaded train derailment rates per ton-mile and car-mile for the track and equipment cause groups in Figure 37b and c. Since these causes are related to car-miles (and by extension ton-miles), they should show similar rates across all train lengths, but instead they are observed to decline with increasing train length. However, this behavior could also be explained if a disproportionate number of long trains are

operating on higher quality tracks where each car-mile and ton-mile has a lower likelihood of derailment. To address this possibility, the team further investigated the relationship between train length and FRA track class for FRA-reportable derailments on mainlines.

Figure 38 shows that over half of loaded unit train derailments with shorter train lengths (e.g., fewer than 100 cars) occurred on FRA track Class I, Class II, and Class III. In comparison, longer trains (e.g., greater than 100 cars) have a greater proportion of derailments on FRA track Class IV and Class V, probably because these longer unit trains are operated on high-tonnage corridors where tracks are maintained like high track classes. This comparison is based on derailment frequency and does not account for traffic volumes by track class (in fact, most of the traffic volume in Class I railroads is on track Class III or higher). Because track-class-specific traffic data was not available, derailment rate calculation by track class and train length in combination was not developed but may be considered in the future if such data become available.

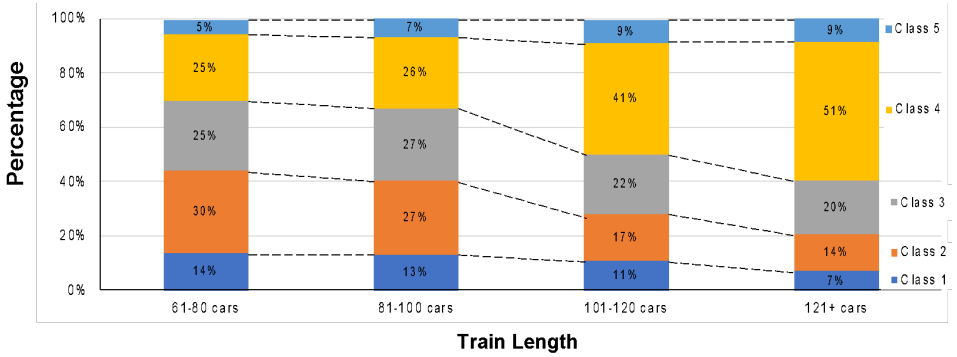

Figure 38. Loaded unit train derailments by train length and FRA track class, Class I mainlines, 1996 to 2018

4.2.6.4 Human Factors in Unit Train and Manifest Train Derailment Rate

In addition to track-caused and equipment-caused derailments, which are mostly car-mile-related and should be associated with train length and train weight, human factor-caused derailment rates also involve significant differences between unit trains and manifest trains (see Figure 35). A previous study (Schafer & Barkan, 2008) concluded that most human factors are train-mile-related causes since the likelihood of these train derailments is proportional to the number of train miles. Moreover, Zhang et al. (2021) used train-miles to normalize accident frequency in modeling human factor-caused freight train accidents in the United States. Thus, researchers primarily focused on the human factor-caused derailment rate, defined as the number of derailments normalized by million train-miles. Figure 36a shows that the human factor-caused manifest train derailment rate per million train-miles (0.122) is roughly twice that of unit train derailments (0.062). In addition, the proportion of train derailments caused by human factors (Figure 34) also emphasizes the much more critical concerns of manifest trains (18.2 percent) over unit trains (7.3 percent).

An in-depth comparative analysis of human factor-caused derailments was conducted using ADL cause groups between unit train derailments and manifest train derailments (Table 24). Train handling (excluding brakes) is among the most frequent human factor causes in both types of train operation, accounting for 18 percent of unit train operation (second to Use of Switches at 21 percent) and 32 percent of all manifest trains. There is a difference in the percentage of total

human factors that cause derailments between the two train types in terms of brake operation (i.e., mainline). While brake operation accounts for over 16 percent of all human factor-caused derailments in manifest trains, it only accounts for 5 percent of the same measure for unit trains.

Previous studies (Schafer & Barkan, 2008; Wang, 2019) classified brake operation (01H) as a car-mile-related cause group after the implementation of statistical learning algorithms with freight train accidents on Class I, and showed that certain causes within the train handling cause group (09H) may be more likely to occur with longer trains. Nevertheless, from the statistics shown in Table 24, the unit trains with longer train length (110 cars per train on average) still have substantially lower derailment rates in these two ADL cause groups than manifest trains (82.6 cars per train on average). This shows that manifest trains have a higher likelihood per train-mile of errors in locomotive engineer operation, excessive buff or slack action, improper train make-up, improper throttle use, excessive horsepower applied by the engineer, and improper brake use. While unit trains are longer and heavier than manifest trains on average, the weight of a unit train is typically uniformly distributed over its length and composed of railcars that are either identical or similar in length. In comparison, manifest trains have an uneven weight distribution with groupings of empty and loaded railcars of varying lengths and gross rail loads distributed throughout the train, making them a particularly difficult train handling challenge in undulating terrain. Like the argument made in previous subsections, the difference in derailment rates between unit trains and manifest trains is confounding and cannot be compared using a single or even several factors.

Table 24. Top ADL causes in human factor-caused derailments of (a) unit trains and (b) manifest trains

(a) Unit trains

ADL Cause Group	Number of Derailments	Percentage	Rate Per Million Train-Miles
11H Use of Switches	38	21.2%	0.013
09H Train Handling (excl. Brakes)	32	17.9%	0.011
10H Train Speed	28	15.6%	0.010
12H Misc. Human Factors	21	11.7%	0.007
07H Switching Rules	15	8.4%	0.005
05H Failure to Obey/Display Signals	14	7.8%	0.005
02H Handbrake Operations	10	5.6%	0.003
01H Brake Operation (Main Line)	9	5.0%	0.003
08H Mainline Rules	9	5.0%	0.003
03H Brake Operations (Other)	2	1.1%	0.001

(b) Manifest trains

ADL Cause Group	Number of Derailments	Percentage	Rate Per Million Train-Miles
09H Train Handling (excl. Brakes)	324	32.2%	0.039
11H Use of Switches	182	18.1%	0.022
01H Brake Operation (Main Line)	163	16.2%	0.020
10H Train Speed	94	9.3%	0.011
12H Misc. Human Factors	58	5.8%	0.007
07H Switching Rules	55	5.5%	0.007
02H Handbrake Operations	48	4.8%	0.006
05H Failure to Obey/Display Signals	39	3.9%	0.005
08H Mainline Rules	23	2.3%	0.003
06H Radio Communications Error	12	1.2%	0.001

Another potential explanation for this difference in unit and manifest train behavior, is the much greater proportion of unit trains that are operated with distributed power (DP). DP train operation involves placing locomotives in the middle and at the end of a train instead of putting all locomotives at the front of the train. Several recent studies (General Electric, 2004; Government Accountability Office, 2019) found that DP operation may offset train handling and brake operation problems and enable more effective train handling for longer and heavier trains, improving braking performance and train safety. Figure 39 illustrates the difference between DP and non-DP train brakes. It is almost impossible to acquire the exact statistics of DP use in unit and manifest trains, but the derailed trains may provide approximate references. In the 23-year train derailment accident data used in this study, over 34 percent of derailed unit trains were operated with DP, compared to only 7 percent for derailed manifest trains. Manifest trains should be more challenging to handle than unit trains in certain circumstances since manifest trains may encounter variations in car length and weight and difficulties in the employment of additional distributed power locomotives.

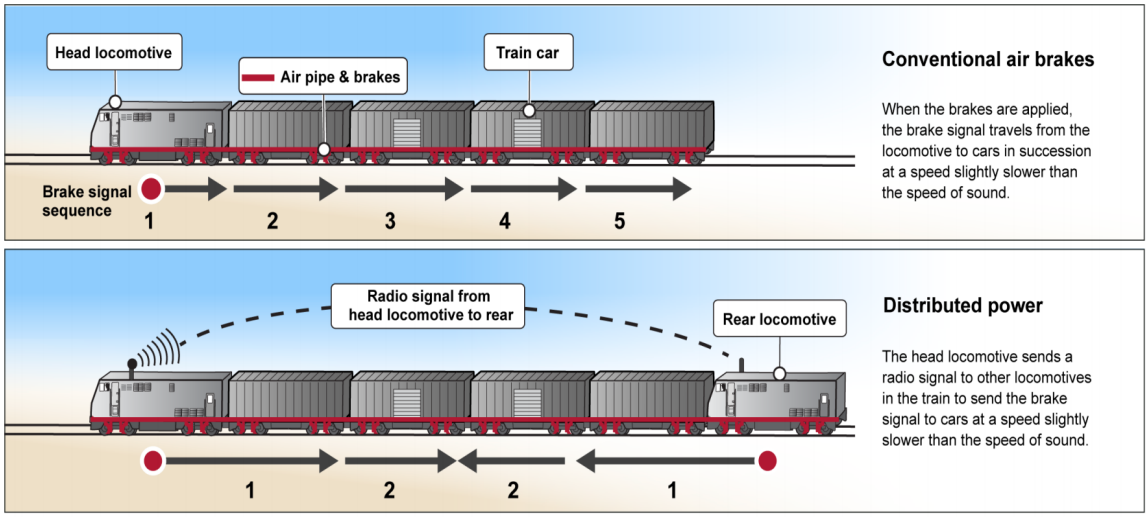

Figure 39. Trains with non-distributed and distributed power (Government Accountability Office, 2019)

4.2.7 Conclusions

The team analyzed freight train derailment rates for manifest trains and unit trains, comparing the effect of loading condition, hazmat loading, train length, and train weight on derailment rates of these two types of trains. Causal analyses were conducted to assist in interpreting the similarities and differences in these accident characteristics. The primary findings of this research are summarized below:

- A unit train (all types combined) has a 27 percent higher derailment rate per million train-miles (0.85 per million train-miles) than a manifest train (0.67 per million train-miles). Unit train derailment rate per million train-miles caused by track failures and equipment failures is over two times the manifest train derailment rate. Meanwhile, manifest trains (0.122 per million train-miles) have approximately twice the human factor-caused derailment rate of unit trains (0.062 per million train-miles).

- A unit train (all types combined) has a 30 percent lower derailment rate per billion ton-miles or per billion car-miles (0.10 per billion ton-miles and 8.14 per billion car-miles, respectively) than a manifest train (0.14 per billion ton-miles and 11.39 per billion car-miles, respectively).
- A loaded unit train has a four-fold higher derailment rate per million train-miles or per billion car-miles than an empty unit train. The rates for loaded and empty unit trains per billion ton-miles are more similar.
- A loaded hazmat unit train has a 30 percent lower rate per million train-miles and a 20 percent lower rate per billion car-miles, as compared to a loaded non-hazmat unit train.
- Hazmat-loaded unit trains have a 28 percent lower derailment rate per billion ton-miles and a slightly lower rate per billion car-miles compared to manifest trains.

This research contributes to the development of a comprehensive and quantitative risk assessment of hazmat unit train transportation. The rail industry has shown a strong interest in understanding how the safety and efficiency of transporting hazmat in unit trains and manifest trains differs under various operating circumstances. Further research could focus on the risks of transporting the same amount of hazmat in unit trains and manifest trains, considering derailment rates on mainline and in the yards, conditional probability of releases, and consequences. Future research could also investigate the tradeoff of transporting hazmat in unit trains and manifest trains in terms of operation efficiency (e.g., number of times hazmat cars need to be transferred in yards) while maintaining at least the same level of safety. Ultimately, the objectives of improving hazmat transportation efficiency and safety will become an optimization problem, and the results presented here form a solid foundation and provide important information to achieve this goal and address these timely and critical railroad transportation questions.

5. Derailment Severity Analyses

5.1 Introduction

To understand the risk of transporting hazmat by rail, it is important to estimate train derailment severity and quantify the relationship between train derailment severity and affecting factors. Understanding the risks can help the rail industry and government develop, evaluate, prioritize, and implement cost-effective safety improvement strategies. There are two approaches to estimating the severity of a train derailment: 1) statistical models, and 2) analytical or simulation models (i.e., physical models).

Statistical models developed from historical accident data estimate expected severity based on factors such as train speed, position of the derailment, and the proportion of loaded and empty cars within the train (Liu, Saat, Qin, et al., 2013; Martey & Attoh-Okine, 2018, 2019a; Nayak et al., 1983). For example, Liu, Saat, Qin, et al. (2013) developed zero-truncated negative binomial regression and quantile regression models to estimate the conditional mean of freight-train derailment severity of historical derailments on U.S. Class I railroad mainlines from 2001 to 2010. Additionally, Saccomanno and El-Hage (1989b, 1991b) developed a TG model to estimate the mean number of cars derailed as a function of derailment speed, residual train length, and accident cause. Martey and Attoh-Okine (2018) developed a joint mixed copula-based model to estimate derailed cars and monetary damage and conducted a combined analysis of the relationship with a set of covariates that might affect both outcomes. Martey and Attoh-Okine (2019a) employed a vine copula quantile regression model (an interval estimation approach) to predict conditional mean and quantiles of derailment severity outcomes. Statistical models are effective in estimating train derailment severity as well as identifying risk factors that influence severity based on historical data.

Physical models are used to model train derailment severity, accounting for the physical dynamics of the derailment and using that information to estimate the number of derailed cars. Physical models can also help researchers understand how factors such as train speed, tonnage, train length, etc., influence derailment severity from the perspective of physical dynamics.

One type of physical model simulates the longitudinal train dynamics, including traction, braking, and longitudinal forces of the coupled cars in the train. The TOES™ model developed for and licensed to AAR-member railroads is a well-established longitudinal train dynamics simulator in North America (Andersen et al., 1991, 1992). TOES has been in use for nearly 30 years, has been validated many times over, and is considered an industry standard for longitudinal train dynamics modeling. The TEDS model is a similar one-dimensional longitudinal dynamics model (Andersen et al., 2012; Sharma & Associates, Inc., 2015). TEDS is a more recently developed tool that calculates the in-line train forces and motions under specified track, traction, and braking conditions. Additional studies that have developed similar longitudinal dynamics models include Mokkapati et al. (2011) and Wu et al. (2014).

Another type of physical model includes two-dimensional (2-D) and three-dimensional (3-D) models of the individual vehicle dynamics, including additional mechanics (e.g., wheel-rail interaction forces, suspension dynamics, derailment kinematics, etc.). For example, Toma developed a detailed 2-D multi-body simulation (MBS) train derailment model (Toma, 1998) that includes significant features from a longitudinal model such as the traction, braking, and coupler forces for the cars on the track. Once derailed, the cars are subject to 2-D motions with a

velocity-dependent ground friction model, impact forces, and uncoupling of cars based on strength and displacement limits. The primary limitations of Toma's model are the simplifications necessary in an MBS model for calculating impact behaviors and the constraint that the model is only 2-D. Other 2-D MBS derailment studies include Paetsch et al. (2006) and Jeong et al. (2007).

As a result of the complexity of post-derailment behaviors, more recent derailment models have relied on 3-D computational solvers to simulate response. An example of this type of model for simulating train derailments using the LS-DYNA finite element solver was performed by Kirkpatrick et al. (2006). The fully 3-D finite element model allows for many additional complex derailment mechanics such as deformation and failure of components and connections (e.g., truck separations and breakup, coupler failures), realistic impact scenarios between derailed cars, and derailment conditions on slopes and elevated rail berms. To investigate the factors that influence derailment severity, the 3-D modeling approach was more complex and computationally intensive than required. In contrast, one-dimensional (1-D) models are less complex and more computationally efficient and are capable of capturing train derailment dynamics. Therefore, the team developed a 1-D train derailment model for this project.

In this research, the team used FRA train accident data to 1) identify factors that influence derailment severity given a train derailment incident, 2) build a statistical model (i.e., TG model) to estimate derailment severity given a set of influencing factors, and 3) build a physical model to understand the mechanical dynamics behind a derailment accident and to estimate derailment severity from the perspective of mechanic dynamics. The remainder of this section is organized as follows.

- Section 5.2 describes the FRA data source and develops a TG model to estimate derailment severity and identify the factors that influence severity.
- Section 5.3 describes a 1-D physical model the team developed to investigate how factors contribute to differences in derailment severity for unit and manifest trains.
- Section 5.4 compares the performance of the TG model and the 1-D model in estimating train derailment severity based on the same FRA dataset.
- Conclusions are drawn in Section 5.5.

5.2 Data Source and Statistical Analysis

FRA's REA Form 6180.54 records the time, cause, severity, consequence, and contributing factors of each listed train accident (FRA, 2019). The research team used REA freight train derailment data for Class I railroads from 1996 to 2018 (the period for which applicable data was available) for train derailment severity analysis.

Many previous studies used "number of derailed cars" to measure derailment severity (Anderson, 2005; Liu, Saat, Qin, et al., 2013; Saccomanno & El-Hage, 1989b, 1991b). The generic term "cars" refers to all types of vehicles (e.g., locomotives, railcars, cabooses, etc.) unless stated otherwise. Monetary damage and the number of casualties are also used to assess derailment severity. However, prior studies (Barkan et al., 2003; Martey & Attoh-Okine, 2018) have shown that monetary damage is prone to substantial variations due to factors such as the cost difference between locomotives and railcars and differences in repair costs between regular track and special track (e.g., turnouts and crossings). These studies also stated that casualties are more appropriate in the measurement of passenger train derailments. As this research focuses on

freight train derailment, the team primarily used the number of cars derailed as a severity metric in unit train and manifest train derailment severity analysis.

Figure 40 shows the average train derailment severity for each year to demonstrate whether there is an increasing or decreasing trend over the studied years. From this figure, an obvious increasing or decreasing trend of average derailment severity is not seen. The Mann-Kendall Trend Test[1] was used instead to verify the significance of increasing or decreasing trends in derailment severity. The team found that train derailment severity does not have a significant increasing or decreasing trend over time, because the p-value (0.342) is greater than the 0.05 confidence level and the null hypothesis (i.e., the data has a significant increasing or decreasing trend) is thus rejected. Therefore, researchers concluded that derailment severity over the 23 years studied does not change over time, and an integrated analysis of the derailment severity for all years from 1996 to 2018 instead of a separate derailment severity analysis for each individual year was performed.

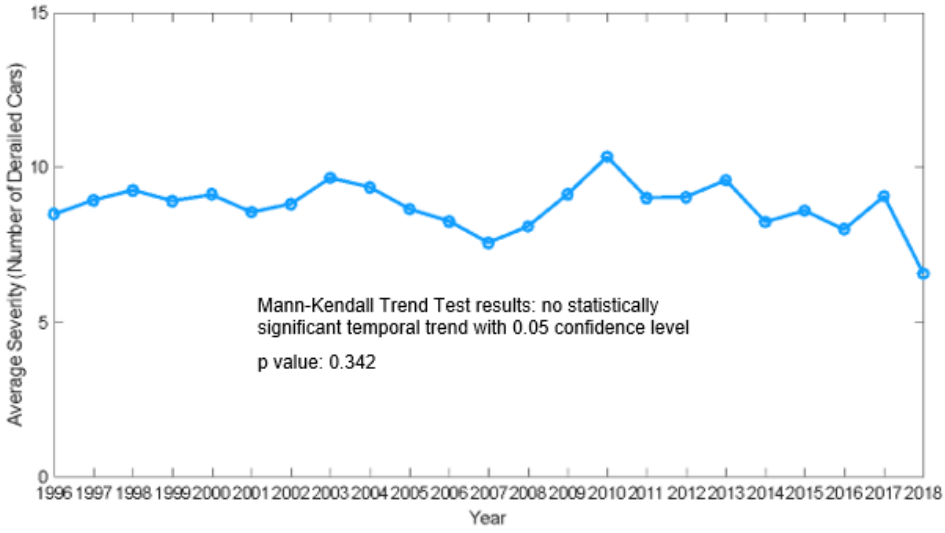

Figure 40. Average derailment severity in each year

From the freight train derailment data collected, the distribution of the number of cars derailed is plotted in Figure 41 (note that these data do not include those with derailment speed equal to "0 mph" and the number of derailed cars equal to "0"). Figure 42. presents the same data separated by train type for the unit trains' and manifest trains' distributions of the number of derailed cars. Table 25 presents descriptive statistics for train derailment severity analysis.

[1] The Mann-Kendall Trend Test (Kendall, 1975) is a non-parametric test for analyzing time series data with consistent increasing or decreasing trends (monotonic trends).

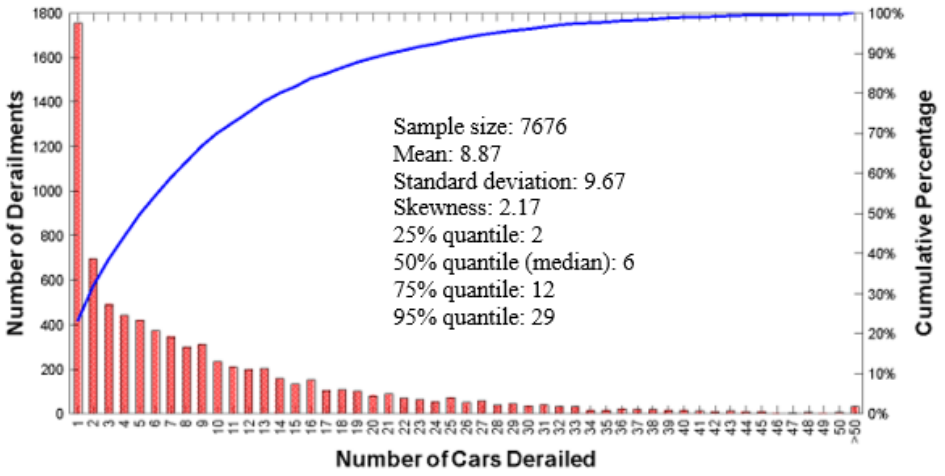

Figure 41. Number of railcars derailed per freight-train derailment (all train types) from 1996 to 2018

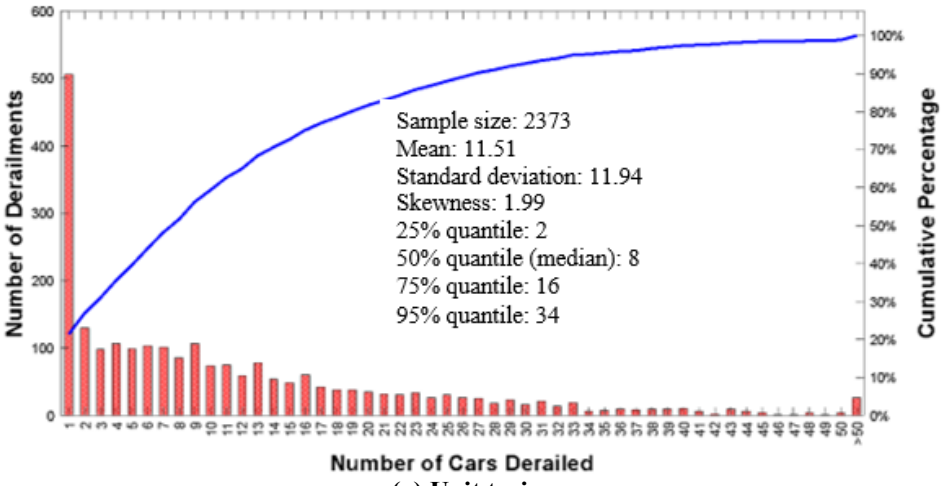

(a) Unit trains

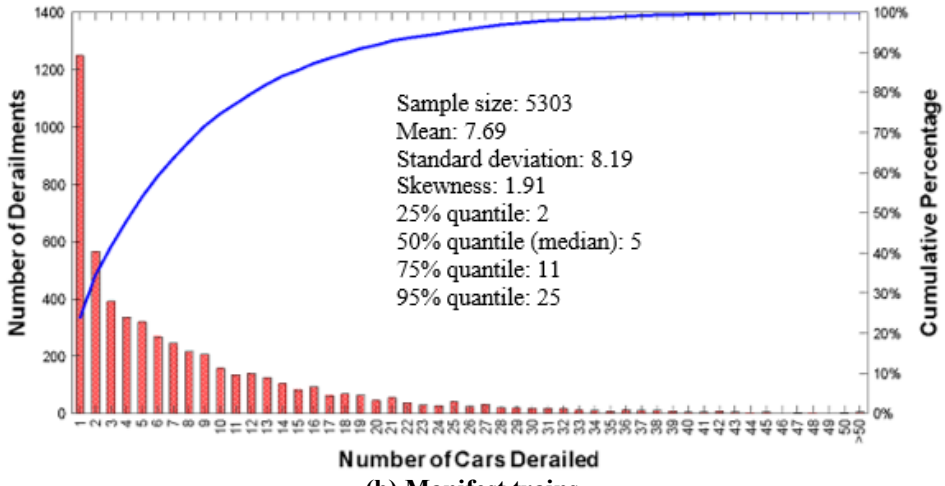

(b) Manifest trains

Figure 42. Number of railcars derailed per freight-train derailment in (a) unit trains and (b) manifest trains

Table 25. Descriptive statistical results

	Sample size (number of train derailments)	Mean (average number of derailed cars)	Median (the median number of derailed cars)	Variance (the variance of numbers of derailed cars)	Standard deviation of numbers of derailed cars
All train types	7,676	8.87	6	93.5	9.67
Unit trains	2,373	11.51	8	142.5	11.94
Manifest trains	5,303	7.69	5	67.1	8.19

Before developing statistical models to estimate train derailment severity, the team conducted data screening to exclude data with inappropriate attributes that could degrade the model's performance. The following screening conditions were applied, and 7,489 train derailments (94.89 percent of all 7,976 derailments) were selected for analysis.

- Speed ≥ 1: In the dataset, 133 derailment incidents showed a speed of 0 mph. Researchers assume that a train will not derail when train speed is extremely slow. Thus, the lowest derailment speed was set as "1 mph" and the 133 derailment incidents at 0 mph were excluded from subsequent analysis. Table 26 shows the descriptive statistical results of derailment speed grouped by 10 mph versus the observed severity by train type.
- 1 ≤ Number of derailed cars ≤ 50: In the original dataset, some derailed car and locomotive numbers were shown as zero. However, when the number of derailed cars is zero, researchers deem that the train did not derail, and thus the accident with zero derailed cars is excluded from analysis. Moreover, the team observed outliers that could start to skew the results for fit, wherein the severity was greater than 50 derailed cars. Therefore, the data with the number of derailed cars greater than 50 are excluded from the analysis. This screening criterion removed 95 derailment incidents from the dataset.
- Number of cars behind POD ≥ number of derailed cars: The number of cars behind POD cannot be less than the number of derailed cars, and thus only data with the number of cars behind POD greater than or equal to the number of derailed cars was considered. In the dataset, 171 derailments where the number of cars behind POD are less than the number of derailed cars were excluded from analysis.
- Other data with apparent errors (139 data records, e.g., tons per car less than 10, two data records only having one derailment incident, etc.) were excluded.

Out of the 7,489 train derailments, 1,932 data points came from loaded unit trains, 371 data points were empty unit train derailments, and 5,186 derailment accidents were manifest train derailments.

The response variable is the total number of railcars derailed, including loaded railcars, empty railcars, and locomotives. Several engineering and operational factors may affect train derailment severity. Based on the literature, several variables, including train derailment speed, residual train length, gross tonnage per car, and train types (e.g., empty unit train, loaded unit train, and manifest train) were identified for statistical analyses.

Table 26. Descriptive statistical results of derailment speed grouped by 10 mph versus the observed severity (a) Unit Trains and (b) Manifest Trains

(a) Unit trains

Derailment Speed (mph)	Sample size (number of train derailments)	Mean (average number of derailed cars)	Median (the median number of derailed cars)	Variance (the variance of numbers of derailed cars)	Standard deviation of numbers of derailed cars
[1,10]	537	6.38	5	26.43	5.14
(10,20]	402	7.33	6	37.35	6.11
(20,30]	553	11.37	11	74.44	8.63
(30,40]	392	14.29	14	137.59	11.73
40+	419	16.37	13	223.49	14.92

(b) Manifest trains

Derailment Speed (mph)	Sample size (number of train derailments)	Mean (average number of derailed cars)	Median (the median number of derailed cars)	Variance (the variance of numbers of derailed cars)	Standard deviation of numbers of derailed cars
[1,10]	1,459	4.80	4	17.96	4.24
(10,20]	899	6.31	4	36.29	6.02
(20,30]	1,122	7.49	6	46.47	6.82
(30,40]	698	10.42	8	88.57	9.41
40+	1,008	11.04	6	134.66	11.60

Train Speed

Train derailment speed is the speed of train operation when the accident occurs. The effect of this factor on derailment severity is most widely studied in the literature (Anderson, 2005; Bagheri et al., 2011; Liu, Saat, Qin, et al., 2013; Saccomanno & El-Hage, 1991b). It has been found that, all other factors being equal, derailment speed is positively associated with the number of cars derailed. This finding is reasonable as speed is an indicator of an accident's kinetic energy.

Residual Train Length

Residual train length is defined as the number of railcars behind the POD (i.e., the maximum number of cars potentially subject to derailment). Figure 43 provides an example. Saccomanno and El-Hage (1991b), Anderson (2005), and Liu, Saat, Qin, et al. (2013) found that a greater residual train length is associated with more derailed cars if a derailment accident occurs.

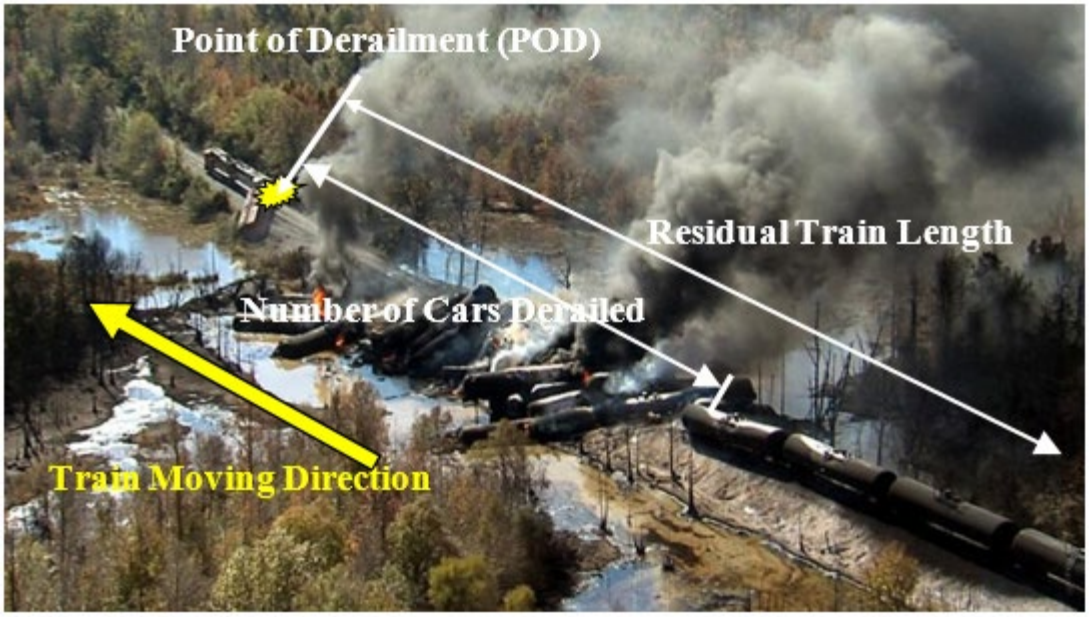

Figure 43. An illustrative example of POD and residual train length

Gross Tonnage Per Car

Liu, Saat, Qin, et al. (2013) verified the hypothesis that a train carrying a larger proportion of loaded cars is expected to derail more cars. Therefore, the gross tonnage per car was considered as a factor that influences derailment severity. Higher gross tonnage per car in the train may also indicate greater kinetic energy in the derailment, thereby causing more cars to derail, all else being equal.

Train Type

Train type is another new factor considered in this research. The team considered three types of trains, including loaded unit trains, empty unit trains, and manifest trains (for the methodology to differentiate train types, please refer to Section 4.2.4.2). There may be a significant difference in train length, gross tonnage, and train speed for loaded unit trains, empty unit trains, and manifest trains, which may influence the derailment severity (see Table 27). Moreover, train type represents some unobserved, hidden factors in addition to tonnage, train length, speed, etc. Therefore, the train type is also treated as a variable.

Table 27. Attributes of loaded unit trains, empty unit trains, and manifest trains

Train types	Average residual train length (number of cars behind POD)	Average tonnage per car	Average total number of cars per train	Average derailment speed (mph)
Loaded unit trains	58	131	109	25.2
Empty unit trains	72	30	110	26.4
Manifest trains	48	84	83	24.7

Table 28 summarizes the input variables considered for the severity estimation model.

Table 28. Variables in derailment severity estimation models

Variables		Data type
Model input	Gross tonnage per car	Continuous
	Train derailment speed (miles per hour)	Continuous
	Number of cars behind POD (point of derailment)	Integer
	Train types considered in this section, including loaded unit trains, empty unit trains, and manifest trains	Categorical
Model output	Number of cars derailed in one derailment	Integer

5.2.1 Model Description

For each train derailment incident, the number of cars derailed must be greater than or equal to "1" and less than or equal to the residual train length. As verified by Bagheri (2010), the number of cars derailed follows a TG distribution and the TG model can truncate the number of derailed cars beyond the range from "1" to the residual train. For a train derailment event with train length L and POD j (the residual train length $Lr = L - j + 1$), the probability of derailing x cars can be calculated by:

$$P(X = x \mid \text{POD at } j) = \begin{cases} \dfrac{p(1-p)^{x-1}}{1-(1-p)^{Lr}} & \text{if } x = 1, 2, \ldots, Lr \\ 0 & \text{otherwise} \end{cases} \tag{5-1}$$

where:

Lr = residual train length

X = number of cars derailed

P = the probability of success at each trial, which is a constant probability. In other words, "x" cars derailing before the first non-derailing car is a geometric distribution and the probability of a car derailing (given that a derailment has occurred) is equal to $(1 - p)$. This probability p is assumed to be related to the factors/covariates through the logit link function:

$$p = \frac{e^Z}{1+e^Z} \tag{5-2}$$

where Z is a linear function (Equation 5-3) of influencing factors, including derailment speed, residual train length, gross tonnage per car, and train type.

$$Z = \beta_0 + \beta_1(speed) + \beta_2(cars\ residual) + \beta_3(tons\ per\ car) + \beta_4(empty\ unit\ train) + \beta_5(loaded\ unit\ train) \tag{5-3}$$

speed = Train derailment speed (mph)

cars residual = Number of cars behind POD

tons per car = Average gross tonnage per car

empty unit train = If the train is an empty unit train, *empty unit train* = 1, otherwise *empty unit train* = 0

loaded unit train = If the train is a loaded unit train, *loaded unit train* = 1, otherwise *loaded unit train* = 0

The model uses the manifest train as a reference, which indicates that the manifest train type variable is not included in the model. A detailed introduction of the TG model can be found in Bagheri (2010).

5.2.2 Model Results

The team used the VGAM package in R to fit the TG model. The VGAM package (Yee, 2020) for R is designed to fit Vector Generalized Linear and Additive Models (VGLMs and VGAMs), as well as reduced-rank VGLMs (RR-VGLMs) and quadratic RR-VGLMs (QRR-VGLMs). It is a general program for maximum likelihood estimation. The VGAM package was able to fit the TG model in this research using the function "truncgeometric ()".

Table 29 presents the results of the model. Except for the variable "empty unit train," all other variables considered in the TG model were significant with all *P*-values being less than 0.05. However, if the confidence level is given to set at 90 percent, the variable "*empty unit train*" is significant with a *P*-value less than 0.1.

Thereafter, the model result of the *Z* function is shown in Equation (5-4).

$$Z = -0.952 - 0.0306(speed) - 0.00180(cars\ residual) - 0.00239(tons\ per\ car) + 0.119(empty\ unit\ train) - 0.339(loaded\ unit\ train) \quad (5\text{-}4)$$

Table 29. TG model results for all train types (with outliers)

Variables	Definition	Coefficient	P-value
Intercept	The constant	-0.952	$< 2\times10^{-16}$
speed	Train derailment speed (miles per hour)	-0.0306	$< 2\times10^{-16}$
cars residual	Number of cars behind POD (point of derailment)	-0.00180	0.00021
tons per car	Average gross tonnage per car	-0.00239	1.49×10^{-5}
empty unit train	If the train is an empty unit train, *empty unit train* = 1, otherwise *empty unit train* = 0	0.119	0.0956
loaded unit train	If the train is a loaded unit train, *loaded unit train* = 1, otherwise *loaded unit train* = 0	-0.339	8.93×10^{-14}

In Equation (5-4), if the coefficient of a variable is negative, then increasing this variable would tend to increase derailment severity; in contrast, if the coefficient of a variable is positive, increasing the variable would tend to decrease derailment severity. Based on Equation (5-2), the probability of a car not to derail (p) is a monotone increasing function of "Z", and thus the probability of a car to derail ($1 - p$) is a monotone decreasing function of "Z". When a variable is increased given that its coefficient in Z function is negative, Z decreases and the probability of a car to derail increases, and thus derailment severity tends to increase, and vice versa. Based on this discussion, the team developed the following interpretation of the obtained model.

- The coefficient of derailment speed is negative (-0.952). This indicates that higher derailment speed is associated with increased derailment severity.

- The coefficient of residual train length is -0.00180, which is negative, indicating that longer residual train length is associated with increased derailment severity.
- Similarly, greater gross tonnage per car is associated with increased derailment severity.
- The coefficient of "empty unit train" is positive (0.119) while the coefficient of "loaded unit train type" is negative (-0.339). This means that a loaded unit train tends to have more cars derailed compared to a manifest train, while an empty unit train tends to derail fewer cars than a manifest train, all else being equal.

The mean number of cars derailed is used as the estimated derailment severity, as formulated by Equation (5-5).

$$D = E[X] = \sum_{x=1}^{Lr} P(x)x = \frac{1}{p\left[1-(1-p)^{Lr}\right]} \tag{5-5}$$

Figure 44 plots the estimated severity versus the observed severity. Due to low-severity outliers (i.e., those incidents where estimated severity was high but observed severity was low) and high-severity outliers (i.e., those incidents where estimated severity was low but observed severity was high), the R square is not sufficiently large (0.61), which indicates that the model does not estimate the severity perfectly.

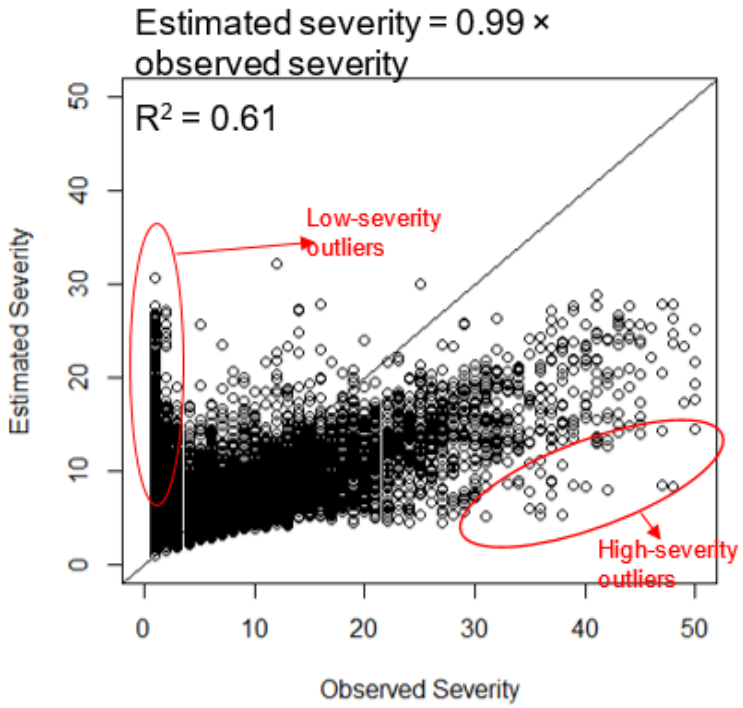

Figure 44. Estimated severity versus observed severity

One of the concerns identified by this result is that there are different types of behaviors in the derailment data and the variation cannot be represented well by this type of model. For example, the derailment data include a significant number (approximately 20 percent) of single-car derailments (severity = 1) over a wide range of derailment speeds. These often occur from mechanisms like a broken wheel or axle where a single truck might derail but the problem is identified, and the train is brought to rest by the operator, with no larger severity of unstable derailment initiated. All the cars in the train remain connected and upright, primarily aligned

with the track, and no impacts occur between any of the cars. These events have a low risk of hazmat release because of the derailment.

In the other extreme derailments, the train was moving very slowly and an initiating event, such as extreme weather, caused a long string of connected cars to fall over, remaining aligned with the track. This also occurs with empty tank cars with double shelf couplers where one car rolls off its trucks in a derailment and the strong rotational coupling between cars results in a long line of trailing cars rolling over. These events can have very high severities at very low or no speed. Again, the only impacts are from a rollover event where the tank impacts the ground and there is a low probability of hazmat release.

As a result, additional analysis was conducted for the data where the high severity and low severity outliers were excluded. The team developed a method to exclude these outliers and then used the TG model again to estimate derailment severity. The derailment data beyond the range from 0.1×derailment speed to 1.6×speed are treated as outliers and are excluded from analysis (Figure 45).

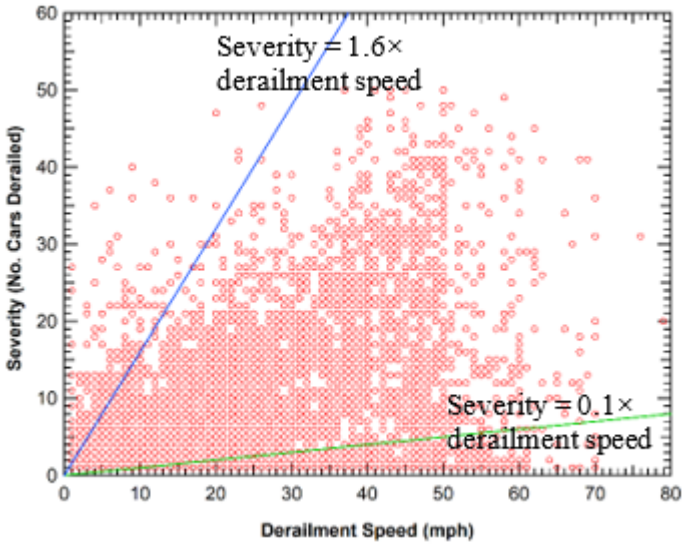

Figure 45. Method to exclude outliers

The derailments outside these bounds were assumed to have a "unique behavior" of derailment compared to the typical derailments that are the primary risk for tank car punctures and hazmat releases. Using this outlier elimination method, 5,400 derailment data were selected from the total 7,489 train derailments. 2,089 outliers were excluded, among which 1,829 derailment data were low-severity outliers and 260 derailment data were high-severity outliers. Among the 5,400 train derailments, 1,448 data records were from loaded unit trains, 274 data records were from empty unit trains, and 3,678 data records were from manifest trains. The result of the TG model is presented in Table 30 and Equation (5-6).

$$Z = -0.586 - 0.0702(speed) - 0.00206(cars\ residual) - 0.00293(tons\ per\ car) - 0.321(loaded\ unit\ train) \quad (5\text{-}6)$$

Table 30. TG model results for all train types (without outliers)

Variables	Definition	Coefficient	P-value
Intercept	The constant	-0.586	7.90×10^{-13}
speed	Train derailment speed (miles per hour)	-0.0702	$< 2\times10^{-16}$
cars residual	Number of cars behind POD (point of derailment)	-0.00206	0.00106
tons per car	Average gross tonnage per car	-0.00293	5.53×10^{-15}
empty unit train	If the train is an empty unit train, *empty unit train* = 1, otherwise *empty unit train* = 0	0.0957	0.295
loaded unit train	If the train is a loaded unit train, *loaded unit train* = 1, otherwise *loaded unit train* = 0	-0.321	6.73×10^{-18}

The team used mean squared error (MSE Equation (5-7)) and mean absolute error (MAE, Equation (5-8)) to measure the performance of the TG models in estimating train derailment severity. For all data with outliers, the MSE and MAE of the model were 60.67 and 5.72, respectively. For the data without outliers, the MSE and MAE of the model were 33.47 and 4.00, respectively. The mean absolute error indicates that the average gap between the estimated number of derailed cars and the observed number of derailed cars was 5.72 and 4.00 for the data with and without outliers, respectively.

$$\text{MSE} = \text{mean}[(\text{estimated severity} - \text{observed severity})^2] \quad (5\text{-}7)$$

$$\text{MAE} = \text{mean}[(\text{estimated severity} - \text{observed severity})] \quad (5\text{-}8)$$

In addition, the team used the TG regression model to fit the derailment severities separately for the loaded unit train, empty unit train, and manifest train. Equations (5-9) and (5-10) present the TG model results for loaded unit train derailment severity based on the data including and excluding outliers, respectively. The effect of average gross tonnage per car on the derailment severity for the data both with and without outliers is insignificant.

$$Z = -1.739 - 0.0390(speed) - 0.00256(cars\ residual) \quad (5\text{-}9)$$

$$Z = -1.380 - 0.0759(speed) - 0.00459(cars\ residual) \quad (5\text{-}10)$$

Equations (5-11) and (5-12) present the TG model results for empty unit train derailment severity based on the data including and excluding outliers, respectively. In the model based on the data with outliers, the effects of average gross tonnage per car on the derailment severity are insignificant. In the model based on the data without outliers, the effects of average gross tonnage per car and residual train length on the derailment severity are insignificant.

$$Z = -0.658 - 0.0338(speed) - 0.00376(cars\ residual) \quad (5\text{-}11)$$

$$Z = -0.518 - 0.0634(speed) \quad (5\text{-}12)$$

Equations (5-13) and (5-14) display the model results for derailment severity of manifest trains based on the data with and without outliers, respectively. All considered variables and the intercept are significant for both models based on the data with and without outliers.

$$Z = -0.878 - 0.0285(speed) - 0.00308(cars\ residual) - 0.00288(tons\ per\ car) \quad (5\text{-}13)$$

$$Z = -0.513 - 0.0694(speed) - 0.00150(cars\ residual) - 0.00353(tons\ per\ car) \quad (5\text{-}14)$$

Table 31 summarizes the performance of TG models in estimating train derailment severity for loaded unit trains, empty unit trains, and manifest trains. Mean square error (Equation (5-7)) and mean absolute error (Equation (5-8)) were used as criteria to measure performance. The team found that the TG model had a better performance when outliers were excluded. Overall, the performance of the TG model was acceptable: the models with outliers all have mean absolute errors less than 7, and the models without outliers all have mean absolute errors less than 4.5.

Table 31. Summary of model performance of TG model

Train types	Data	Model results	Mean Square Error (MSE)	Mean Absolute Error (MAE)
All Train Types	With Outliers	$Z = -0.952 - 0.0306\times(speed) - 0.00180\times(cars\ residual) - 0.00239\times(tons\ per\ car) + 0.119\times(empty\ unit\ train) - 0.339\times(loaded\ unit\ train)$	60.67	5.72
	Without Outliers	$Z = -0.586 - 0.0702\times(speed) - 0.00206\times(cars\ residual) - 0.00293\times(tons\ per\ car) - 0.321\times(loaded\ unit\ train)$	33.47	4.00
Loaded unit trains	With Outliers	$Z = -1.739 - 0.0390\times(speed) - 0.00256\times(cars\ residual)$	82.53	6.84
	Without Outliers	$Z = -1.380 - 0.0759\times(speed) - 0.00459\times(cars\ residual)$	33.64	4.12
Empty unit trains	With Outliers	$Z = -0.658 - 0.0338\times(speed) - 0.00376\times(cars\ residual)$	57.98	5.44
	Without Outliers	$Z = -0.518 - 0.0634\times(speed)$	42.25	4.41
Manifest trains	With Outliers	$Z = -0.878 - 0.0285\times(speed) - 0.00308\times(cars\ residual) - 0.00288\times(tons\ per\ car)$	52.37	5.27
	Without Outliers	$Z = -0.513 - 0.0694\times(speed) - 0.00150\times(cars\ residual) - 0.00353\times(tons\ per\ car)$	32.39	3.91

5.3 Physical Modeling of Derailment Severity

Statistical models may have difficulty predicting extreme derailment events that fall outside historical experience. Physical models, however, can capture the conditions of a specific train derailment scenario by mathematically describing the physical dynamics of the derailment, which could help determine the derailment mechanism by train speed, tonnage, train length, etc. Therefore, physical models are expected to estimate train derailment severity more accurately.

5.3.1 Introduction

A simplified 1-D model for derailment kinematics was developed to investigate factors that contribute to differences in derailment severity for unit and manifest trains. The objective was to have a clear understanding of the effects of different train characteristics that most influence the risk for a given hazmat car shipment. The model includes the primary factors that contribute to the deceleration of train cars behind the point of derailment after the derailment event is initiated. These include:

- Length and weight of the rail cars behind the POD
- Train braking effects
- Derailment blockage forces
- Grade of the track
- Train rolling and aerodynamic resistance

The model was developed as a time stepping algorithm. At each time step, the braking, train resistance, and blockage forces are updated and applied to the cars behind the POD to calculate and update the deceleration rate. The speed and time steps then are applied to determine the train length (i.e., number of cars) passing the POD.

Rather than develop a model for the air brake system from first principles, a simplified approach was adopted that applies data obtained from various derailments. Three derailments were selected with different residual train lengths behind the POD and trailing locomotives with event recorders that provided data on the brake pressure and deceleration response of the cars behind the derailment. These three derailments are:

- Aliceville, AL, 11/7/2013: 39 mph, loaded unit oil train, 90 loads/0 empties, 26 cars derailed (car numbers 1-26)
- Brainerd, MN, 7/10/2011: 27 mph, loaded unit coal train, 121 loads/0 empties, 20 cars derailed (car numbers 66-85)
- Wagner, MT, 2/13/2013: 37 mph, loaded unit grain train, 104 loads/0 empties, 10 cars derailed (car numbers 88-97)

Given the available data for these derailments, they were also used as initial cases to investigate and validate the modeling.

5.3.1.1 Train Braking Effects

The brake cylinder pressure histories for the three derailments are shown in Figure 46. All three are characterized by a steady state increase in pressure over most of the application with a transition phase at the beginning and end of brake application. The primary difference in the curves appears to be a shift in the time for which the steady state increase in brake pressure occurs. This shift is correlated to the residual length of the train behind the POD where the shorter residual train length (Wagner, 18 cars behind POD) resulted in an earlier application of brakes and the longer residual train length (Aliceville, 90 cars behind POD) resulted in a delayed brake application.

The recorded brake application curves were applied to analyze the specific responses in these three derailments. However, for most derailments, this data was not available. Therefore, an approach was developed to estimate a brake application curve for other derailments by applying a time shift to a baseline pressure curve. In this case, the Brainerd derailment pressure curve was used as a baseline.

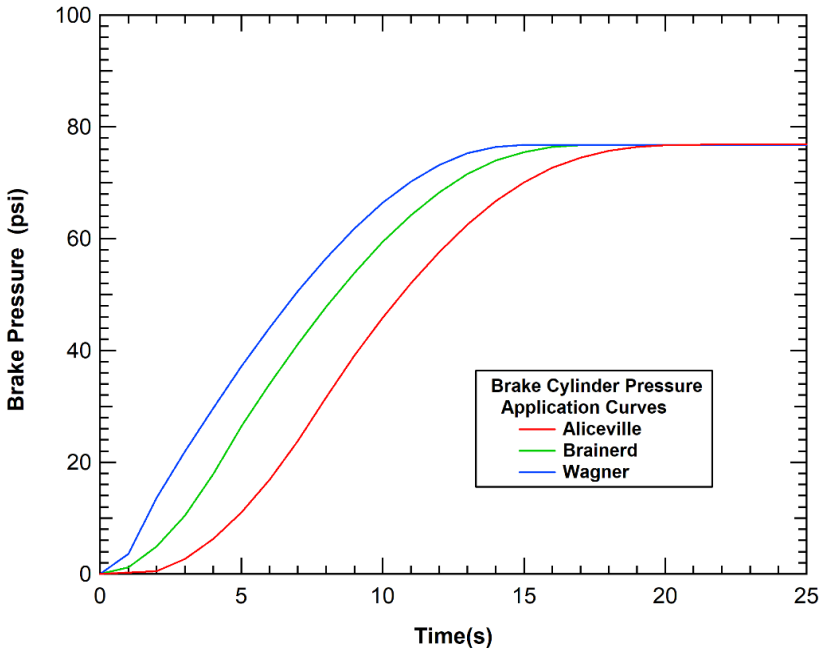

Figure 46. Brake cylinder pressure curves for various derailments

The equation used to shift the brake application curves for the various derailments is:

$$T_s = T_0 + [(N_c L_C - L_0)/1150] \quad (4\text{-}9)$$

T_s is the shifted time, T_0 is the baseline (i.e., reference) time, N_c is the number of cars in the residual train, L_C is the length of the cars in the residual train (in feet), and L_0 is the baseline train length. The equation effectively shifts the time based on the difference in the length of the residual train divided by the sound speed in the air pipe (1150 ft/s). For the corrections performed here, the reference residual train length used for Brainerd was 2852 ft.

A comparison of the time-shifted brake pressure curves with the event recorder curves for the Aliceville and Wagner derailments is shown in Figure 47. The comparison shows that the time shifted curve is a good approximation of the actual brake application behavior and a suitable approach to estimate braking for derailments where brake pressure data was unavailable.

An additional feature of the brake application model is the addition of brake application delay time. The brake application curves, shown in Figure 47, used a derailment initiation reference time from the event data recorder (time = 0). This time was determined from the brake pressure change that initiates the onset of emergency braking. However, this refers to the time when a separation occurs in the brake pipe rather than the time when an initial car derails.

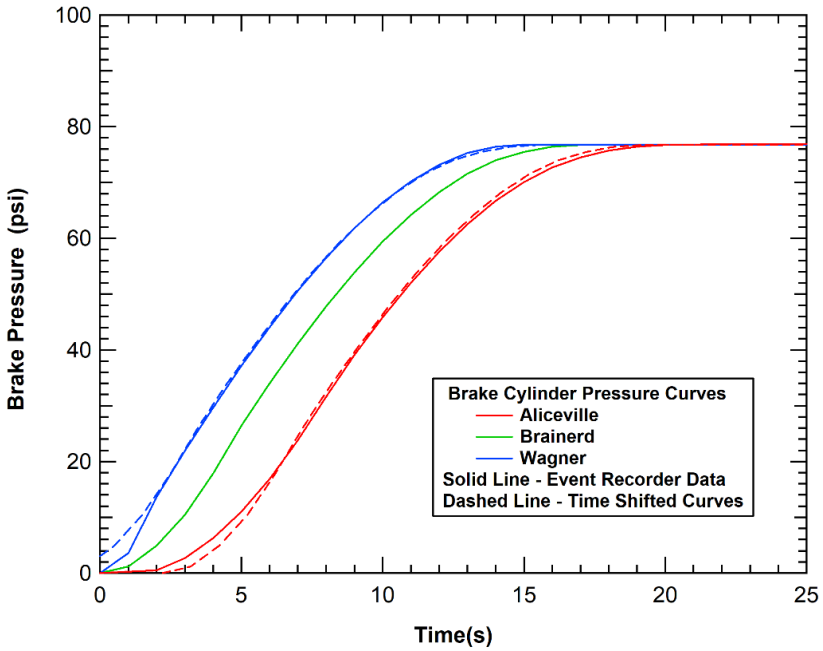

Figure 47. Comparison of the time-shifted brake pressure curves and event recorder curves

In a typical derailment, the initiation will occur from some failure of the rail, equipment, or excess in lateral loads at the wheel-rail interface. The initial cars that derail are typically still connected to the leading and trailing cars and are initially aligned closely with the original rail orientation. There will typically be a delay between the time when the initial wheel derails and the time when the additional forces on the derailed cars result in a failure of the coupled connection and separation from the leading cars ahead of the POD. It is typically only after this delay that the brake pipe will be broken, and the brake initiation will begin. As a result, a brake application delay time was added to shift (i.e., delay) the brake application curve from the time of the derailment initiation. The magnitudes of the brake application delay times are discussed further in the model validation analyses.

The braking forces are assumed to be proportional to the brake application and use an emergency braking force of 7800 lb brake force per car at full pressure (Lovette & Thivierge, 1992). This level results in a 3 percent brake ratio for a 263K gross rail load (GRL) loaded car and a 12 percent brake ratio for a 65K lightweight empty car. Similarly, an 18 percent brake ratio is assumed to be typical for locomotives in emergency braking with an application that follows the same pressure curve.

5.3.1.2 Derailment Blockage Force

The next factor in the derailment model is the derailment blockage force. The blockage force is the in-line train force produced by the derailed cars that acts on the remaining cars on the rail behind the POD. The kinematics of a car approaching and passing the POD in a derailment is illustrated in Figure 48. The blockage resistance is a combination of higher rolling or sliding resistance between the car and ground after leaving the rail and the forces from impacts against a pileup of previously derailed cars in the forward portion of the derailment. The force is either transmitted through the draft gear or by any point of contact from impacts between cars. The

magnitude of the force transmitted longitudinally aft from the derailed cars will also be a function of the constantly changing alignment of cars resulting from the lateral buckling of derailed cars.

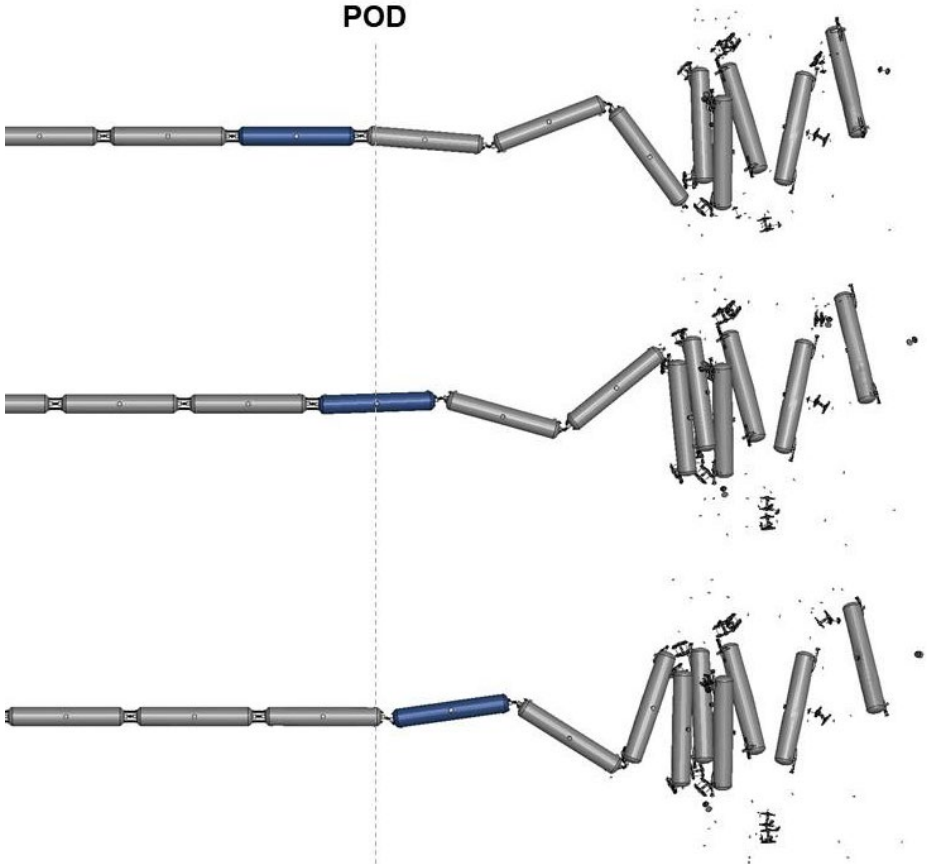

Figure 48. Example kinematics of a car passing the point of derailment

Previous studies have investigated and analyzed the magnitude of this blockage force. Brosseau (2014) analyzed several derailments and compared the deceleration response to the calculated deceleration that would occur from braking alone, calculating blockage forces between 500,000 and 650,000 lb. Similarly, an analysis of the Lac Mégantic derailment (Transportation Safety Board of Canada, 2014a) found an average blockage force of approximately 400,000 lb. In this case, the train was a runaway with no braking applied so the blockage force was acting alone to stop the motion of the cars on the rail behind the POD.

Although the blockage force is not expected to be a smooth profile due to the buckling and impact behaviors of the cars (Transportation Safety Board of Canada, 2014a), it is commonly approximated as a smooth force in models, as illustrated in Figure 49. In addition, there is a potential period at the initiation of the derailment where the cars ahead of the derailment provide a traction force until separation occurs. Thus, the blockage is modeled with a delay time before blockage forces begin, a ramp time over which the blockage force is linearly increased, and then a steady state when blockage force is fully developed. This blockage force is applied in the model as a force fixed at the POD acting on the remaining cars (i.e., mass) on the rails behind that position.

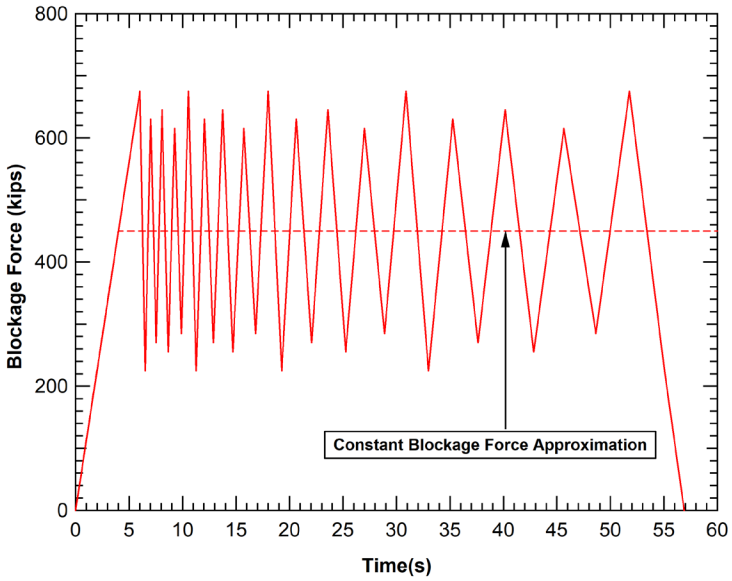

Figure 49. Schematic illustration of the blockage force profile in a derailment

5.3.1.3 Train Resistance

The final set of forces included in the model is the standard train resistance forces. Gravitational acceleration is added to a train on either an uphill or downhill grade. A model for the train resistance is also added based on existing models (Hay, 1982). Resistance to motion is an important input for any such simulation, and the Davis equation, which is a well-known resistance formula, is widely used for freight trains. The Davis equation is a quadratic form in velocity:

$$R = A + Bv + Cv^2 \tag{5-10}$$

with constant coefficients based on experimental work done by W.J. Davis (1926). It has multiple variants known as the Modified Davis and Adjusted Davis equations. The resistance calculations of the Davis equation are commonly defined as a force per unit train weight.

In the Davis equation, the constant term A represents the journal rolling resistance. The second term in the Davis equation represents the flange resistance and is proportional to the train speed. The final term is the wind resistance and is proportional to the square of the train speed.

For the model, the team used the following values for the resistance:

$$\begin{aligned} A &= 1.3 + 29/w \ (lbs/ton) \\ B &= 0.045 \ (lbs/ton - mph) \\ C &= 5.2 \ (lbs/ton - mph^2) \end{aligned} \tag{5-11}$$

where w is the axle load in tons. These coefficients produce the resistance magnitudes shown in Figure 50 for a 263k GRL loaded freight car. An assessment of these resistance forces indicates that they are most significant at high speed and, as a result, have little effect on most derailments. However, they were kept in the model for completeness.

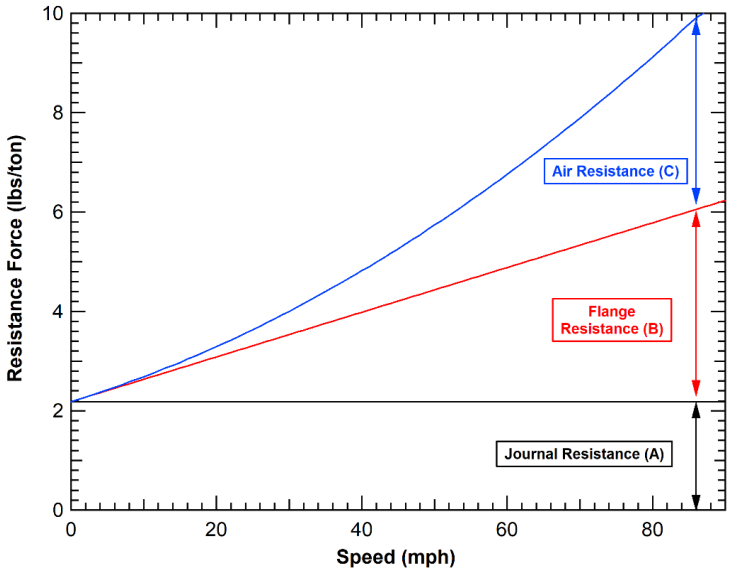

Figure 50. Resistance model for a conventional freight train

5.3.2 Model Architecture

The derailment model was developed as a simple time stepping algorithm. A general flowchart for the model methodology is provided in Figure 51.

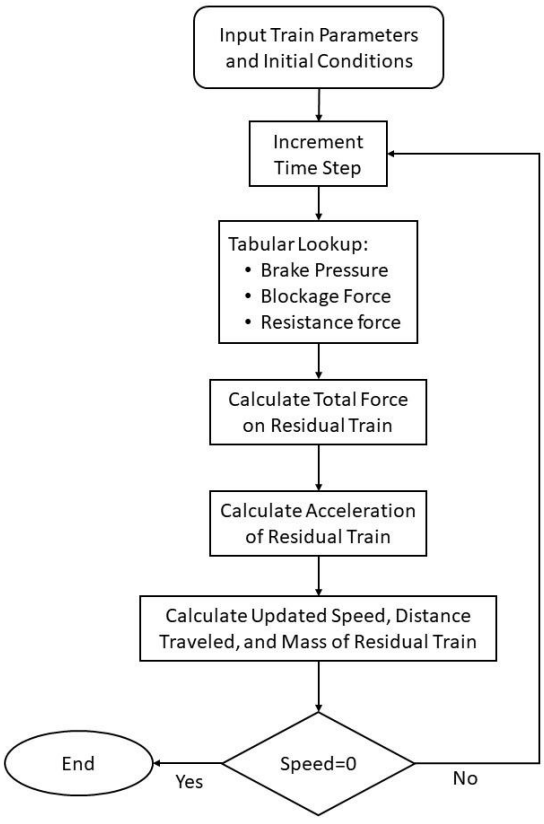

Figure 51. Derailment model flowchart

The required input parameters begin with a description of the train (behind the POD) that includes the number of cars, the weight of each car, the car lengths, and additional features (e.g., a trailing locomotive). The derailment speed and curves such as the braking and blockage forces and rolling resistance are specified as input conditions at the start of the analysis. The algorithm then steps through time updating the motions of the residual train (the portion of the train behind the POD) and forces on the residual train until the train comes to rest.

For derailments with a trailing locomotive included in the residual train, the weight of the locomotive, position of the locomotive, and locomotive brake ratio are all specified.

The equations of motion for the residual train are solved with a computational approach. At each time step, the sum of the forces acting on the train (i.e., braking, blockage, rolling resistance, and gravitational) is calculated, along with the distance traveled, residual length, and residual train mass. The total force and residual train mass are used to calculate an updated derailment acceleration of the residual train. This process is solved by incremental time steps up to the point where the residual train comes to rest.

5.3.3 Model Validation Analyses

The primary model validation was achieved via a comparison to a series of derailments where quantitative data was available on the derailment response. Data from three different derailments were obtained from the event recorder in a trailing locomotive. The three cases analyzed were:

- Aliceville, AL, 11/7/2013: 39 mph, loaded unit oil train, 90 loads/0 empties, 26 cars derailed (car numbers 1-26), 90 cars behind POD
- Brainerd, MN, 7/10/2011: 27 mph, loaded unit coal train, 121 loads/0 empties, 20 cars derailed (car numbers 66-85), 56 cars behind POD
- Wagner, MT, 2/13/2013: 37 mph, loaded unit grain train, 104 loads/0 empties, 10 cars derailed (car numbers 88-97), 17 cars behind POD

In addition to providing data from an event recorder in a trailing locomotive, these three derailments represent good tests of the model because they have significantly different residual train lengths (number of cars behind the POD). Such length variation tests the relative importance of different aspects of the model. For example, the blockage force is applied at the POD. As a result, the blockage forces are much more significant for a small residual train length (less mass behind the POD) than they will be for a long residual train.

5.3.3.1 Aliceville Derailment Analysis

A contractor's letter to the Environmental Protection Agency (EPA) states: "At around midnight on November 7, 2013, an Alabama & Gulf Coast Railway train hauling crude oil from Amory, Mississippi, to Walnut Hill, Florida, derailed just south of Aliceville, Alabama, at railroad milepost 683. The train was composed of 90 railcars, 26 of which derailed into a wetland slough located along the east and west sides of the rail line. During high water, the slough connects to Lubbub Creek, which discharges into the Tombigbee River approximately 3.5 miles southwest of the derailment." The locomotive passed the derailment point and remained on the tracks, and the buffer car was pulled along by the locomotive and derailed but never separated from the locomotive (Croft & Johnson, 2013).

The cause of the derailment was not conclusively determined but has been identified in one unpublished report as a possible broken rail. The derailment occurred on a slightly curved track, but the slight curvature was ignored, and the derailment was modeled with straight track in the simulations. The derailment speed was 39 mph.

The description of the Aliceville train consist as incorporated in the 1-D analysis is summarized in Figure 52. The train was defined as a loaded unit oil train that had 90 263K GRL tank cars behind the POD followed by a single 415 Kip trailing locomotive.

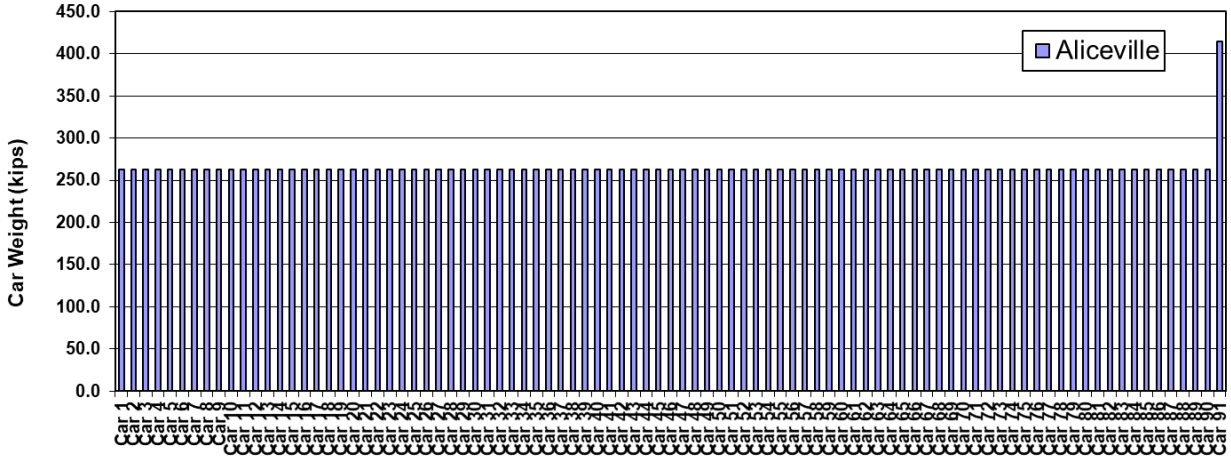

Figure 52. Train makeup for the Aliceville derailment analysis

The primary model parameters used for the Aliceville 1-D analysis were:

- 91 cars behind POD
- 59.3-foot car lengths
- 500-kip blockage force
- 6 s blockage delay
- 4 s blockage ramp
- 39 mph derailment
- 0.0 percent grade
- event recorder brake pressure curve
- 6 s brake delay

The event recorder velocity and displacement data are compared with the 1-D model analysis in Figure 53. Note that the derailment time from the event recorder was shifted by 4.5 seconds so that the correct length of the train (i.e., number of cars) reaches the point of derailment. This comparison of the event recorder displacement and the number of cars derailed was used to provide insight into the delayed brake application after the time of the derailment initiation. In addition, one of the derailed cars was the buffer car that remained attached to the locomotive and was pulled away from the derailment. Thus, the team considered the primary derailment severity to be the 25 cars behind the point of separation between the buffer car and the first tank car.

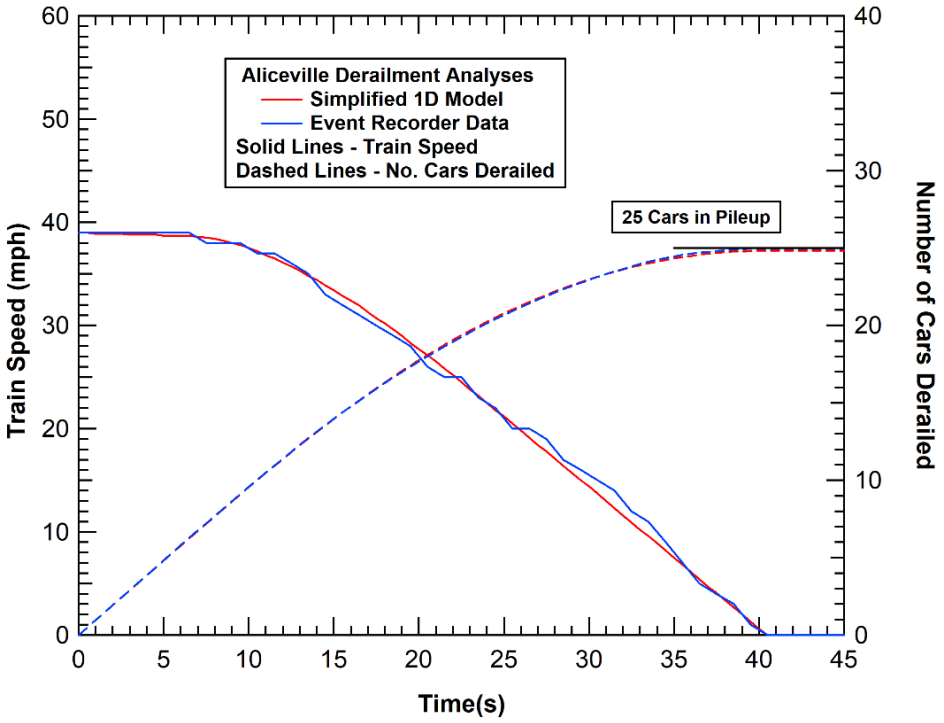

Figure 53. Comparison of the measured and modeled Aliceville derailment kinematics

One of the objectives of the model development for this study was to investigate the relative severity of derailments between manifest and unit trains. One method for this comparison is the total kinetic energy of the vehicles past the point of derailment. The derailment energy for the Aliceville incident is summarized in Figure 54. The derailment response results in cumulative derailment energy of 232 million ft-lb. Comparisons to a similar derailment condition for a corresponding manifest train are provided in the Brainerd Derailment Analysis below.

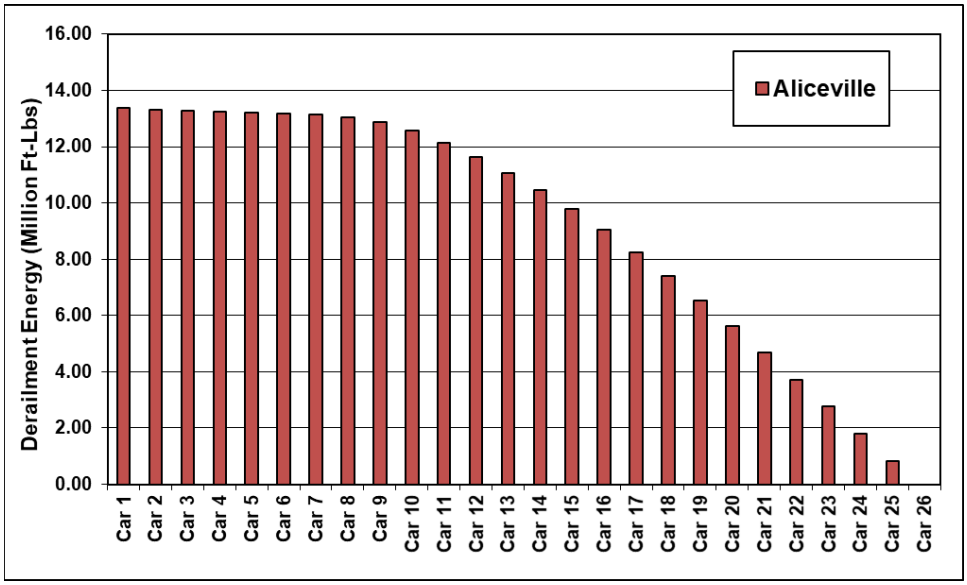

Figure 54. Calculated car derailment energies for the Aliceville derailment

5.3.3.2 Brainerd Derailment Analysis

The Brainerd, MN, derailment of a loaded coal unit train occurred on July 10, 2011. The train carried 121 loads but derailed in the middle of the train with car 66 as the first car behind the POD and 20 cars derailed (cars 66-85). The event recorder data showed the train traveling at 27 mph at the time the emergency was initiated at the rear end of the train (Brosseau, 2014). According to the raw event recorder data, the train came to a stop after 22 seconds.

The description of the Brainerd train consist as incorporated in the 1-D analysis is summarized in Figure 55. The residual train was defined as a loaded unit coal train comprising 61 286K GRL coal cars behind the POD followed by a single 420 Kip trailing locomotive.

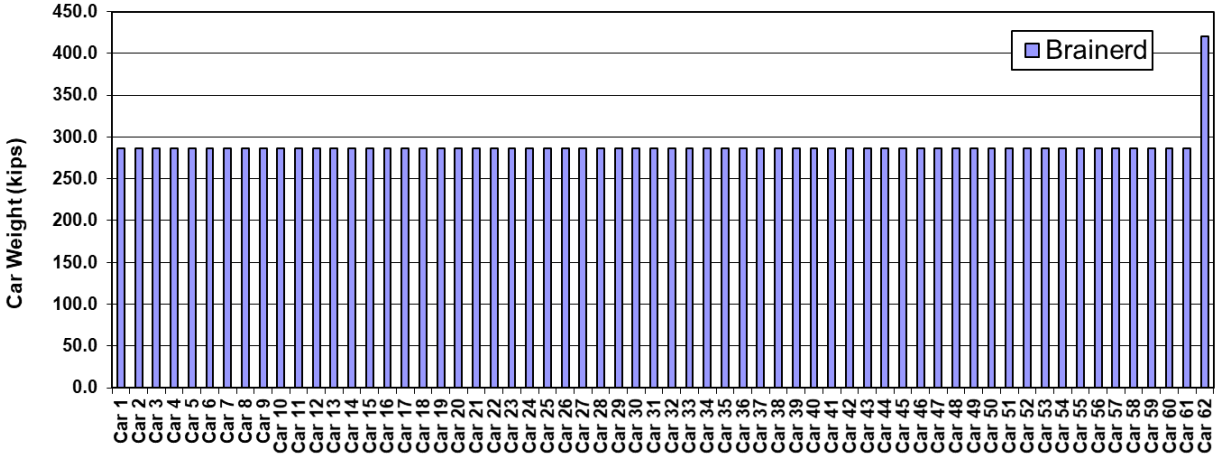

Figure 55. Train makeup for the Brainerd derailment analyses

The primary model parameters used for the Brainerd 1-D analysis were:

- 62 cars behind POD
- 53.1-foot car lengths
- 420-kip trailing locomotive
- 460-kip blockage force
- 14 s blockage delay
- 4 s blockage ramp
- 27 mph derailment
- 0.0 percent grade
- event recorder brake pressure curve
- 14 s brake delay

The event recorder velocity and displacement data are compared with the 1-D model analysis in Figure 56. The derailment energy for the Brainerd derailment is summarized in Figure 57. The derailment response results in a cumulative derailment energy of 101 million ft-lb.

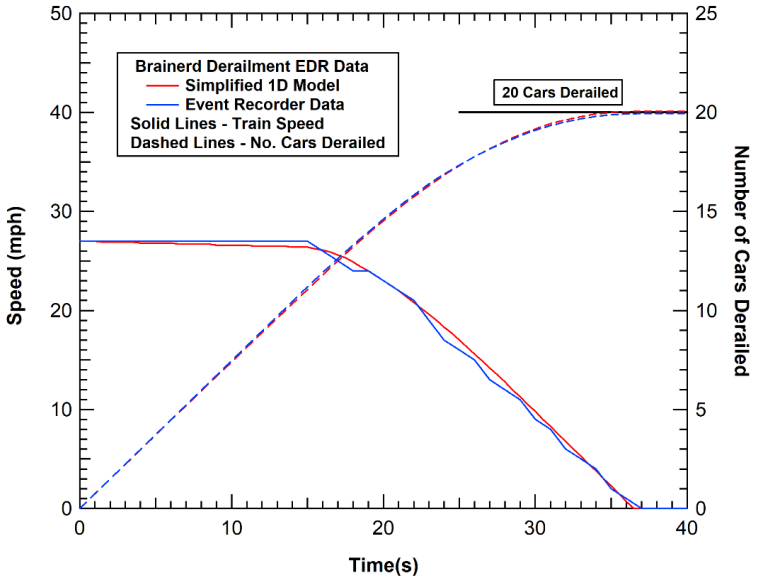

Figure 56. Comparison of the measured and modeled Brainerd derailment kinematics

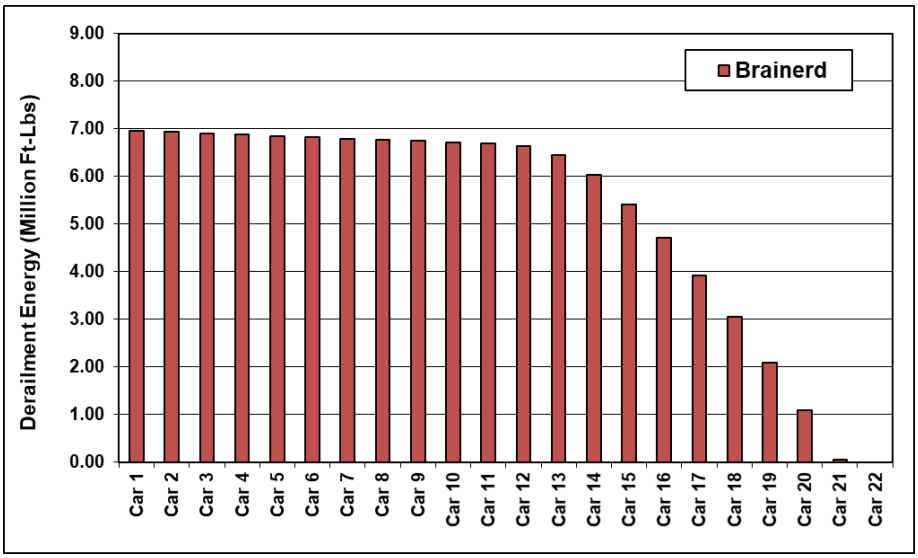

Figure 57. Calculated car derailment energies for the Brainerd derailment

5.3.3.3 Wagner Derailment Analysis

The Wagner, MT, derailment of a loaded unit grain train occurred on February 13, 2013. The train carried 104 loads but derailed in the rear of the train with car 88 as the first car behind the POD and 10 cars derailed (cars 88-97). The event recorder data showed the train traveling at 37 mph at the time the emergency was initiated at the rear of the train (Brosseau, 2014). According to the raw event recorder data, the train came to a stop after 11 seconds.

The description of the Wagner train consist as incorporated in the 1-D analysis is summarized in Figure 58. The residual train was defined as a loaded unit grain train comprising 18 263K GRL grain hopper cars behind the POD followed by a single 415 Kip trailing locomotive.

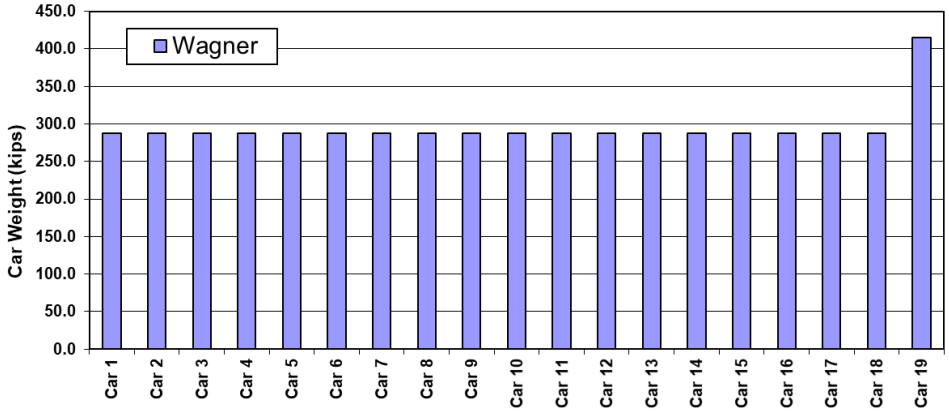

Figure 58. Train makeup for the Wagner derailment analyses

The primary model parameters used for the Wagner 1-D analysis were:

- 19 cars behind POD
- 59.3-foot car lengths
- 415-kip trailing loco
- 400-kip blockage force
- 2.5 s blockage delay
- 4 s blockage ramp
- 38 mph derailment
- 0.0 percent grade
- event recorder brake pressure curve
- 2.5 s brake delay

The event recorder velocity and displacement data are compared with the 1-D model analysis in Figure 59. The derailment energy for the Wagner derailment is summarized in Figure 60.

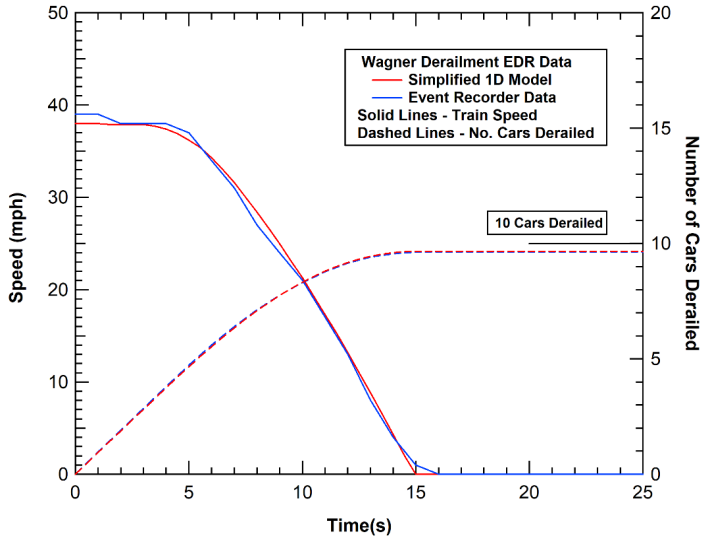

Figure 59. Comparison of the measured and modeled Wagner derailment kinematics

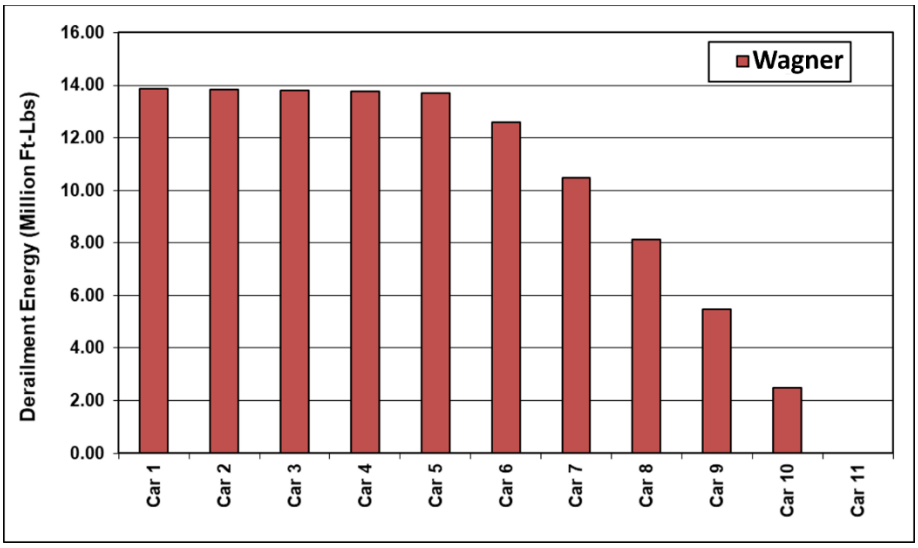

Figure 60. Calculated car derailment energies for the Wagner derailment

5.3.3.4 Graettinger Derailment Analysis

The Graettinger, IA, derailment of a loaded ethanol train occurred on March 10, 2017. The train carried 100 loads and derailed at car 21 leaving 80 cars and a trailing locomotive behind the POD. The event recorder data showed the train traveling at 29 mph at the time of derailment and 20 cars derailed (cars 21-40). According to the raw event recorder data, the train came to a stop in 11 seconds.

The Graettinger train consist is incorporated in the 1-D analysis as a string of 80 cars loaded to 254K GRL followed by a single 415 Kip trailing locomotive.

The primary model parameters used for the Graettinger 1-D analysis were:

- 80 cars behind POD
- 59.9-foot car lengths
- 415-kip trailing locomotive
- 450-kip blockage force
- 12 s blockage delay
- 4 s blockage ramp
- 29.5 mph derailment
- 0.2 percent ascending grade
- model adjusted brake pressure curve
- 12 s brake delay

The event recorder velocity and displacement data are compared with the 1-D model analysis in Figure 61.

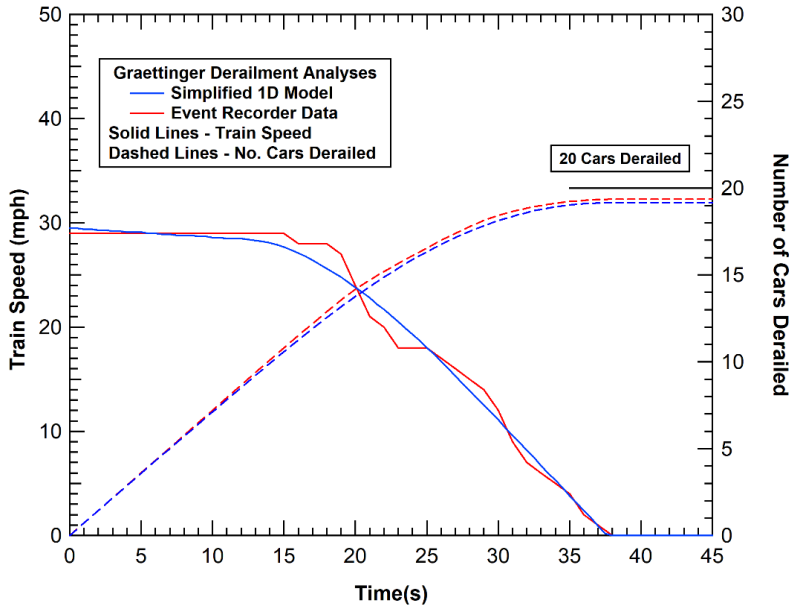

Figure 61. Comparison of the measured and modeled Graettinger derailment kinematics

5.3.3.5 Casselton Derailment Analysis

The Casselton, ND, derailment occurred on December 30, 2013, when a westbound BNSF train carrying 112 cars loaded with grain derailed 13 cars while traveling on main track 1 at milepost 28.5. The first car that derailed (the 45th car) fouled the adjacent main track. Approximately one minute later, an eastbound BNSF train with 104 tank cars loaded with petroleum crude oil, traveling on main track 2, struck the derailed car that was fouling the track. As a result of the collision, the oil train derailed both head-end locomotives, a buffer car, and 20 cars loaded with crude oil.

Event recorder data was available for analysis of the ride-down behavior from a trailing locomotive on the second oil train involved in the accident. The event recorder data showed the train traveling at 43 mph while approaching the point of collision and derailment initiation. According to the raw event recorder data, the train came to a stop approximately 45 seconds after the application of emergency braking.

The Casselton train consist is incorporated in the 1-D analysis as a string of 2 lead locomotives, 106 cars loaded to 252K GRL followed by a single 415 Kip trailing locomotive. The primary model parameters used for the Casselton 1-D analysis were:

- 106 cars behind POD
- 59.6-foot car lengths
- 2 415-Kip leading locomotives
- 415-kip trailing locomotive
- 400-kip blockage force
- 7 s blockage delay
- 6 s blockage ramp

- 43 mph derailment
- 0.1 percent descending grade
- model adjusted brake pressure curve
- 7 s brake delay

The event recorder velocity and displacement data are compared with the 1-D model analysis results in Figure 62.

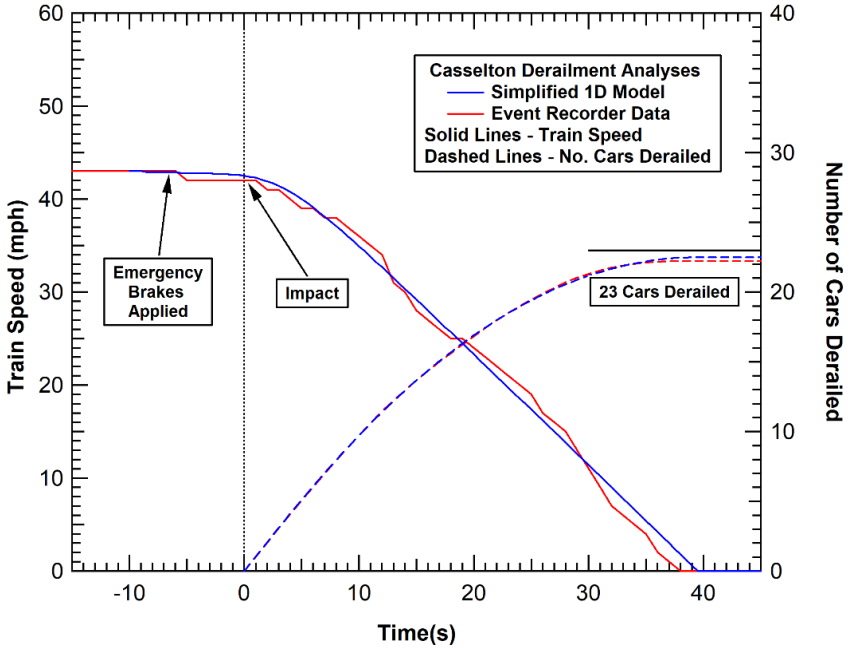

Figure 62. Comparison of the measured and modeled Casselton derailment kinematics

5.3.3.6 Saskatoon Derailment Analysis

The Saskatoon, SK, derailment of a loaded unit grain train occurred on January 22, 2019. The train carried 155 loaded cars and derailed with 130 cars behind the POD and 30 cars derailed (cars 33-62). Note that there was a distributed power locomotive in the derailed string at position 52 in the consist. From the length and trailing tons, the team calculated an average car length of 56.7 feet and an average weight of the loaded grain hoppers of 285,000 lb.

An aerial photograph of the Saskatoon derailment is shown in Figure 63. As seen in the photo, the derailment occurred at a grade crossing where multiple cars were stopped. The derailment response was captured by different video cameras at the grade crossing ("Canadian Traindude," 2019; Nathan Zeller, 2019). These videos were analyzed by Geordie Roscoe (2019) to determine the deceleration profile of the derailing train. This deceleration profile was used as a comparison to the 1-D model analysis.

Figure 63. Photograph of the Saskatoon derailment event

The primary model parameters used for the Saskatoon 1-D analysis were:

- 130 cars behind POD
- 56.7-foot car lengths
- 415-kip DP locomotive at position 26 in derailed string
- 600-kip blockage force
- 7 s blockage delay
- 4 s blockage ramp
- 36 mph derailment
- 0.3 percent descending grade
- 7 s brake delay

The video analysis velocity and displacement data are compared with the 1-D model analysis in Figure 64.

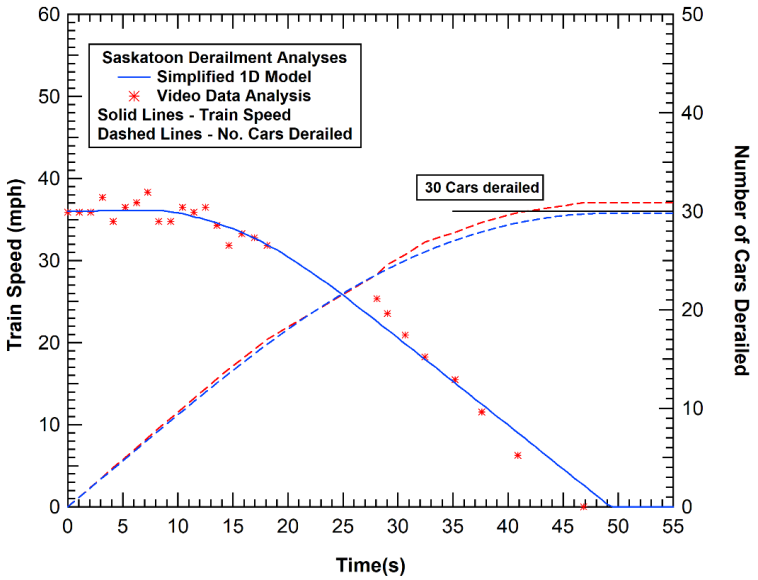

Figure 64. Comparison of the measured and modeled Saskatoon derailment kinematics

The derailment energy for the Saskatoon derailment is summarized in Figure 65. The derailment response resulted in a cumulative derailment energy of 266 million ft-lb.

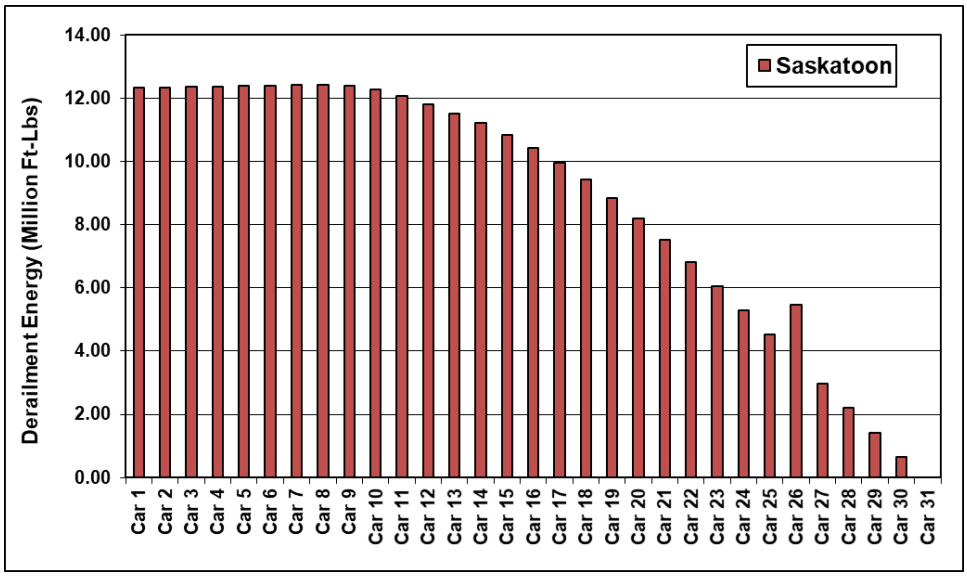

Figure 65. Calculated car derailment energies for the Saskatoon derailment

5.3.3.7 Lac-Mégantic Derailment Analysis

The Lac-Mégantic, Quebec, derailment occurred on July 6, 2013. The derailment involved a unit train carrying petroleum crude oil that was in a runaway condition. Due to the damage and casualties caused by this derailment, the results and data from a significant investigation were available for analysis.

The train carried a buffer car and 72 loaded tank cars and was in a runaway condition traveling at 65 mph when it derailed. The derailment occurred at the front of the train with the buffer car derailing as well as 63 of the 72 tank cars. Although the quantitative data from an event recorder behind the POD was not available, a significant amount of information about the derailment was available from the Transportation Safety Board (TSB) investigation (2014b). A photograph of the derailment is shown in Figure 66.

The derailment was applied to the model validation primarily due to the unique characteristics of the runaway condition involved. Since the brake system was not functional in the derailment, the deceleration was almost exclusively the result of blockage forces. Thus, this derailment provides a unique scenario for investigating blockage effects. Based on the reported train length and trailing tons, the team calculated that the consist behind the POD was primarily 72 loaded tank cars with a length of 59.3 feet and an average weight of 282,000 lb.

The primary model parameters used for the Lac-Mégantic 1-D analysis were:

- 72 cars behind POD
- 282,000 lb average car weight
- 59.3-foot car lengths
- 450-kip blockage force

- 2 s blockage delay
- 4 s blockage ramp
- 65 mph derailment
- 1.26 percent descending grade
- no braking force

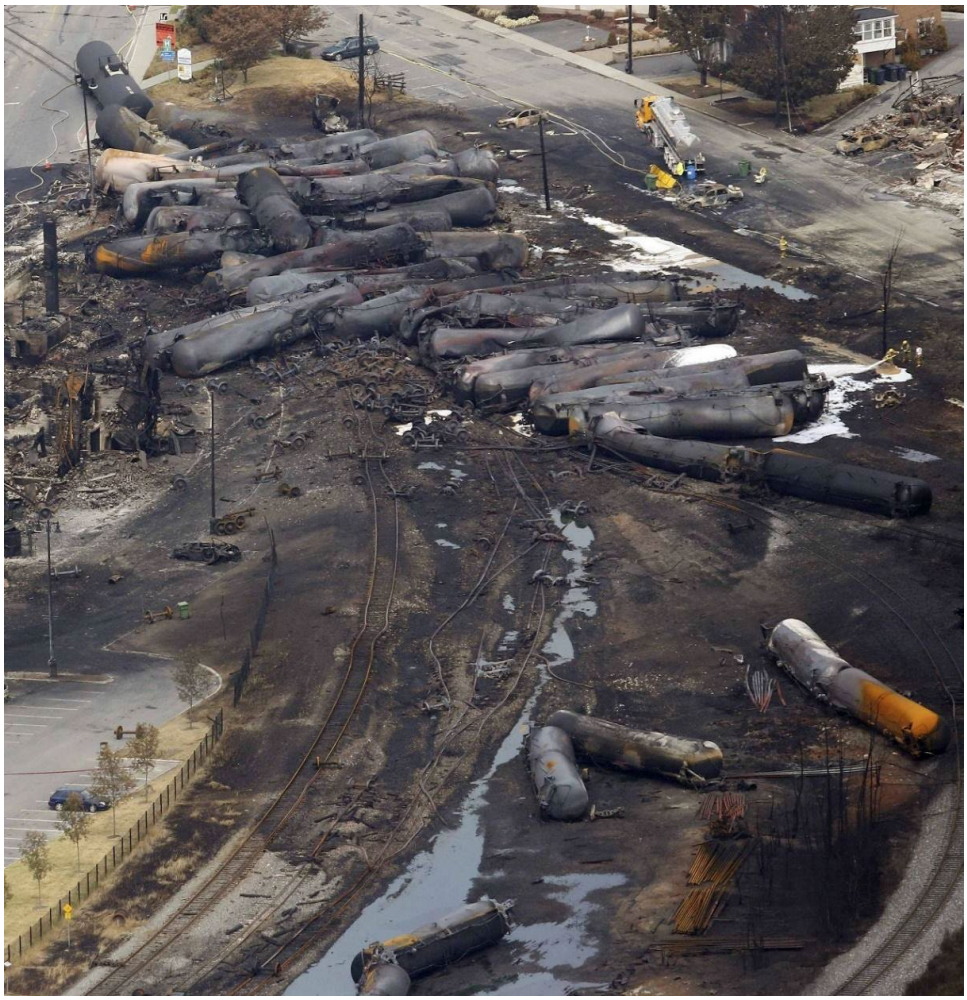

Figure 66. Photograph of the Lac-Mégantic derailment event

The calculated velocity and displacement data from the 1-D model analysis of the Lac-Mégantic derailment are shown in Figure 67. The parameters selected for the model resulted in 62 cars derailed, compared to the 64 observed cars derailed. However, the first three tank cars were observed to be pulled along the curve past the primary POD by a significant distance. Therefore, they may have derailed from overspeed on the curve rather than leaving the rail at the POD.

The derailment energy for the Lac-Mégantic derailment is summarized in Figure 68. The derailment response resulted in a cumulative derailment energy of 1.82 billion ft-lb. Also shown in the figure are the corresponding derailment energies for the Aliceville and Minot derailments. The comparison shows the severe magnitude of this derailment compared to other events.

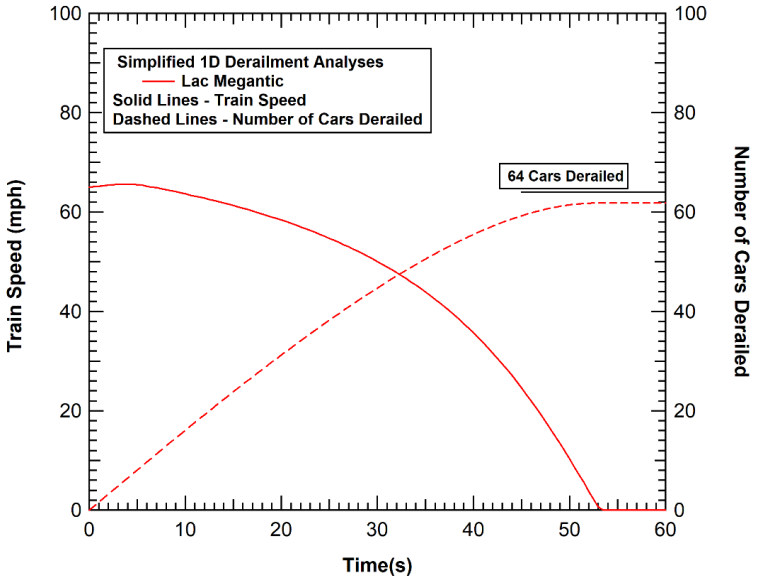

Figure 67. Calculated Lac-Mégantic derailment kinematics and observed severity

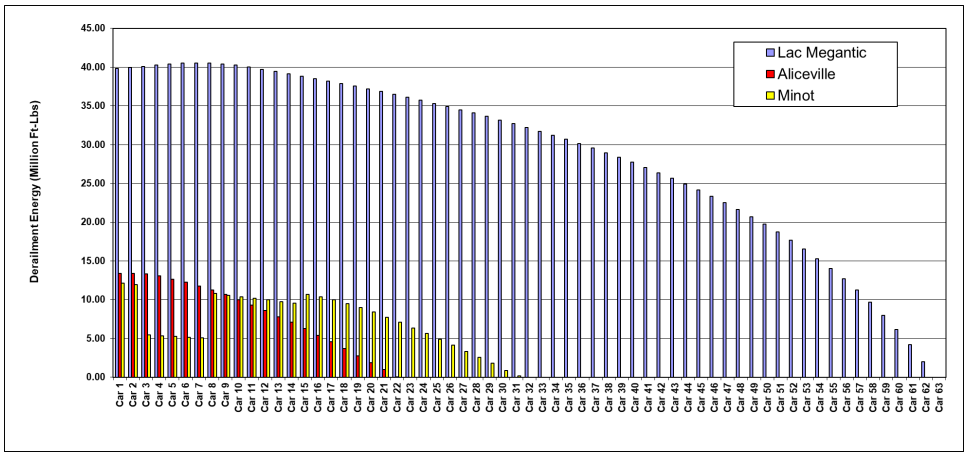

Figure 68. Calculated car derailment energies for the Lac-Mégantic derailment compared to Aliceville and Minot derailments

5.3.3.8 Minot Derailment Analysis

One of the primary objectives of the model development is to investigate the differences in severity between unit trains and revenue trains with mixed manifests. The derailments analyzed in the previous sections were all unit trains. Unfortunately, the team did not obtain any data for a revenue train where an event recorder was located behind the POD. As a result, the January 18, 2002, derailment of a freight train near Minot, ND, was used in this study as a reference revenue train derailment. The train comprised 112 cars and derailed near the front of the train with car 4 as the first car behind the POD and 31 cars derailed (cars 4-34). Although the quantitative data from an event recorder behind the POD was not available, a significant amount of information about the derailment was available from both the National Transportation Safety Board (NTSB) investigation (2004) and other studies of this derailment (Kirkpatrick, 2005). A photograph of the derailment is shown in Figure 69.

Figure 69. Photograph of the Minot derailment event (Kirkpatrick, 2005)

The following is a description of the event according to the NTSB Railroad Accident Report (2004): "At approximately 1:37 a.m. on January 18, 2002, eastbound Canadian Pacific Railway freight train 292-16, traveling about 41 mph, derailed 31 of its 112 cars about 1/2 mile west of the city limits of Minot, North Dakota."

A description of the Minot train consist as incorporated in the 1-D analysis is summarized in Figure 70. As expected for a revenue train, the consist includes various blocks of different car types including both loaded and empty cars. The power for the train was provided by leading locomotives ahead of the POD.

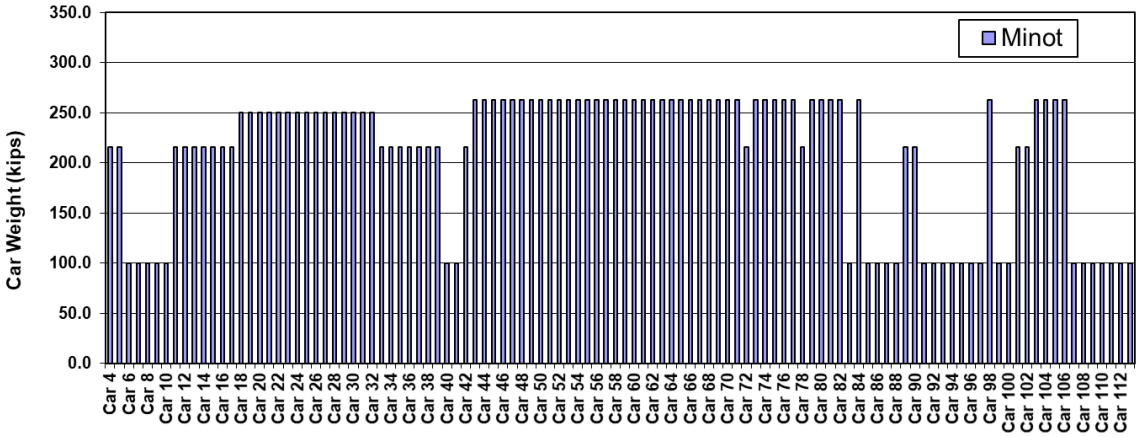

Figure 70. Train makeup for the Minot derailment analyses

The primary model parameters used for the Minot 1-D analysis were:

- 108 cars behind POD
- various car weights from manifest
- 59-foot car lengths
- 400-kip blockage force
- 8 s blockage delay
- 4 s blockage ramp
- 41 mph derailment
- 0.0 percent grade
- 1-D model brake pressure curve
- 8 s brake delay

Since event recorder data was not available for this derailment, the parameters were estimated without information to guide the selection. For example, the braking and blockage delay times were set at 8 seconds, which is between the 4-second delays in the Aliceville and Wagner derailments and the 14-second delay in the Brainerd derailment.

The calculated velocity and displacement data from the 1-D model analysis are shown in Figure 71. The parameters selected for the model resulted in 30 cars derailed compared to the 31 observed cars derailed. The derailment energy for the Minot derailment is summarized in Figure 72.

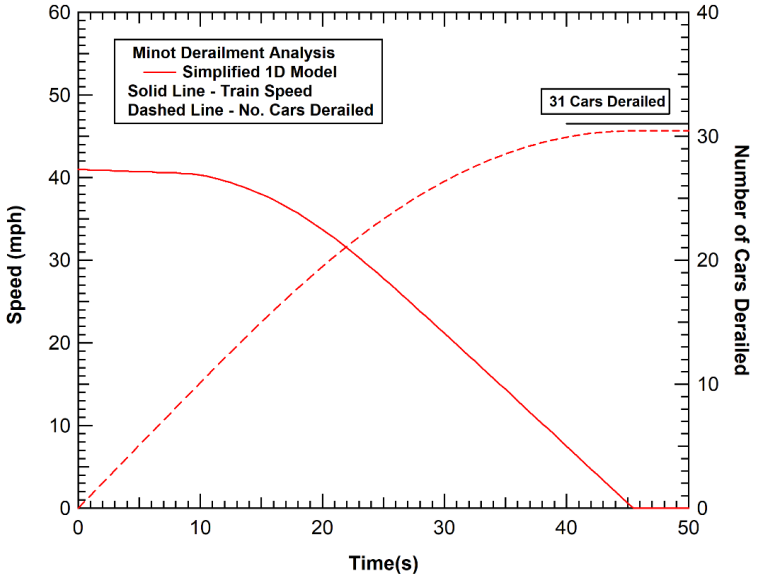

Figure 71. Calculated Minot derailment kinematics and observed severity

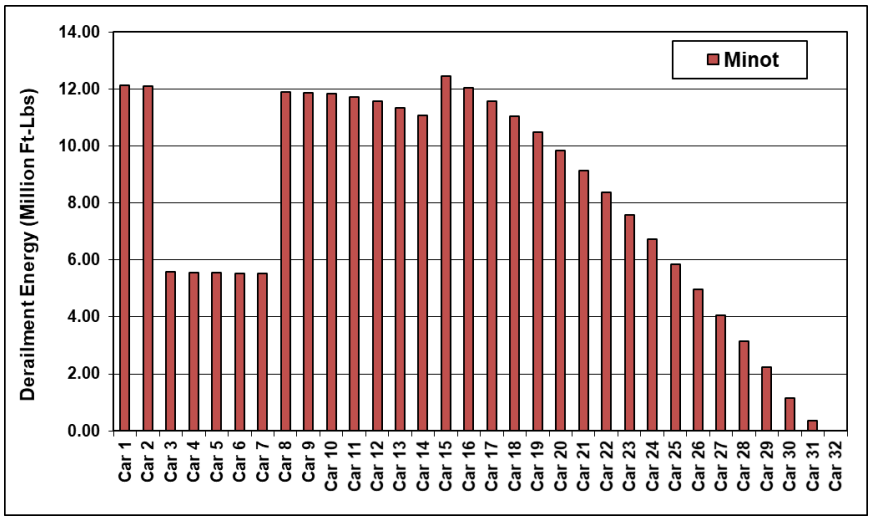

Figure 72. Calculated car derailment energies for the Minot derailment

5.3.3.9 Braking Model Validation Analyses

Since part of the data collection effort to obtain derailments can be used for the primary validation cases, a few examples were identified where the event recorder data was available for the locomotive ahead of the POD. This data cannot provide any insight into the mechanics of the derailment behind the POD, but it can be used in an evaluation of the emergency braking model in the analysis.

As described previously in the Casselton Derailment Analysis, the Casselton, ND, derailment and collision was initiated when a unit grain train derailed 13 cars. The first car that derailed (the 45th car) fouled the adjacent track. Approximately one minute later, an eastbound BNSF train carrying 104 tank cars loaded with petroleum crude oil, traveling on main track 2, struck the derailed car that was fouling the track and derailed two head-end locomotives, a buffer car, and 20 cars loaded with crude oil.

The ride-down behavior of the second oil train involved in the accident was analyzed. However, data was also available from the event recorder of a lead locomotive in the first train that derailed. The data showed the grain train traveling at 28 mph when approaching the point of derailment initiation. According to the raw event recorder data, the lead section of the train (ahead of the POD) came to a stop approximately 36 seconds after the application of emergency braking.

The Casselton train consist is incorporated in the 1-D analysis as a string of 2 lead locomotives and 44 grain hoppers loaded to 263K GRL. The primary model parameters used for the 1-D braking analysis of the Casselton train were:

- 44 cars ahead of POD
- 2 415-kip leading locomotives
- 28 mph derailment
- 0.10 percent descending grade
- 18 percent locomotive brake ratio

- model adjusted brake pressure curve

A comparison of the event recorder data and 1-D analysis of the braking ride-down behavior for Casselton is shown in Figure 73. The comparison shows that the braking model is capable of accurately reproducing the ride-down response for the lead section of the train in this derailment.

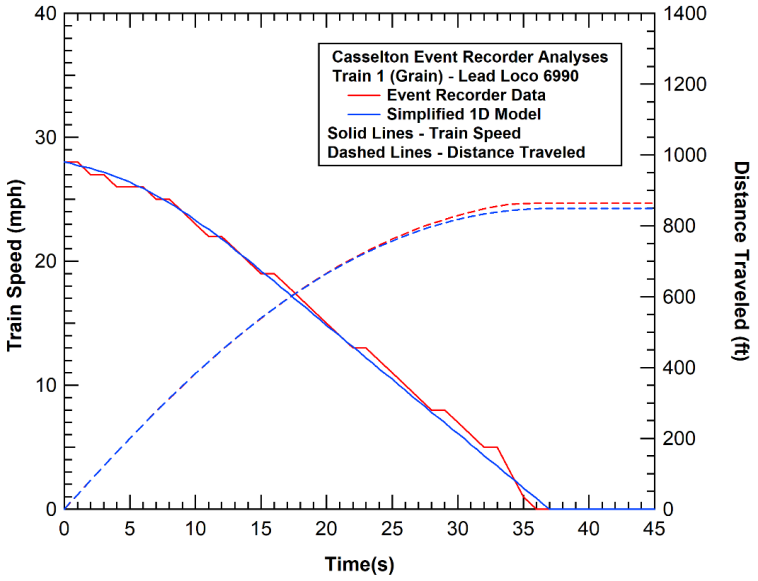

Figure 73. Comparison of the measured and modeled Casselton emergency braking response

The second derailment evaluated to validate the braking behavior is the April 30, 2014, derailment in Lynchburg, VA. The CSX crude oil unit train was traveling eastbound on the number 2 track when the train derailed at car 35 as the result of a broken rail. Data showed the train traveling at 24 mph when approaching the point of derailment initiation. According to the raw event recorder data, the lead section of the train (ahead of the POD) came to a stop approximately 31 seconds after the application of emergency braking.

The Lynchburg train consist is incorporated in the 1-D analysis as a string of 2 lead locomotives and 34 tank cars loaded to 257K GRL. The primary model parameters used for the 1-D braking analysis of the Lynchburg train were:

- 34 cars ahead of POD
- 2 415-kip leading locomotives
- 24 mph derailment
- 0.0 percent grade
- 18 percent locomotive brake ratio
- model adjusted brake pressure curve

A comparison of the event recorder data and 1-D analysis of the braking ride-down behavior for Lynchburg is shown in Figure 74. The comparison shows that the braking model is again capable of accurately reproducing the ride-down response for the lead section of the train in this derailment.

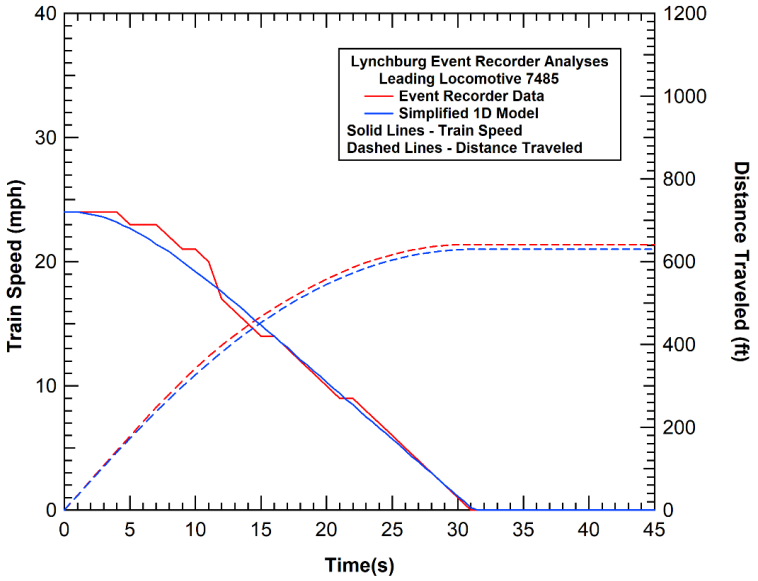

Figure 74. Comparison of the measured and modeled Lynchburg emergency braking response

The third and final derailment evaluated to validate the braking behavior is the June 19, 2009, derailment at Cherry Valley, IL. The eastbound Canadian National Railway Company freight train U70691-18 derailed at a highway/rail grade crossing. The train consisted of 2 locomotives and 112 cars (78 loaded and 36 empty cars), 19 of which derailed. The data showed the train traveling at 35.7 mph when approaching the point of derailment initiation. According to the raw event recorder data, the lead section of the train (ahead of the POD) came to a stop approximately 32 seconds after the application of emergency braking.

The description of the leading portion of the Cherry Valley consist (ahead of the POD), as incorporated in the 1-D analysis, is summarized in Figure 75. As a revenue train, the consist included blocks of different car types including both loaded and empty cars. The power for the train was provided by two leading locomotives ahead of the POD. In the Cherry Valley consist, the locomotives were followed by 2 loaded cars (cars 1-2), 36 empty cars (cars 3-38), and 20 additional loaded cars (cars 39-58).

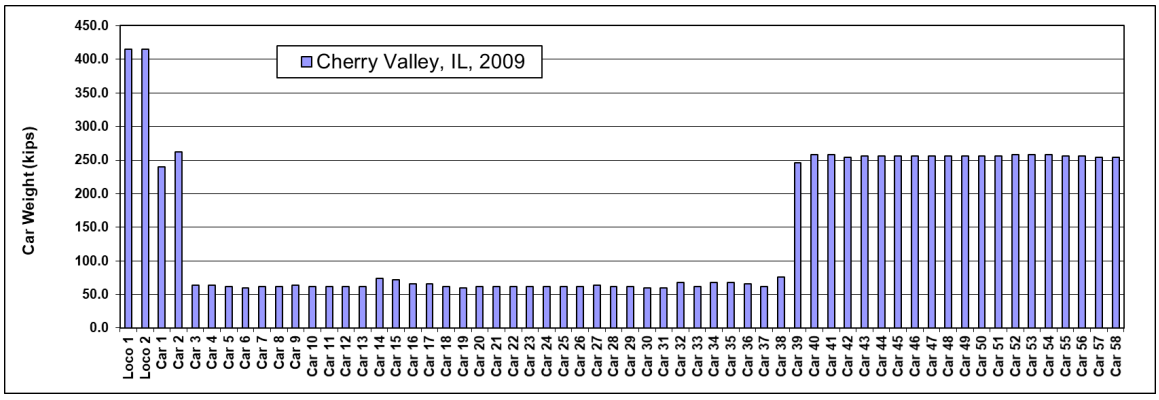

Figure 75. Train makeup for the Cherry Valley braking analyses

The primary model parameters used for the 1-D braking analysis of the Cherry Valley train were:

- 58 cars ahead of POD
- 2 415-kip leading locomotives
- 35.7 mph derailment
- 0.26 percent descending grade
- 18 percent locomotive brake ratio
- model adjusted brake pressure curve

A comparison of the event recorder data and 1-D analysis of the braking ride-down behavior for Cherry Valley is shown in Figure 76. The comparison again shows that the braking model is capable of accurately reproducing the ride-down response for the lead section of the train in this derailment.

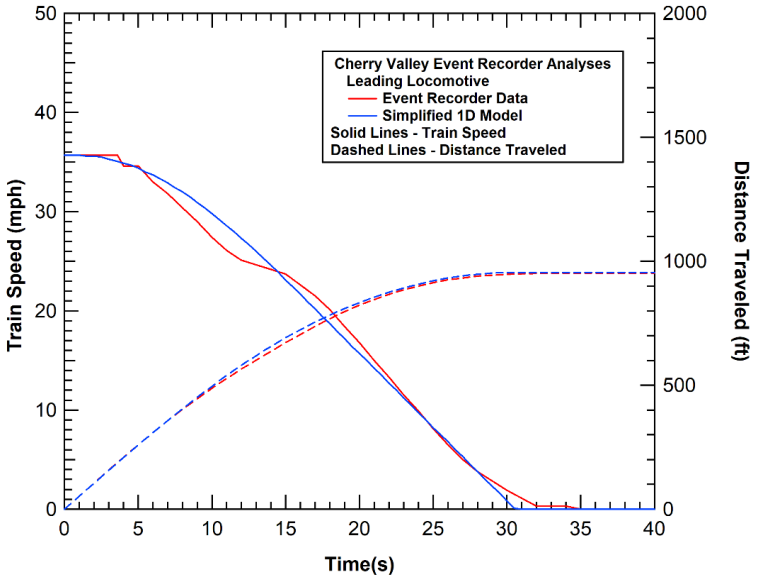

Figure 76. Comparison of the measured and modeled Cherry Valley emergency braking response

In summary, the ride-down braking acceleration history was obtained from the leading locomotives for three separate derailments. The simplified 1-D model was modified to evaluate the response of the train section ahead of the POD. In this scenario, there are no blockage forces and the primary factors that influence the deceleration are the braking forces of the locomotives and cars ahead of the POD, the effect of grade, and a small contribution from the rolling resistance. In all three scenarios, the model predicted a ride-down response that closely matches the event recorder data.

5.3.3.10 Primary Validation Analysis Summary

The above analyses of specific derailments, for which detailed information was available, validate the model's capabilities of reproducing the derailment kinematics for the class of derailments resulting in unstable pileups (typical for broken rail derailments). Performing these

analyses serves two purposes. The first is a primary validation of the model. The second is to provide insight into the magnitude of various parameters for which no other data sources were available. These include parameters such as the braking and blockage delay times and the blockage force magnitude. A summary of the model parameters used in the derailment analyses is provided in Table 32.

Table 32. Validation analysis parameter summary

Parameter	Units	Aliceville	Brainerd	Graettinger	Casselton	Wagner	Saskatoon	Lac-Mégantic	Minot
Number of Cars	Each	91	62	81	109	19	130	72	109
Length of cars	Feet	59.3	53.1	59.9	59.6	59.3	56.7	59.3	59.0
Avg. Mass per Car	lb	264,670	288,162	255,981	256,484	263,000	286,002	282,008	210,917
Trail Loco Mass	lb	415,000	420,000	415,000	415,000	414,994	415,000	n/a	n/a
Residual Train Mass	M lb	24.1	17.9	5.6	20.7	28.0	37.2	23.0	20.3
Blockage Force	lb	500,000	460,000	450,000	400,000	450,000	600,000	450,000	400,000
Blockage Delay	s	4	14	12	0	2.5	7	2	8
Blockage Ramp Time	s	4	4	4	6	4	4	4	4
Car Braking Force	lb	7,800	7,800	7,800	7,800	7,800	7,800	0	7,800
Total Energy into pile	M ft-lb	204.2	98.0	107.5	379.6	103.3	265.6	1,815.3	229.6
Total cars into pile	Cars	22.8	19.8	19.2	33.0	9.7	29.8	61.8	28.9
Grade	Percent	0	0	0.2	-0.1	0	-0.3	-1.26	0
Derailment Speed	MPH	39	27	29.5	43	38	36	65	41
Braking Delay	s	4	14	12	7	2.5	7	2	8
Trailing Locos	Each	1	1	1	1	1	1	0	0

5.3.3.11 Secondary Validation Analyses

The primary model validation described above was performed via a detailed comparison of the model against data of the derailment response for events where the quantitative derailment kinematics were well known. However, in addition to providing the primary model validation, these analyses were also a model calibration where the magnitude of the blockage and braking delay and blockage force were varied to obtain the best match with the measured derailment behavior. As a result, there remains a need to perform a secondary model validation against an independent set of derailments.

The approach used for the secondary validation was to collect a larger set of derailments and train the model using reported input parameter values. The team performed a search of FRA and TSB railroad accident reports to collect data on derailments to find accidents where the derailment speed, trailing cars (and tons) behind the point of derailment, grade, average car length, and presence of trailing locomotives were all known. Since the positions of the loaded and empty cars are not reported for most manifest trains, these could not typically be used in the

assessment and trailing tons behind the POD could not be determined. Thus, the secondary validation derailments primarily consist of loaded or empty unit trains.

A set of 70 train derailments were identified for which the required analysis inputs were known. Records of these derailments included a range of derailment speeds, train weights, residual train lengths, grades, and derailment severities. A summary of the derailments is provided in Table 33.

The model input parameters used for the secondary validation analyses were:

- blockage delay equals braking delay
- 4 s blockage ramp
- brake pressure curves based on the length behind POD

The blockage force variable was assigned with different values. For longer cars, such as a loaded oil tank car, a 450-kip blockage force was used. For shorter coal gondolas, a 400-kip blockage force was used. This is because shorter car lengths have less resistance to lateral buckling with a shorter wavelength. Finally, empty cars were assumed to have a blockage force equal to two times the average car weight. This is one area of the model where additional investigation would be beneficial.

A nominal combined blockage and braking delay time was input into the model to calculate severity. Additionally, the delay time was varied in the model to determine the delay required to match the observed severity. Delay time is not the only uncertain variable in these analyses, but delay time is known to have a very significant effect on severity and a range of delay times were observed in the primary validation scenarios. Thus, this evaluation was thought to provide some additional insight into the range and distribution of potential delay times in derailments. The severity predicted by the 1-D model, as well as the calculated blockage and delay time required to match the reported severity, are also summarized in Table 33.

Table 33. Additional derailments analyzed for secondary model validation

Date	Location	Speed (mph)	No. Cars behind POD	No. Trailing Locos	Avg. Car Weight (kips)	Avg. Car Length (feet)	Grade	Blockage Force (lbs)	Observed Severity	1-D Model Severity	Delay Time to Match (s)
6/6/2019	Stanwood, IA	47	141	2	268	52.9	0.26%	400,000	37	45.7	-1.7
2/16/2019	Cloquet, MN	39	98	1	280	51.2	0.00%	400,000	39	36.0	10.9
1/22/2019	Saskatoon, SK	33	130	1	285	56.7	-0.30%	450,000	30	30.0	8.4
6/22/2018	Doon, IA	47	95	1	279	57.1	0.40%	450,000	35	35.9	5.7
4/7/2018	Oswego, MT	52	44	0	286	56.6	0.00%	450,000	30	29.2	7.1
10/3/2017	Antelope, SK	48	64	1	285	47.4	0.00%	400,000	37	38.9	4.6
9/15/2017	Blucher, SK	46	90	1	285	46.9	0.00%	400,000	37	44.7	-0.3
8/13/2017	Dominion City, MB	40	44	1	259	57.1	0.00%	450,000	22	20.1	10.1
8/11/2017	Heron, MT	43	113	1	286	53.1	0.47%	400,000	33	37.1	2.5
6/30/2017	Plainfield, IL	40	41	2	281	59.0	0.00%	450,000	21	20.6	8.0

Date	Location	Speed (mph)	No. Cars behind POD	No. Trailing Locos	Avg. Car Weight (kips)	Avg. Car Length (feet)	Grade	Blockage Force (lbs)	Observed Severity	1-D Model Severity	Delay Time to Match (s)
3/10/2017	Greattinger, IA	28	80	1	254	59.9	0.20%	450,000	20	16.5	14.8
2/4/2017	Hearne, TX	19	108	2	284	54.0	-0.59%	400,000	18	16.0	13.3
6/23/2016	Mosier, OR	24	78	1	273	60.8	0.15%	450,000	16	13.8	13.7
11/8/2015	Watertown, WI	27	30	0	280	59.4	0.00%	450,000	15	17.3	5.0
9/19/2015	Lesterville, SD	10	97	1	257	59.4	0.00%	450,000	7	5.2	17.4
7/16/2015	Culbertson_MT	44	32	2	277	59.3	0.00%	450,000	22	19.8	9.9
5/6/2015	Heimdal, ND	24	29	0	275	59.0	0.00%	450,000	6	11.1	-0.8
3/7/2015	Gogama, ON	43	89	0	387	59.4	0.00%	450,000	39	32.5	15.1
3/4/2015	Galena, IL	23	101	1	279	56.2	0.14%	450,000	21	15.4	20.3
2/17/2015	Louisville, NE	35	100	1	270	51.8	-0.05%	400,000	33	29.8	11.9
2/16/2015	Mt Carbon, WV	33	108	0	272	59.0	-0.05%	450,000	27	25.3	10.7
2/15/2015	Gogama, ON	38	94	0	387	59.4	0.00%	450,000	29	28.3	8.7
2/11/2015	McGrew, NE	49	62	1	271	52.9	-0.25%	400,000	45	36.3	16.2
2/5/2015	Dubuque, IA	24	83	0	255	59.3	-0.03%	450,000	14	14.7	7.9
11/25/2014	Belden, CA	23	67	1	282	60.0	-1.00%	450,000	12	16.4	2.9
5/11/2014	Pillager, MN	43	118	1	266	50.0	-0.15%	400,000	45	43.4	8.7
4/30/2014	Lynchburg, VA	24	71	0	269	59.8	-0.10%	450,000	17	14.5	13.8
12/30/2013	Casselton, ND	28	45	1	264	59.1	0.00%	450,000	13	14.3	6.7
11/7/2013	Aliceville, AL	39	90	1	260	59.3	0.00%	450,000	26	27.7	5.6
7/20/2013	Rushville, MO	15	27	0	274	52.0	0.00%	400,000	8	7.2	12.0
7/6/2013	Lac Mégantic	65	72	0	282	59.3	-1.26%	450,000	64	62.8	7.5
4/28/2013	Provost, AB	23	154	3	286	47.0	0.40%	400,000	17	19.3	5.3
3/17/2013	East Haven, CT	10	30	0	35	43.2	0.00%	70,000	3	4.8	4.4
2/13/2013	Wagner, MT	37	104	1	286	57.0	0.00%	450,000	10	12.8	3.3
2/3/2013	Fairbury, NE	50	113	1	269	54.0	0.40%	400,000	39	47.6	-1.6
12/9/2012	St. Charles, VA	8	28	3	189	53.1	-0.20%	400,000	6	3.7	20.0
7/4/2012	Northbrook, IL	38	110	1	271	52.9	0.00%	400,000	32	33.5	6.1
7/2/2012	Mesa, WA	48	63	1	266	51.9	-0.14%	400,000	32	35.6	2.8
12/21/2011	Cariboo, BC	29	65	0	275	58.6	0.20%	450,000	19	17.0	12.0
7/10/2011	Brainerd, MN	27	56	1	275	54.0	0.00%	400,000	20	17.0	13.9
3/8/2011	Fernie, BC	25	84	1	271	54.7	-1.20%	400,000	27	22.4	14.8

Date	Location	Speed (mph)	No. Cars behind POD	No. Trailing Locos	Avg. Car Weight (kips)	Avg. Car Length (feet)	Grade	Blockage Force (lbs)	Observed Severity	1-D Model Severity	Delay Time to Match (s)
2/12/2011	Fort Fraser, BC	45	62	0	269	54.0	-0.25%	400,000	36	33.2	10.1
3/6/2010	Wilson Creek, WA	38	73	2	286	58.0	0.00%	450,000	25	25.7	6.9
2/15/2010	Providence, VA	48	47	0	57	51.6	0.01%	114,000	32	22.7	15.1
2/6/2010	Meyersdale, PA	65	130	0	266	51.0	-1.47%	400,000	108	96.1	14.9
9/20/2009	Bill, WY	37	94	1	284	53.1	-1.00%	400,000	33	38.5	2.8
6/23/2009	Fort Scott, KS	25	55	3	284	55.4	-1.00%	400,000	21	17.7	13.9
6/19/2009	Cherry Valley, IL	36	56	0	263	59.6	-0.26%	450,000	19	21.6	4.5
1/16/2009	Littleton, CO	44	21	1	240	44.8	-1.03%	400,000	17	19.3	3.7
1/1/2009	Manzanola, CO	47	101	2	286	53.1	-0.37%	400,000	41	45.8	2.3
11/9/2008	Littleswan, MN	48	93	1	268	34.7	0.00%	400,000	65	58.3	12.0
10/24/2008	Baring, MO	49	83	0	264	58.3	-0.72%	450,000	36	40.0	2.6
6/3/2008	Eglin, TX	44	68	0	286	43.0	0.52%	400,000	39	37.5	8.7
5/27/2008	Gladstone, VA	29	119	0	269	50.0	-0.05%	400,000	33	26.0	18.0
3/19/2008	Vienna, IL	8	127	1	269	54.1	-1.00%	400,000	7	7.8	8.8
3/7/2008	Fairfield, Ne	43	81	1	293	54.0	-0.26%	400,000	38	37.0	8.3
1/1/2008	Lusk, WY	34	81	1	286	54.0	-0.40%	400,000	32	28.0	13.0
10/20/2006	New Brighton, PA	37	60	0	259	61.5	0.00%	450,000	23	19.4	13.5
11/4/2005	Riga, KS	50	63	1	220	54.0	0.45%	400,000	43	31.1	19.5
10/27/2005	Cherokee, IA	28	127	1	280	53.1	-1.00%	400,000	21	31.7	-2.2
10/22/2005	Worden, MT	48	102	1	263	56.6	-0.16%	400,000	43	40.0	9.9
10/5/2005	Broadwater, NE	47	24	0	280	54.0	0.00%	400,000	20	19.0	8.0
10/3/2005	Mason, ND	46	63	0	286	59.9	-0.60%	450,000	33	33.1	6.7
10/1/2005	Kit Carson, CO	39	49	1	286	51.0	0.00%	400,000	21	25.6	2.0
9/13/2005	Gibbon, NE	49	53	1	283	54.0	0.00%	400,000	27	32.4	0.2
9/10/2005	Hanna, WY	50	67	0	274	53.6	-0.08%	400,000	39	38.7	6.7
8/27/2005	Bear, WY	48	70	0	284	53.1	0.37%	400,000	39	36.3	9.6
8/2/2005	Thrall, TX	48	51	0	256	40.9	0.00%	400,000	36	36.6	5.9
5/15/2005	Bill, WY	48	69	1	276	49.2	0.60%	400,000	29	36.0	-0.8
5/5/2005	Casselton, ND	36	52	0	279	59.8	0.00%	450,000	25	20.6	14.3

The calculated delay time to match the observed severity of the derailment is plotted against the derailment speed for the secondary validation derailments in Figure 77. Also shown in the figure is a linear fit to the data. The correlation of delay time against derailment speed indicates that the delay time is reduced at higher speeds. This trend of reduced delay time is logical since more cars pass the POD in each delay duration at a higher speed. As a result, there is a greater potential for more rapid development of unstable lateral buckling initiation, which produces a separation between cars that initiate emergency braking and blockage force development. As a result, this linear fit was incorporated into the model for the calculation of a baseline delay time in each derailment analysis.

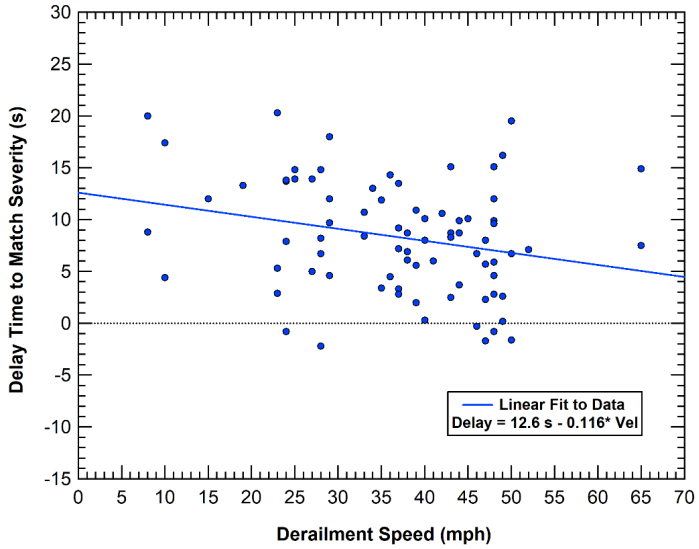

Figure 77. Comparison of the calculated and observed derailment severities in the secondary model validation

The predicted model severity is plotted against the observed derailment severity for the secondary model validation cases in Figure 78.

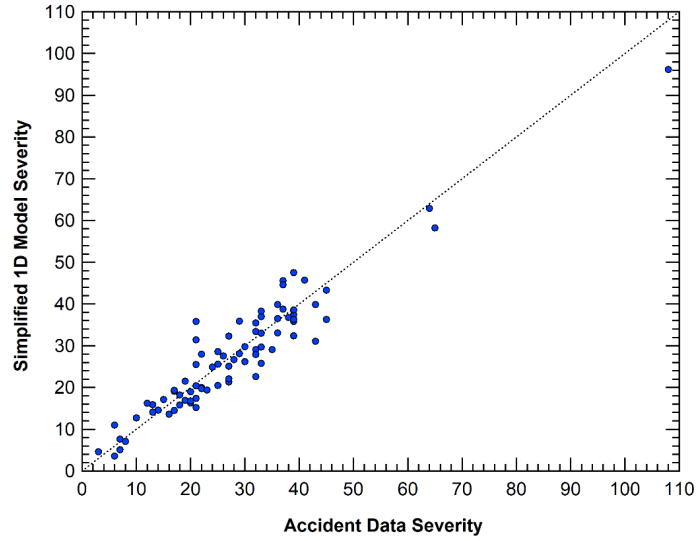

Figure 78. Comparison of the calculated and observed derailment severities in the secondary model validation

The comparison shows a good correlation of the model with the observed derailment behavior. Any single derailment may have a predicted severity that is higher or lower than the observed severity by several cars. This magnitude of variation is expected because of variability in factors such as braking or blockage delay, grade, slope and terrain, etc. However, the trend and average severities are in good agreement.

Overall, the level of agreement between modeled and observed derailment severities provides confidence in the model for predicting this type of derailment event. The average predicted severity for the secondary derailment matches the average observed severity. However, to further validate the model, the performance of various factors in the analyses were also investigated. The difference between the observed and predicted severities is plotted against the grade in Figure 79. The difference versus grade shows that the model slightly underpredicts the severity for steep descending grades. However, this is probably skewed from the derailment scenario on the steepest grade (1.47 percent descending). This was an extreme derailment event that derailed 108 cars compared to the model's prediction of 96.1 cars (11 percent error). As a result, there is insufficient data on steep descending grades to determine whether the trend is significant.

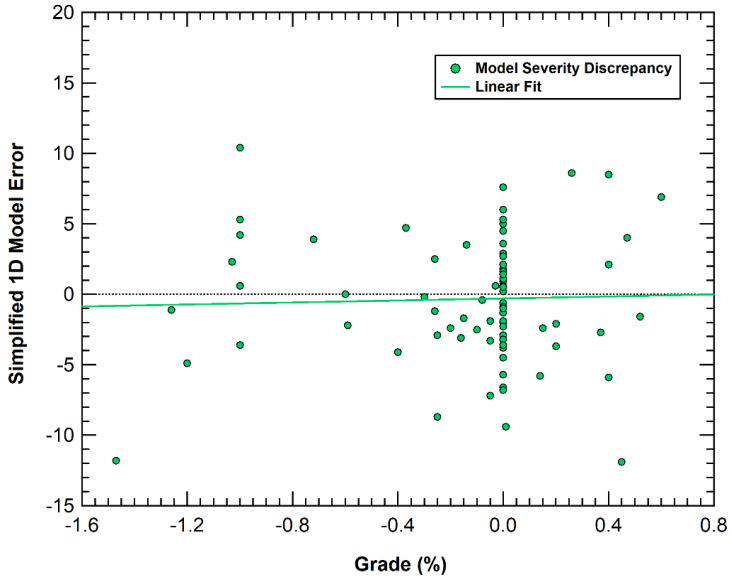

Figure 79. Discrepancy in the calculated and observed severity as a function of grade

A similar plot of the differences between the observed and predicted severities is plotted against derailment speed in Figure 80. The difference between model prediction and speed does not show a strong trend. The slight trend of underpredicting the highest speed derailments may be a result of the same extreme severity derailment on the steep descending grade.

A final plot of the difference between the observed and predicted severities is plotted against the residual train length (i.e., number of cars behind the POD) in Figure 81. Again, the comparison of model discrepancy and length does not show a strong trend.

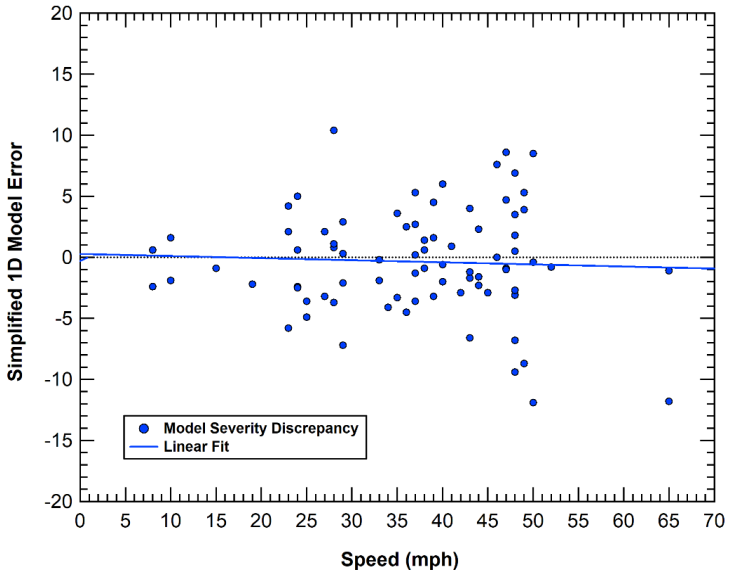

Figure 80. Discrepancy in the calculated and observed severity as a function of speed

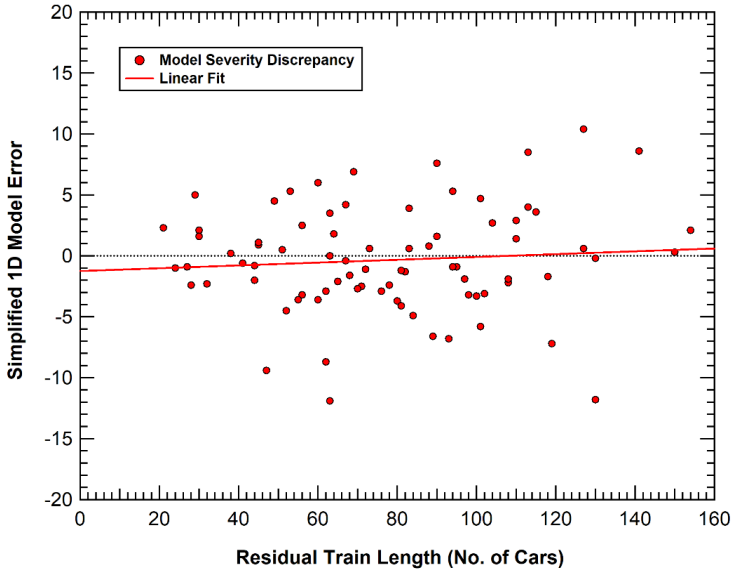

Figure 81. Discrepancy in the calculated and observed severity as a function of residual train length

Overall, the secondary model validation efforts indicate that the simplified model can predict severity reasonably well for a wide range of derailment conditions. The effects of individual parameters such as speed, grade, and residual train length appear to be represented well by the model. Note that the derailments represented by the model are of the type that results in a separation of the train and large-scale lateral buckling common for broken rail derailments (as well as many other initiating events). In a significant percentage of derailments this behavior is not representative. One such example would be derailments where a single wheel or truck derails, but the train remains upright and in-line as it is brought to a halt.

Another observation of the secondary model validation efforts is that the cases investigated are not a random sampling of all derailments. Since the information on the sample derailment events was obtained from FRA and TSB accident investigation reports, the derailments selected will be biased toward more severe derailments. This is because the investigating authorities only investigate events above a threshold of severity (e.g., costs associated with damage to the track and equipment). Additional information on lower speed derailments would be helpful to determine if they follow similar behaviors represented by the model.

5.3.4 Model Application

5.3.4.1 Model Main Effects Analyses

An investigation into the effects of individual derailment parameters was performed using a set of unit train derailments. The objective was to both investigate the effects of parameter variation for uncertain inputs and to gain insight into the importance of other factors for train derailment severity (e.g., car brake ratio).

The baseline model input parameters used for this effects study were:

- 263 GRL unit trains
- 59-foot-long cars
- no trailing locomotive
- 450-kip blockage force
- 8 s blockage delay
- 1 s blockage ramp
- 0.0 percent grade
- brake pressure curves based on the length behind POD
- 8 s brake delay

The derailments selected for these analyses were all loaded trains with similar characteristics (primarily tank cars) where the consist is easily described. A set of 18 loaded unit train derailments were identified from various sources that span a range of derailment speeds, residual train lengths, and derailment severities. A summary of the derailments is provided in Table 34. Also included in the table is a comparison between the observed derailment severity and the severity estimated by the 1-D model.

The estimated model severity is plotted against the observed derailment severity for the secondary model validation cases in Figure 82. The comparison shows a good correlation of the model with the observed derailment behavior. Any single derailment may have a predicted severity that is higher or lower than the observed severity by up to four cars. This magnitude of variation is a result of expected variability in factors such as braking or blockage delay, grade, slope, and terrain. However, the trend and average severities are in good agreement.

The average predicted severity for the secondary derailment analysis is 96 percent of the average observed severity. However, this may be partially due to the discretization of results. The model severity is listed as a fractional severity and the observed severity is a discrete value. Thus, the

model severity prediction of 21.2 cars for New Brighton indicates that 20 percent of the 22nd car has passed the POD. In a real derailment, this might mean that the forward truck has derailed, and the severity reported would be represented as 22 cars.

Table 34. Additional derailments analyzed for secondary model validation

Location	Date	Derailment Speed	No. Cars Behind POD	Observed Severity	1-D Model Severity
New Brighton, PA	10/20/2006	37 mph	60	23	21.2
Luther, OK	8/22/2009	19 mph	81	14	9.5
Cherry Valley, IL	6/19/2009	36 mph	55	19	19.6
Gainford, AB	10/19/2013	24 mph	118	13	15.1
Aliceville, AL	11/7/2013	39 mph	90	26	27.4
Casselton, ND	12/302013	42 mph	45	21	21.7
Dubuque, IA	2/5/2015	24 mph	82	14	13.1
Gogama, ON	2/15/2015	38 mph	89	29	31.2
Mt. Carbon	2/16/2015	33 mph	105	27	22.9
Heimdal, ND	5/6/2015	24 mph	27	7	8.1
Culbertson, MT	7/16/2015	44 mph	33	22	19.2
Lesterville, SD	9/19/2015	10 mph	97	7	4.2
Watertown, WI	11/8/2015	27 mph	33	15	10.6
Mosier, OR	6/23/2016	25 mph	78	16	13.7
Graettinger, IA	3/10/2017	30 mph	77	20	17.6
Plainfield, IL	7/3/2017	40 mph	41	21	19.4
Doon, IA	6/22/2018	48 mph	85	32	35.9
Saint-Lazare, MB	2/16/2019	46 mph	105	37	37.2
Guernsey, SK	2/6/2020	42 mph	77	32	28.4

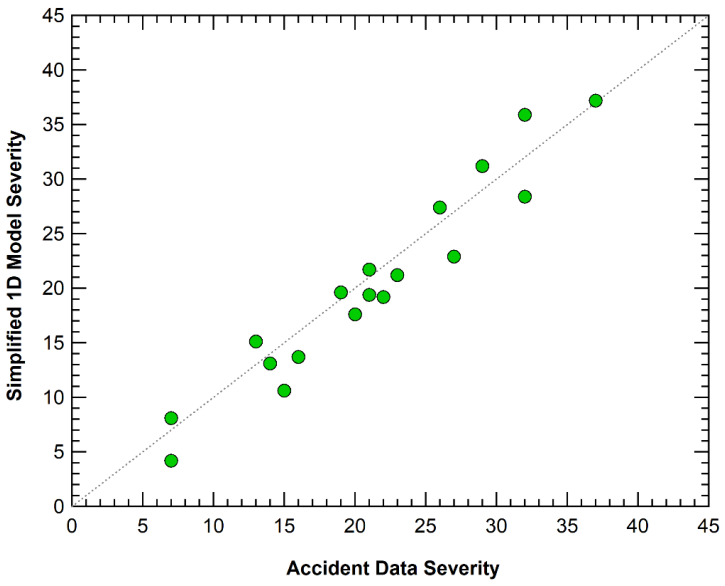

Figure 82. Comparison of the calculated and observed derailment severities in the additional secondary model validation

The derailment parameters investigated are listed in Table 35. The first two parameters are related to the application of braking. The brake application delay is the time between the initiation of the derailment and the separation of the brake pipe that initiates the brake application. In the primary model validation, the values of the brake application varied between 3 and 15 seconds. In the secondary model validation, a value of 8 seconds was used as the estimated average value. For this effects analysis, a low value of no braking delay was used, and a high value of 16 seconds was used. Although it is possible that a delay time greater than 16 seconds could occur in limited derailment events, these values are believed to be bound on a large majority of actual derailment braking delays. Similarly, the baseline braking force used for each car in emergency braking was 7800 lb (Lovette & Thivierge, 1992). The low and high variations used on this braking force were 4000 and 12000 lb, respectively. This variation in braking forces is larger than expected for freight vehicles in normal operating conditions.

Table 35. Parameter variations used in the main effects analyses

Parameter	Baseline Value	Low Value	High Value
Brake Application Delay	8 Seconds	0 Seconds	16 Seconds
Brake Force	7,800 lb	4,000 lb	12,000 lb
Blockage Initiation Delay	8 Seconds	0 Seconds	16 Seconds
Blockage Force	450,000 lb	300,000 lb	600,000 lb
Rolling Resistance	1X	0X	2X
Grade	Flat	1% Down Grade	1% Up Grade
Combined Brake/Blockage Delay	8 Seconds	0 Seconds	16 Seconds

The next two parameters are related to derailment blockage forces. The blockage initiation delay is the time between the initiation of the derailment and the development of a pileup in front of the derailment that significantly retards the motion of the cars behind the POD. In the primary model validation, the values of the blockage delay ranged between 4 and 14 seconds. In the secondary model validation, 8 seconds was used as the estimated average value. This effects analysis uses a low value of no blockage delay and a high value of 16 seconds. There are derailments that occur at the edge of an embankment or on an elevated right of way (e.g., bridge) where a significant blockage would not occur. However, these values are believed to be bound on a large majority of actual derailment blockage delays. The primary model validation efforts resulted in blockage forces between 400,000 and 500,000 lb, and the baseline blockage force used was 450,000 lb. Other studies have indicated values of the blockage force as high as 650,000 lb (Brosseau, 2014). In addition, some derailments have occurred along steep embankments or on raised bridges where the blockage forces should be quite low. The low and high variations used on this blockage force were 300,000 and 600,000 lb, respectively. This variation in blockage forces is believed to be sufficiently large to capture the blockage levels for most derailments.

The next parameter evaluated was rolling resistance. In the model development process, the addition of rolling resistance was found to have relatively modest effects on derailment severity. As a result, little effort was made to optimize this model. Some variability would be expected in rolling resistance based on environmental conditions (e.g., wind, elevation, humidity, and

temperature), equipment (e.g., car types, weight, etc.), and the condition of the rail. For this effects analysis, the baseline parameters provided previously varied from a lower limit of no rolling resistance to an upper limit of two times the baseline level.

The sixth parameter evaluated was the effect of grade. The baseline analyses were all performed on level track (i.e., no grade). The effects analyses evaluated the variations caused by a 1 percent downgrade and a 1 percent upgrade. There have been documented derailments that have occurred on steeper grades than these limits (e.g., Lac Mégantic occurred when the train was on a 1.2 percent downgrade). However, the majority of track and derailments fall within the limits of a 1 percent grade.

The grade was modeled by the addition of the gravitational acceleration forces acting on the residual train. However, it is likely that a train on an uphill grade would be subjected to traction forces from the locomotive prior to separation at the POD. Similarly, a train on a downhill grade is more likely to have some level of brake application prior to separation. These initial traction or braking forces were not included in the model. Thus, the effects of grade could potentially be overpredicted in the analyses.

The final parameter evaluated was a combined delay in the initiation of the blockage and braking forces. In the initial phase of derailment, the first derailed cars are still connected to the leading cars ahead of the POD and the derailed cars continue to move in an upright condition, primarily along the initial alignment. In this phase, the brake pipe is still intact (emergency braking is not yet initiated) and a pileup of derailed cars has not yet begun. It is reasonable to assume that both the initiation of the emergency braking and the development of unstable deformation behaviors that initiate a blockage are dependent on the time at which the first coupled connection between cars fails. Consequently, the blockage delay and braking delay times are not independent parameters; rather, they are coupled because of the derailment mechanics. Thus, the final parameter investigated is the change in the time of delay for both braking and blockage forces by an equal duration (i.e., combined delay). As was applied in the investigation of independent delay times, a low value of no delay and a high value of 16 seconds were used.

For each derailment, the model was run an additional 14 times using the low and high values of each of the 7 derailment parameters analyzed. In each simulation, only the single parameter being investigated in that analysis was varied from the baseline values. A summary of the calculated severities for all the analyses is provided in Figure 83. The analyses resulted in a much wider spread in predicted severities for any given derailment than previously observed from the baseline parameters in Figure 82.

A summary of the main effects analyses is provided in Figure 84. Each parameter is represented by a diagonal line where the point on the left represents the lower limit value of the parameter and the value on the right represents the upper limit. The vertical heights of the points at either end of the line represent the average change in severity over the 18 derailments analyzed at that level of the derailment parameter. For example, with no braking delay, the derailment severity was on average 86 percent of the baseline derailment analyses. Similarly, the analyses with a 16-second braking delay had a severity that was on average 110 percent of the baseline analyses. Thus, a quick comparison of the lengths of the lines gives an indication of the relative importance of the parameters for calculated severity.

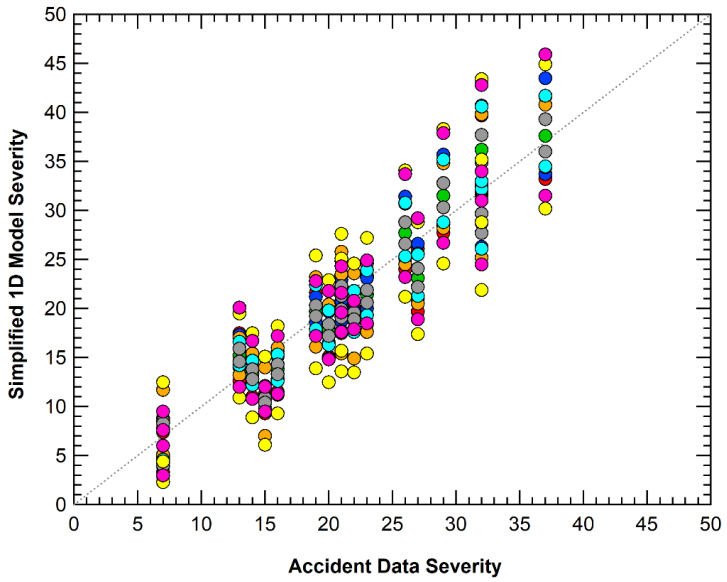

Figure 83. Calculated derailment severities in the supplemental model validation

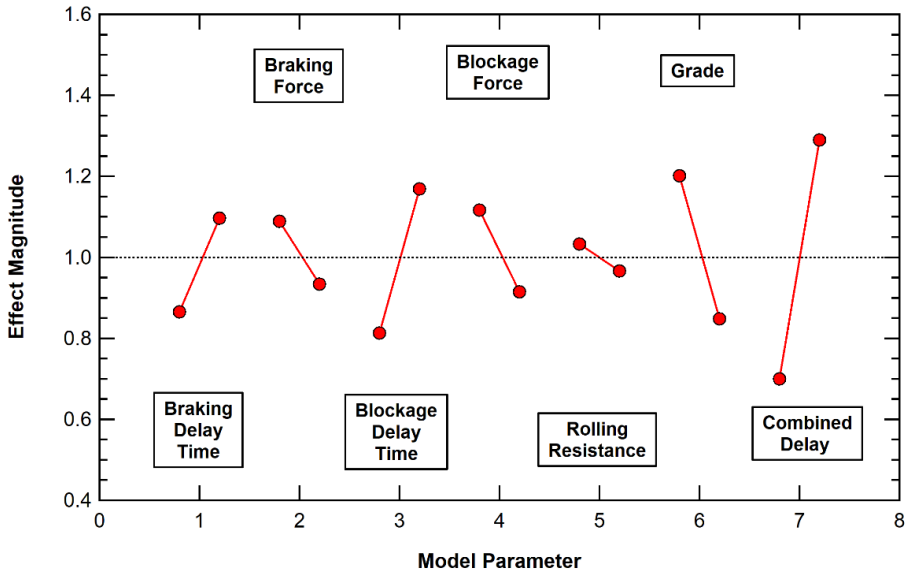

Figure 84. Calculated derailment severities in the supplemental model validation

Caution should be taken in interpreting the main effects plot in Figure 84 because the magnitudes of the variation in the parameters used for the analyses are not necessarily equal. The team attempted to use some engineering judgment in the selection of the range, based on knowledge of the variation possible and level of uncertainty in the various parameters. However, the selection of the range could have an impact on the conclusions that are made from the comparison.

Comparing the parameter effects from Figure 84 resulted in the following observations and conclusions:

- The variations in the braking and blockage delay times were found to have a greater effect on severity than the braking and blockage forces. This indicates the importance of

both including this effect in analyses and performing further investigations into the range and distributions of these delay times in derailments.

- Blockage effects are equal to or greater than braking effects on derailment severity. Any analysis of derailment that does not accurately account for this blockage effect could draw misleading conclusions.
- Rolling resistance has a small effect on derailment severity. A relatively large range of variation was included in this assessment, from no rolling resistance to a level two times that of the baseline Davis model parameters. At these extremes, the rolling resistance produced only a 3 percent change in average derailment severity.
- The effect of grade has a significant influence on derailment severity in the main effects analyses. However, additional analyses of the distribution of grade levels in derailments would be required to draw any significant conclusions on the effect of grade in overall fleet conditions.
- Of the parameters investigated, the combined braking and blockage delay has by far the largest effect on derailment severity, with an approximately 30 percent change in severity at both the low and high values as compared to the baseline. There is good reason to believe that these two parameters would not be independent of each other since both the initiation of braking (i.e., brake pipe failure) and the unstable buckling behaviors that develop a blockage would be delayed until coupled connection failure occurs in the derailment response.

5.3.4.2 Analysis of Train Manifest Effects

A primary objective of developing the 1-D derailment model was to investigate the effects of the train consist and understand the potential differences in derailments between revenue and unit trains. The first method applied to investigate this effect was to analyze identical derailment conditions where the only variation is in the specification of the consist (i.e., car weight distribution). Examples of this type of analysis are provided in Figure 85 through Figure 87. The analyses pertain to the Aliceville, Brainerd, and Wagner derailments described previously. In each of the figures, the team compared the energy of the derailing cars from the baseline unit train analysis with that of an identical derailment condition but with the train consist definition from the Minot derailment, shown previously in Figure 72. In each case, the revenue train consist is defined as starting at car 4 of the Minot train consist. However, the Minot train consist is truncated to match the same number of cars as the residual unit train in each case.

The Aliceville unit train derailment, as compared with the approximately identical derailment of the Minot manifest train (shown in Figure 85), had two fewer cars derailed and an overall reduction in derailment energy of 40 percent. The Aliceville train did come to rest more rapidly due to the action of braking and blockage forces on a smaller mass behind the POD. However, the lower weight of vehicles passing the POD exerted an equal or more significant effect, leading to a direct reduction of derailment energy. The Brainerd unit train derailment alongside the approximately identical derailment with the Minot manifest train, which is compared in Figure 86, had one fewer car derailed and an overall reduction in derailment energy of 41 percent. Similarly, the Wagner unit train derailment with an approximately identical derailment as the Minot manifest train, compared in Figure 87, had one fewer car derailed and an overall reduction

in derailment energy of 56 percent. The larger reduction for the Wagner derailment is a result of the smaller derailment severity and the number of empty cars located near the POD.

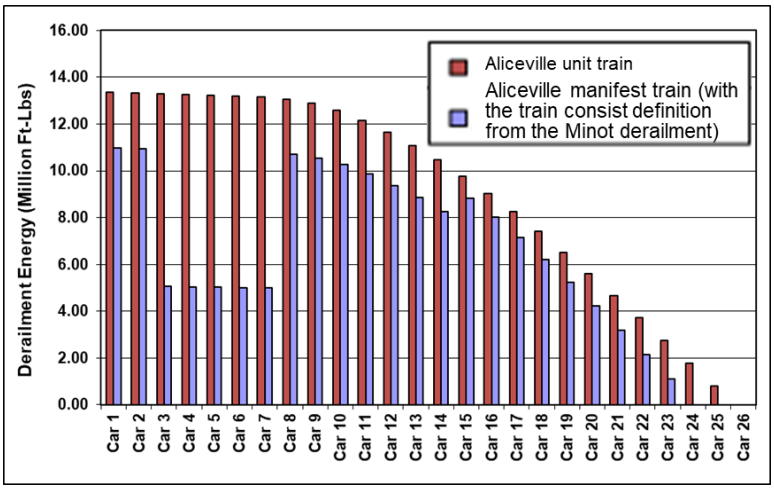

Figure 85. Calculated car derailment energies for the Aliceville derailment

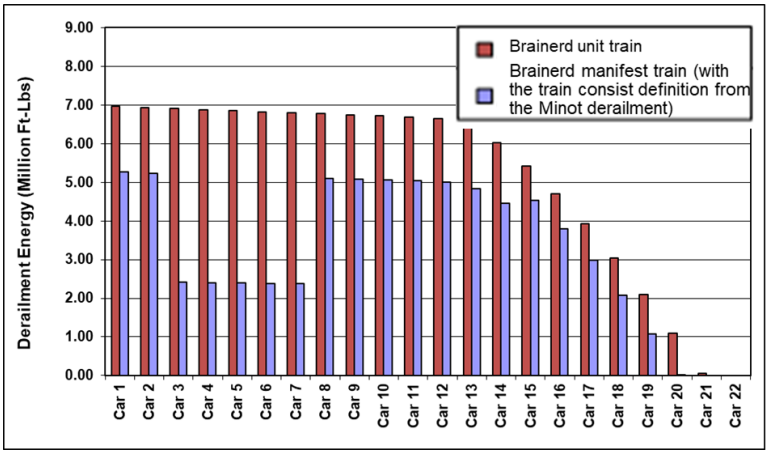

Figure 86. Calculated car derailment energies for the Brainerd derailment

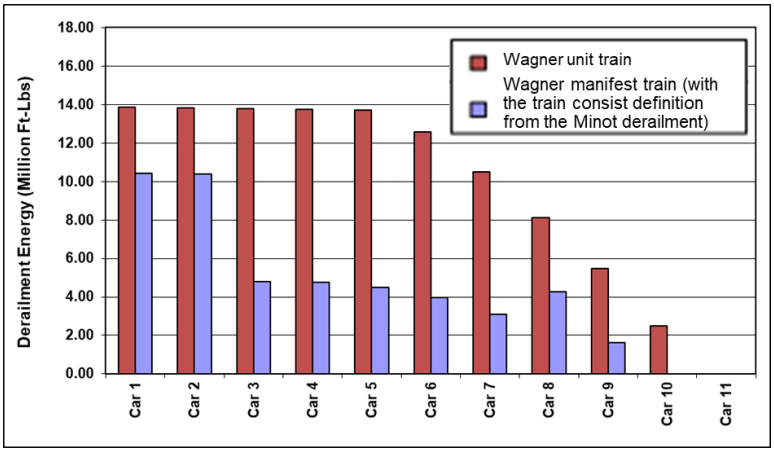

Figure 87. Calculated car derailment energies for the Wagner derailment

The corresponding analysis of the Minot revenue train derailment was performed using an equal length unit train consist comprising loaded 263K GRL cars. Again, the comparison of the derailment energies for the two analyses is presented in Figure 88. The unit train consist resulted in approximately 3.5 more cars derailed and an overall increase in derailment energy of 42 percent. In this scenario, the train came to rest more slowly due to the impact of braking and blockage forces on the increased mass behind the POD. Additionally, the increased weight of vehicles passing the point of derailment directly increased the derailment energy.

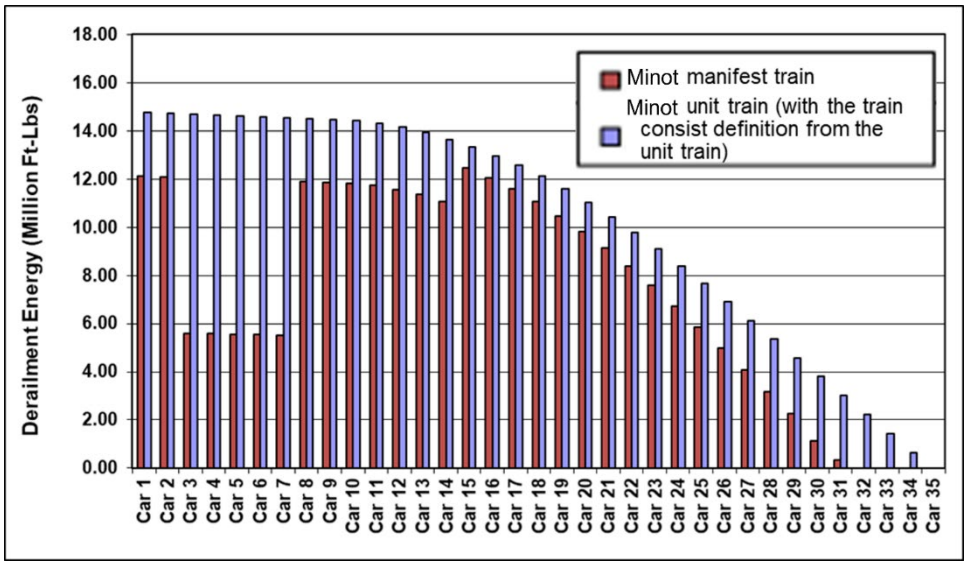

Figure 88. Calculated car derailment energies for the Minot derailment

5.3.4.3 Analysis of Derailments in Rail Equipment Accident/Incident Form 6180.54

The team used the same data in Section 5.2 (i.e., the Rail Equipment Accident/Incident Form 6180.54 including the freight train derailment data on the main tracks of Class I railroads from 1996 to 2018) to validate 1-D model. This database contains derailment speed, number of derailed cars and locomotives, total number of cars and locomotives, point of derailment, locomotive positions, and gross tonnage, which can be directly used as 1-D model input parameters. However, some model input parameters are not included in the database, prompting the team to optimize these parameters so that the mean absolute error (MAE, defined by Equation (5-8)) was minimized for different train types.

The 1-D model also showed a significant fraction of derailments considered low-severity outliers and high-severity outliers. This is probably because the 1-D model was developed for derailment incidents whose derailment process follows the physical mechanism of an unstable lateral buckling derailment, common for broken rail derailments and similar events. No effort was made to capture outlier behaviors with the 1-D model, such as broken wheel single-car derailments. The team therefore conducted an additional analysis for the 1-D model based on the data excluding these outliers. The parameters of the 1-D model are given in Table 36.

Table 36. One-dimensional model input parameters

Parameters		Data with outliers	Data without outliers
Car length (feet)		59	59
Grade		0.00%	0.00%
Braking delay (seconds)	All train types	5	10
	Manifest train	4	9
	Loaded unit train	9	12
	Empty unit train	4.5	9
Blockage delay (seconds)	All train types	5	10
	Manifest train	4	9
	Loaded unit train	9	12
	Empty unit train	4.5	9
Blockage ramp time (seconds)	All train types	2	2.5
	Manifest train	1.5	2.5
	Loaded unit train	3	3.5
	Empty unit train	1.5	2
Blockage force (kip)		400	400

Table 37 presents the performance of the 1-D model in estimating the derailment severity based on the data including and excluding outliers. Two criteria, mean squared error (MSE) and MAE, are used to measure the performance of the 1-D model in estimating train derailment severity.

The model results based on all data including outliers are analyzed below. For all train types, the MSE and MAE obtained by the model are 75.70 and 6.14, respectively. The MAE indicates that the average gap between the estimated number of cars derailed and the observed number of cars derailed is 6.14. The team also found that the observed mean derailment severity (8.63) and the estimated mean derailment severity (8.61) were very similar, with the relative gap being only 0.23 percent ((8.63 – 8.61)/8.63×100% = 0.23%). The team used the 1-D model to separately fit the data for three train types: manifest train, loaded unit train, and empty unit train. The model results for the three train types are presented in Table 37.

Table 37. Results of the 1-D model

Train types	MSE		MAE		Observed mean		The mean of estimated derailment severities	
	With outliers	Without outliers	With outliers	Without outliers	With outliers	Without outliers	With outliers	Without outliers
All train types	75.70	34.56	6.14	4.06	8.63	10.84	8.61	10.44
Loaded unit train	109.70	34.18	6.98	4.05	11.56	14.39	13.08	14.01
Empty unit train	63.77	39.52	5.69	4.27	7.50	9.29	6.73	8.23
Manifest train	65.64	33.52	5.74	3.99	7.61	9.56	7.27	9.12

The model results based on the data excluding outliers are analyzed below. For all train types, the MSE and MAE obtained by the model were 34.56 and 4.06, respectively. This indicates that the 1-D model can significantly improve estimation performance when outliers are excluded. The team also used the 1-D model to separately fit the data excluding outliers for three train types (i.e., manifest train, loaded unit train, and empty unit train) and drew a similar conclusion.

Figure 89 plots the estimated severity obtained by the 1-D model versus the observed severity. This R squared increases from 0.54 to 0.83 when the outliers are excluded, indicating that the 1-D model improves the estimation performance when outliers are excluded.

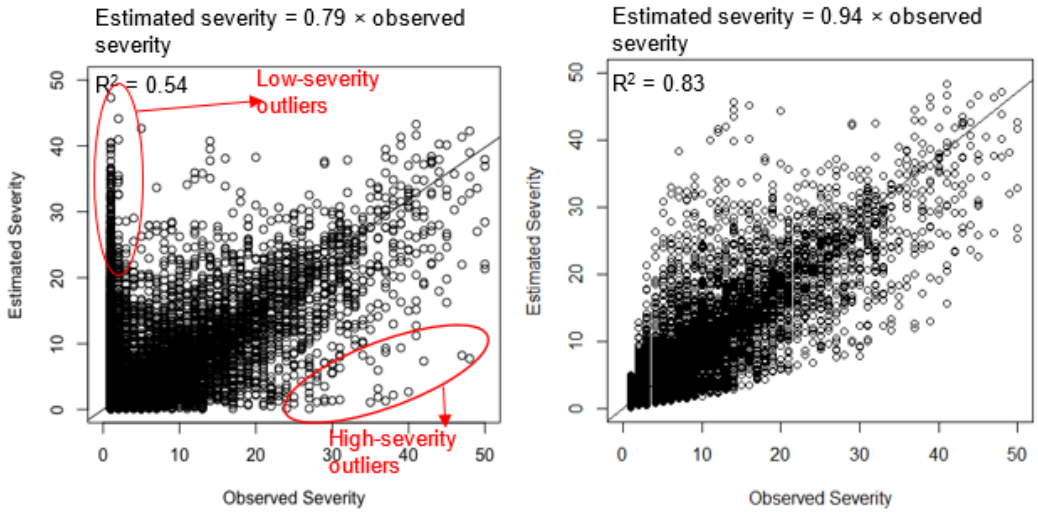

Figure 89. Estimated severity versus observed severity (1-D Model): (a) data with outliers, (b) data without outliers

5.4 Comparison of TG Model and 1-D Model

In Section 5.2 and Section 5.3, the same data are used to estimate the performance of the TG model and the 1-D model. Table 38 presents the comparative results based on MAE and MSE against the full set of derailments including outliers and the set of derailments excluding outliers. The bold numbers represent better performance.

Table 38. Estimation performance of the TG model and 1-D model in terms of MAE and MSE

	MAE				MSE			
	Outliers included		Outliers excluded		Outliers included		Outliers excluded	
	TG model	1-D model	TG model	1-D model	TG model	1-D model	TG model	1-D model
All train types	**5.72**	6.14	**4.00**	4.06	**60.67**	75.70	**33.47**	34.56
Loaded unit train	**6.84**	6.98	4.12	**4.05**	**82.53**	109.70	**33.64**	34.18
Empty unit train	**5.44**	5.69	4.41	**4.27**	**57.98**	63.77	42.25	**39.52**
Manifest train	**5.27**	5.74	**3.91**	3.99	**52.37**	65.64	**32.39**	33.52

The team developed a full set of derailment data including outliers. The TG model outperformed the 1-D model in estimating the severity for all train types combined, as well as loaded unit trains, empty unit trains, and manifest trains, respectively.

For the set of derailment data excluding outliers, overall the 1-D model and the TG model had similar accuracies in estimating train derailment severity. The TG model slightly outperformed the 1-D model in estimating the severity of all train types combined, as well as the manifest train type. In estimating derailment severity of loaded unit trains, the two models had very close

performance, in which the MAE of the TG model (4.12) was slightly higher than the 1-D model, while the MSE of the TG model (33.64) was slightly lower than the 1-D model. The 1-D model outperformed the TG model for empty unit train derailment severity estimation.

Overall, the 1-D model's estimation accuracy significantly improved after outliers were excluded. This finding is not surprising since the 1-D model was developed to model the typical derailment with unstable lateral buckling behavior seen commonly in broken rail derailments and similar events, and thus performs better at estimating the derailment severity for the data excluding outliers. No effort was made in the 1-D model to account for the significant number of outliers.

Figure 90 presents the regression results of observed severity versus estimated severity against the data excluding the outliers. R squared values of the 1-D model were very close to the TG model for all train types, including unit loaded trains, empty unit trains, and manifest trains, given that outliers were excluded.

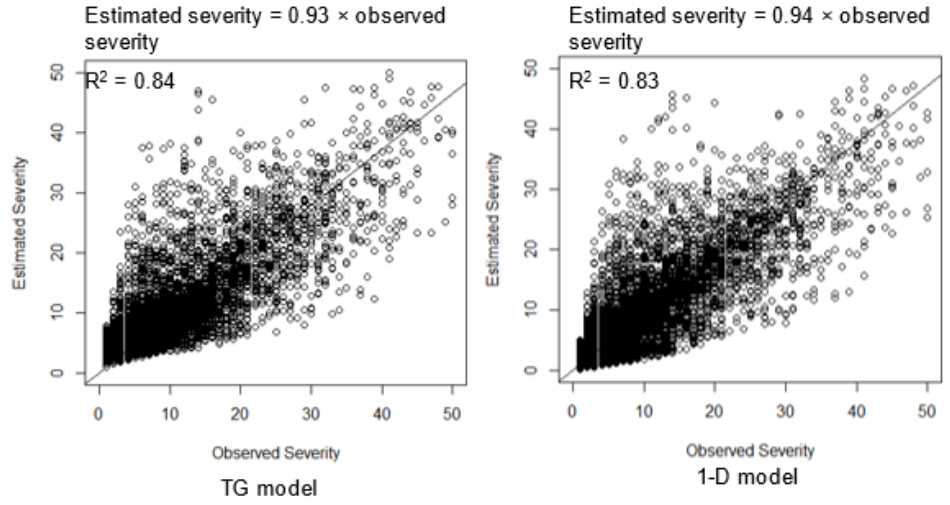

(a) All Train Types

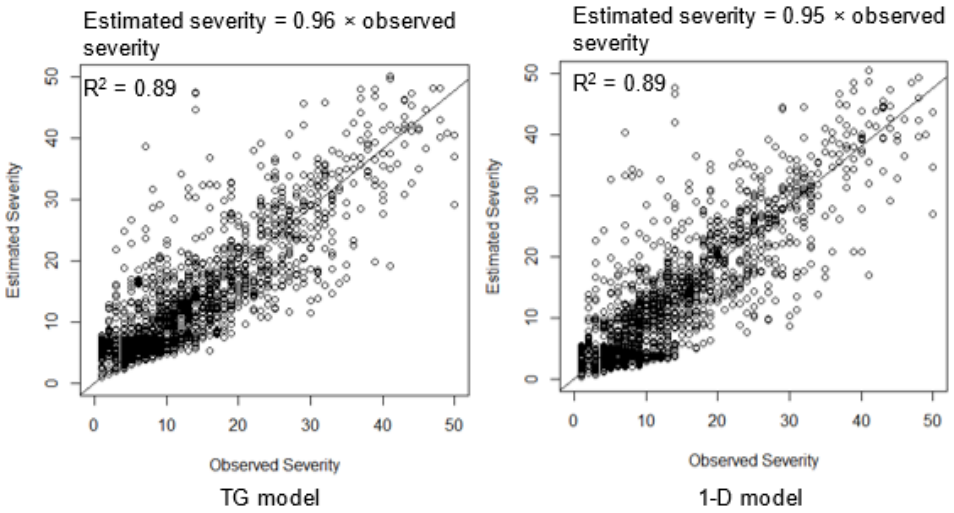

(b) Loaded Unit Trains

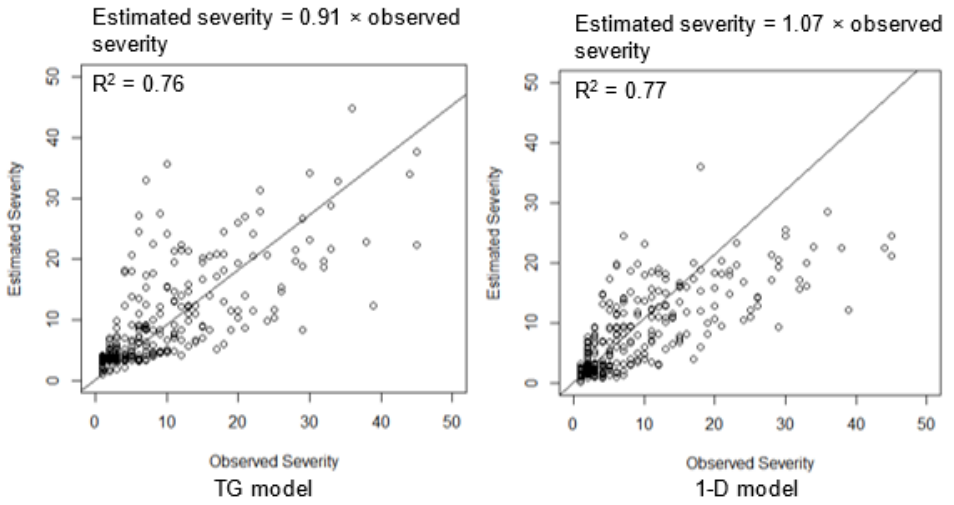

(c) Empty Unit Trains

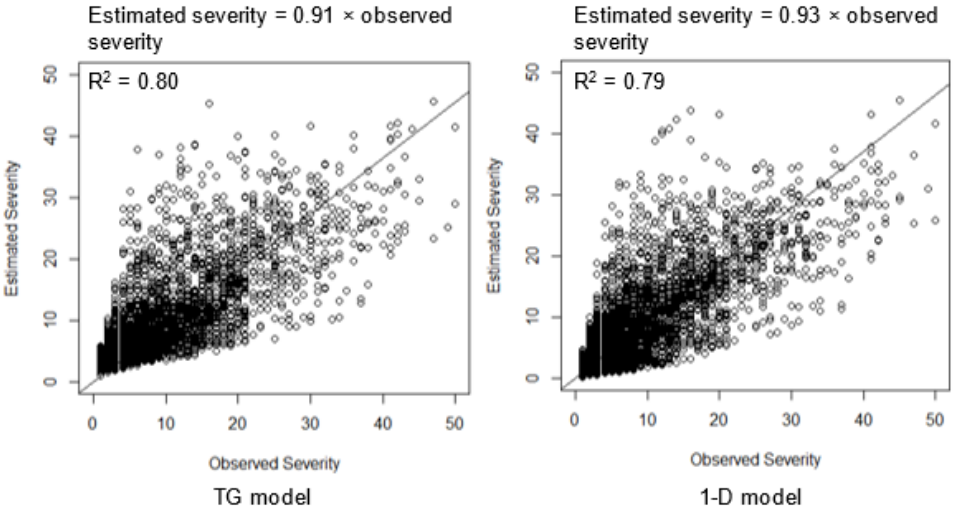

(d) Manifest Trains

Figure 90. Observed severity versus estimated severity obtained by the TG model and the 1-D model based on the data excluding outliers: (a) all train types (b) loaded unit trains (c) empty unit trains (d) manifest trains

A simple comparison between the TG model and the 1-D model based on the data with all levels of severity combined cannot demonstrate their relative performance in estimating some extreme derailment incidents (e.g., severe derailments). Thus, the team conducted a comprehensive comparison between the 1-D model and the TG model at different levels of derailment severity. Derailment incidents were divided into six categories: $1 \leq$ severity ≤ 5; $5 <$ severity ≤ 10; $10 <$ severity ≤ 15; $15 <$ severity ≤ 20; $20 <$ severity ≤ 25; and severity > 25. The MAE and MSE of the 1-D model and TG model were calculated in estimating each category of severity level. The comparison results are presented in Figure 91 (outliers are included). As Figure 91 shows, the 1-D model did not perform as well as the TG model in estimating low-severity derailment incidents (e.g., severity ≤ 10), since it is shown that the MAE and MSE obtained by the 1-D model are higher than those obtained by the TG model at low severity. However, the 1-D model tends to significantly outperform the TG model for high-severity derailments (e.g., severity >

10), which is reflected in the finding that the 1-D model obtained smaller MSE and MAE in estimating high-severity derailments. Moreover, Figure 91 demonstrates that the 1-D model had the highest estimation performance for the derailment severity of loaded unit trains, which typically have larger train length and gross tonnage compared with other train types and are more likely to have severe train derailments. These important findings indicate that the 1-D model is better at estimating extreme derailments that fall outside historical experience and can better capture the conditions of a specific train derailment scenario by mathematically describing the physical dynamics of a derailment, while the TG model can better estimate relatively lower severity derailments that fall within the historical experience.

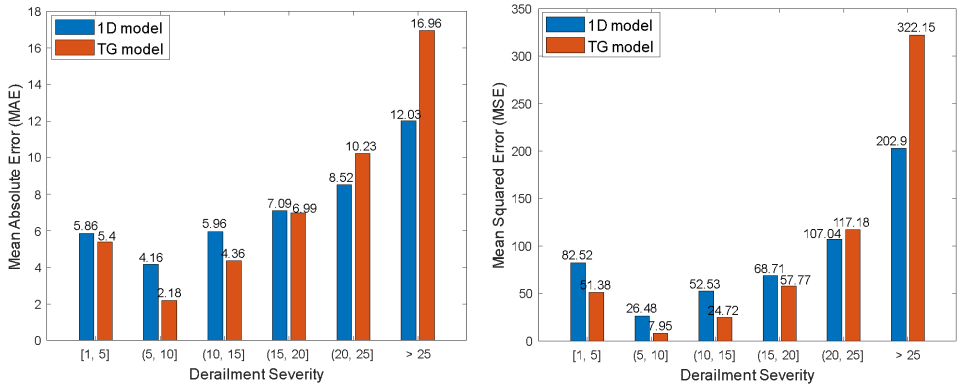

(a) All train types

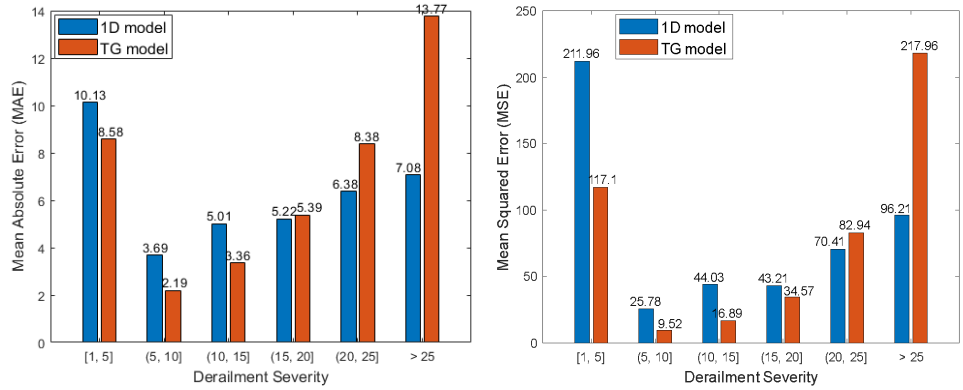

(b) Unit loaded trains

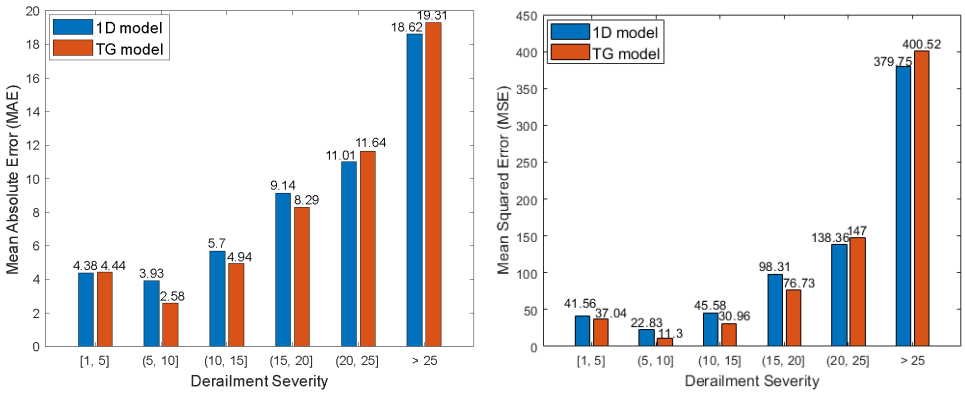

(c) Unit empty trains

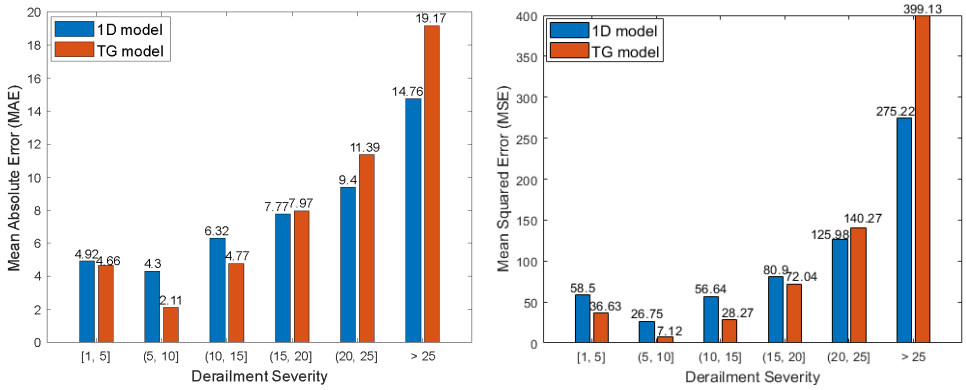

(d) Manifest trains

Figure 91. Comparison between 1-D model and TG model for different severity levels (outliers are included): (a) all train types (b) loaded unit trains (c) empty unit trains (d) manifest trains

The summary of the main effects (i.e., speed, gross tonnage per car, and residual train length) analyses is provided in Figure 92.

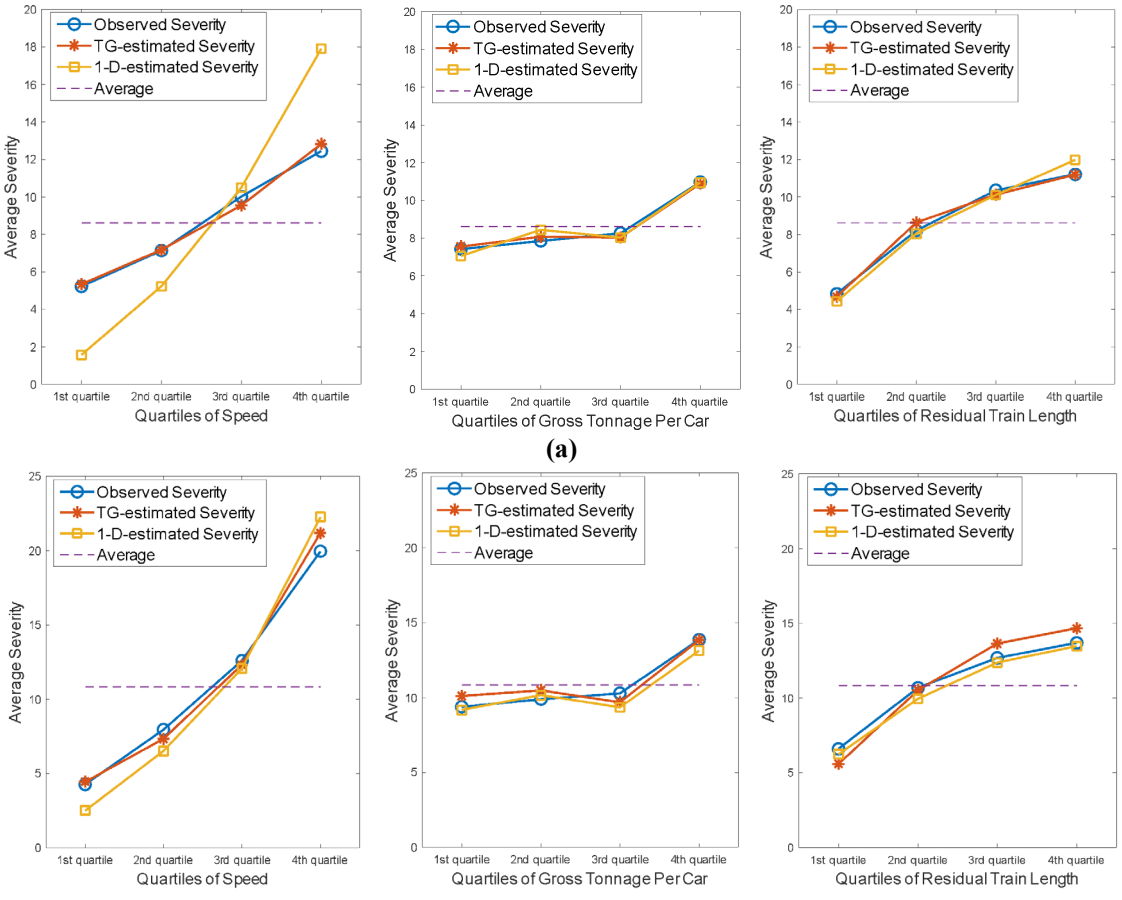

(a)

(b)

Figure 92. Calculated derailment severities in quartiles of factors (speed, gross tonnage per car, and residual train length): (a) all data with outliers (b) data excluding outliers

Each factor is represented by three lines (one line for observed severity, one line for TG-estimated severity, and one line for the 1-D-model-estimated severity). The main effects analysis is based on the four quartiles of three factors: speed, gross tonnage per car, and residual train length. The dash line represents the average severity of the derailments analyzed in the database (7,489 derailments for all data, 5,400 derailments for data excluding outliers).

Figure 93 presents the effect analysis of train types, showing average derailment severity of unit loaded train versus manifest trains with the gross tonnage per car between 135 and 145. Thus, a quick comparison of the slopes of the lines gives an indication of the relative importance of factors for calculated severity.

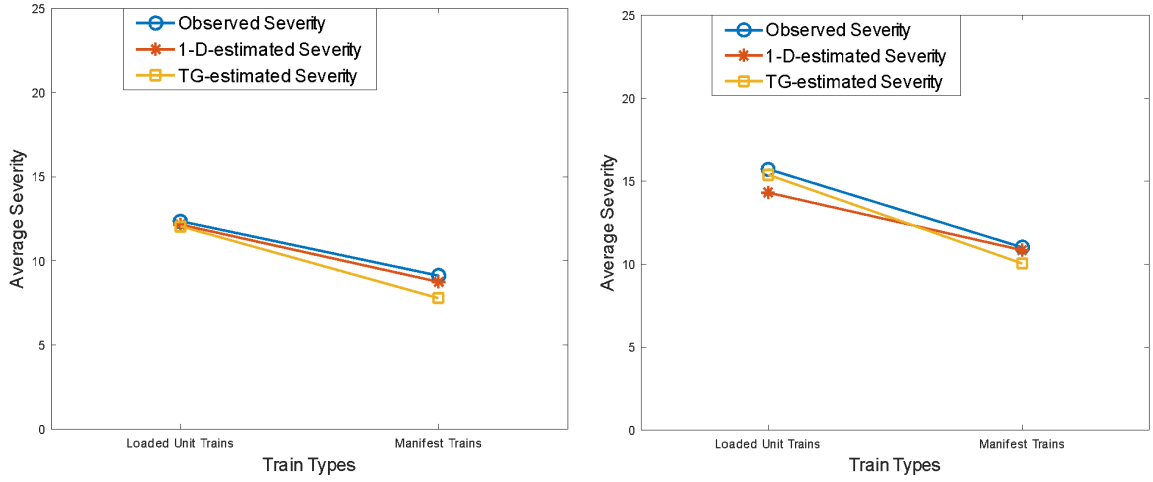

Figure 93. Calculated derailment severities for different train types (gross tonnage per car between 135 and 145): (a) all data with outliers (b) data excluding outliers

5.5 Summary and Conclusions

The team developed a statistical TG model and a 1-D physical model (1-D model) to estimate train derailment severity. Based on the severity estimation results obtained by the TG model and the 1-D model, the team drew the following conclusions.

- The TG model identifies the factors that can significantly influence train derailment severity, including train speed, residual train length, gross tonnage per car, and train type (i.e., unit loaded train, unit empty train, and manifest train). In addition, the TG model quantifies the influence of these factors contributing to derailment severity.
- The 1-D model can better capture the conditions of a specific train derailment scenario by mathematically describing the physical dynamics of a derailment, given that the key parameters of a derailment incident can be accurately estimated. However, it requires estimates of parameters (e.g., blockage delay, braking delay, blockage force, etc.) of a derailment incident that may significantly influence the model's performance.
- The team used data from FRA's REA Incident Form 6180.54 to test the performance of the TG model and 1-D model. Overall, the TG model outperformed the 1-D model in estimating severity because some parameters of the 1-D model were unknown and

difficult to accurately estimate. However, the comparison results show that the 1-D model had a better estimation performance for high-severity derailments.

- There exists a set of outliers in the REA database which are not the typical derailments and not the primary risk for tank car punctures and hazmat releases, which thus degrades the estimation performance of both the TG model and 1-D model. Thus, the team conducted a severity analysis based on the data excluding outliers. The results showed that both the TG model and the 1-D model achieve better estimation performance after outliers are excluded.

6. Analysis of Yard and Terminal Derailments

In the context of North American railroads, efficient shipment of individual carloads of freight via manifest trains requires railcars arriving at a yard from multiple origins and bound for different destinations to be re-sorted and classified into trains departing for common intermediate destinations. The sorting (i.e., switching or shunting) process at these intermediate classification yards results in extra risk of derailment and release for carload shipments of hazmat moving in manifest trains. In contrast, unit trains transport multiple carloads together as a group directly from origin to destination terminals without the need for intermediate switching at classification yards. Although unit trains do not incur the additional risks associated with switching railcars in classification yards, both unit and manifest trains are subject to derailment risk during arrival and departure operations at loading and unloading terminals and classification yards. To effectively compare the overall risk of transporting hazmat in unit and manifest trains, the derailment risk of manifest trains during A/D processes at origin, intermediate, and destination yards, switching operations at intermediate yards, and unit trains during A/D at origin and destination terminals, must be quantified and used to supplement the mainline analysis outlined in previous chapters (Figure 94).

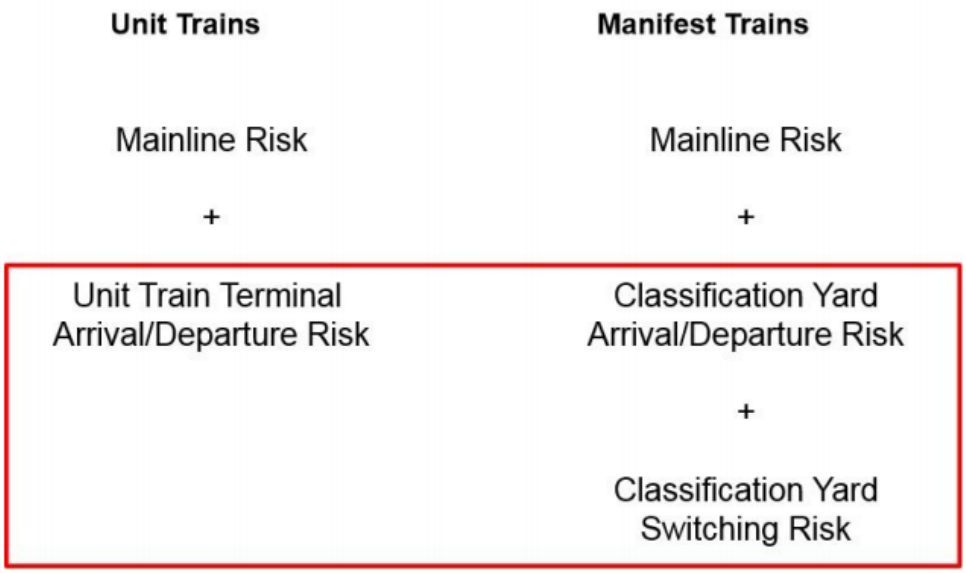

Figure 94. Comparison of unit and manifest train risk

To address this need, the team performed a quantitative analysis and statistical comparison of freight train yard and terminal derailment characteristics and rates for unit trains and non-unit manifest trains. Yard and terminal derailment data on Class I railroads between 1996 and 2018 were analyzed for both manifest trains and unit trains. To help justify separate treatment of different yard and terminal operations, a causal analysis was conducted for the unit train terminal and manifest train classification yard arrival and departure processes, and for the yard switching process in both flat switching and hump classification yards. This analysis suggests that unique derailment mechanisms may predominate for different yard processes and yard types, lending support for the need to calculate specific derailment rates for each appropriate combination of train type (i.e., unit or manifest), yard/terminal type (i.e., unit terminal, flat switching, or hump classification yard) and yard process (i.e., A/D or yard switching).

To normalize the Class I railroad yard and terminal derailment data, appropriate traffic data was obtained for the years 1996 to 2018. Derailment rates, calculated by two methodologies (i.e., generic mileage-based and detailed route-based), were estimated and compared for both A/D and yard switching events. The subsequent analysis also presents a case study to quantitatively compare the derailment rates for equivalent unit and manifest train trips.

To support the process of analyzing the consequences and overall risks of yard and terminal derailments, the team developed statistical models and approaches for estimating the severity of these derailments. Because train arrivals and departures at both yards and terminals are an extension of mainline operations and involve the same types of train consists, a position-based derailment severity model was developed for yards and terminals in a similar manner to the mainline. The position-based derailment severity approach consists of two steps: the normalized point of derailment distribution, and a distribution of number of cars derailed given the normalized point of derailment. Because yard switching derailments involve a cut of railcars and not the entire manifest train, the mainline definitions of normalized point of derailment and position in train no longer apply, requiring a distinct approach for yard switching derailment severity. To analyze yard switching events, a distribution of number of cars derailed per yard switching derailment was developed for both flat switching and hump classification yards.

For both yard switching and yard and terminal A/D derailments, the distribution of the number of cars derailed must be further transformed into a distribution of number of railcars carrying hazmat (i.e., hazmat railcars) derailed, and then subsequently into a distribution of hazmat railcars releasing lading, and a distribution of the estimated quantity of hazmat released. This next step is straightforward for unit train terminal A/D derailments since, by definition, all the derailed unit train railcars must be carrying hazmat. The situation is more complicated for manifest train A/D and yard switching derailments, since the manifest train will also be transporting non-hazmat railcars and the distribution of number of hazmat cars derailed will be heavily dependent on the position of the hazmat railcars within the manifest train and how they are switched relative to non-hazmat railcars.

The remainder of this section is structured as follows: Section 6.1 reviews the yard and terminal operating framework used to complement the mainline analysis; Section 6.2 reviews the primary derailment and traffic data sources, collection, and processing; Section 6.3 summarizes the resulting yard and terminal derailment statistics and causes of these incidents; Section 6.4 presents calculations of the various yard and terminal derailment rates; Section 6.5 details the analysis of yard and terminal derailment severity; and Section 6.6 describes how the derailment severity analysis supports further extension to the release and consequence analysis described in other sections.

6.1 Yard and Terminal Operating Framework

Each year, freight railroads in the United States transport approximately 100 million carloads involving two million hazmat shipments (AAR, 2019b). Most rail shipments involve more than one train movement due to the long distances traveled and the need to move railcars between sidings, branchlines, and major mainline routes that may be owned by different rail carriers. In addition to the line-haul (i.e., mainline) movements, the arrival and departure process at terminals and yards, and disassembly and assembly railcar switching in classification yards produce additional derailment and subsequent hazmat release risks. However, this risk is distinct between two main types of freight trains: manifest trains and unit trains.

Manifest trains consist of a mixture of empty and loaded railcars for various shippers. To economically transport freight from multiple origins to multiple destinations, small groups of railcars moving from common points typically pass through numerous yards and are switched between trains several times during their trip. A railcar moving a single shipment in carload service spends, on average, 62 percent of its time in classification yards and only 14 percent of its time in actual line-haul mainline movement (Kumar, 2011). The remaining 24 percent of the time is spent at shipper origin and destination spurs. In comparison, a unit train is composed of a single type of railcar carrying a single commodity from one origin to one destination. Unit trains reduce operating expenses by realizing economies of scale through bulk transportation.

When comparing the risks of manifest train and unit train shipments, the fundamental operating differences between these two train types require consideration of different trip components (see Figure 94). In addition to the mainline, both train types encounter accident risks during arrival and departure events at terminals and yards. These movements are similar to mainline freight operations but with reduced speed on non-mainline track. At classification yards (Figure 95), these events typically take place in the receiving yard where manifest trains arrive from the connection to the mainline, in the departure yard where manifest trains leave the classification yard for the mainline, or on the lead and running tracks connecting the receiving and departure yards to the mainline. At unit train terminals, these events typically take place on loop or "balloon" tracks used to sequentially load or unload each railcar in the unit train as it advances at low speed, or on the lead tracks connecting these facilities to the mainline. Within this research, events associated with unit train arrivals and departures from terminal facilities and manifest train arrivals and departures from classification yards are referred to as "freight consist" events (also known as "arrival and departure" events) to be consistent with how they are labeled and categorized in the FRA Incident/Accident Database.

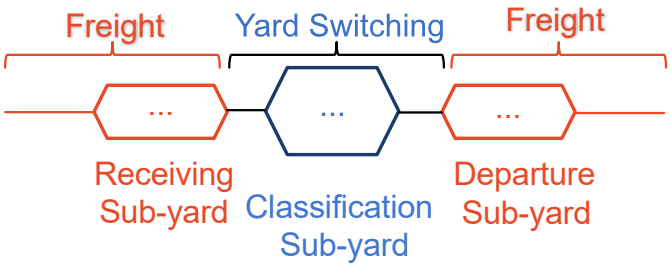

Figure 95. Yard and terminal accident location and train consist type

For manifest trains, railcar switching and sorting by destination in classification yards poses an additional accident likelihood due to causes such as switching rule violations and track and turnout defects. Within this research, events associated with the actual railcar classification, sorting, switching, and train assembly process in classification yards are referred to as "yard switching consist" events (or simply "yard switching" events) to similarly be consistent with the incident/accident database. These events typically take place in the main classification yard and its associated tracks used for accumulating railcars into blocks by destination, on the switching lead tracks used to actively sort the railcars and connect the receiving and departure tracks to the classification tracks, or on other ancillary tracks used to process railcars as they pass through the classification yard. Yard switching typically involves the movement of a single railcar, a cut of cars, or a portion of a train (potentially moving in reverse or in a shoving movement) at restricted speed by a yard switching crew using a switch engine and not the mainline locomotive power

used to transport the train over the mainline. Therefore, the traditional mainline definitions of a train consist, point of derailment, and position-based accident probability are not readily applicable. While the analysis of A/D risk can consider the same unit train and manifest train consists studied on the mainline, by definition, the yard switching process will alter the arriving manifest train consist into a new departing manifest train consist as the group of hazmat railcars comprising the shipment transfer from one manifest train to another. Thus, the yard switching approach outlined in this section must consider the hazmat railcars being processed together as a single group independent of their position within the specific arriving and departing train consists.

6.2 Yard and Terminal Derailment Data, Traffic Data, and Processing

6.2.1 Derailment Data

To be consistent with the mainline analysis, the team again extracted data on train A/D accidents and yard switching accidents in railway terminals and yards involving Class I railroads over the period from 1996 to 2018 from the FRA REA database (Form 6180.54). The REA database records accidents that exceed a monetary threshold for damage and loss to rail infrastructure and equipment (Federal Railroad Administration, 2012). The yard accidents (indicated by the "typtrk" field) were filtered by the field "typeq" (i.e., train consist) to associate the accident with a particular yard and terminal operational activity:

- 1 (freight train) is classified as a train arrival and departure accident at yards and terminals (i.e., freight consist).
- 4 (work train), 5 (single car), 6 (cut of cars), 7 (yard/switching), 8 (light loco(s)), 9 (main/inspec. Car), A (spec. MoW eq.) were classified as yard switching accidents (i.e., yard consist).
- All other entries, such as 2 (passenger train-pulling), 3 (commuter train-pulling), B (passenger train-pushing), C (commuter train-pushing), D (DMU), and E (EMU) were excluded from this study.

6.2.2 Traffic Data and Processing

Traffic data was collected from the 1996-2018 STB Class I Railroad Annual Reports (Form R-1) summarizing various annual financial and operating statistics for each Class I railroad. Specific annual traffic data including mainline train-miles, mainline car-miles, mainline ton-miles, number of loaded cars transported, and yard switching hours were assembled from Schedule 755 for unit trains and manifest trains, respectively. Using mainline train-miles, car-miles, and number of loaded cars, the number of manifest trains and unit trains operated over the study period can be estimated as follows:

$$Average\ mainline\ train\ length\ (excluding\ locomotives) = \frac{total\ train\ miles}{total\ car\ miles} \quad (6\text{-}1)$$

$$Number\ of\ empty\ and\ loaded\ railcars\ operated = number\ of\ loaded\ railcars\ operated\ \times loading\ factor \quad (6\text{-}2)$$

$$Number\ of\ trains\ operated = \frac{number\ of\ empty\ and\ loaded\ railcars}{average\ mainline\ train\ length} \quad (6\text{-}3)$$

The unit train loading factor is assumed to equal two, indicating that empty and loaded railcars each account for half of the total unit train car-miles. A manifest train loading factor of 1.73 is applied since the number of empty cars moving on manifest trains is approximately 73 percent of the number of loaded cars on manifest trains (based on further analysis of the empty and loaded car-miles by railcar type in the R-1 data). Applying these factors to the number of loaded railcars reported in the R-1 data and dividing by the average train length yields the number of trains of each type operated per year over the study period (Figure 96).

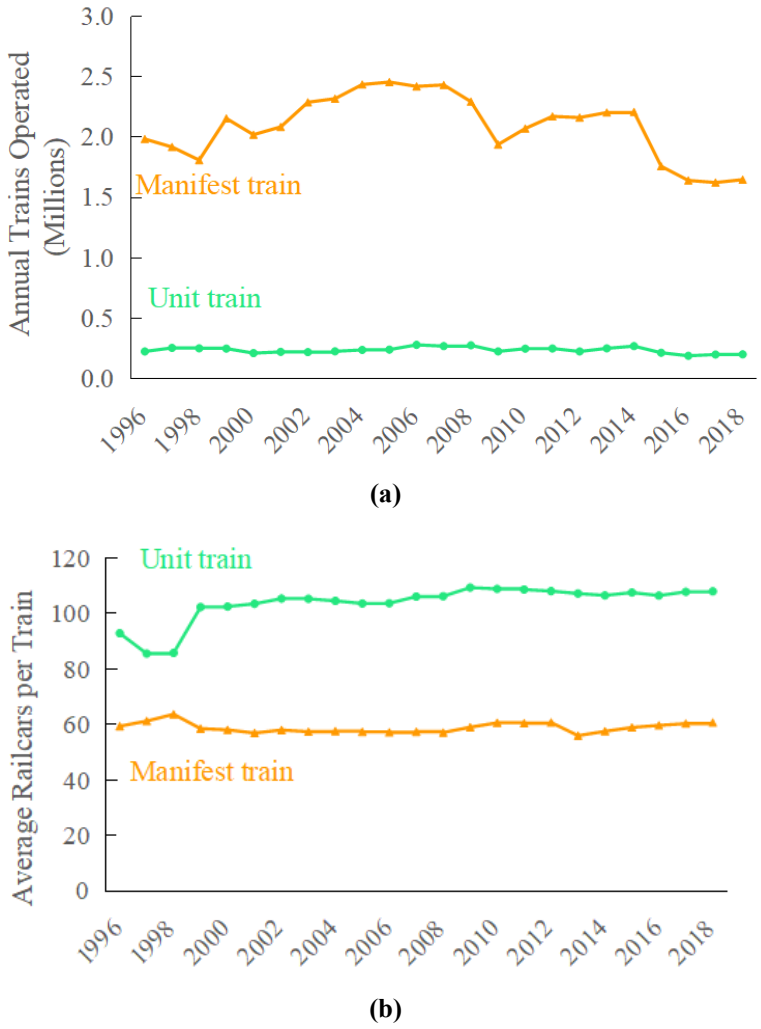

Figure 96. Comparison of Class I manifest train and unit train (a) annual number of mainline trains operated and (b) average train length in railcars (1996-2018)

6.2.3 Train Type Identification

Since yard switching activities only apply to manifest train operations, all trains causing or involved in yard switching type accidents are classified as manifest train consists. However, arrival and departure type accidents apply to both manifest trains and unit trains. Therefore, a scheme to identify the unit trains and manifest trains in the REA database arrival and departure derailments (i.e., freight consist) using information such as operator and train number, train

length, narrative, and causing railcar number (Figure 97), was adapted from the mainline methodology.

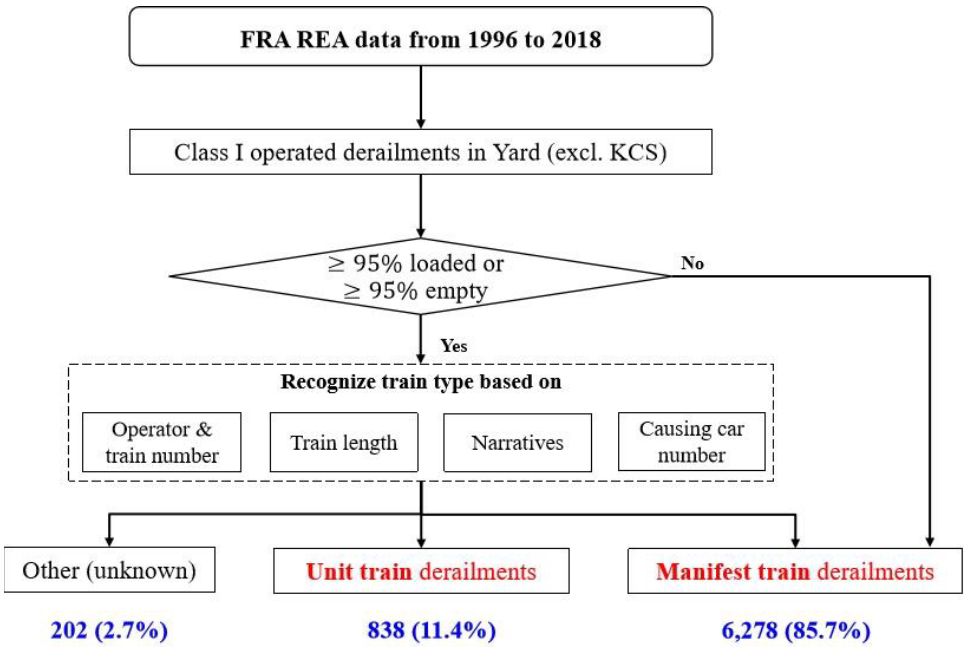

Figure 97. Methodology for classifying trains in yard A/D derailments

A train is classified as fully loaded if 95 percent or more of its cars are loaded, or empty if 95 percent or more of its cars are empty, considering the presence of buffer cars. These percentages were calculated by dividing the number of loaded or empty cars by the total number of cars in the train. By definition, trains that are not fully loaded or empty are not unit trains and are thus classified as manifest trains. To further classify fully loaded or empty trains, four criteria were applied:

1) The REA database fields for railroad operator and train number were compared to individual railroad train symbol systems for unit and manifest trains and classified accordingly. If no train symbol match was found, additional criteria were considered.
2) All trains with fewer than 40 railcars were classified as manifest trains. For trains of 40 railcars or more, additional criteria were considered.
3) Keywords in derailment narrative fields, such as "boxcar," "trailer," "container," or "local train," are likely to be indicative of manifest train derailments and were classified accordingly.
4) The reporting mark and number field for the first car involved in the derailment was used to assist the identification of train type since certain car types are uncommon for unit trains.

To be consistent with the mainline portion of this research, this classification scheme was only applied to yard accidents on six U.S. Class I railroads: BNSF, CSX, Grand Trunk Corporation (Canadian National's U.S. operations), Norfolk Southern, Soo Line Corporation (Canadian Pacific's U.S. operations), and Union Pacific. Kansas City Southern was not included in this research due to data limitations and some inconsistencies in historical traffic data.

From 1996 to 2018, among all the yard and terminal A/D accidents (i.e., freight consist), 838 were unit trains, 6,278 were manifest trains, and 202 were classified as "other" trains of unknown type and excluded from further analysis.

6.2.4 Yard Type Identification

To better understand manifest train derailments during yard switching at classification yards, researchers investigated derailment characteristics and rates at two major yard types: flat yards (cars are sorted using shoving engines) and hump yards (automated sorting using gravity). The different operating procedures between flat and hump yards may cause significant differences in derailment likelihood.

The FRA REA database does not contain a specific field to indicate the type of yard where each accident occurred. Multiple REA data fields, including central coordinates, yard engine ID, station name, milepost, cause, and narrative were used to identify incidents occurring in hump yards. The classification procedure is as follows:

1) Where available, compare derailment coordinates to central coordinates of known hump and mini-hump yards to within +/- 0.02° or one mile.
2) Examine yard engine ID field for abbreviations related to yard names.
3) Compare station name and milepost of derailment location with those associated with known hump and mini-hump yards.
4) Check for hump-yard-specific causes including:
   T305 – Retarder worn, broken, or malfunctioning
   T306, H314 – Retarder yard skate defective, improperly applied
   S006 – Hump yard automatic switch control failure
   S007, H313 – Hump yard automatic retarder control failure
   S016, H316 – Hump yard automatic control failure
   M407 – Retarder ineffective due to contaminated wheels
   M411 – Bypassed couplers in hump yard bowl
5) Narrative fields with keywords such as "hump lead," "group retarders," etc. are indicative of hump yard accidents.
6) If none of the above applies, the accident is considered a flat yard accident.

Applying this procedure to all 17,392 yard switching accidents indicated that 6,899 (40 percent) occurred in hump yards (Figure 98a) and 10,493 (60 percent) occurred in flat yards (Figure 98b). Eliminating non-Class I railroad incidents, out of 13,300 yard switching derailments, 7,438 (56 percent) occurred in hump yards and 5,862 (44 percent) occurred in flat yards.

A challenging aspect of this classification is that the number of hump yards decreased from 57 to 35 over the study period (Figure 98a) due to mergers, closures, conversion to flat switching, and other operating adjustments. Various references were used to construct a timeline summarizing the status of every U.S. hump classification yard during the study period (

Table 39), and derailments were classified according to the status of the yard (ownership and yard type) at the time of the incident.

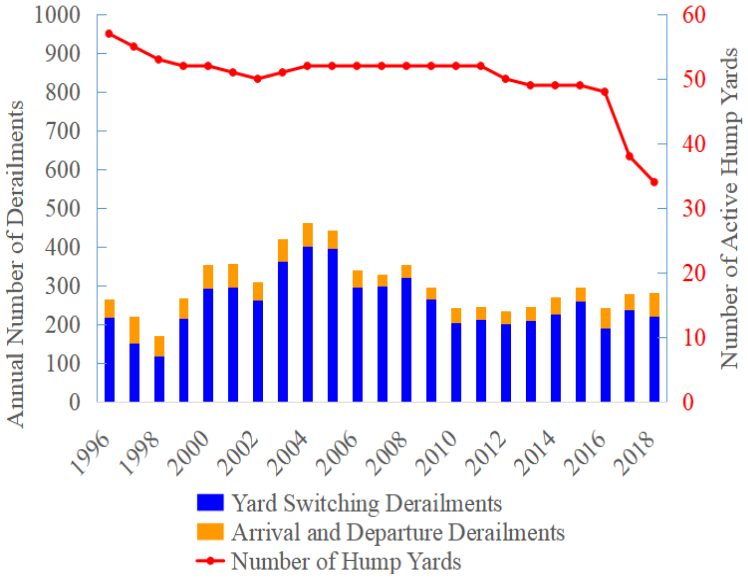

(a)

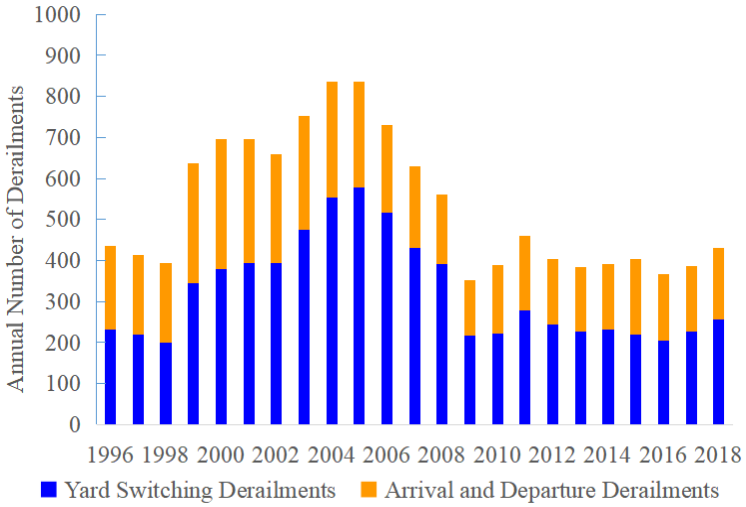

(b)

Figure 98. Number of active hump classification yards and annual yard derailment frequency for (a) hump yards and (b) flat switching yards

Table 39. Hump classification yard status timeline

Yard Name	Owner	Location	Type	Current Disposition	Ownership and Name Changes
Gateway	A&S	East St. Louis, IL	Hump	Active	
Barstow	BNSF	Barstow, CA	Hump	Active	
Galesburg	BNSF	Galesburg, IL	Hump	Active	
Argentine	BNSF	Kansas City, KS	Hump	Active	
Hobson	BNSF	Lincoln, NE	Mini H	Active	

Yard Name	Owner	Location	Type	Current Disposition	Ownership and Name Changes
Tennessee	BNSF	Memphis, TN	Hump	Active	
Northtown	BNSF	Minneapolis, MN	Hump	Active	
Pasco	BNSF	Pasco, WA	Hump	Active	
Balmer	BNSF	Seattle, WA	Mini H	Active	
Cherokee	BNSF	Tulsa, OK	Hump	Active	
Flynn	BNSF	Oklahoma City, OK	Mini H	Converted to flat in 1997	
Murray	BNSF	Kansas City, MO	Hump	Converted to flat in 1998	
Clearing	BRC	Chicago, IL	Hump	Active	
Kirk	CN	Gary, IN	Hump	Active	EJ&E before 2013
Flat Rock	CN	Flat Rock, MI	Hump	Converted to flat in 1997	
Harrison	CN	Memphis, TN	Mini H	Active, flat before 2009	Flat Johnston Yard before 2009
Oak Island	CR	Newark, NJ	Hump	Active	
North	CR	Detroit, MI	Hump	Converted to flat in 1998	
Pavonia	CR	Camden, NJ	Hump	Converted to flat in 2017	
Selkirk	CSX	Albany, NY	Hump	Active	CR before 1999
Queensgate	CSX	Cincinnati, OH	Hump	Active	
Avon	CSX	Indianapolis, IN	Hump	Active	CR before 1999
Rice	CSX	Waycross, GA	Hump	Active	
Frontier	CSX	Buffalo, NY	Hump	Closed in 2009	CR before 1999
Tilford	CSX	Atlanta, GA	Hump	Closed in 2017	
Boyles	CSX	Birmingham, AL	Hump	Closed in 2017	
Cumberland	CSX	Cumberland, MD	Hump	Closed in 2017	
Hamlet	CSX	Hamlet, NC	Hump	Closed in 2017	
Osborn	CSX	Louisville, KY	Hump	Closed in 2017	
Radnor	CSX	Nashville, TN	Hump	Closed in 2017	
Stanley	CSX	Toledo, OH	Hump	Closed in 2017	
Willard	CSX	Willard, OH	Hump	Closed in 2017	
Blue Island	IHB	Chicago, IL	Hump	Active	
Norris	NS	Birmingham, AL	Hump	Active	
Elkhart	NS	Elkhart, IN	Hump	Active	CR before 1999
Brosnan	NS	Macon, GA	Hump	Active	
Norfolk	NS	Norfolk, VA	Hump	Active	
Conway	NS	Pittsburgh, PA	Hump	Active	CR before 1999
Buckeye	NS	Columbus, OH	Hump	Closed in 2009	CR before 1999
Shaffers	NS	Roanoke, VA	Hump	Closed in 2013	
Sevier	NS	Knoxville, TN	Hump	Closed in 2016	
Allentown	NS	Allentown, PA	Hump	Closed in 2020	CR before 1999
Bellevue	NS	Bellevue, OH	Hump	Closed in 2020	
Spencer	NS	Linwood, NC	Hump	Closed in 2020	
Sheffield	NS	Sheffield, AL	Hump	Closed in 2020	

Yard Name	Owner	Location	Type	Current Disposition	Ownership and Name Changes
Debutts	NS	Chattanooga, TN	Hump	Converted to flat in 2017; Partially converted back to hump in 2018, active	
Enola	NS	Harrisburg, PA	Hump	Flat before 2003; Converted to flat in 2020	
St. Paul	SOO	St. Paul, MN	Hump	Active	
Bensenville	SOO	Bensenville, IL	Hump	Converted to flat in 2012	
Madison	TRRA	East St. Louis, IL	Hump	Active	
Beaumont	UP	Beaumont, TX	Mini H	Active	
West Colton	UP	Colton, CA	Hump	Active	
Davidson	UP	Fort Worth, TX	Hump	Active	Centennial Yard before 2007
Englewood	UP	Houston, TX	Hump	Active	
Settegast	UP	Houston, TX	Mini H	Active	
Strang	UP	La Porte, TX	Mini H	Active	
Livonia	UP	Livonia, LA	Mini H	Active	
North Little Rock	UP	North Little Rock, AR	Hump	Active	
Bailey	UP	North Platte, NE	Hump	Active	
Davis	UP	Roseville, CA	Hump	Active	Roseville Yard before 1999
Proviso	UP	Chicago, IL	Hump	Closed in 2019	
Hinkle	UP	Hermiston, OR	Hump	Closed in 2019	
Neff	UP	Kansas City, MO	Hump	Closed in 2019	
Pine Bluff	UP	Pine Bluff, AR	Hump	Closed in 2019	
Pocatello	UP	Pocatello, ID	Hump	Converted to flat in 2002	
City of Industry	UP	City Of Industry, CA	Mini H	Converted to flat in 2012	
East Los Angeles	UP	Los Angeles, CA	Hump	Closed in 2001	Converted to intermodal

A&S: Alton & Southern
BRC: Belt Railway of Chicago
CR: Conrail
EJ&E: Elgin Joliet & Eastern
IHB: Indiana Harbor Belt
TRRA: Terminal Railroad Association of St. Louis

6.3 Train and Yard Type-Specific Derailment Analysis

6.3.1 Yard Derailment Statistics

After classifying all yard accidents from 1996 to 2018 by process (i.e., A/D or yard switching), train type (i.e., unit or manifest), and yard type, summary statistics for each group of yard derailments were made (

Table 40). These yard and terminal statistics can also be compared to equivalent metrics for manifest and unit train derailments on the mainline developed in earlier sections. Like the mainline, train length includes all loaded railcars, empty railcars, and locomotives in the train consist.

Table 40. Derailment characteristics by process and yard type (1996-2018)

Process	Yard/ Train Type	Derailment Frequency	Average Train/ Consist Length	Average Tons per Car (excl. locomotive)	Average Speed (mph)	Average Number of Cars Derailed
Yard or Terminal Arrival and Departure (freight consist)	Unit Trains	838	105.7	107.2	7.0	6.0
	Manifest Trains	6,278	60.8	71.8	6.3	4.5
	Hump Yards	1,143	59.5	58.1	6.3	4.0
	Flat Yards	5,135	61.1	74.8	6.2	4.6
Yard Switching	Hump Yards	7,438	28.3	33.8	4.6	2.2
	Flat Yards	5,862	41.5	44.8	7.0	4.1
Mainline	Unit Trains	2,462	110.0	113.8	25.1	11.3
	Manifest Trains	5,514	82.6	80.7	24.3	7.6

Average yard and terminal arrival and departure derailment speeds of manifest trains and unit trains are substantially lower than speeds for the same train types on mainlines. The average weight of unit trains arriving and departing terminals is nearly twice that of manifest trains arriving and departing hump yards. Correspondingly, in terms of derailment severity, unit train arrival and departure derailments result in more cars derailed per accident compared to manifest trains. The same result is observed on the mainline where both train types derail substantially more cars per incident compared to incidents at yards and terminals. This result is consistent with hypotheses proposed by Martey & Attoh-Okine et al. (2019b) and Liu, Saat, Qin, et al. (2013) that derailment severity is affected by train length, train weight, and derailment speed. For yard and terminal arrival and departure accidents, despite similar average speeds, a higher value of total train length and greater train weight appear to result in more cars derailed in a unit train incident compared to a manifest train. Compared to both yard arrival and departure incidents and mainline incidents, yard switching incidents involve fewer railcars, lower consist weights, lower speeds, and fewer railcars derailed per incident.

Comparing hump yards and flat yards, the manifest trains involved in derailments during arrival and departure at hump yards are shorter than at flat yards, consistent with yard switching events, where the cuts of cars in hump yards are also shorter than in flat yards. The average derailment speed of hump yard accidents is lower than flat yards for yard switching accidents due to the distinct classification operations in the two types of yards. A minor difference in derailment severity is observed between hump and flat yard arrival and departure derailments, but yard switching derailments in hump yards exhibit fewer derailed railcars than in flat yards. Overall, the derailment statistics suggest differences in risk between hump yards and flat yards for both freight consist and yard switching consist accidents, demonstrating the need to consider yard type and process when studying the derailment risk of carload shipments.

6.3.2 Causal Analysis

Since yard and terminal derailments exhibit different characteristics based on process, train type, and yard type, it may be assumed that some causes are more prevalent in certain yard/terminal situations than others. The FRA REA database categorizes train accidents into five major cause groups: track, equipment, human factor, signal, and miscellaneous. In the early 1990s, Arthur D. Little (ADL) Inc., with the assistance of AAR and railroad experts, further developed a systematic grouping of FRA cause codes to better associate causes with similar or related preventative measures. Using the 1996-2018 yard accident data, the top ADL cause groups for manifest and unit train arrival and departure derailments were ranked by number of derailments (Table 41).

Table 41. Top ten most frequent yard/terminal A/D causes by train type on Class I railroads (1996-2018)

Cause Group	Number of Derailments		Average Number of Cars Derailed
	Frequency	Percent of Total	
Unit Train Terminal Arrival/Departure			
Broken rails or welds	224	26.8	6.8
Wide gauge	106	12.7	6.7
Turnout defects: switches	105	12.6	5.6
Use of switches	79	9.4	4.8
Switching rules	42	5.0	3.4
Miscellaneous track and structure defects	29	3.5	5.7
Track geometry (excluding wide gauge)	27	3.2	5.8
Other miscellaneous	26	3.1	5.4
Other wheel defects (car)	19	2.3	6.3
Roadbed defects	18	2.2	8.4
Manifest Train Yard Arrival/Departure			
Switching rules	908	15.4	2.8
Use of switches	766	13.0	3.8
Broken rails or welds	685	11.7	5.7
Wide gauge	625	10.6	6.4
Turnout defects: switches	486	8.3	4.3
Train handling (excluding brakes)	407	6.9	5.6
Other miscellaneous	206	3.5	4.1
Handbrake operations	195	3.3	2.3
Train speed	183	3.1	3.1
Miscellaneous track and structure defects	155	2.6	5.4

Broken rails or welds is the leading cause group for unit train terminal A/D accidents, while switching rules and use of switches accounts for approximately the same percentage of manifest train A/D derailments. This result is consistent with manifest train operations in yards requiring more use of turnouts and switches during arrival and departure events compared to unit train terminal operations.

Previous studies have classified each ADL cause group as being train-mile related, car-mile related, or ton-mile related (Wang, 2019). Most of the top cause groups for both train types are train-mile related causes (independent of train length), except for "broken rails or welds." This result is different from the mainline where the most common cause groups are car-mile related (i.e., related to train length). For the 1996-2018 period studied, most unit train terminal derailments resulted from track-related causes (66 percent) while human factor-related causes accounted for almost half (47 percent) of the yard derailments for manifest trains. The extensive manifest train handling operations at arriving and departing yards is consistent with this dominance of human factor-related accidents. Similarly, since unit train consists involve heavier and more cars on average, this is consistent with these trains experiencing more track-related accidents than manifest trains.

When considering the derailment severity of yard/terminal A/D accidents, the same cause groups show more cars derailed in unit trains than manifest trains (Figure 99). In interpreting this figure, the green dot labeled "Track" represents the average number of cars derailed per track-caused unit train accident (approximately 6.5), and the number of track-caused unit train derailments accounts for approximately 70 percent of the total number of unit train terminal A/D derailments. Causes at the top right of the figure are of greatest concern since they are both severe and frequent. For both train types, signal-caused A/D derailments are infrequent. This result is not unexpected, given that most yard and terminal trackage is unsignaled.

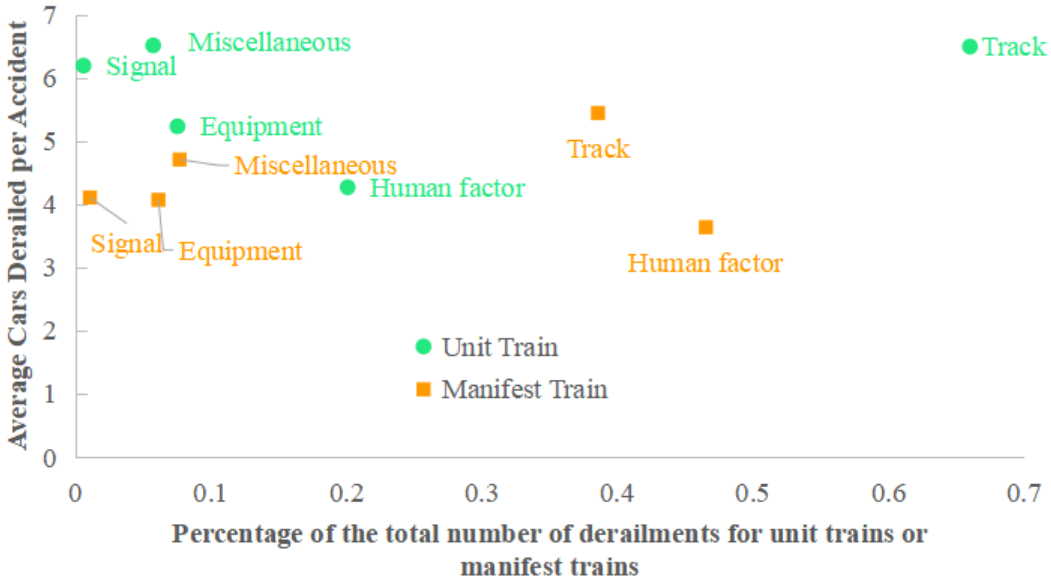

Figure 99. Cause group frequency and average severity of unit and manifest train derailments during A/D at yards and terminals (1996-2018)

Derailment causes can also be categorized by yard type and train consist (Figure 100 and Figure 101). The figures include any cause group accounting for more than 4 percent of all derailments for that combination of yard type and process. The most frequent arrival and departure derailment cause groups are identical for hump yards (Figure 100a) and flat yards (Figure 100b), but have slightly different frequencies. Broken rails or welds ranks first for trains arriving/departing hump yards, while switching rules is the most common cause at flat yards. The accident causes are more distinct for yard switching derailments with different frequent

cause groups present for the two yard types. Railcars switched in hump yards (Figure 101a) are more vulnerable to miscellaneous, switching rules and signal failure causes (all three causes largely associated with the hump speed control system), while railcars in flat yards (Figure 101b) tend to derail due to switching rules and use of switches. Handbrakes are also a leading accident cause in flat yards but are not a primary cause in hump yards, likely because typical hump yard classification tracks are specifically profiled to control railcars without the use of handbrakes.

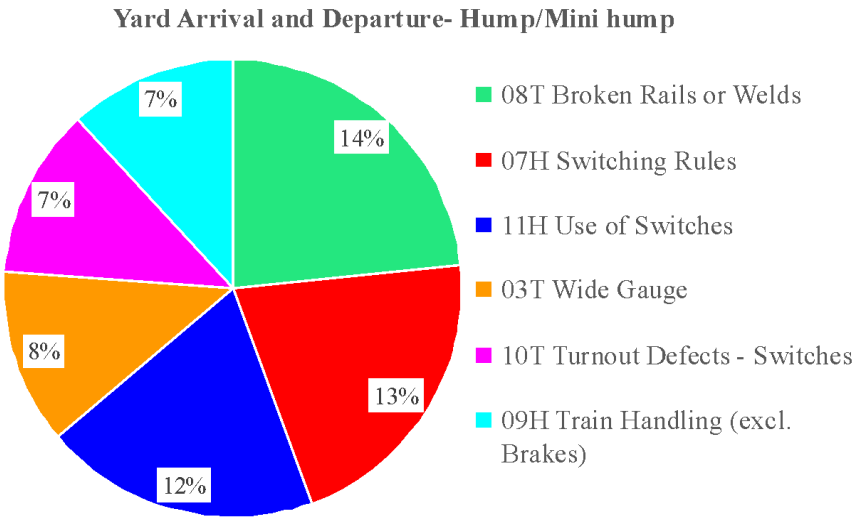

(a)

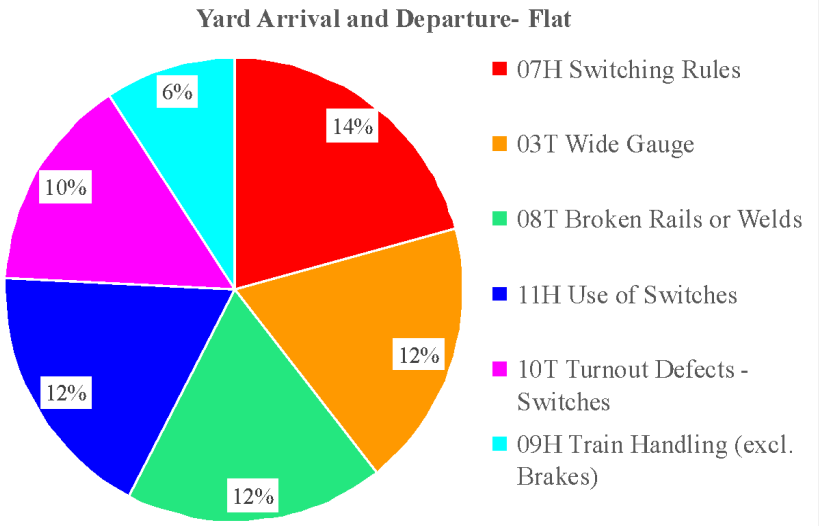

(b)

Figure 100. Leading derailment cause groups (1996-2018) for (a) arrivals/departures at hump yards, and (b) arrivals/departures at flat yards

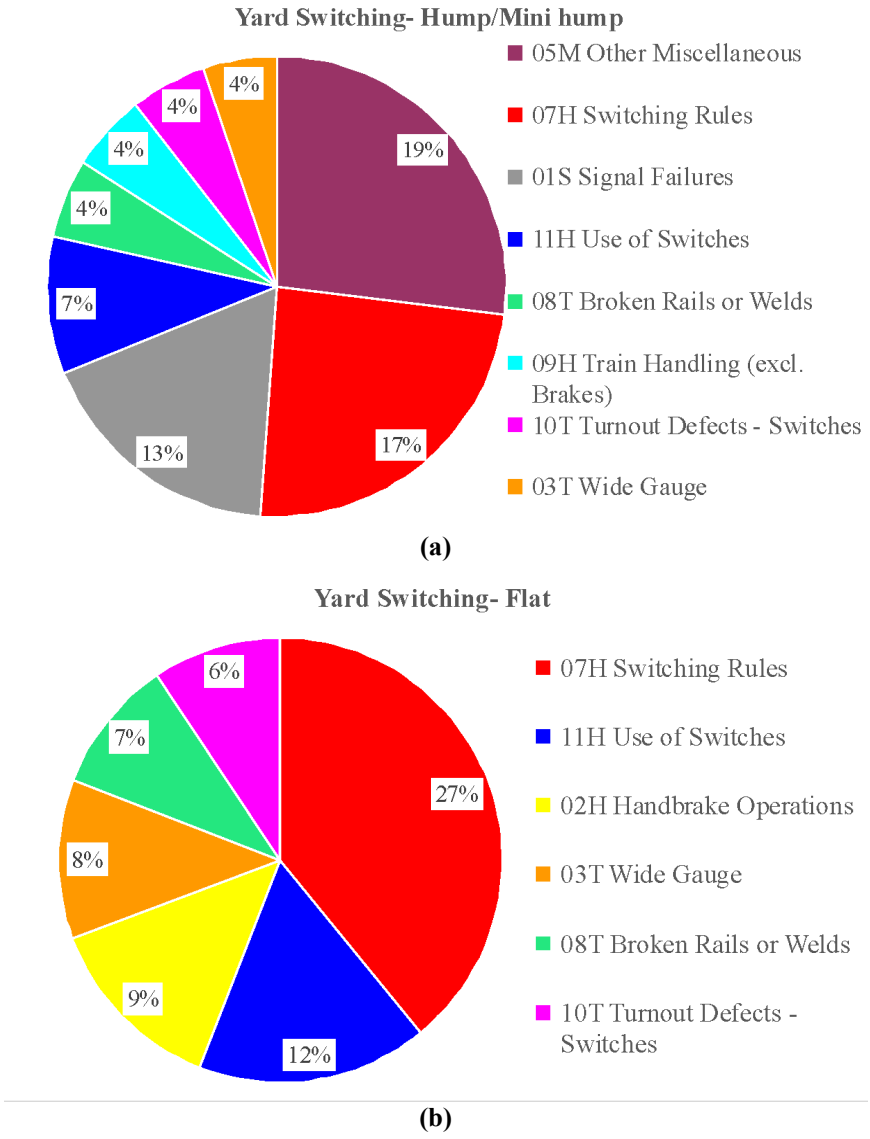

Figure 101. Leading derailment cause groups (1996-2018) for (a) yard switching in hump yards and (b) yard switching in flat yards

The difference in derailment causes between yard types and processes (i.e., train consist) affects the probability of derailments for various trains in different yard operations. Therefore, to better estimate the likelihood of derailments under different operating circumstances, the team calculated derailment rates separately for different train consists and yard types.

6.4 Yard and Terminal Derailment Rates by Train Type

Yard and terminal derailment rates are calculated by normalizing the historical yard and terminal accident frequency data by historical yard traffic metrics. See Section 6.2 for a detailed description of the collection and processing of both the historical accident frequency data and the historical traffic data for the years 1996 to 2018.

As described in Section 3, although the mainline travel distance between origin and destination can typically be estimated for a given carload freight shipment, detailed information on the exact sequence of manifest trains and number and type of classification yards involved may not be known beforehand. To provide flexibility in this regard, two approaches were proposed to develop yard derailment rates for manifest trains:

- **Generic Mileage-Based Approach** is used if the number and type of intermediate classification yards is not known. This approach looks at the average rate of yard A/D and switching events as a function of mainline traffic metrics. The underlying assumption is that the number of intermediate yards (and associated expected number of yard derailments) is linearly proportional to the overall mainline distance traveled from origin to destination.
- **Detailed Route-Based Approach** is used if the exact number and type of intermediate classification yards is known. This approach develops specific rates of occurrence for yard A/D and yard switching events as a function of actual yard traffic metrics, such as the number of train arrivals and departures or number of railcars processed. Different rates are developed for hump and flat switching classification yards. Because it is more specific to actual yard operating metrics and the exact yards involved in the shipment, the detailed route-based approach should produce more accurate estimates than the generic mileage-based approach when specific yard details are known.

By definition, loaded unit trains operate from an origin loading terminal directly to a destination unloading terminal. Thus, each unit train movement involves one origin train departure and one destination train arrival. Since this terminal pattern is fixed, the detailed route-based approach can always be applied to unit trains. However, for the purposes of comparison and to provide context for the calculated manifest train derailment rates, generic mileage-based metrics were also calculated for unit train terminal A/D events.

6.4.1 Generic Mileage-based Rate Calculation

The generic mileage-based approach is used when the total mainline distance for a given shipment is known, but the exact pattern of intermediate classification yards is not known. Without prior information on the exact number of yards to be visited by the shipment, there is no basis on which to determine an exact number of train A/D events and railcar yard switching activity experienced by the railcars involved in the shipment during their trip from origin to destination. As a proxy for these exact values, the generic mileage-based approach assumes that the number of manifest train A/D and yard switching events are proportional to the mainline distance traveled, as shipments covering greater distances are more likely to involve train connections at multiple intermediate classification yards. Based on this assumption, the occurrence of yard derailments can be normalized by mainline traffic metrics to produce mileage-based rates of yard and terminal derailments per mainline train-mile, car-mile, or ton-mile. The resulting composite metrics account for the typical distances traveled by manifest trains between intermediate classification yards and the relative likelihood of A/D and yard switching derailments at those facilities.

6.4.1.1 A/D Derailments

For arrival and departure (i.e., freight consist) derailments, three mileage-based derailment rates were calculated (per million mainline train-miles, per billion mainline ton-miles, and per billion mainline car-miles) for both manifest trains and unit trains, using the following equations:

$$A/D\ Derailment\ rate\ per\ million\ train\ miles\ =\ \frac{Number\ of\ A/D\ train\ derailments}{million\ mainline\ train\ miles} \quad (6\text{-}4)$$

$$A/D\ Derailment\ rate\ per\ billion\ ton\ miles\ =\ \frac{Number\ of\ A/D\ train\ derailments}{Billion\ mainline\ ton\ miles} \quad (6\text{-}5)$$

$$A/D\ Derailment\ rate\ per\ billion\ car\ miles\ =\ \frac{Number\ of\ A/D\ train\ derailments}{Billion\ mainline\ car\ miles} \quad (6\text{-}6)$$

For a given train type, each derailment rate was calculated using the number of yard/terminal A/D derailments assigned to that train type by the classification process described in Section 6.2.3. This quantity of derailments was normalized by the train-type specific train-miles, ton-miles, and car-miles obtained from the Class I railroad STB R-1 financial report traffic data described in Section 6.2.2.

6.4.1.2 Yard Switching Derailments

One yard-specific traffic metric included in the Class I railroad STB R-1 financial report traffic data is the number of yard switching hours. Thus, it is possible to calculate the manifest train yard switching derailment rate by normalizing the number of yard switching derailments by the number of yard switching hours:

$$YS\ Derailment\ rate\ per\ million\ yard\ switching\ hours\ =$$
$$\frac{Number\ of\ manifest\ train\ yard\ switching\ derailments}{million\ yard\ switching\ hours} \quad (6\text{-}7)$$

However, for a given hazmat shipment moving in manifest trains, it is difficult to estimate the incremental or total number of yard switching hours that should be allocated to a given shipment. This estimate is particularly difficult to make for a case where it is assumed that the number of intermediate classification yards visited by the shipment is not known. As a proxy, the assumption is made that the number of yard switching hours allocated to a shipment is proportional to the mainline train-miles required to transport the shipment, and is also proportional to the number of mainline car-miles, since trains with a greater number of railcars per train require additional switching effort and time to sort at classification yards:

$$YS\ hours\ per\ mainline\ train\ miles\ =\ \frac{yard\ switching\ hours}{mainline\ train\ miles} \quad (6\text{-}8)$$

$$YS\ hours\ per\ thousand\ mainline\ car\ miles\ =\ \frac{yard\ switching\ hours}{thousand\ mainline\ car\ miles} \quad (6\text{-}9)$$

The implication of this assumption is that like A/D derailments, manifest train yard switching (i.e., yard consist) derailment rates can be calculated per mainline train-mile and mainline car-mile using the following equations:

$$YS\ Derailment\ rate\ per\ million\ train\ miles = Derailment\ rate\ per\ million\ yard\ switching\ hours \times Yard\ switching\ hours\ per\ mainline\ train\ miles \quad (6\text{-}10)$$

$$YS\ Derailment\ rate\ per\ billion\ car\ miles = Derailment\ rate\ per\ million\ yard\ switching\ hours \times Yard\ switching\ hours\ per\ thousand\ mainline\ car\ miles \quad (6\text{-}11)$$

$$YS\ Derailment\ rate\ per\ million\ million\ train\ miles = \frac{Number\ of\ \ YS\ derailments}{million\ mainline\ manifest\ train\ miles} \quad (6\text{-}12)$$

$$YS\ Derailment\ rate\ per\ billion\ car\ miles = \frac{Number\ of\ \ YS\ derailments}{billion\ mainline\ manifest\ train\ car\ miles} \quad (6\text{-}13)$$

Each derailment rate was calculated using the number of yard switching derailments identified in the FRA REA database. This quantity of derailments was normalized by the manifest train-miles and car-miles obtained from the Class I railroad STB R-1 financial report traffic data.

6.4.1.3 Calculated Generic Mileage-based Yard and Terminal Derailment Rates

Using the above equations, generic mileage-based yard and terminal derailment rates were calculated for different train types and traffic metrics for the years 1996-2018 (Table 42).

Table 42. Generic mileage-based yard and terminal derailment rates (1996-2018) for various train types and mainline traffic metrics

	Arrival/Departure (Freight Consist)			Yard Switching (Yard Consist)	
Train Type	Derailments per Million Mainline Train-Miles	Derailments per Billion Mainline Car-Miles	Derailments per Billion Mainline Ton-Miles	Derailments per Million Mainline Train-Miles	Derailments per Billion Mainline Car-Miles
Manifest Train	0.70	11.88	0.14	1.57	26.86
Unit Train	0.29	2.81	0.03	N/A	N/A
Empty Unit	0.10	1.00	0.03	N/A	N/A
Loaded Unit	0.48	4.63	0.03	N/A	N/A

For yard and terminal arrivals/departures and all three traffic metrics, unit trains have substantially lower average derailment rates than manifest trains. There are two likely explanations for this result: 1) unit trains travel greater mainline distances than manifest trains and tend to be longer and heavier, thus having a higher traffic mileage denominator per A/D compared to manifest trains; and 2) unit train terminals are far less complex than classification yards served by manifest trains, with fewer turnouts and other common points of failure that may lead to derailments. This effect of overall train weight is demonstrated within the category of unit trains where, when measured by million train-miles or per billion car-miles, a loaded unit train has a four-times higher derailment rate than an empty unit train. If the unit train derailment rate

is measured by billion ton-miles, the rates are independent of loading condition, as this metric effectively normalizes for differences in weight between train types (Figure 102).

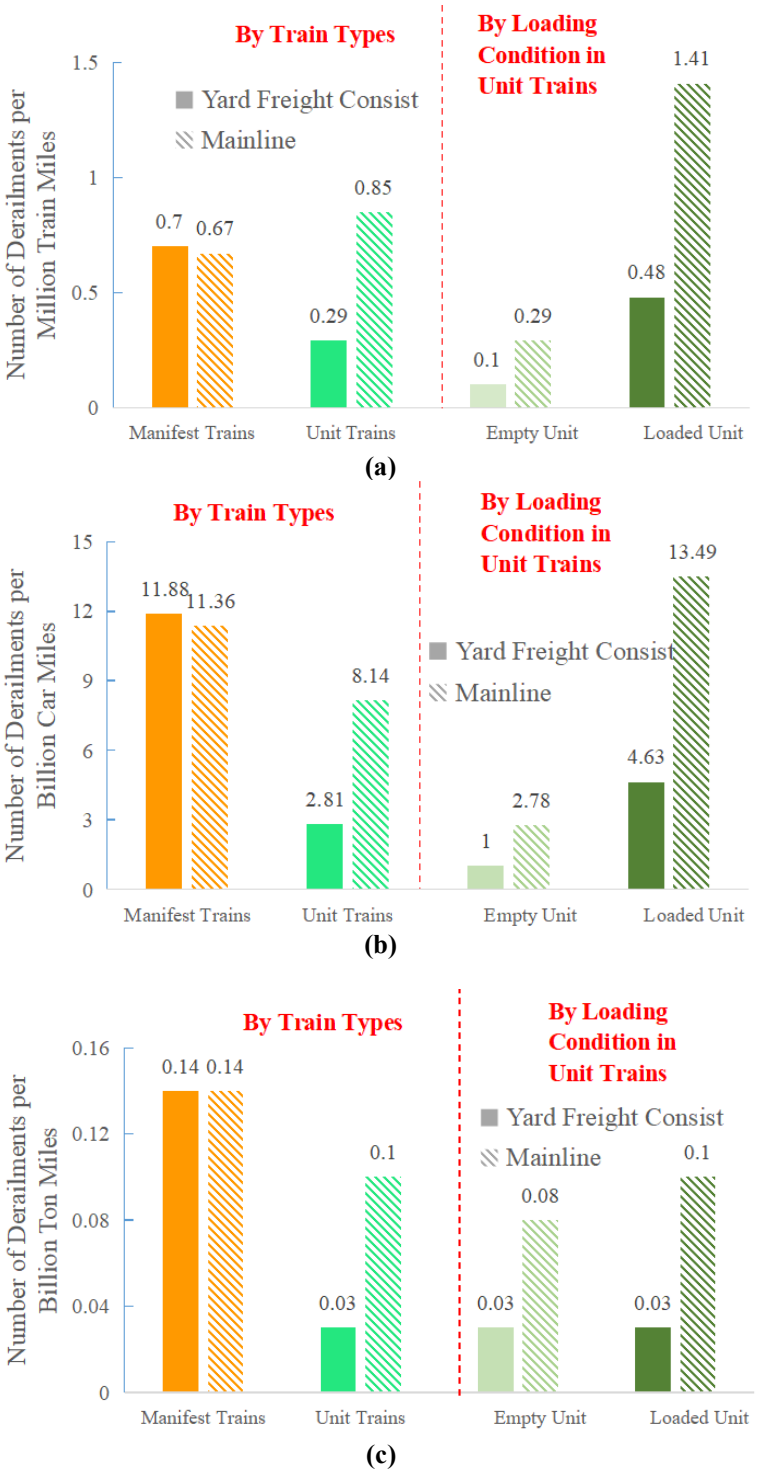

Figure 102. Comparison of mainline and generic mileage-based A/D derailment rates (1996-2018) for different train types and normalized by (a) mainline train-miles, (b) mainline car-miles, and (c) mainline ton-miles

Since they are calculated based on mainline mileage, the generic yard and terminal arrival and departure (i.e., freight consist) derailment rates can be directly compared to the mainline train derailment rates calculated in previous sections (Figure 102a-c). The mainline and classification yard A/D derailment rates for manifest trains are similar. A manifest train traveling one unit of mainline distance has a similar probability of derailing on the mainline or during its classification yard arrival or departure events. However, a unit train traveling one unit of mainline distance is three times more likely to derail on the mainline than during a terminal A/D event. This result is consistent with unit trains having relatively less involvement with terminal operations during shipments compared to manifest trains which visit multiple intermediate classification yards.

6.4.1.4 Application and Example Calculation

Table 42 presents multiple yard and terminal derailment rates normalized by different traffic metrics (i.e., train-mile basis versus car-mile basis); a key consideration is how to apply these different metrics. Independently calculating expected derailment likelihood solely based on train-miles or car-miles can produce confounding results when comparing two trains of disparate lengths (i.e., number of railcars). A long train with a lower derailment likelihood than a short train on a train-mile basis may have a higher derailment likelihood than the short train when compared on a car-mile basis. Thus, an approach that accounts for both factors is needed.

As described in Section 3, in terms of derailment probability, different accident causes are more closely associated with different traffic metrics. Thus, when calculating derailment likelihood per shipment, instead of performing a simple calculation using a single traffic metric, the relative influence of multiple causes and their associated traffic metrics can be considered. The overall derailment rate should be a weighted combination of the train-mile and car-mile rates, with the weights set to reflect the proportion of yard and terminal derailments attributable to causes associated with each traffic metric.

Analysis of all yard and terminal derailments (both A/D and yard switching) from 1996 to 2018 yields the proportion of derailments attributable to train-mile or car-mile causes for both unit trains and manifest trains (Table 43). While approximately three-quarters of manifest train yard derailments are attributed to train-mile causes, two-thirds of unit train terminal derailments are attributed to train-mile causes.

Table 43. Proportion of yard and terminal derailments attributed to train-mile and car-mile causes by train type (1996-2018)

Train Type	Train-Mile Causes	Car-Mile Causes
Manifest Train	78.1%	21.9%
Unit Train	62.8%	37.2%

To illustrate the application of these generic mileage-based yard and terminal derailment rates, consider the previously introduced example shipment of 100 railcars using manifest trains to travel 2,000 miles between origin and destination classification yards, and a comparable 100-railcar unit train shipment that travels 2,000 miles directly from origin to destination (Figure 6). Assume that the number of intermediate yards is unknown for the manifest train shipment, requiring the mileage-based yard and terminal derailment rates to be applied. Considering the

number of train-miles and car-miles accumulated from origin to destination by each train type, the generic mileage-based yard and terminal derailment rates by train type (Table 42), and the proportion of derailments attributed to train-mile and car-mile causes by train type, the expected number of derailments during each shipment can be estimated (Table 44).

Table 44. Train type yard and terminal derailment likelihood comparison for example shipment using generic mileage-based rates

Train Type / Traffic Metric	Expected Yard/Terminal Derailments per 100-car Shipment			
	Calculation Process	Result	Weight	Weighted Result
Manifest Train Train-mile Basis	(Manifest A/D Derailments per Mainline Train-mile) × (2,000 Train-miles) + (Yard Switching Derailments per Mainline Train-mile) × (2,000 Train-miles)	4.55E-03	0.781	3.55E-03
Manifest Train Car-mile Basis	(Manifest A/D Derailments per Mainline Car-mile) × (2,000 × 100) Car-miles + (Yard Switching Derailments per Mainline Car-mile) × (2,000 × 100) Car-miles	7.75E-03	0.219	1.70E-03
Manifest Train Overall Total				*5.24E-03*
Unit Train Train-mile Basis	(Unit A/D Derailments per Mainline Train-mile) × (2,000 Train-miles)	5.78E-04	0.628	3.64E-04
Unit Train Car-mile Basis	(Unit A/D Derailments per Mainline Car-mile) × (2,000 × 100) Car-miles	5.62E-04	0.372	2.09E-04
Unit Train Overall Total				*5.73E-04*

For the example shipment considering a unit train and manifest train of the same train length traveling the same mainline distance, using the generic mileage-based approach per train shipment, the likelihood of the manifest train derailing in a classification yard is almost 10 times that of the unit train derailing in terminals. For a manifest train shipment, the probability of experiencing a derailment during the yard switching process is more than double that while arriving at or departing from the yard. This result shows the need to study the derailment risks associated with the yard switching process in classification yards for manifest trains. To further quantify this yard switching derailment likelihood, the team developed an alternative approach that quantifies the impact of the specific number and types of intermediate classification yards in a manifest train shipment. With this approach, a shipment connecting the same origin and destination with the same mainline travel distance, but passing through different patterns of intermediate classification yards, will display distinct derailment probabilities and severities, providing a better estimation of the risks associated with manifest train shipments.

6.4.2 Detailed Route-based Rate Calculation

The detailed route-based approach is used when the exact number and type of intermediate classification yards involved in a manifest train shipment is known, or for a unit train shipment (since, by definition, a unit train movement only involves one departure from an origin terminal and one arrival at a destination terminal). This approach requires specific rates of occurrence for yard A/D and yard switching derailments normalized by actual yard traffic metrics such as the number of train arrivals and departures or number of railcars processed. The team developed different derailment rates for hump and flat switching classification yards, and for unit train terminals. Because it is more specific to actual yard operating metrics and the exact yards involved in the shipment, the detailed route-based approach should produce more accurate estimates of derailment likelihood than the generic mileage-based approach when specific yard details are known. Differences between this detailed approach and the generic mileage-based approach are magnified for manifest train shipments with especially longer or shorter mainline travel distances between classification yards compared to the average manifest train.

6.4.2.1 A/D Derailments

For arrival and departure (i.e., freight consist) derailments, the number of arrival and departure derailments is normalized by the number of train and railcar A/D events (i.e., the total number of trains arriving or departing yards and terminals, and the total count of railcars on those trains). By definition, unit train shipments usually only consist of one departure event at the origin terminal and one arrival event at the destination terminal. For shipments moving on manifest trains, in addition to the origin departure and destination arrival events, each additional intermediate classification yard visited adds one train arrival and one train departure event and a corresponding number of railcar arrivals and departures. Using this approach, the number of yards and terminals involved in a particular shipment route can be used with the calculated rates to estimate and compare the A/D derailment likelihood for manifest and unit trains.

Although the total number of A/D events is not directly reported in the STB R-1 traffic data, since each train operated has one arrival and one departure event, the annual train A/D metric for manifest and unit trains (Figure 103) can be calculated by doubling the number of trains operated (as calculated using Equations (6-1)-(6-3) and STB R-1 traffic metrics for total train-miles, car-miles, and number of loaded railcars):

$$Number\ of\ train\ arrival\ and\ departure\ events = number\ of\ trains\ operated \times 2 \quad (6\text{-}14)$$

To account for cause groups that are classified as being related to train-miles or car-miles, two rates with different traffic metrics (train A/Ds and railcar A/Ds) are calculated for the yard and terminal A/D derailments. Given the number of A/D derailments and train or railcar A/D events for a particular train type, the corresponding derailment rates were calculated:

$$Derailment\ rate\ per\ million\ train\ arrival/departure\ event = \frac{number\ of\ A/D\ train\ derailments}{million\ train\ A/D\ events} \quad (6\text{-}15)$$

$$Derailment\ rate\ per\ million\ car\ arrival/departure\ event = \frac{number\ of\ A/D\ train\ derailments}{million\ train\ A/D\ events \times average\ train\ length} \quad (6\text{-}16)$$

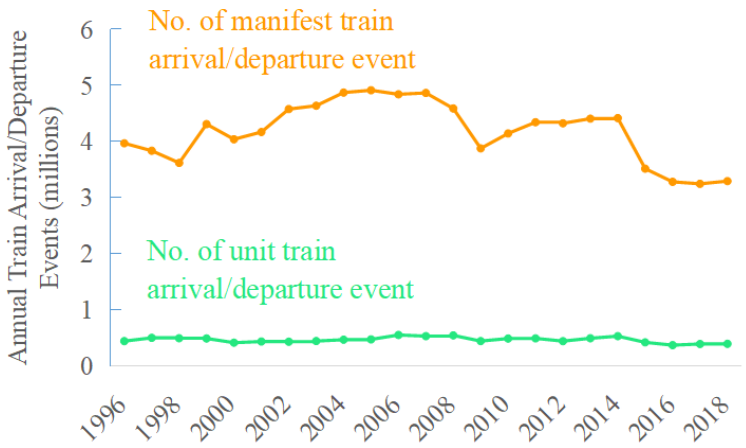

Figure 103. Annual number of Class I unit and manifest train yard and terminal A/D events (1996-2018)

In the above equations, the average train length in railcars for a given train type was calculated using Equation (6-1) as described in Section 6.2.2. In addition to the overall rates for unit trains at terminals and manifest trains at arriving and departing yards, more detailed rates by loading condition (i.e., loaded and empty unit train) and yard type (i.e., hump yard and flat yard) can be computed by changing the scope of the numerator and denominator accordingly.

6.4.2.2 Yard Switching Derailments

In past studies, the yard switching (i.e., yard consist) derailment rate for manifest trains in classification yards has been expressed in terms of yard-switching hours or yard-switching miles, since these traffic metrics are available in the STB R-1 data. However, these rates are difficult to implement in a comparative risk analysis of hazmat shipments via different manifest and/or unit train plans. Since there is no direct calculation to quantify the incremental yard switching miles or hours corresponding to the addition of a given number of hazmat carloads to the existing traffic through a given classification yard, the incremental risk calculation is not straightforward.

This approach normalizes the number of yard switching accidents by the total number of railcars switched (i.e., the total counts of railcars being processed in classification yards). Although not reported directly in the STB R-1 data, the number of railcars switched in classification yards can be estimated as the sum of empty cars and loaded cars transported in non-unit trains, assuming that each railcar transported needs to be classified once before departing on each leg of its trip. This calculation is possible because the STB reports the number of railcars transported and does not report origin-destination carload shipments. For example, a single carload shipment that moves in three different manifest trains from origin to destination is reported as three railcars transported. Hence, the yard switching derailment rate is calculated as follows, given that the number of loaded and empty railcars operated was previously calculated using Equation (6-2):

$$Derailment\ rate\ per\ million\ car\ switching\ event = \frac{number\ of\ \ yard\ switching\ derailments}{million\ empty\ and\ loaded\ railcars\ operated} \quad (6\text{-}17)$$

Calculating yard switching derailment rates specific to hump yards and flat yards requires further assumptions since public data separating manifest train traffic by yard type is not available. In the absence of detailed yard-specific railcar processing data, an alternative approach was

proposed based on discussions with several industry experts on yard operations and the relative breakdown of classification operations in flat and hump yards over time. The portion of total railcars processed in hump yards was estimated by considering the number of active hump yards in a given year (Figure 98a) and average hump and flat yard processing rates (Zhang et al., 2021). Over the study period, this corresponds to 44 percent of railcars switched in hump yards while the remaining 56 percent of railcar switching occurs in flat yards.

6.4.2.3 Calculated Detailed Route-based Yard and Terminal Derailment Rates

Using the above equations, detailed route-based yard and terminal derailment rates were calculated for different train types and traffic metrics for the years 1996-2018 (Table 45). Using million train arrivals/departures as the traffic metric, unit trains showed slightly larger derailment likelihoods compared to manifest trains. However, when normalized by train length using million car A/D events as the traffic metric, unit trains showed a lower rate due to their longer train lengths. Within the category of manifest trains, trains or railcars arriving or departing at flat yards have three times the derailment likelihood associated with hump yards. For unit trains, empty unit trains only experience around 20 percent of the derailment rate of loaded unit trains during terminal arrival and departure. The difference in the yard switching accident (i.e., yard consist) rates between flat yards and hump yards is minor, particularly given the assumptions required to estimate traffic in each yard type. Given that each railcar processed corresponds to two railcar A/D, a railcar processed in a hump yard is just over five times more likely to derail during yard switching than while arriving at or departing from the hump yard.

Table 45. Detailed route-based yard and terminal derailment rates (1996-2018) for various train and yard types

	Arrival/Departure (Freight Consist)		Yard Switching (Yard Consist)
Train/Yard Type	A/D Derailments per Million Train Arrival/Departures	A/D Derailments per Million Car Arrival/Departures	YS Derailments per Million Cars Processed in Classification Yards
Manifest Train	61.52	1.04	6.43
Flat Yard	118.92	2.02	6.38
Hump Yard	36.53	0.62	6.49
Unit Train	76.95	0.74	N/A
Empty Unit	27.59	0.27	N/A
Loaded Unit	126.31	1.22	N/A

Since the rates in Table 45 were calculated using all incidents and traffic over the 23-year duration of the study period, it is also important to consider derailment rate variation over time (Figure 104). A decreasing trend was observed for manifest train rates per train and railcar A/D events between 2000 and 2014. A relatively stable derailment rate emerged over the last three years of the study period and is consistent with the overall average rates. Similarly, for manifest train yard switching derailments, a large drop in derailment rate was observed after 2006. The recent rates between 2008 and 2018 are generally lower than the 23-year average. However, it is cause for industry attention that both manifest train yard A/D and yard switching derailment rates have shown increasing trends since 2012.

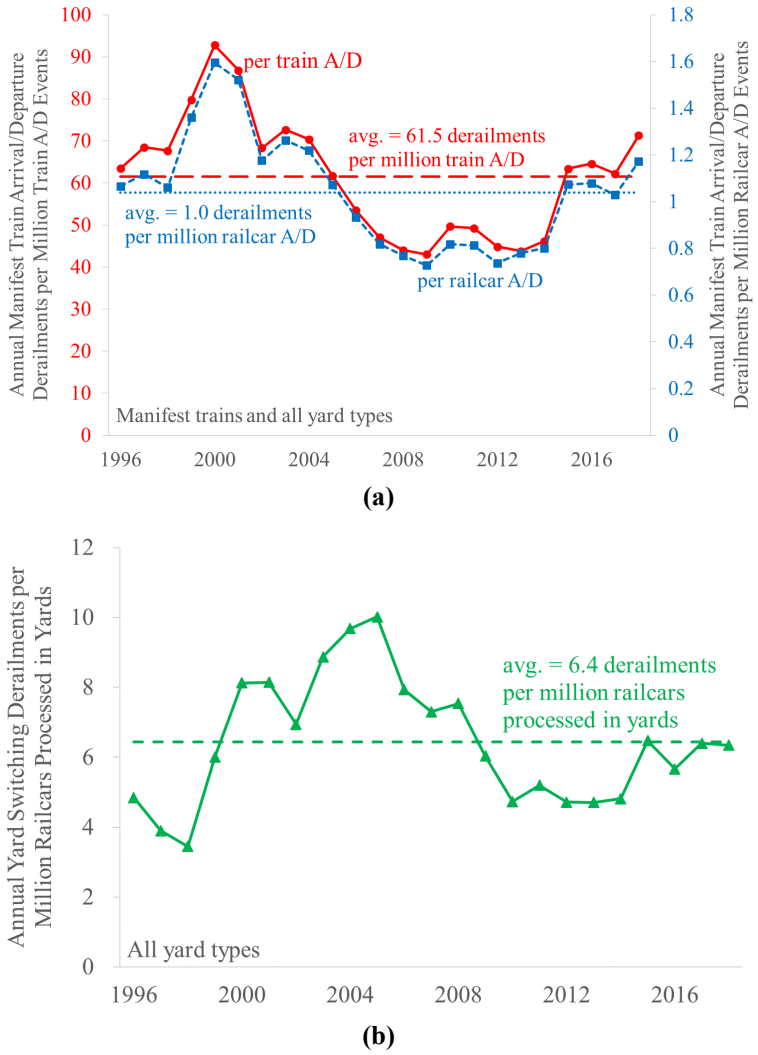

Figure 104. Annual Class I manifest train yard derailment rate and 23-year average for (a) yard arrival and departure accidents and (b) yard switching accidents (1996-2018)

6.4.2.4 Application and Example Calculation

Since Table 45 presents yard and terminal A/D derailment rates normalized by different traffic metrics (i.e., train A/D events or car A/D events), a key consideration is how to apply these different metrics to manifest and unit train shipments. As described in Section 3, in terms of derailment probability, different accident causes are more closely associated with different traffic metrics (e.g., train-miles or car-miles). To analyze yard and terminal A/D derailments, it is assumed that accident cause groups associated with train-miles will also be a function of the number of train A/D, and that those associated with car-miles will also be a function of the number of railcar A/Ds.

Given this assumption, the overall yard and terminal A/D derailment rates for each train type is a weighted combination of the train-A/D and car-A/D rates. The weights are set to reflect the proportion of yard and terminal derailments attributable to causes associated with each traffic metric, as previously presented in Table 43.

Revisiting the earlier example, consider a hypothetical 2,000-mile shipment of 100 railcars using manifest trains, and a comparable 2,000-mile 100-railcar unit train shipment (Figure 7). Unlike the previous example where the details of the manifest train route were not known, now assume that the manifest train shipment is composed of two separate legs, with the shipment connecting between trains at one intermediate classification yard. In this scenario, the manifest train shipment involves a total of four yard A/D events, compared with two terminal A/D events for the unit train. In addition, a total of 200 railcar switching events are required for the manifest train shipment (100 railcars switched at the origin yard and 100 railcars switched at the intermediate yard). Considering this exact pattern of A/D and yard switching events, but assuming the specific yard types (i.e., hump versus flat) are unknown, the detailed route-based yard and terminal derailment rates by train type (Table 45) are used to estimate the expected number of derailments (Table 46).

Table 46. Train type yard and terminal derailment likelihood comparison for example shipment using detailed route-based rates

Train Type / Traffic Metric	Expected Yard/Terminal Derailments per 100-car Shipment			
	Calculation Process	Result	Weight	Weighted Result
Manifest Train Train-A/D Basis	(Manifest A/D Derailments per Manifest Train A/D Event) × (4 A/D Events) + (Yard Switching Derailments per Railcar Processed) × (200 Railcars Switched)	1.53E-03	0.781	1.20E-03
Manifest Train Car-A/D Basis	(Manifest A/D Derailments per Manifest Car A/D Event) × (4 A/D Events × 100 Railcars) + (Yard Switching Derailments per Railcar Processed) × (200 Railcars Switched)	1.70E-03	0.219	3.73E-04
Manifest Train Overall Total				*1.57E-03*
Unit Train Train-A/D Basis	(Unit A/D Derailments per Unit Train A/D Event) × (2 A/D Events)	1.54E-04	0.628	9.66E-04
Unit Train Car-A/D Basis	(Unit A/D Derailments per Unit Train A/D Event) × (2 A/D Events × 100 Railcars)	1.48E-04	0.372	5.51E-05
Unit Train Overall Total				*1.52E-04*

Compared to the generic mileage-based results (Table 44), the derailment likelihood calculated using the detailed approach (Table 46) is far lower. This example illustrates how the detailed approach better captures the yard and terminal derailment likelihood for a relatively long mainline trip with only one intermediate yard used by the manifest train shipment. Since many manifest and unit train trips are far shorter than 2,000 miles, the generic mileage-based approach using mainline train-miles and car-miles overestimates the amount of yard and terminal operations involved in this example trip. If the example shipment were shortened from 2,000 to 200 mainline miles but still involved one intermediate classification yard for the manifest train, the mileage-based values in Table 44 would decrease by a factor of ten, while the detailed route-based values in Table 46 would remain the same to reflect the constant pattern of yards and terminals encountered by each train. Because of this tendency, the detailed route-based approach should be used whenever information on the number of intermediate yards and terminals

involved in the manifest train shipment is available; the generic mileage-based approach should only be used as an initial approximation when no specific manifest train yard and terminal routing information is available.

6.5 Analysis of Yard and Terminal Derailment Severity

To further understand the risk of transporting hazmat in railroad terminals and yards, the team developed statistical models to estimate yard and terminal derailment severity (i.e., number of railcars derailed) based on various associated affecting factors. Developed from the same historical accident data used when calculating the yard and terminal derailment rates, the statistical models consider factors that influence train derailment severity such as train speed, position of the first railcar derailed, and average railcar weight in tons. The typical operating characteristics of railroad yards and terminals, especially during yard switching procedures, involve lower speeds, different braking actions, and movements of smaller groups (i.e., cuts) of railcars compared to mainline manifest and unit trains. Thus, the severity model and associated affecting factors previously developed and used for mainline derailment severity were re-evaluated in the context of yard and terminal arrival and departure events. Similarly, a new model was developed for manifest train yard switching derailments. In summary, the team used the historical FRA REA data from 1996-2018 to:

1) Estimate the position of the first car derailed given a yard or terminal A/D derailment incident
2) Identify factors that influence derailment severity given a yard and terminal A/D derailment incident with the first car derailed at a certain position
3) Build a statistical model to estimate yard and terminal A/D derailment severity given a set of influencing factors
4) Develop a statistical model fitting the distribution of the number of cars derailed given a manifest train yard switching incident

The remainder of this section presents the underlying statistical analysis of yard and terminal derailment severity and applies the developed statistical models to example shipments. Section 6.5.1 describes the source derailment data and data screening process to remove outliers before presenting summary statistics for the severity of different types of yard and terminal derailments. Section 6.5.2 presents a statistical model (i.e., beta distribution model) to estimate the position of the first derailed railcar for yard and terminal arrival and departure derailments. Section 6.5.3 describes a statistical model, namely a TG model, to identify factors that influence yard arrival and departure derailment severity and to estimate the distribution of the number of railcars derailed per yard and terminal A/D incident. Finally, Section 6.5.4 describes a non-position-based statistical model to predict the distribution of derailment severity for manifest train yard switching derailments.

6.5.1 Data Screening and Trends in Yard and Terminal Derailment Severity

The FRA REA derailment dataset also was used for the derailment severity analysis. In the context of this research, the number of railcars derailed is the primary derailment severity metric. Subsequent sections of this report will present techniques to transform this metric into a quantity of hazmat release and resulting consequence.

6.5.1.1 Data Screening

Before developing statistical models to estimate train derailment severity, the team conducted data screening to exclude outliers and data with incorrect attributes which might degrade the performance of resulting statistical models. The following necessary screening conditions were applied, with any incidents failing to meet any single condition excluded from further analysis:

- **Speed ≥ 1:** Derailment incidents with reported speeds of zero miles per hour were excluded from further analysis since these incidents are assumed to have different derailment severities and release mechanisms than a train in motion. Thus, the team set the lowest derailment speed as "1 mile per hour" for further analysis.
- **Number of Derailed Railcars ≥ 1**: In the original dataset, the entries for some derailment incidents list the number of derailed railcars and locomotives as zero. Since these trains did not actually derail and are unlikely to lead to the same damage and release mechanisms modeled in later steps, the accidents with zero derailed cars were excluded from subsequent analysis.
- **Number of Derailed Railcars ≤ 50:** The original dataset includes entries for yard and terminal derailments where more than 50 railcars derail. Many of these incidents involved extreme weather events at yards and terminals, representing outliers that could skew the statistical analysis of severity for more typical derailment conditions. Therefore, records with more than 50 derailed cars were excluded from further analysis.
- **Number of Cars Behind the POD ≥ Number of Derailed Cars**: The statistical models of derailment release described in other sections assume that the derailment propagates backward from the POD. Derailments where the number of derailed railcars exceeds the number of railcars behind the POD violate this assumption and suggest that different derailment mechanisms are at work. To be consistent with the mainline analysis and the assumptions underlying these later models, the team only considered derailment records where the number of cars behind the POD was greater than or equal to the number of derailed cars.
- **Tons Per Car Outside the Range of 10 to 300 Tons:** Values of tons per railcar outside this range are unlikely and suggest errors in the derailment data, and these derailment records were excluded from further analysis.

6.5.1.2 Derailment Severity Trends and Statistics

The team applied the screening conditions to the FRA REA yard derailment data and found 6,336 A/D derailments and 11,203 yard switching derailments for further analysis. To determine if there is a temporal trend in derailment severity over the study period, the annual average train A/D derailment (i.e., freight consist) and yard switching derailment (i.e., yard switching consist) severity in cars derailed per incident were calculated (Figure 105).

There is no obvious increasing or decreasing trend of average derailment severity from 1996 to 2018 for either A/D or yard switching derailments. To statistically support this observation, the team used the Mann-Kendall Trend Test[2] to verify the significance of any increasing or

[2] The Mann-Kendall Trend Test (Kendall, 1975) is a non-parametric test for analyzing time series data with consistently increasing or decreasing trends (i.e., monotonic trends).

decreasing trend in derailment severity. The team found that train derailment severity does not have a significant increasing or decreasing trend over time, because the p-value (0.059 and 0.177) is greater than the 0.05 confidence level and the null hypothesis is rejected (the data has a significant increasing or decreasing trend). Therefore, the team concluded that the annual average yard and terminal derailment severity for the 23 years studied does not change over time, and an integrated analysis of the derailment severity for all years from 1996 to 2018 can be conducted instead of a separate derailment severity analysis for each individual year.

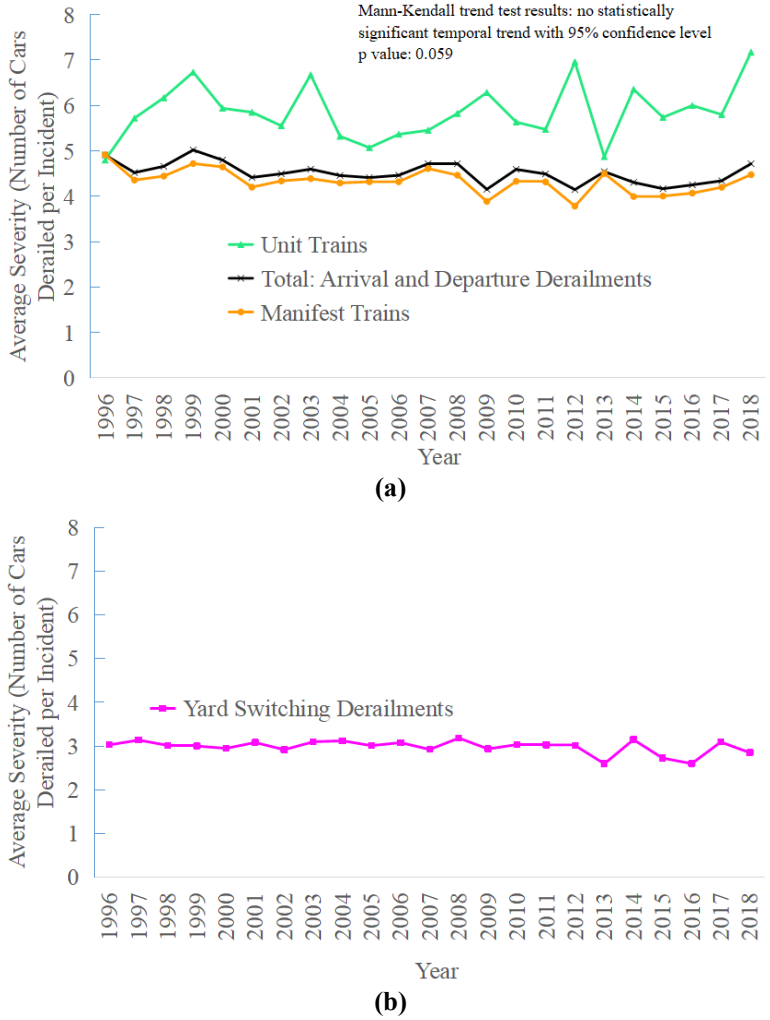

Figure 105. Annual average severity of yard and terminal derailments (1996-2018) for (a) yard A/D accidents and (b) yard switching accidents

Aggregating the screened yard derailment data from 1996 to 2018, descriptive statistics for each train type and yard and terminal process (Table 47) quantify the differences in observed severity. The average unit train terminal A/D derailment tends to derail the most railcars, followed by the manifest train A/D incident, and finally the manifest train yard switching incident.

Cumulative distributions of the number of cars derailed per incident further illustrate the nature of the differences between the severities of unit train terminal A/D derailments, manifest train yard A/D derailments, and yard switching derailments (Figure 106). These distributions begin at one car derailed since incidents with zero cars derailed were removed during the data screening

process. Yard switching derailments feature approximately twice as many one and two-car derailments as arrival and departure derailments.

Table 47. Derailment severity in cars derailed per incident by yard process (1996-2018)

Derailment Type		Number of Derailments	Railcars Derailed per Incident			
			Mean	Median	Variance	Standard Deviation
Arrival and Departure Derailments (Freight Consist)	All Train Types	6,336	4.7	4	10.6	3.3
	Unit Trains	809	5.9	5	13.5	3.7
	Manifest Trains	5,527	4.5	4	9.9	3.2
Yard Switching Derailments (Yard Switching Consist)	Manifest Trains	11,203	3.6	3	8.9	3.0

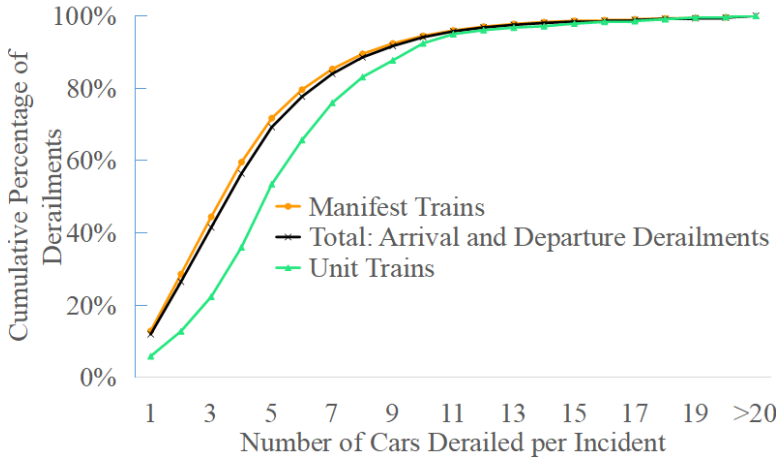

(a)

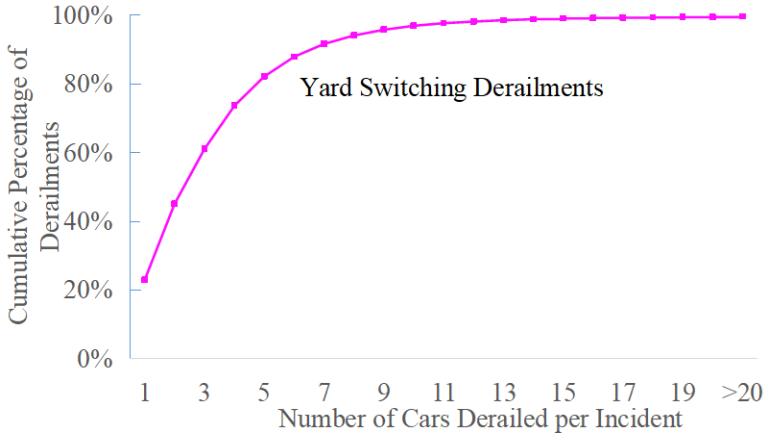

(b)

Figure 106. Cumulative distribution of number of cars derailed per incident for yard and terminal derailments (1996-2018) for (a) yard A/D accidents and (b) yard switching accidents

6.5.2 POD for A/D Derailments

Based on previous studies of mainline derailments, it was expected that the number of railcars derailed for yard and terminal A/D events also would be dependent on the position of the POD. To account for different train lengths, the NPOD was calculated by dividing the POD by the train length for each incident. Plotting the probability distribution of NPOD for manifest train and unit train A/D derailments suggests that the manifest train NPOD distribution is more heavily skewed toward the front of the train relative to the unit train NPOD distribution (Figure 107).

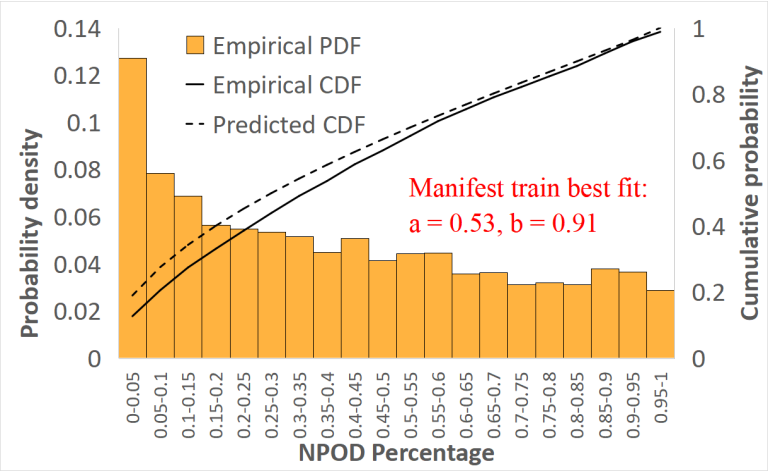

(a)

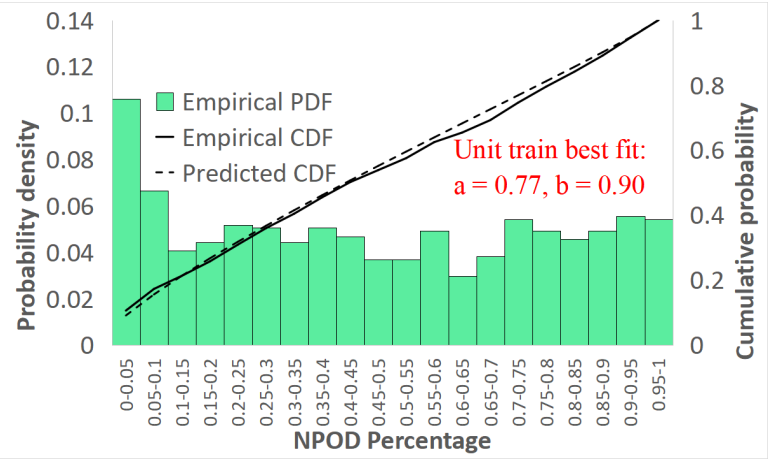

(b)

Figure 107. Normalized point of derailment distribution and beta distribution fitting for (a) manifest train and (b) unit train arrival and departure derailments (1996-2018)

According to prior mainline derailment research, the NPOD follows a beta distribution. Using this distribution, given a train length L, the probability that the POD is at the Kth position, $Pod(K)$, can be estimated using the following equation:

$$Pod(K) = F(\frac{K}{L}) - F(\frac{K-1}{L}) \quad (6\text{-}18)$$

where:

Pod(K) = POD probability at the K^{th} position of a train

F(X) = cumulative density distribution of the fitted distribution

L = train length in railcars

The team used the Python 3.7.3 scipy.stats.beta.fit package to determine the best fit parameters for manifest train and unit train arrival and departure derailments; the resulting beta distribution parameter values are shown in Figure 97. The R scores for the empirical and predicted probability densities with 1 percent NPOD bin for a manifest train and unit train are 0.997 and 0.986, respectively, indicating a good correlation between the NPOD data and the beta distribution. The fitted model can be used to calculate the POD distribution for both manifest and unit train A/D events in subsequent steps of the analysis.

6.5.3 Predicting Number of Cars Derailed for A/D Derailments

Section 6.5.1 presented an empirical distribution of derailment severity (i.e., railcars derailed per incident) across all yard and terminal A/D events that passed the screening process. These events represent A/D derailments across a wide range of operating conditions and train consists that may influence the severity of an individual A/D derailment. As demonstrated by Bagheri (2010), the number of cars derailed for a mainline derailment follows a TG distribution, and the TG model can truncate the number of derailed cars within the range from one car up to the residual train length behind the POD.

Applying this model to a train derailment with train length *L* and POD *j* (and thus residual train length $L_r = L - j + 1$), the probability of derailing *k* cars is calculated by:

$$P(X = x \mid \text{POD at } j) = \begin{cases} \dfrac{p(1-p)^{x-1}}{1-(1-p)^{Lr}} & \text{if } x = 1, 2, \ldots, Lr \\ 0 & \text{otherwise} \end{cases} \quad (6\text{-}19)$$

where:

Lr = residual train length

X = number of cars derailed

P = probability of success at each trial, which is a constant probability.

The probability of *x* cars derailing before the first non-derailing car is a geometric distribution with the probability of a car derailing (given that a derailment has occurred) equal to $(1 - p)$. This probability *p* is assumed to be related to the factors/covariates through the logit link function:

$$p = \frac{e^{Z}}{1 + e^{Z}} \quad (6\text{-}20)$$

where:

Z is a linear function of influencing factors, including (for the mainline) derailment speed, residual train length, gross tonnage per car, and train type:

$$Z = \beta_0 + \beta_1 X_1 + \beta_2 X_2 + \beta_3 X_3 \ldots \quad (6\text{-}21)$$

where:

x1, x2, x3... are factors affecting car derailment probability

$\beta_0, \beta_1, \beta_2, \beta_3$... are parameters associated with each affecting factor

Based on the literature review of mainline models, factors to consider as possibly influencing yard and terminal A/D derailment severity include train derailment speed, gross tons per railcar, train type (e.g., empty unit train, loaded unit train, and manifest train), residual train length (i.e., number of railcars behind the POD), and overall train length. The following section summarizes a single-variable screening analysis of several of these possible factors.

6.5.3.1 Analysis of Potential Factors

Plotting the average speed of yard and terminal A/D derailments with a given severity (i.e., number of cars derailed) does not indicate a strong trend between the number of railcars derailed and derailment speed for various train types (Figure 108). A possible explanation is that yard and terminal arrivals and departures typically take place at restricted speeds under 20 miles per hour. Since all the data clusters within the small speed range, it is difficult for train speed to be significantly higher for one subset of derailments than another.

Plotting the average gross tons per car of yard and terminal A/D derailments with a given severity does not indicate a strong trend of increasing number of railcars derailed with increasing tons per car for various train types (Figure 109). The figure does indicate that, as expected, the average tons per car for manifest trains (consisting of a mixture of empty and loaded railcars) falls between the extreme tons per car exhibited by loaded and empty unit trains. Also, as expected, average loaded unit train tons per car clustered around the typical maximum loaded gross railcar loads of 131.5 to 143 tons per railcar, while average empty unit train values clustered around the typical railcar tare weight range of 20 to 30 tons per railcar. Overall, for a given train type, yard and terminal A/D derailments with many cars derailed did not exhibit a substantially higher average gross tons per car than derailments with fewer cars derailed. Thus, any effect of tons per car on derailment severity is likely best captured by specifying the train type instead of the actual value of tons per car.

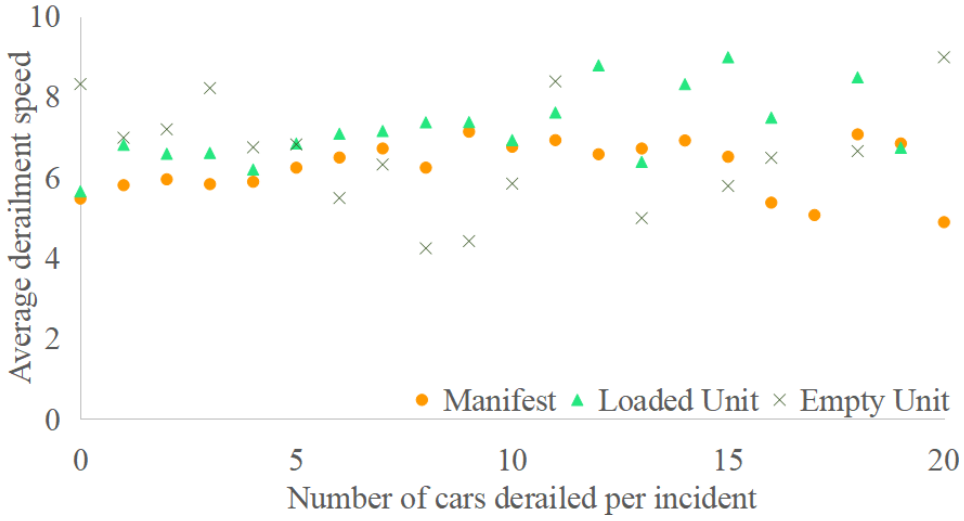

Figure 108. Average derailment speed for manifest and unit train A/D derailments with a given severity (1996-2018)

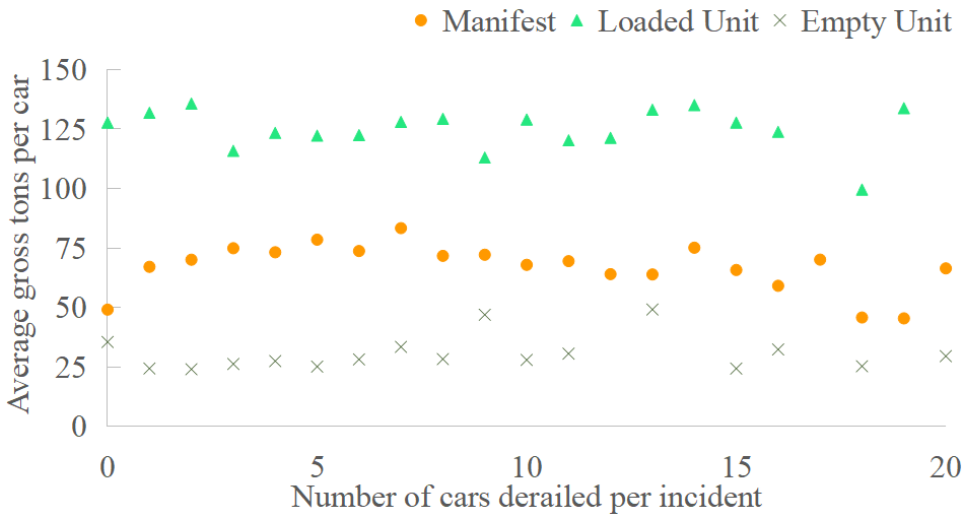

Figure 109. Average gross tons per railcar for manifest and unit train A/D derailments with a given severity (1996-2018)

Plotting the average residual train length of yard and terminal A/D derailments with a given severity (number of cars derailed) did not indicate a slight trend of increasing number of railcars derailed with increasing residual train length for manifest trains and loaded unit trains (Figure 110). The larger the residual train length, the more severe the derailment. However, this effect was not observed for empty unit trains.

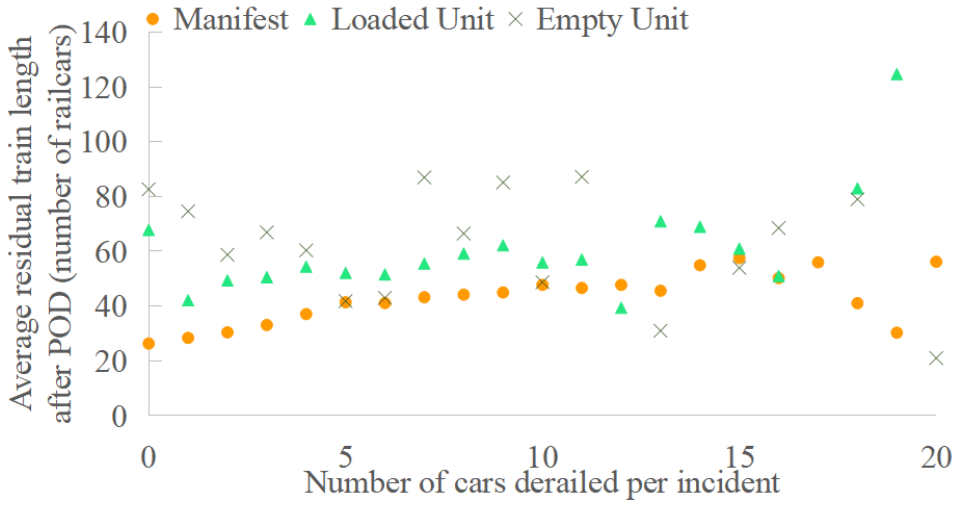

Figure 110. Average residual train length for manifest and unit train A/D derailments with a given severity (1996-2018)

To better evaluate using residual train length as an influencing factor in the TG model, the average residual train length and average total train length were compared for manifest train A/D derailments with a given severity (Figure 111). For manifest trains, train length appears to have a larger influence on derailment severity than residual train length, as indicated by the steeper slope of the linear trend line. Based on this result, total train length was considered for inclusion

in the TG model developed for determining manifest train and loaded unit train yard and terminal A/D derailment severity.

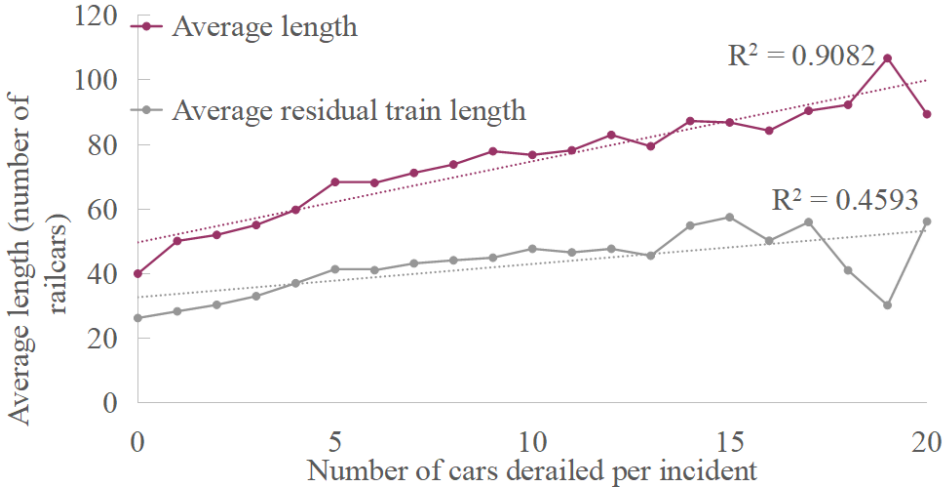

Figure 111. Comparison of correlation between derailment severity and average residual train length and average train length for manifest train yard A/D derailments (1996-2018)

6.5.3.2 Fitted TG Model

Considering the previous analysis, a different TG model to predict the number of railcars derailed in each incident was fit to the 1996-2018 yard and terminal A/D derailment data for loaded unit trains, empty unit trains, and manifest trains. Multiple potential explanatory variables (Table 48) were considered as inputs to the model fitting process using Python 3.7.3 and maximum likelihood estimation. Using a unique combination of these explanatory variables, the ability of each candidate model to predict the number of railcars derailed in each incident was evaluated and compared using the mean square error and mean absolute error.

The model fitting process was conducted twice for each of the three train types, yielding six models in total (Table 49). For each train type, one model was fit to the original dataset and a second model was fit to the data with outliers removed. In this analysis, outliers were defined as individual derailments with severity greater than 20 railcars derailed or a derailment speed greater than 20 miles per hour, as these were judged not to be representative of typical yard and terminal A/D derailment conditions. In general, removing the outliers improved the overall fit, reducing the mean square and absolute error of the models for each train type.

Table 48. Candidate variables for A/D severity estimation models

Variables		Data type
Model input	Total number of cars in the consist (train length)	Integer
	Number of cars behind POD (point of derailment)	Integer
	Train types considered in this section, including loaded unit trains, empty unit trains, and manifest trains	Categorical
Model output	Number of cars derailed in one derailment	Integer

Table 49. A/D severity estimation models fit to 1996-2018 data

Yard Arrival and Departure Derailments (Freight Consist)				
Train Type	Data	Model results	Mean Square Error (MSE)	Mean Absolute Error (MAE)
Loaded Unit Trains	With Outliers	Z = –1.561 – 0.00175×(train length)	8.097	2.139
	Outliers Removed	Z = –1.574– 0.00160×(train length)	7.932	2.121
Empty Unit Trains	With Outliers	Z = –1.698	34.861	3.968
	Outliers Removed	Z = –1.575	17.697	3.329
Manifest Trains	With Outliers	Z = -1.602 – 0.004973× (train length)	14.179	2.511
	Outliers Removed	Z = –1.595 – 0.002932× (train length)	9.788	2.348

The fitted models suggest that yard and terminal A/D severity is primarily a function of overall train length for loaded unit trains and manifest trains. As train length increases, loaded unit trains and manifest trains tend to derail an increasing number of railcars per yard and terminal A/D derailment. Empty unit trains tend to derail a consistent number of railcars regardless of train length. A possible explanation for the non-sensitivity of empty unit trains to train length is that the relatively light weight of empty railcars (compared to loaded railcars) reduces the amount of additional kinetic energy imparted to the derailment per extra railcar of train length. Since each empty railcar only adds a small incremental amount of energy to the derailment, longer empty trains are less likely to derail additional railcars.

6.5.3.3 Application and Example Calculation of Number of Hazmat Railcars Derailed

Section 6.5.2 described a beta distribution for calculating the probability that the POD is at the k^{th} position of the train ($POD_i(k)$) during an A/D derailment at yard/terminal i. The previous paragraphs described fitting a TG model to describe the probability of derailing x vehicles given the POD is at the k^{th} position at yard/terminal i ($Pi\ (x \mid k)$). Combining these two models, the probability that the railcar in the j^{th} position of the train derails at yard/terminal i (defined as $PD_i(j)$) can be calculated for manifest train and unit train arrival and departure derailments as:

$$\mathrm{PD_i(j)} = \sum_{k=1}^{j}[\mathrm{POD_i(k)} \times \sum_{x=j-k+1}^{L_r} \mathrm{P_i(x|k)}] \quad (6\text{-}22)$$

where:

$\sum_{x=j-k+1}^{L_r} \mathrm{P_i(x|k)}$ is the sum of the probability that the derailment has spread to j^{th} position given the POD is at k^{th} position.

To illustrate this process of calculating the probability that a railcar at a given position in a unit train or manifest train derails due to an A/D derailment and the resulting distribution of number

of hazmat railcars derailed, reconsider the earlier hypothetical example of a train with seven railcars used in Section 3. As a first step, the beta distributions for manifest and unit trains developed in Section 6.5.2 can be applied to this seven-car scenario to calculate the probability that the POD is at a certain position in the train, given that a yard and terminal A/D derailment occurs (Table 50). The manifest train has a larger conditional probability of the POD being at the front of the train compared to the unit train. However, while the unit train POD conditional probability is relatively consistent along the remainder of its length, the manifest train POD conditional probability exhibits a more rapid decrease along the remaining train length.

Table 50. Example conditional probability of pod at k^{th} position of manifest train or unit train given a yard or terminal A/D derailment

k		1	2	3	4	5	6	7
POD(k)	Manifest	3.37E-01	1.52E-01	1.21E-01	1.05E-01	9.64E-02	9.19E-02	9.65E-02
	Unit	2.06E-01	1.48E-01	1.34E-01	1.27E-01	1.24E-01	1.24E-01	1.38E-01

Similarly, the TG model described earlier in this section can be applied to the seven-car manifest train and seven-car unit train to calculate the probability of derailing railcars given the POD (Table 51).

Table 51. Conditional probability of derailing *x* railcars given POD at *k*th position of example manifest or unit train given a yard or terminal A/D derailment

		$P_i(x\|k)$						
	k	$x = 1$	$x = 2$	$x = 3$	$x = 4$	$x = 5$	$x = 6$	$x = 7$
Manifest Train	1	2.31E-01	1.92E-01	1.60E-01	1.34E-01	1.12E-01	9.32E-02	7.77E-02
	2	2.50E-01	2.09E-01	1.74E-01	1.45E-01	1.21E-01	1.01E-01	
	3	2.78E-01	2.32E-01	1.94E-01	1.61E-01	1.35E-01		
	4	3.21E-01	2.68E-01	2.24E-01	1.87E-01			
	5	3.95E-01	3.30E-01	2.75E-01				
	6	5.45E-01	4.55E-01					
	7	1.00E+00						
Unit Train	1	2.33E-01	1.94E-01	1.61E-01	1.33E-01	1.11E-01	9.19E-02	7.63E-02
	2	2.53E-01	2.10E-01	1.74E-01	1.44E-01	1.20E-01	9.95E-02	
	3	2.81E-01	2.33E-01	1.93E-01	1.60E-01	1.33E-01		
	4	3.24E-01	2.69E-01	2.23E-01	1.85E-01			
	5	3.97E-01	3.30E-01	2.73E-01				
	6	5.46E-01	4.54E-01					
	7	1.00E+00						

Equation (6-22) is then applied to calculate the conditional probability that the railcar in the k^{th} position of the train derails at a yard/terminal given an A/D derailment (Table 52). For this

extremely short seven-car example train, the differences between a manifest train and unit train are minimal.

Table 52. Example conditional probability that railcar at k^{th} position of manifest train or unit train derails given a yard or terminal A/D derailment

Position *j*		1	2	3	4	5	6	7
PD(j)	Manifest	3.37E-01	4.11E-01	4.29E-01	4.15E-01	3.78E-01	3.21E-01	2.42E-01
	Unit	3.37E-01	4.11E-01	4.28E-01	4.13E-01	3.76E-01	3.18E-01	2.41E-01

While the conditional derailment probability of each individual railcar position in the train is of interest, a more useful result related to overall severity and eventual estimates of consequence is the overall distribution of number of cars derailed for a given incident. Multiplying the conditional probability distribution of railcars derailed given POD (Table 51) by the corresponding conditional probability of each POD (Table 50) yields the conditional probability of x number of cars derailing due to a derailment starting at position k given a yard A/D derailment occurs (Table 53). Note that combinations of x and k below the diagonal are infeasible since the number of cars derailed cannot exceed the residual train length.

Table 53. Example conditional probability of x railcars derailing due to derailment starting at k^{th} position of manifest or unit train given an A/D derailment

		$P_i(x\|k)$						
	k	$x = 1$	$x = 2$	$x = 3$	$x = 4$	$x = 5$	$x = 6$	$x = 7$
Manifest Train	1	7.77E-02	6.48E-02	5.41E-02	4.51E-02	3.76E-02	3.14E-02	2.62E-02
	2	3.80E-02	3.17E-02	2.65E-02	2.21E-02	1.84E-02	1.54E-02	
	3	3.36E-02	2.80E-02	2.34E-02	1.95E-02	1.63E-02		
	4*	3.38E-02	2.82E-02	2.36E-02	1.96E-02			
	5	3.81E-02	3.18E-02	2.65E-02				
	6	5.01E-02	4.18E-02					
	7*	9.65E-02						
Unit Train	1*	4.80E-02	3.99E-02	3.31E-02	2.75E-02	2.28E-02	1.89E-02	1.57E-02
	2*	3.73E-02	3.10E-02	2.57E-02	2.13E-02	1.77E-02	1.47E-02	
	3*	3.75E-02	3.11E-02	2.58E-02	2.14E-02	1.78E-02		
	4*	4.10E-02	3.40E-02	2.82E-02	2.34E-02			
	5*	4.91E-02	4.07E-02	3.38E-02				
	6*	6.80E-02	5.64E-02					
	7*	1.38E-01						

*Indicates position k is a hazmat railcar. Shading colors indicate total number of hazmat cars derailed for that combination of k and x: Gray = 7, Blue = 6, Pink = 5, Purple = 4, Red =3, Orange = 2, Yellow =1, Green = 0

If the specific position *j* of each hazmat railcar transported by the manifest train is known, the number of hazmat cars derailed can be determined, corresponding to each combination of POD position *k* and number of railcars derailed *x*. In this example, it is assumed that the manifest train consists of hazmat railcars at positions four and seven. If the POD is the third railcar and only one railcar is derailed, zero hazmat railcars will derail as positions four and seven will not be involved in the derailment. If the POD is still the third railcar but two, three, or four railcars derail, one hazmat railcar will derail in each of these cases as all these derailment conditions will involve the railcar in the fourth position. If the POD of three and five railcars derailed, both positions four and seven will be among the derailed cars and a total of two hazmat railcars will derail. Applying this approach across all combinations of *k* and *x* for the manifest train, the cells in Table 53 are shaded to reflect the number of hazmat cars derailed (orange = two hazmat cars derailed, yellow = one, and green = zero hazmat cars derailed).

By definition, the unit train has hazmat railcars at every position. Under this condition, since every railcar derailed is a hazmat car, the number of hazmat cars derailed reduces to the number of cars derailed (*x*) and each column of equal *x* value is shaded a solid color corresponding to that number of hazmat railcars derailed regardless of POD *k*.

Grouping and summing each probability in Table 53 by the number of hazmat cars derailed (i.e., sum all cells shaded the same color) yields the conditional probability of *y* hazmat cars derailed given the example seven-car consist and a manifest or unit train A/D derailment has occurred (Table 54). For the example seven-car manifest train with two hazmat railcars at positions four and seven, approximately 42 percent of yard A/D derailments do not result in any hazmat railcars derailed, approximately 50 percent result in one derailed hazmat railcar, and approximately 8 percent derail both hazmat railcars. Since all railcars on the seven-car unit train are, by definition, hazmat cars, approximately 42 percent of the terminal A/D derailments will result in one hazmat railcar derailed. Approximately 1.6 percent of the example unit train terminal A/D derailments will result in all seven hazmat railcars derailing.

Table 54. Conditional probability of *y* hazmat railcars derailing in example manifest or unit train given an A/D derailment occurs

Hazmat Cars Derailed (y)	Conditional Probability	
	Manifest Train	Unit Train
0	4.20E-01	0
1	5.02E-01	4.19E-01
2	7.75E-02	2.33E-01
3	0	1.47E-01
4	0	9.36E-02
5	0	5.83E-02
6	0	3.36E-02
7	0	1.57E-02
Sum	1	1

Note that the values in Table 53 are conditional on a derailment occurring and thus do not reflect any differences in the base manifest and unit train derailment rate per train A/D. Further, 3.5 manifest trains are required to transport the same number of railcars as the unit train. Finally, the

manifest train incurs an additional yard switching risk, and the severity of these events is explored in the next section.

6.5.4 Predicting Number of Cars Derailed for Yard Switching Derailments

The movements of single railcars or cuts of railcars during yard switching activities eliminate the sense of POD location, train length, residual train length, and even railcar position in the train consist used to quantify and predict derailment severity for yard A/D derailments. Thus, a different non-position based statistical model is necessary to predict the severity of manifest train yard switching derailments.

6.5.4.1 Fitting Statistical Distribution for Number of Cars Derailed

As a basis for statistical analysis, the empirical probability density distribution of number of railcars derailed per incident for yard switching derailments was developed for all yards combined (Figure 112), and separately for flat switching yards (Figure 113a) and hump yards (Figure 113b).

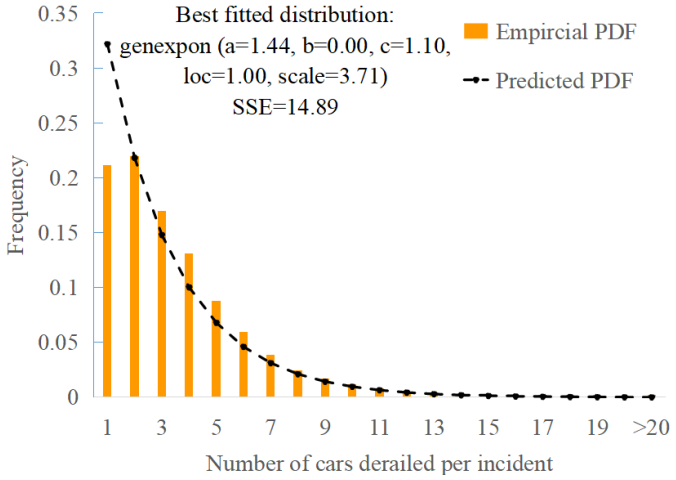

Figure 112. Distribution of number of railcars derailed per incident for manifest train yard switching derailments in all yard types (1996-2018)

Fitting an appropriate statistical model to each empirical distribution allows it to predict the severity for yard switching derailments regardless of position within the group of railcars being switched. To identify an appropriate distribution fitting the historical yard switching derailment data, each continuous distribution model built into the *Python 3.7.3 scipy.stats* function was iteratively checked to find the best fitting model with the least sum of squared errors (SSE). After examining all 89 potential distribution models, the generalized exponential distribution was found to be the best fitting distribution, with an SSE of 14.89 for manifest train yard switching derailments in all yards combined. The parameters of the distribution are specified in Figure 112. To better estimate the yard switching derailment severity for different classification yard types, the generalized exponential distribution was also fit to the data for hump yard derailments and flat yard derailments, respectively. Different sets of optimal parameters describe the severity of derailments for the two yard types, as shown by the parameters specified in Figure 113 *a* and *b*. Using these statistical models, the derailment severity can be specified for the pattern of flat and

hump classification yard types involved in a particular manifest train shipment if this information is available.

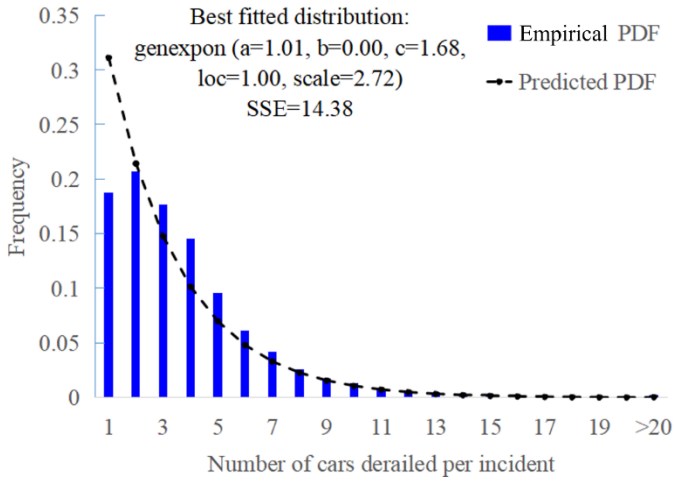

(a)

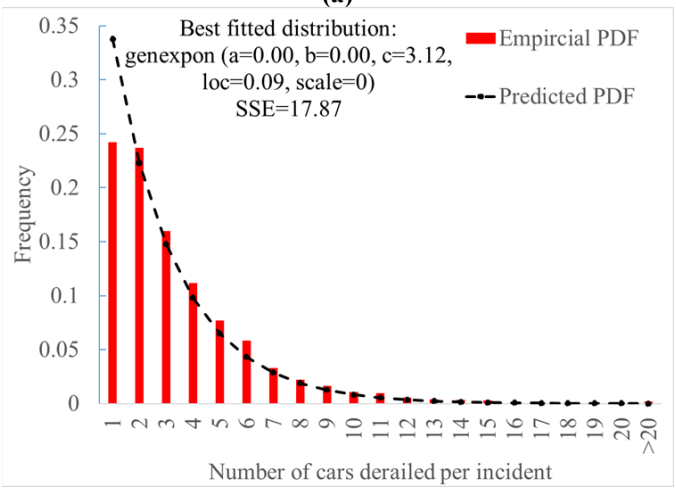

(b)

Figure 113. Distribution of number of railcars derailed per incident for manifest train yard switching derailments (1996-2018) in (a) flat yards and (b) hump yards

As a result of fitting the generalized exponential distribution, the number of railcars derailed during a yard switching type derailment can be estimated regardless of the POD, the type of railcars in the cut of railcars being switched, or the cause of a yard switching derailment in a yard of unknown type (Table 55). Similar tables were developed for flat switching yards (Table 56) and hump yards (Table 57).

The length of the cut of cars being switched has no impact on the severity of a yard switching derailment other than to restrict the maximum number of railcars that can derail. The statistical distribution derived from historical data includes the possibilities of derailing from 1 to 20 or more railcars, with an overall probability summing to 1. For circumstances in which the cut of railcars being switched is shorter than 20 railcars in length, the maximum number of railcars that can derail is constrained by the length of the cut. In such cases, the possibility of derailing all railcars in the block is truncated. The value *Pi'*(*xmax*) is defined as the truncated probability of derailing *x* railcars when *xmax* is the maximum number of cars that can derail due to the length

of the group of cars under study. Hence, if the cut of cars is only one car long, given at least one railcar derailed, the probability of derailing one car under this condition is 1 (*Pi'(1)=1*).

Table 55. Conditional probability of *x* railcars derailing given a yard switching derailment occurs (all yard types combined, 1996-2018)

x	1	2	3	4	5	6	7
CDF(x)	3.22E-01	5.40E-01	6.88E-01	7.88E-01	8.57E-01	9.03E-01	9.34E-01
$P_i(x)$	3.22E-01	2.18E-01	1.48E-01	1.00E-01	6.81E-02	4.62E-02	3.13E-02
$P_i'(x_{max})$	1.00E+00	6.78E-01	4.60E-01	3.12E-01	2.12E-01	1.43E-01	9.73E-02
x	**8**	**9**	**10**	**11**	**12**	**13**	**14**
CDF(x)	9.55E-01	9.70E-01	9.79E-01	9.86E-01	9.91E-01	9.94E-01	9.96E-01
$P_i(x)$	2.12E-02	1.44E-02	9.77E-03	6.62E-03	4.49E-03	3.05E-03	2.07E-03
$P_i'(x_{max})$	6.60E-02	4.48E-02	3.04E-02	2.06E-02	1.40E-02	9.47E-03	6.42E-03
x	**15**	**16**	**17**	**18**	**19**	**20**	**>20**
CDF(x)	9.97E-01	9.98E-01	9.99E-01	9.99E-01	9.99E-01	1.00E+00	1.00E+00
$P_i(x)$	1.40E-03	9.51E-04	6.45E-04	4.37E-04	2.97E-04	2.01E-04	1.36E-04
$P_i'(x_{max})$	4.36E-03	2.95E-03	2.00E-03	1.36E-03	9.21E-04	6.25E-04	4.24E-04

Table 56. Conditional probability of *x* railcars derailing given a yard switching derailment occurs in a flat switching yard (1996-2018)

x	1	2	3	4	5	6	7
CDF(x)	3.11E-01	5.25E-01	6.73E-01	7.75E-01	8.45E-01	8.93E-01	9.26E-01
$P_i(x)$	3.11E-01	2.14E-01	1.48E-01	1.02E-01	7.01E-02	4.83E-02	3.32E-02
$P_i'(x_{max})$	1.00E+00	6.89E-01	4.75E-01	3.27E-01	2.25E-01	1.55E-01	1.07E-01
x	**8**	**9**	**10**	**11**	**12**	**13**	**14**
CDF(x)	9.49E-01	9.65E-01	9.76E-01	9.83E-01	9.89E-01	9.92E-01	9.95E-01
$P_i(x)$	2.29E-02	1.58E-02	1.09E-02	7.49E-03	5.16E-03	3.55E-03	2.45E-03
$P_i'(x_{max})$	7.36E-02	5.07E-02	3.49E-02	2.41E-02	1.66E-02	1.14E-02	7.86E-03
x	**15**	**16**	**17**	**18**	**19**	**20**	**>20**
CDF(x)	9.96E-01	9.97E-01	9.98E-01	9.99E-01	9.99E-01	9.99E-01	1.00E+00
$P_i(x)$	1.69E-03	1.16E-03	8.00E-04	5.51E-04	3.80E-04	2.61E-04	5.79E-04
$P_i'(x_{max})$	5.42E-03	3.73E-03	2.57E-03	1.77E-03	1.22E-03	8.40E-04	5.79E-04

Table 57. Conditional probability of *x* railcars derailing given a yard switching derailment occurs in a hump yard (1996-2018)

x	1	2	3	4	5	6	7
CDF(x)	3.38E-01	5.61E-01	7.09E-01	8.07E-01	8.72E-01	9.15E-01	9.44E-01
$P_i(x)$	3.38E-01	2.23E-01	1.48E-01	9.80E-02	6.50E-02	4.31E-02	2.86E-02
$P_i'(x_{max})$	1.00E+00	6.62E-01	4.39E-01	2.91E-01	1.93E-01	1.28E-01	8.50E-02
x	**8**	**9**	**10**	**11**	**12**	**13**	**14**
CDF(x)	9.63E-01	9.75E-01	9.84E-01	9.89E-01	9.93E-01	9.95E-01	9.97E-01
$P_i(x)$	1.90E-02	1.26E-02	8.35E-03	5.54E-03	3.68E-03	2.44E-03	1.62E-03
$P_i'(x_{max})$	5.64E-02	3.74E-02	2.48E-02	1.65E-02	1.09E-02	7.24E-03	4.81E-03
x	**15**	**16**	**17**	**18**	**19**	**20**	**>20**
CDF(x)	9.98E-01	9.99E-01	9.99E-01	9.99E-01	1.00E+00	1.00E+00	1.00E+00
$P_i(x)$	1.07E-03	7.12E-04	4.72E-04	3.13E-04	2.08E-04	1.38E-04	9.14E-05
$P_i'(x_{max})$	3.19E-03	2.11E-03	1.40E-03	9.30E-04	6.17E-04	4.09E-04	2.72E-04

6.5.4.2 Application and Example Calculation of Number of Hazmat Railcars Derailed

To explain the process of calculating the total number of hazmat cars derailed during the yard switching process, consider a hypothetical example with seven railcars being switched. During the yard switching process, the specific order of railcars, especially the position of the hazmat cars, is usually unknown and may change multiple times as the railcars are moved around the yard. However, since the objective of yard switching is to sort and group railcars by common destination, a simplifying assumption is made that all the hazmat cars under study remain grouped together during railcar shunting. This assumption presents two possible approaches for analyzing the hazmat railcars during the yard switching process:

- **Switched Alone** considers the group of hazmat cars under study to be isolated during the yard switching process. Only derailments initiated by one of the hazmat cars are considered when calculating the distribution of hazmat railcars derailed. Any derailments caused by other cars in the yard are assumed to have zero probability of derailing any of the hazmat railcars under study and are thus ignored. This represents a "best case" scenario as the hazmat railcars are assumed to be switched alone and are not subject to any risk of derailment related to incidents triggered by other railcars processed through the yard.
- **Switched *En Masse*** assumes that the group of hazmat railcars under study are coupled to a group of non-hazmat railcars for the duration of the yard switching process. In calculating the distribution of hazmat railcars derailed, this approach considers both the derailments initiated by the hazmat railcars themselves, as well as any derailments caused by the group of non-hazmat railcars to which they are coupled. This represents a "worst case" scenario as the hazmat railcars switched *en masse* are subject to additional risk of

derailment incidents related to non-hazmat railcars simultaneously being processed throughout the yard.

The train in this example has five non-hazmat cars (positions 1 to 3 Non-Hazmat, and 6 and 7 Non-Hazmat) and two hazmat cars (positions 4 and 5 Hazmat). In this example, it is assumed that the two hazmat railcars are switched *en masse* in a flat switching yard with the five non-hazmat cars (three positioned ahead of the hazmat cars and two behind).

The number of hazmat cars derailed in a yard switching derailment is determined by the combination of the position of the POD, the total number of railcars derailed, and the position of the hazmat railcars. The same inspection process described for A/D derailments in the previous section also is used to identify the number of hazmat railcars derailed resulting from each combination of POD and number of railcars derailed, as shown by the matrix for the example railcar composition (Table 58). As explained previously, table cells below the diagonal are infeasible as the total number of railcars derailed cannot exceed the residual train length following the POD.

Table 58. Example number of hazmat railcars derailing given POD and number of cars derailed in a yard switching derailment

	POD	Total Number of Cars Derailed						
		1	**2**	**3**	**4**	**5**	**6**	**7**
Non-Hazmat	**1**	0	0	0	1	2	2	2
Non-Hazmat	**2**	0	0	1	2	2	2	
Non-Hazmat	**3**	0	1	2	2	2		
Hazmat Car	**4***	1	2	2	2			
Hazmat Car	**5***	1	1	1				
Non-Hazmat	**6**	0	0					
Non-Hazmat	**7**	0						

As described earlier in this section, the conditional probability of *x* number of cars derailed given a yard switching derailment has occurred was calculated for a flat switching yard (Table 56) based on the fitted generalized exponential distribution of yard switching derailment severity.

A key difference between the yard switching methodology and that used for mainline and train A/D events is that these same derailment size probabilities (Table 56) are applied to any railcar switched in a flat yard, regardless of its position within the group of railcars being switched. This assumption is made since the probability of a yard switching derailment is calculated per railcar processed (Table 45) and, given that railcar positions are either unknown or change during the switching process, there is no basis to adjust either the per-railcar probability of causing a derailment or the probability distribution of the number of railcars derailed based on the railcar position. However, the POD has an influence on the maximum possible number of cars derailed and on when the truncated probability should be applied to account for the case where all railcars after the POD derail.

In the example with seven railcars being switched, if the derailment starts at the 6th railcar, a maximum of two railcars can derail (the 6th and 7th). The complete example probability of number of cars derailed given POD (Table 59) is derived by truncating the flat yard switching derailment size distribution in Table 56 when appropriate. In addition, as explained above, the

probability of the POD occurring at any specific railcar position is assumed to be equal for all possible positions, and is 1/7 (0.143) in the example.

Table 59. Example conditional probability of POD at position k and conditional probability of *x* railcars derailing given POD k in a flat yard switching derailment

POD Prob.	POD *k*	*x* Cars Derailed 1	2	3	4	5	6	7	Sum
0.143	1	0.311	0.214	0.148	0.102	0.070	0.048	0.107	1.000
0.143	2	0.311	0.214	0.148	0.102	0.070	0.155		1.000
0.143	3	0.311	0.214	0.148	0.102	0.225			1.000
0.143	4*	0.311	0.214	0.148	0.327				1.000
0.143	5*	0.311	0.214	0.475					1.000
0.143	6	0.311	0.689						1.000
0.143	7	1.000							1.000

Combining the probability distribution of *x* cars derailed given POD and the probability of each POD position *k* by multiplying the corresponding values in Table 59, the conditional probability of *x* number of cars derailed given that a yard switching derailment occurs cab be plotted (Table 60). The number of hazmat cars involved in each derailment scenario (Table 58) is indicated in Table 60 by various colors of shading: orange = two hazmat cars derailed, yellow = one hazmat car derailed, and green = zero hazmat cars derailed.

Grouping and summing each conditional probability in Table 60 by the number of hazmat cars derailed yields the conditional probability of *y* number of tank cars derailed given a flat yard switching derailment occurs for this example cut of cars (Table 61).

Table 60. Example conditional probability of *x* railcars derailing due to derailment starting at k^{th} position of cut of railcars given yard switching derailment

POD *k*	*x* Cars Derailed 1	2	3	4	5	6	7	Sum
1	0.044	0.031	0.021	0.015	0.010	0.007	0.015	0.143
2	0.044	0.031	0.021	0.015	0.010	0.022		0.143
3	0.044	0.031	0.021	0.015	0.032			0.143
4*	0.044	0.031	0.021	0.047				0.143
5*	0.044	0.031	0.068					0.143
6	0.044	0.098						0.143
7	0.143							0.143

Shading color code: Orange = 2 TC derailed, Yellow =1, Green = 0

Table 61. Conditional probability of *y* hazmat railcars derailing in example cut of railcars given a flat yard switching derailment occurs

Hazmat Cars Derailed (y)	Conditional Probability
0	0.5
1	0.254
2	0.246
Sum	1

6.5.5 Total Yard/Terminal Derailment Severity

While the distribution of derailment severity for unit trains is characterized solely by the terminal A/D calculation (Section 6.5.3), the overall yard derailment severity distribution for a manifest train includes two components: A/D (Section 6.5.3) and yard switching (Section 6.5.4).

For a manifest train shipment, the overall yard derailment severity distribution of number of hazmat cars derailed can be calculated by:

$$P(y)_{YardTotal} = P(y|\,derail)_{YardAD} \times P\,(derailment)_{YardAD} + P(y|\,derail)_{YardSwitching} \times P\,(derailment)_{YardSwitching} \quad (6\text{-}23)$$

Specifically, for the scenario of unknown yard type and count (i.e., generic mileage-based approach), the *P(derailment)* is calculated based on the mainline mileage accumulated during the shipment.

where:

$$P(y)_{YardTotal} = P(y|\,derail)_{YardAD} \times P\,(derailment\ per\ trainmiles/carmiles\ on\ mainline)_{YardAD} \times P\,(trainmiles/carmiles\ on\ mainline\ during\ the\ shipment) + P(y|\,derail)_{YardSwitching} \times P\,(derailment\ per\ trainmiles/carmiles\ on\ mainline)_{YardSwitching} \times P\,(trainmiles/carmiles\ on\ mainline\ during\ the\ shipment) \quad (6\text{-}24)$$

For the scenario of known yard type and count (i.e., detailed route-based approach), the *P(derailment)* is calculated based on the specific number and type of yard A/D events and the yard switching events the train experiences during the shipment.

where:

$$P(y)_{YardTotal} = P(y|\,derail)_{YardAD} \times P\,(derailment\ per\ A/D\ events)_{YardAD} \times P\,(number\ of\ A/D\ events\ during\ the\ shipment) + P(y|\,derail)_{YardSwitching} \times P\,(derailment\ per\ yard\ switching\ events)_{YardSwitching}\ x \times P\,(number\ of\ yard\ switching\ events\ during\ the\ shipment) \quad (6\text{-}25)$$

In the example of shipping seven railcars, assume the manifest train originates at a flat switching yard, re-classifies at an intermediate flat switching yard, and arrives at its destination, while the unit train departs from a terminal and arrives at a terminal without stopping at any intermediate yards. Given that both trains are only 7 railcars long and travel 100 miles between origin and destination, the probability of derailment can be calculated (Table 62).

Combining the derailment probability in Table 62 with the conditional probabilities of hazmat derailment in Table 54 for yard A/D, and in Table 61 for yard switching using Equation (6-25), the overall probability of derailing hazmat railcars during the shipment can be calculated (

Table 63).

Table 62. Probability of derailment for example shipment comparison

Metric	Weight	Manifest Train			
		A/D		Switching	
Train processed	78.08%	(Manifest train derailments per train A/D event) × (4 A/D events)	4.76E-04	(2 yards) × (7 cars switched/yard) × (Yard switching derailments per car processed)	8.93E-05
Car processed	21.92%	(Manifest train derailments per car A/D event) × (4 A/D events × 7 cars)	5.66E-05		
Known yard	Combined		**3.84E-04**		**8.93E-05**

Metric	Weight	Unit Train	
		A/D	
Train processed	62.80%	(unit train derailments per train A/D event) × (2 A/D events)	2.53E-04
Car processed	37.20%	(unit train derailments per car A/D event) × (2 A/D events × 7 cars)	1.71E-05
Known yard			**1.65E-04**

Table 63. Combining yard A/D and switching likelihood of hazmat derailment for example manifest train shipment

Hazmat Cars Derailed (y)	Arrival/Departure		Yard Switching		Total
	Probability of Derailment	Conditional Probability of Derailing y Hazmat Cars	Probability of Derailment	Conditional Probability of Derailing y Hazmat Cars	
0	3.84E-04	4.20E-01	8.93E-05	5.00E-01	2.06E-04
1		5.02E-01		2.54E-01	2.15E-04
2		7.75E-02		2.46E-01	5.17E-05
Sum		1		1	4.73E-04

Similarly, the total unit train derailment likelihood can be calculated by combining the derailment probability in Table 54 with the conditional probabilities of hazmat derailments of differing numbers of cars derailed in Table 54 for yard arrival and departure events, since there is no yard switching operation in the unit train shipment. Since all railcars in the unit train carry hazmat, the total derailment likelihood for events with specific numbers of hazmat railcars derailed (Error! Not a valid bookmark self-reference.) includes events involving a greater number than is possible for the manifest train (

Table 63) and the likelihood of zero hazmat cars derailed given a derailment is zero.

For the example seven-railcar long manifest train and unit train shipments, the manifest train has a significantly larger likelihood of overall hazmat derailment than the unit train. However, recall that one sample manifest train carries only two hazmat railcars while the unit train carries seven. Thus, to transport an equivalent amount of hazmat between origin and destination, 3.5 sample

manifest trains must operate for each sample unit train. Hence, the overall yard derailment likelihood for manifest train shipments must be multiplied by a factor of 3.5 before directly comparing it with that of the unit train. Considering this factor, the example manifest train operation shows an even greater likelihood of derailing hazmat railcars in yards compared to unit trains in terminals for the example shipments. However, despite being more likely, these manifest train yard derailments cannot involve more than two hazmat railcars while the less likely unit train terminal derailments can involve up to seven railcars for the example shipment.

Table 64. Calculating yard A/D likelihood of hazmat derailment for example unit train shipment

Hazmat Cars Derailed (y)	Arrival/Departure		Total
	Probability of Derailment	Conditional Probability of Derailing y Hazmat Railcars	
0	1.65E-04	0	0
1		4.19E-01	6.91E-05
2		2.33E-01	3.84E-05
3		1.47E-01	2.43E-05
4		9.36E-02	1.54E-05
5		5.83E-02	9.62E-06
6		3.36E-02	5.54E-06
7		1.57E-02	2.59E-06
Sum		1	1.65E-04

6.6 Yard/Terminal Derailment Release Probability and Consequence

Using the methods in Section 6.5, the team calculated the probability distribution of the total number of hazmat cars derailed, which was denoted as $P(y)_{YardTotal}$. As explained in Section 3, the CPR of a non-pressurized, 30,000-gallon tank car should be multiplied by a factor of 0.35 to reflect the fact that most yard accidents have lower severities and chances of release than mainline accidents in general, due to lower yard operating speeds relative to mainline speeds. Let $P(x)_{YardRel}$ denote the probability that there are x hazmat cars releasing contents per shipment and let TT denote the total number of tank cars in a train. $P(x)_{YardRel}$ can be calculated by:

$$P(x)_{YardRel} = \sum_{y=x}^{TT} \binom{y}{x} (0.35 \times CPR)^x \times (1 - 0.35 \times CPR)^{y-x} \times P(y)_{YardTotal} \quad (6\text{-}26)$$

where:

$P(x)_{YardRel}$ = the probability that there are x hazmat cars releasing contents per shipment

$P(y)_{YardTotal}$ = the probability that there are y number of hazmat cars derailed

TT = the total number of tank cars in a train

CPR = the conditional probability of releasing

Knowing the number of tank cars releasing contents, the methodology developed in Section 3.1 for mainline risk analysis can be adapted to calculate the probability distribution of the releasing quantity and release consequence.

7. Tank Car Release Probability and Release Quantity

This section presents the models that were used to derive the CPR and the expected quantity of release (EQR) of railroad tank cars for the calculation of hazmat transportation risk (described in Section 3.1.5). The CPR model was developed by Treichel et al. (2019a) and was funded by the industry partners of the Advanced Tank Car Collaborative Research Program (ATCCRP) using data from the RSI–AAR Railroad Tank Car Safety Research and Test Project and EQR models developed for that project (2014). This chapter presents a summary of these models and how they were integrated into the mainline and yard hazmat transportation risk framework. For detailed information on these models, the two technical reports mentioned above may be found in the References section.

7.1 Tank Car Release Probability

7.1.1 Definition of CPR

A conditional probability is the probability of an event occurring given a specific condition. The CPR for a tank car is the probability that a single tank car releases any quantity of lading, given that it is derailed in an FRA-reportable accident, which is any accident that causes damage to track, equipment, and/or structures exceeding a certain dollar threshold that is adjusted each year. In 2021, this threshold was $11,200 (FRA, 2021).

7.1.2 Analytical Approach

A logistic regression analysis was conducted to derive formulas for the four tank car components that can release lading: shell, head, top fittings, and bottom fittings (Figure 114).

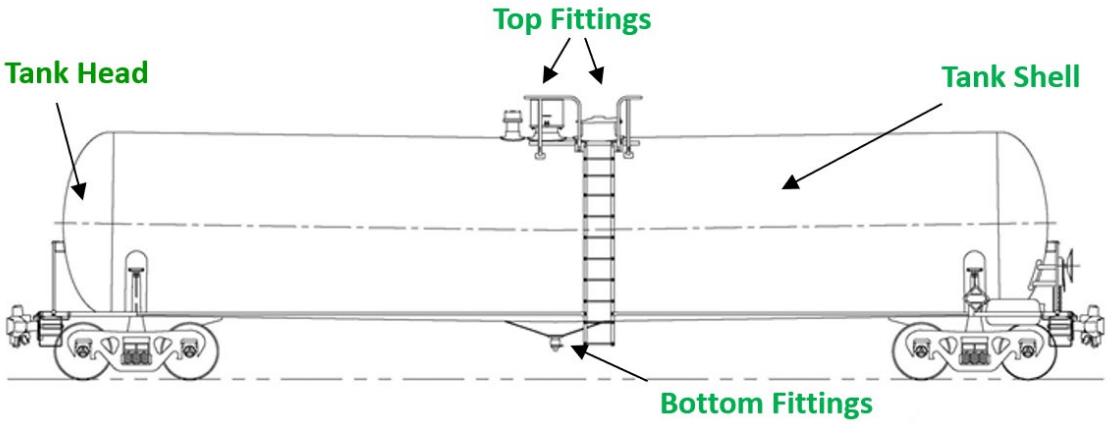

Figure 114. Four components of a tank car that can lose lading (Treichel et al., 2019a)

Historical tank car accident records from the RSI-AAR Railroad Tank Car Safety Research and Test Project were used to perform the regression analysis. A set of train accident characteristics and tank car features was considered, and the group minimax concave penalty approach (gMCP) was applied to account for the effects of correlated variables and to facilitate variable selection for the logistic regression. As a result, each of the formulas selected as most representative of the data from the regression generates estimated CPRs that are specific to one of four components of

the tank car. These formulas contain variables that affect CPRs of the specific component of the tank car and the interaction terms among those variables.

The component CPR formulas are expressed as:

$$CPRi = \exp(L(Xi)) / [1 + \exp(L(Xi))] \times F, \quad (7\text{-}1)$$

where:

i = index to the car component (i.e., head, shell, top fittings, or bottom fittings)

CPRi = the estimated CPR from component i

L(Xi) = the linear combination of input variables for component i

F = FRA multiplier

The FRA multiplier adjusts the condition on the release probability from "given that the car is damaged in any accident" to "given that the car is derailed in an FRA-reportable accident." This is important when CPR estimates are used as part of a larger quantitative risk assessment and combined with FRA accident rates and other data based on that metric. The FRA-compatible probability is the form of CPR that is most often used by the industry. In the study presented by Treichel et al. (2019a), this value is estimated to be 1.0; however, future studies using updated tank car accident data and methods may yield different values.

The CPR for the tank car as a whole is:

$$CPRcar = 1 - \prod_i (1 - CPRi) \quad (7\text{-}2)$$

Use of this formula assumes that the component CPRs are independent, given a set of accident circumstances. This is not strictly true. However, the results of the previous study showed that the dependence is not large enough to significantly bias the results and is additionally mitigated by the design of the full models (Treichel et al., 2019a).

7.1.3 CPR Calculator

A calculator was used based on the CPR models derived by Treichel et al. (2019a) to produce CPR estimates for various rail hazmat transportation risk assessment. The calculator allowed the input of various train accident characteristics (e.g., derailment speed, number of cars derailed, position of tank car, etc.) and tank car features (e.g., tank head and shell thicknesses, presence of jacket, head shields, or fitting protection, tank steel material types, etc.). The output of the calculator is the CPR estimate based on input variables and the logistic regression formulas for tank car CPR described in the previous subsection. Figure 115 shows a screenshot of the calculator.

Note that the input to the calculator is not a car specification like "111A100W1," but a set of values that precisely describe each car's actual physical characteristics and accident conditions. This approach enables the wide range of tank car features to enhance the statistical power and robustness of the analysis and to provide flexibility in assessing the CPR for different designs and configurations. Table 65 presents an example CPR calculation for a DOT-117J tank car under an average accident condition for a freight car in an FRA-reportable mainline accident caused by broken rails or welds, as derived from FRA mainline and siding freight train accidents for the period 2003-2012 (Treichel et al., 2019a). Note that the general train accident condition for the CPR study (Treichel et al., 2019a) was based on all broken-rail derailments. However, the

derivation of CPR itself was based on *all* releases, not just broken rail releases. Thus, the CPR formulas themselves are general. The broken-rail-based characteristics only refer to the accident conditions (e.g., train speed, number of cars derailed, first derailed vehicle) as the input to obtain CPRs, not the CPRs themselves. The resulting CPR estimate, 0.043, was used in the mainline hazmat release risk calculation presented in Section 3.1.

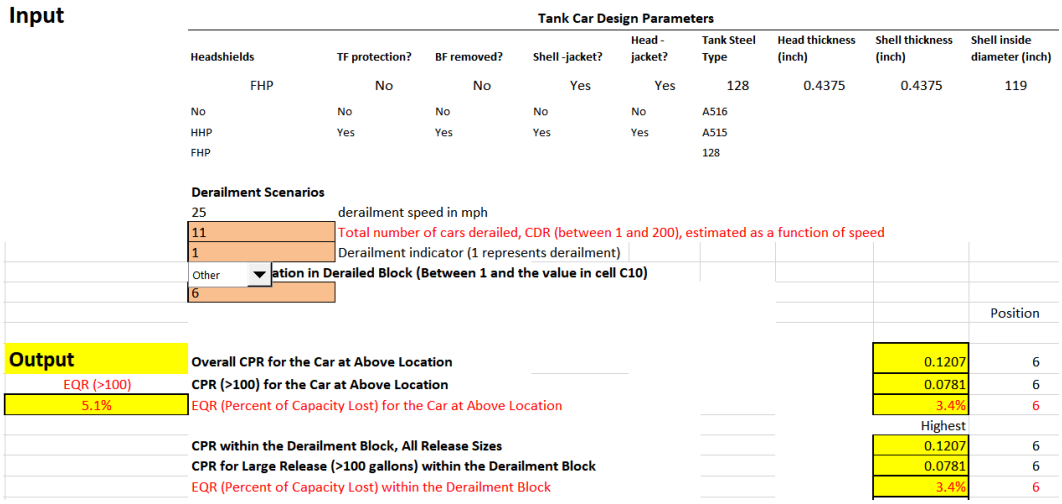

Figure 115. A screenshot of a portion of the CPR calculator

Table 65. An example calculation of CPR

Variable Input (for a DOT-117J tank car)	
Tank Shell Thickness (inch.)	0.5625
Tank Head Thickness (inch.)	0.5625
Tank Head Shield Type	Full Head Shield
Presence of Top Fitting Protection	Yes
Bottom Fitting Removal	No
Presence of Tank Jacket	Yes
Tank Shell Inside Diameter (inch.)	119
Derailment Speed (mph)	25
Total Number of Cars Derailed	11
Position of the Tank Car in Derailment Block	6
Output CPR Estimate (for a single car)	0.043

7.1.4 CPR in the Yard

CPRs on yard or industrial track are generally lower than CPRs for the same cars on mainline or siding track. However, the variable for track type in the regression was not statistically significant in any of the component CPR models, so the dominant factors are lower speeds and smaller derailments. A separate analysis was conducted to compare the fraction of lading loss between mainline and yard tank car records in the previous study (Treichel et al., 2019a), and based on that, a factor of 0.35 was applied to the FRA mainline multiplier for yard CPR estimates.

7.2 Tank Car Release Quantity

Railroad tank cars have a wide range of capacities, and a loss of a given gallon volume can represent a different severity of outcome for different cars. For example, a 16,000-gallon loss is 50 percent of the lading from a 32,000-gallon car, but is an 80 percent loss from a 20,000-gallon car, and a total loss from a 16,000-gallon car. Therefore, quantity lost data are represented in terms of percentage of car capacity lost. The RSI-AAR Railroad Tank Car Safety Research and Test Project (2014) conducted a series of quantity of loss analyses using their tank car accident database, and these were later elaborated on and used by Treichel et al. (2019a). The distribution of various percentages of lading loss for different types of cars and accident conditions were developed. For example, Figure 116 shows the distribution of the percentage of quantity lost for non-pressure tank cars in mainline and siding accidents by tank car components. It was found that many of the releases either had a small amount of release (<5 percent of total capacity) or an almost total loss (>80 percent of total capacity).

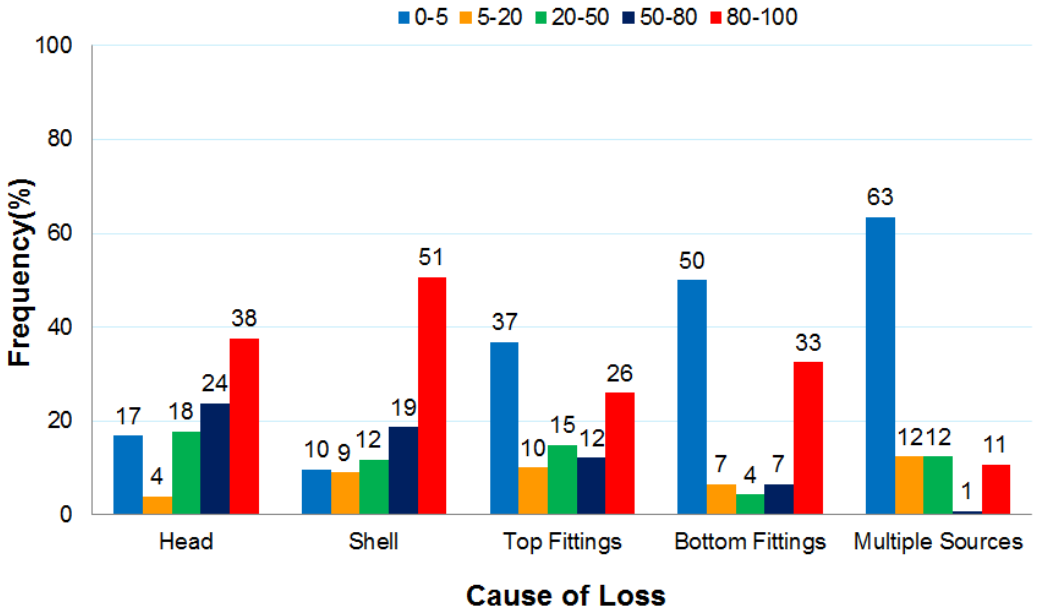

Figure 116. Distribution of quantity of lading lost, expressed as a percentage of loaded quantity, for each car component (bar color indicates category of the quantity lost, as a percentage of total capacity) (Treichel et al., 2019a)

Given the tank car capacity, tank car type, and track type, a distribution of percentage of quantity loss can be developed. An example was shown in the mainline hazmat release calculation in Section 3.1 (Figure 6 and Table 9). In that example, the tank car was assumed to be a 30,000-gallon non-pressure tank car, and the accident was assumed to be a mainline/siding accident. If tank car features or accident conditions changed, a different quantity of loss distribution could be derived.

Using the results from the quantity of loss analysis conducted previously, an EQR calculator was developed. Given an average capacity of a specific type of tank car and the probability distribution of number of tank cars releasing, the probability distribution of EQR can be generated using the quantity of loss distribution derived from the previous study. An example calculation of the probability distribution of EQR was presented in Section 3.1.

Note that the distributions of EQR for various tank car capacities, tank car types, and accident conditions were derived from empirical data. In the future, when new tank car accident records are available, the derived EQR distribution may change. For more information regarding different empirical-based EQR distributions, see the technical report prepared by Treichel et al. (2019a).

8. Consequence Analyses

Researchers originally planned to determine the relative numbers or quantity of releases resulting from movements of hazmat materials in either a unit train or distributed in multiple manifest trains. A true consequence analysis was not included in the proposed project scope. However, there was interest in evaluating the potential consequences beyond just quantity released. This section describes how the team performed a small pilot study that can demonstrate how the results from the unit and manifest risk assessments can be applied to perform a more complete consequence assessment.

8.1 Scope of the Consequence Analyses

Performing full consequence analyses of unit train operations (to injuries/fatalities for all hazmat commodities, routes, etc.) is a very large task. Thus, the team evaluated a range of options and existing models or analysis tools that could be applied to reduce and simplify the problem. An analysis of the unit hazmat shipments by commodity, shown in Figure 117 (and discussed earlier in Section 4.1), indicates that crude oil and ethanol combined comprise a significant majority of hazmat unit train shipments. Therefore, one of the initial simplifications identified is to reduce the scope of the problem by limiting the commodities evaluated to flammable liquids (e.g., crude oil and ethanol).

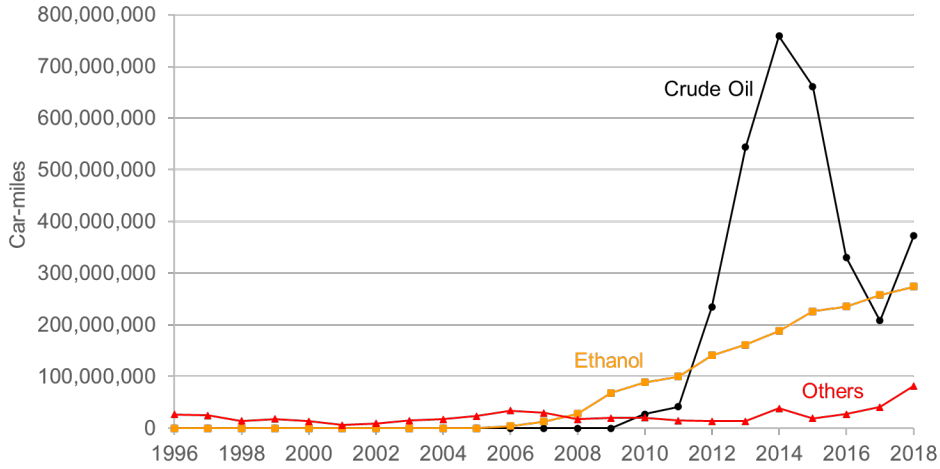

Figure 117. Hazmat unit train car-miles by commodity

The consequence analyses performed here demonstrate an approach to analyzing consequences resulting from change in severity of flammable liquid releases resulting from shipments in unit trains versus manifest trains.

One difficulty in performing consequence analyses is that often the results are controlled by the most severe events, which are extremely rare. Consequence analyses also have difficulty including and quantifying consequences from conditions that have not been previously observed. A consequence analysis for rail transportation of flammable liquids performed prior to 2013 would likely not have considered that an event like the Lac-Mégantic rail disaster, which resulted in 47 fatalities and more than 30 buildings destroyed, was possible.

One such type of severe consequence that has not been significantly considered for flammable liquids by rail is an uncontrolled fire spread. Over the past few decades there have been significant increases in both the number and size of uncontrolled wildfires, as indicated by data on area burned shown in Figure 118 (NIFC (National Interagency Fire Center), 2021; Short, 2015; US EPA, 2021). As a result, for this consequence assessment, the research team felt it was important to evaluate the risk of fire spread with a flammable liquid derailment as the initiating event.

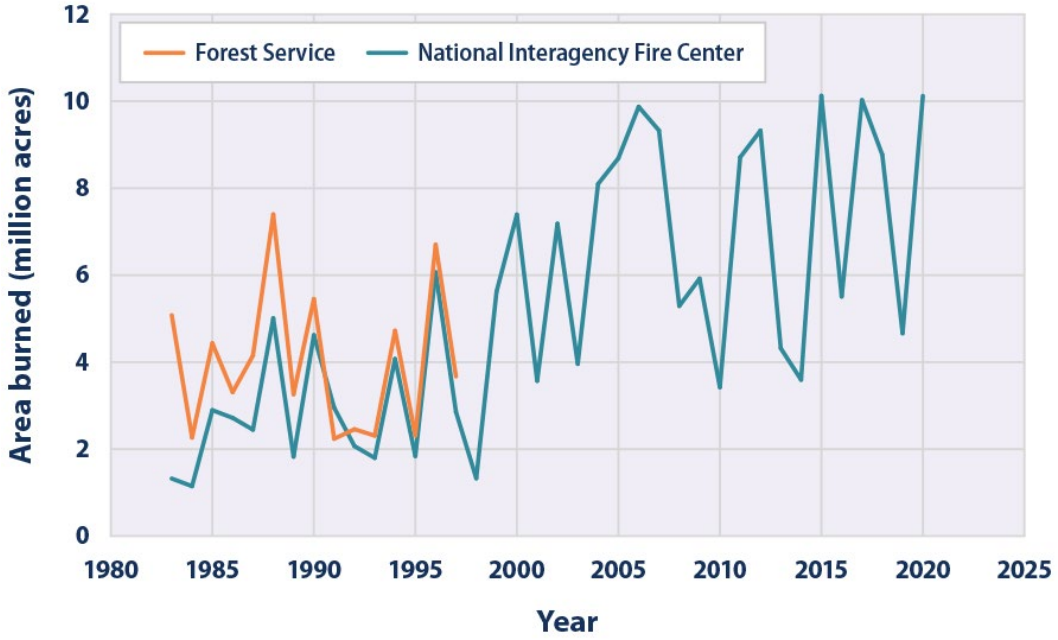

Figure 118. Wildfire extent in the United States, 1983–2020 (NIFC (National Interagency Fire Center), 2021; Short, 2015; US EPA, 2021)

In modern wildfires/firestorms, obstacles such as traffic jams, rubble, and disabled/abandoned vehicles have obstructed evacuation routes, leading to fatalities. However, studies of wildfires show a casualty rate of less than 0.01 percent for the evacuating population and most fatalities are caused by waiting too long to evacuate (Etheridge, 2020a). However, the examples show that, due to the potentially large populations exposed, an uncontrolled wildfire can result in a significant number of fatalities.

8.2 Consequence Analysis Methodology

The approach proposed for this study was to leverage existing toolsets developed to assess the consequences of military or terrorist attacks (e.g., detonations, etc.) as well as industrial accidents (e.g., hazmat spill fires). This toolset comprises the Hazard Prediction and Assessment Capability (HPAC) with its associated analysis modules, and the Nuclear Capabilities Services (NuCS) framework.

The proposed approach applies the HPAC and NuCS toolsets to analyze a series of derailment events (i.e., flammable liquid releases) at representative real-world locations with varying population densities and release sizes. The code runs quickly and provides a range of consequence measures (e.g., injury hazard area as a function of time, number of people within

hazard area, structures damaged). Based on the results of these analyses, the team developed a set of consequence curves that are fit to the results of the simulations. These consequence curves could subsequently be applied to a given route with appropriate weighting assumptions within a simple consequence calculator.

The following is a brief description of various steps, tools, and assumptions applied in the consequence analysis. The first step is the selection of representative derailment sites. For simplicity, the sites were selected along a single rail line running through a region in the existing NuCS database of at least 25 metropolitan areas. For each of these areas, the ground geometry, buildings, and vegetation density (for fire fuel) are all fully characterized within the database. The team then picked three representative locations (urban, suburban, and rural) along a rail line for the derailment sites. The NuCS database then populated all the additional required input data regarding the selected sites.

The HPAC tool contains an OILSPILL model that predicts the area and volume of contained and uncontained crude oil spills. The amount of oil spilled can be estimated using railcar volumes. The oil spill can be ignited, and HPAC contains a transport and dispersion model as well as a weather model, which creates a plume of soot that spreads from the source and deposits over the local area.

The oil spill modeling uses a Microsoft Excel spreadsheet-based tool (FluxCalc.xlsx) to calculate the evaporative flux rate of a variety of potentially toxic components from hydrocarbons pooled on the ground. FluxCalc was developed by the professional services company RPS and is based on the algorithms used in the RPS oil spill trajectory and fate model OILMAP. A description of FluxCalc capabilities and references for the model development are provided by Chowdhury (2016).

The fuel spill distribution is mapped on the ground into the fuel files for the fire spread/casualty code (QUIC-FST) (Crepeau & Etheridge, 2019; Etheridge, 2020b). A flowchart for the QUIC-FST framework is shown in Figure 119.

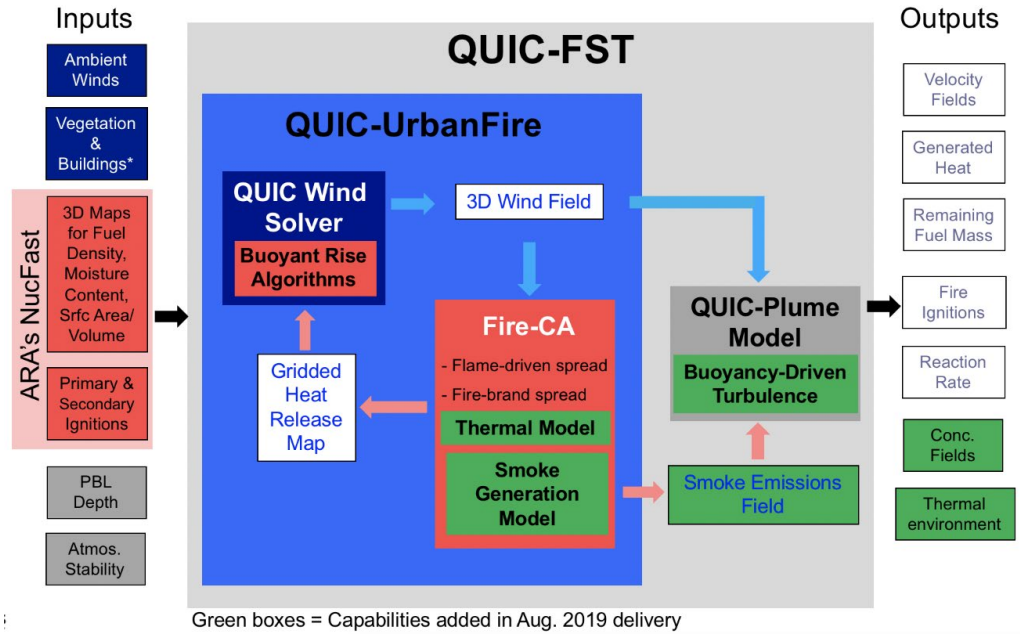

Figure 119. QUIC-FST fast-running fire spread model framework (Linn et al., 2020)

Again, the tool is geo-referenced and can import building, vegetation, and population data based on an input location. The assumption is that all fuel in the spill footprint will ignite once a fire event occurs. This would be modeled in the code by placing fuel in all cells inside the spill footprint and setting the probability of ignition in that region to 1. The fire spread code is then run to provide a time-dependent map of the fuel consumed by fire. The fire casualty model provides a time-dependent map of the casualties (fatalities and injuries) due to the propagating fire with a breakdown of casualties due to burns and smoke inhalation.

The fire spread/casualty code can be applied to a given region with a defined population to provide an estimate of fire casualties for that location and population. It calculates the probability of injury and fatality due to a thermal dose in each computational cell in the scene. Applying a random number generator and the probabilities to the population density, it arrives at an estimate of casualties for each computational cell. For a given spill, casualties are dependent on the vegetation and building distribution in the area. This approach gives an estimate of casualties for a given spill as a function of population.

By performing a series of analyses with the above tool at a series of hypothetical locations with varying population densities, and using various release sizes, the team developed a set of consequence curves for the affected area, buildings burned, or casualties as a function of time. For this application, the time was limited (e.g., the initial two hours after a derailment).

Most of the validation done with QUIC-FST (QUIC-Fire/Smoke/Thermal) have been comparisons to the FIRETEC high-fidelity, rad-hydro code (e.g., line fires, Atlanta cases). There has also been a lot of testing on specific types of fires (e.g., two nearby line fires, circular fire, crown fires, moisture dependency) to ensure QUIC-FST is predicting the correct fire behavior qualitatively. Data on the validation of the fire spread models is available in prior research (Crepeau & Etheridge, 2019; Linn et al., 2020). Additional validation work has also been performed but is not currently documented.

8.2.1 Casualty Analyses

QUIC-FST casualties are divided into two groups: fire casualties and smoke casualties. For fire casualties, Thermal Dose Units (TDUs) are used to determine injuries and fatalities. The thermal output of the fire is used to calculate the TDU of a cell which can then be used to calculate fatalities. The criteria and fitted line are summarized in Table 66 and shown in Figure 120 (O'Sullivan & Jagger, 2004).

Table 66. Thermal dose injury relationship (O'Sullivan & Jagger, 2004)

Harm Caused	Infrared Radiation Thermal Dose (TDU) $(kW/m2)^{4/3}s$
Pain	92
1st degree burn threshold	105
2nd degree burn threshold	290
3rd degree burn threshold (~LD05)	1,000
LD50 (Lethal Dose, 50%)	2,000
100% Fatality (no Personal Protective Equipment)	3,500

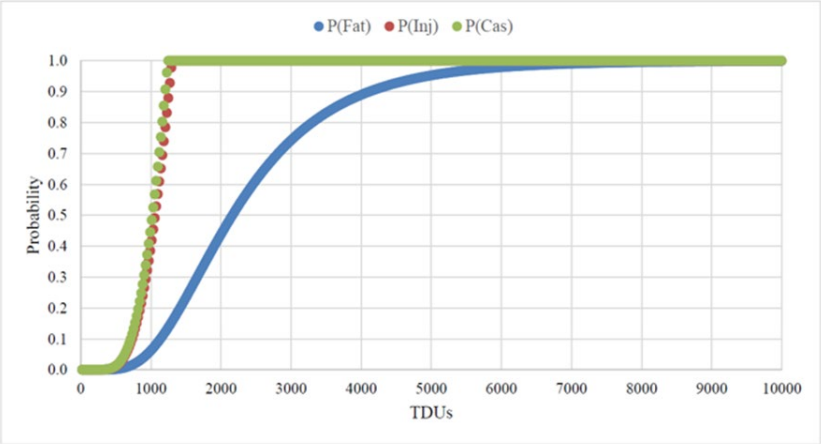

Figure 120. Injury and fatality curves used for TDU casualty assessments

Injuries are subsequently obtained as a function of the number of fatalities. According to historical data, the injury-to-fatality ratio is about 6.4. As a result, the number of serious fire injuries is equal to 6.4 times the number of fire fatalities. This methodology for calculating fire casualties is summarized in Table 67.

Table 67. Probability of fatality and serious injury.

Fatality Probability	Probability of Severe Injury
$Y = -10.7 + 1.99 \ln(TDU \cdot 0.1)$	$P(SI) = 6.4 \cdot P(Fatality)$

Smoke casualties are calculated similarly. The ratios for smoke-to-fire casualties are found from historical data and this ratio is applied to obtain the smoke casualties of a run. These smoke casualty ratios are summarized in Table 68.

Table 68. Summary of smoke to fire casualty proportionalities.

	Fatalities (%)	Injuries (%)
Inhalation	86	64
Burns	14	36

8.2.2 Advantages of This Approach

Assessing the risk of hazmat transport in unit train versus manifest train services requires tools that can assess differences between dissimilar release sizes. This is not possible with simplified assumptions, such as using the Emergency Response Guidelines (ERG) to define the hazard area. However, the proposed toolset can easily assess the consequences of different sized events.

The primary advantage of this approach is that the existing tools, which have already been highly developed for assessing consequences in the military, security, and industrial accident fields, can be leveraged; the team performed a limited scope assessment with the available resources for consequence assessment in this program. The tools also have the fidelity to address more complex consequences at various types of locations, which was beyond the scope of many past railroad consequence assessments. These include both the assessment of the initial conditions

and the growth of affected area from fire spread, as well as the extension from the thermal environment in the affected area to an assessment of potential casualties.

A second advantage is that consequence analyses are often dominated by assumptions based on extremely rare but high consequence events. Considering potential casualties as the consequence metric in this study, the primary differences would likely be from the increased probability of a larger spill event in an urban area. This tool is designed to evaluate the types of events for which there are very limited real-world data.

The primary limitation of this approach is that the team had resources to evaluate only a limited number of scenarios. Ideally, a much larger set of locations, wind/weather conditions, and spill sizes would be assessed to prevent bias in the results based on the scenarios evaluated.

8.2.3 Required Inputs for Proposed Process

Below is a summary of the inputs required for the QUIC-FST fire spread and casualty analyses.

Transportation Incident Model:

- User Input – Incident site (by Lat/Lon), lading material (choice from ~130 and user-defined), transportation method (e.g., rail, road, water), vehicle/container (e.g., rail car, …), accident/explosion, type of accident (e.g., overturn/collision), number of containers (e.g., 1 - 5), fraction full of all containers
- Output – Viable pooled mass

Oil Spill Model:

- User Input – Viable pooled mass
- Output – Pool diameter

Fire Spread Model:

- User Input – Incident site (by Lat/Lon), ambient wind, modified fuel files mapped with pool
- Database inputs – Vegetation, buildings, population density
- Output – burnt/unburnt fuel mass, fire spreading area, and fire-related casualties (e.g., smoke inhalation, burns) as a function of time

These analyses are performed to provide the data needed for the consequence calculator. For example, if a user is interested in consequences at 30 minutes after a release incident and they input the amount of release, site information, and wind information, the combined model will calculate and report the size, number of structures, and estimated population in the affected zone. The results of these analyses are built into the calculator with the appropriate corrections and weighting functions as described in the following sections.

8.2.4 Assumptions

Below is a summary of the primary assumptions required for the QUIC-FST fire spread and casualty analyses.

Transportation Incident Model:

- All container contents are spilled and create a pool
- All containers have the same volume of material

Oil Spill Model:

- Circular spill if using HPAC model (used for this study)
- Terrain conforming if using ArcGIS Pro model

Fire Spread Model:

- Pool achieves final footprint before igniting
- Entire pool ignites simultaneously
- Fire spread over flat terrain
- Fire spread through convection/radiation and firebrands
- No firefighting measures employed
- No evacuation of population (evacuation corrections are subsequently applied in the calculator)

8.2.5 Annual Fuel Load Moisture Content Correction

The fire spread analyses were performed for a low moisture content, which is a worst-case fire spread scenario that occurs during the worst time of the year (i.e., fire season). It is unrealistic to apply this condition uniformly throughout the year and doing so would lead to an overestimation of the fire spread risk. Thus, a correction was applied to the fire spread analysis to account for seasonal changes.

US Government Data on annual distribution of wildfire acreage burned indicates that fire season runs effectively one quarter of the year, June through August, as shown in Figure 121 (MTBS (Monitoring Trends in Burn Severity), 2019; US EPA, 2021).

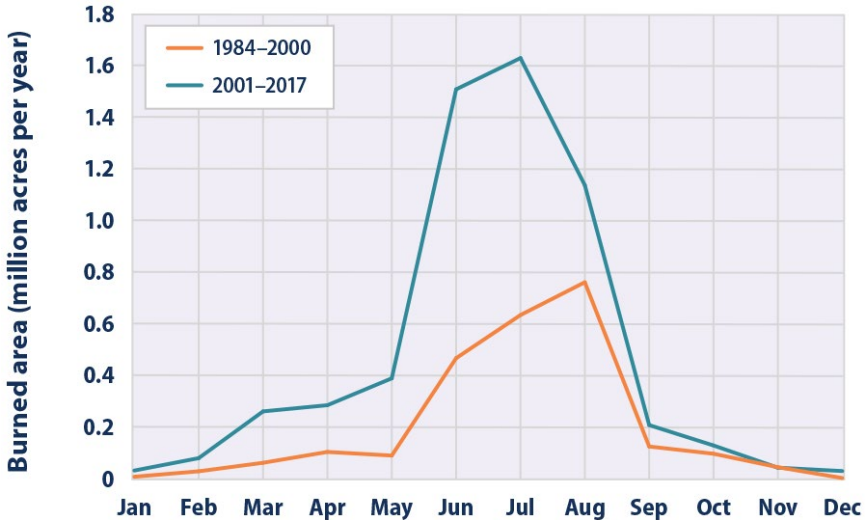

Figure 121. Comparison of monthly burned area due to wildfires in the United States between 1984–2000 and 2001–2017 (US EPA, 2021)

To account for the duration of fire season each year, a simplified approximation was used that assumes fire spread after five minutes and associated increases in other consequence measures are scaled by a factor of 0.25. The early time fire behavior (i.e., first five minutes) was unchanged because it is assumed to be primarily controlled by the spilled fuel from the derailment rather than the presence or absence of low-moisture vegetation at the site.

8.2.6 Population Evacuation Corrections

The initial casualty estimates from the QUIC-FST analysis are based on population density (i.e., occupancy) remaining in place. This assumption results in unrealistic over-predictions of the number of casualties without accounting for the mitigating effects of evacuations. Ideally, a detailed evacuation model could be coupled to the analyses (Brokaw, 2021). However, incorporating the evacuation modeling was beyond the scope of this demonstration study. As a result, an approach is needed to account for the evacuation of occupants within the burn area hazard zone.

When discussing occupant evacuation, there are different zones and time scales that need to be considered. First, there is a nearfield evacuation of buildings at risk of fires immediately adjacent to or within the initial pool fire zone. These nearfield evacuations are typically initiated by fire alarms and often are experienced by populations that have previously experienced evacuation procedures as part of fire drills.

There is a significant amount of information in the open literature on building evacuation data and modelling (Fahy, 2006; Purser, 2010). It was beyond the scope of this effort to perform a full review of this information or to develop and incorporate a detailed evacuation model. The team developed a relative occupancy curve for the buildings in the nearfield hazard zone. An example relative occupancy nearfield building evacuation curve assuming a 4-minute evacuation time is shown in Figure 122.

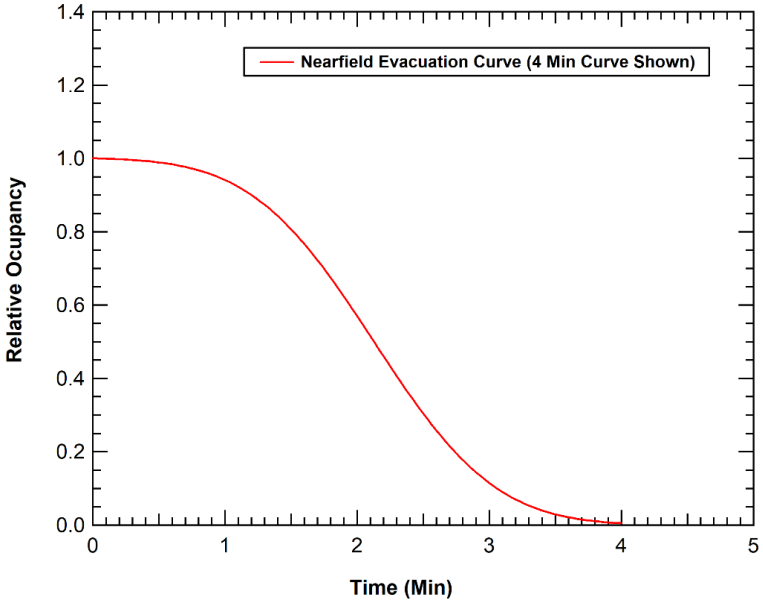

Figure 122. Example 4-minute nearfield building relative occupancy evacuation curve

This time frame is consistent with the data from an evacuation of a 7-story office building with 381 occupants where the last occupant exited at 286 seconds and most of the occupants exited within 220 seconds (Fahy, 2006). Within the consequence calculator, this nearfield building evacuation time is a user-controlled variable that can be changed based on the location, type of buildings, etc., considered for the scenarios analyzed.

In assessing casualties of uncontrolled wildfires, the historical data is likely the best estimator for determining potential casualties. However, this study only considered the consequences up to a duration of two hours after the derailment. In this case, a fire may be running through an urban or suburban region in a high wind fuel growth scenario. An evacuation for this "far field" zone (i.e., exposed to fire hazard in the initial two hours) is needed.

The data on evacuation times for larger far field zones is not as plentiful as the available building evacuation data and modelling information. However, an EPA report (Hans, 1974) provides summary data of 64 evacuation events covering a total of 1,142,336 evacuated persons. The studied events cover a wide range of population sizes, disaster agents, number of people evacuated, meteorological conditions, times of day, and roadway conditions. The 1974 study found an inverse relationship between population density and evacuation time, as shown in Figure 123. This evacuation time was defined as the sum of notification time plus preparation time plus response time.

The five events with the shortest evacuation times all had times of around two hours. Assuming a two-hour characteristic time for far field evacuation in the fire spread modeling shows the relative occupancy curve (Figure 124). Again, within the consequence calculator, this far field evacuation time is a user-controlled variable that can be changed based on the location, hazard area size, population density, etc., with consideration to the scenarios analyzed.

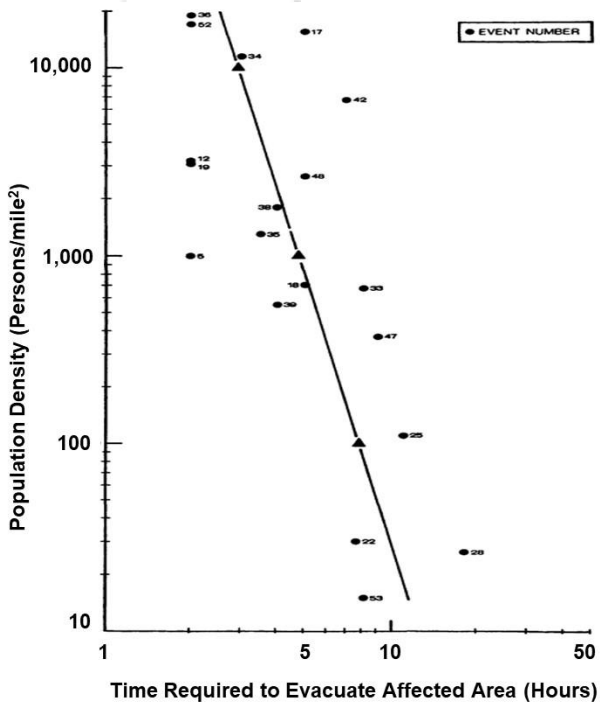

Figure 123. Population density versus evacuation time (Hans, 1974)

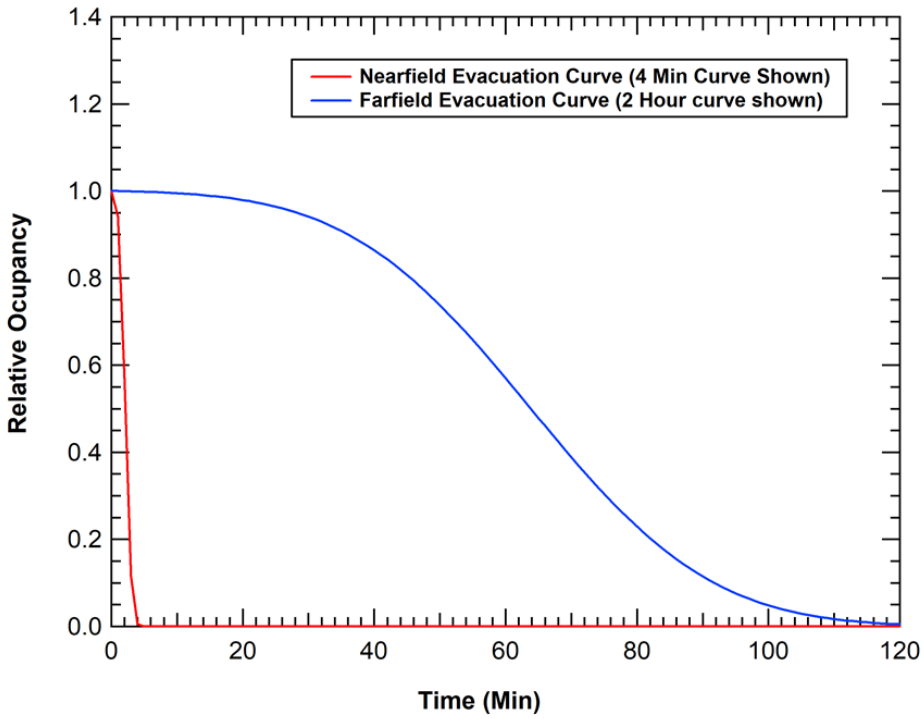

Figure 124. Example 4-minute nearfield and 2-hour far field evacuation curves

8.3 Consequence Analyses

QUIC-FST analyses were applied to all factorial combinations of the experimental factor level conditions listed in Table 69. The analyses considered three locations (i.e., rural, suburban, and urban) with corresponding population densities, spill sizes, and different wind conditions, for a total of 27 fire spread scenarios.

Table 69. Factor level matrix of fire spread consequence analyses

Factor	Level 1	Level 2	Level 3
Location (Description and Lat. and Lon.)	Rural Lat: 33.620294° Lon: -83.586634°	Suburban Lat: 33.818623° Lon: -84.226467°	Urban Lat: 33.750259° Lon: -84.385777°
Spill Size	30,000 Gallons	60,000 Gallons	90,000 Gallons
Wind Condition	Low: 1 mph	Medium: 10 mph	High: 20 mph

The three locations selected were all along a single rail line that runs through the greater Atlanta metropolitan area. The three locations are shown in Figure 125 through Figure 127. At each location, three different size spills were evaluated to be equivalent to one, three, and five tank cars spilling all their contents into the initial pool for the fire spread analyses. Similarly, for each combination of location and spill size, analyses were performed with steady wind conditions at 1, 10, and 20 mph.

(a) Location selected for the rural fire spread analyses [Google Earth]

(b) Analysis zone for the potential QUIC-FST fire spread

Figure 125. Location for the rural QUIC-FST fire spread analyses

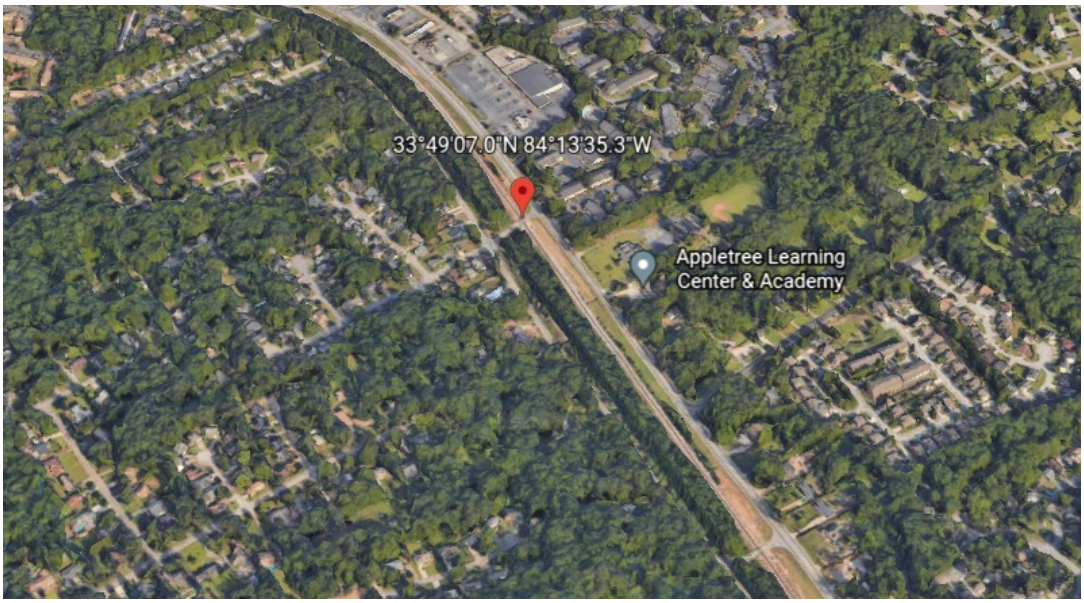

(a) Location selected for the suburban fire spread analyses [Google Earth]

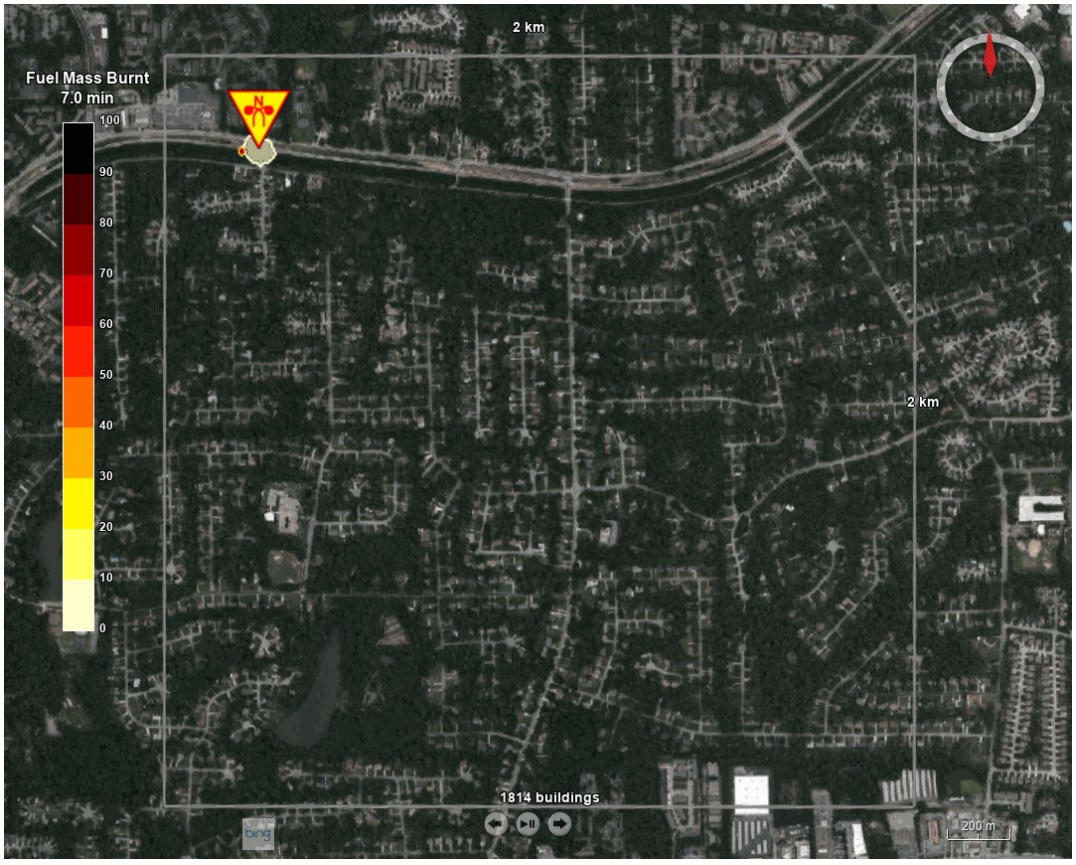

(b) Analysis zone for the potential QUIC-FST fire spread

Figure 126. Location for the suburban QUIC-FST fire spread analyses

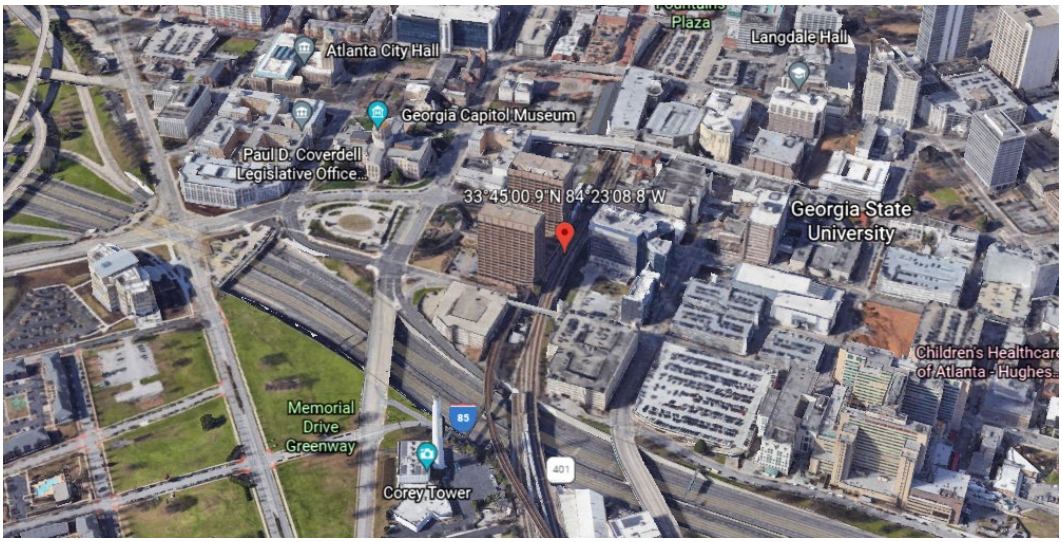

(a) Location selected for the urban fire spread analyses [Google Earth]

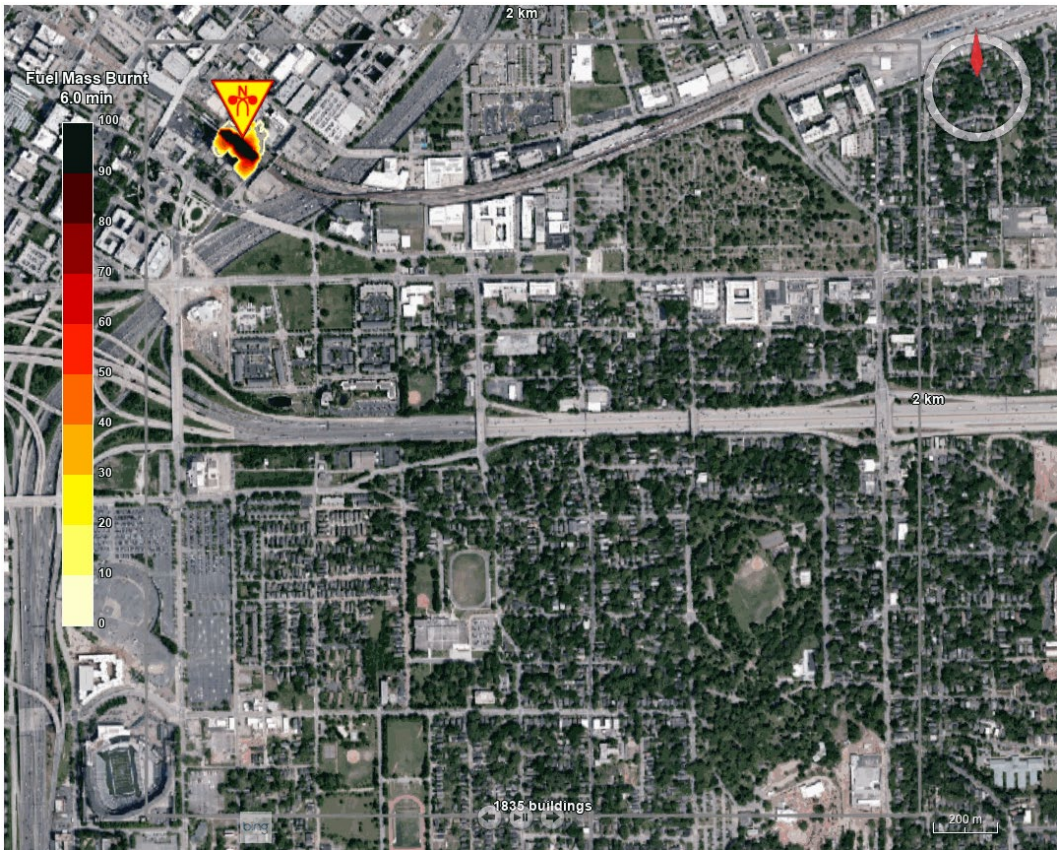

(b) Analysis zone for the potential QUIC-FST fire spread

Figure 127. Location for the urban QUIC-FST fire spread analyses

Estimates of the annual wind conditions were obtained from open-source weather data such as that obtained from the Iowa Environmental Mesonet (IEM). For example, a wind rose summarizing the annual wind conditions at the DeKalb-Peachtree Airport northeast of Atlanta is shown in Figure 128. The most common wind direction is from the northwest (blowing

southeast). This is the wind direction that was used in the QUIC-FST fire spread analyses. Furthermore, the data can be used to determine the weighting of typical wind conditions. For example, at this location, the wind is less than 5 mph 44.5 percent of the time, between 5 and 15 mph 51.6 percent of the time, and greater than 15 mph 3.9 percent of the time.

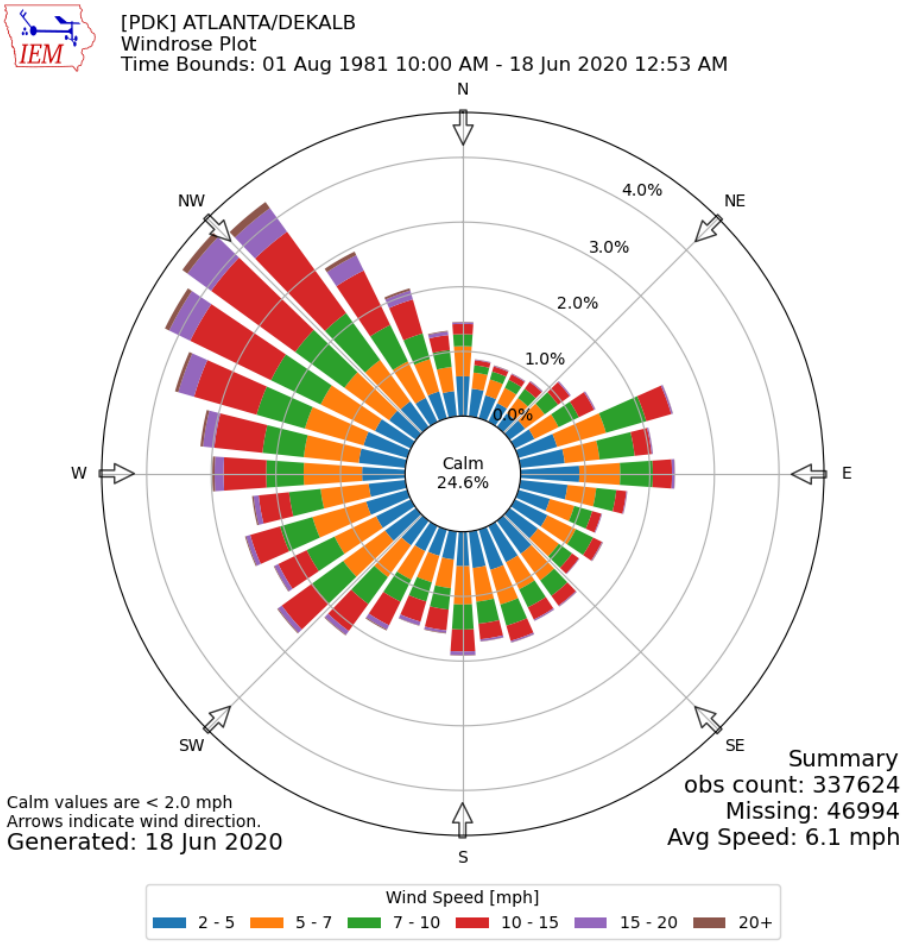

Figure 128. Wind rose for the annual wind profile outside Atlanta (Iowa State University, Department of Agronomy, 2022)

An accurate incorporation of wind effects would require a more detailed assessment of weather at each location throughout the year. The corresponding IEM wind rose summarizing the July wind conditions at the DeKalb-Peachtree Airport northeast of Atlanta is shown in Figure 129. The data show that the wind patterns in the summer (when there is a higher wildfire risk) have a more easterly direction. Additionally, there is a lower percentage of high winds in July with winds less than 5 mph 49.5 percent of the time, between 5 and 15 mph 49.2 percent of the time, and greater than 15 mph 1.3 percent of the time. These percentages can be used in the consequence analyses to weight results for the 1, 10, and 20 mph wind condition scenarios.

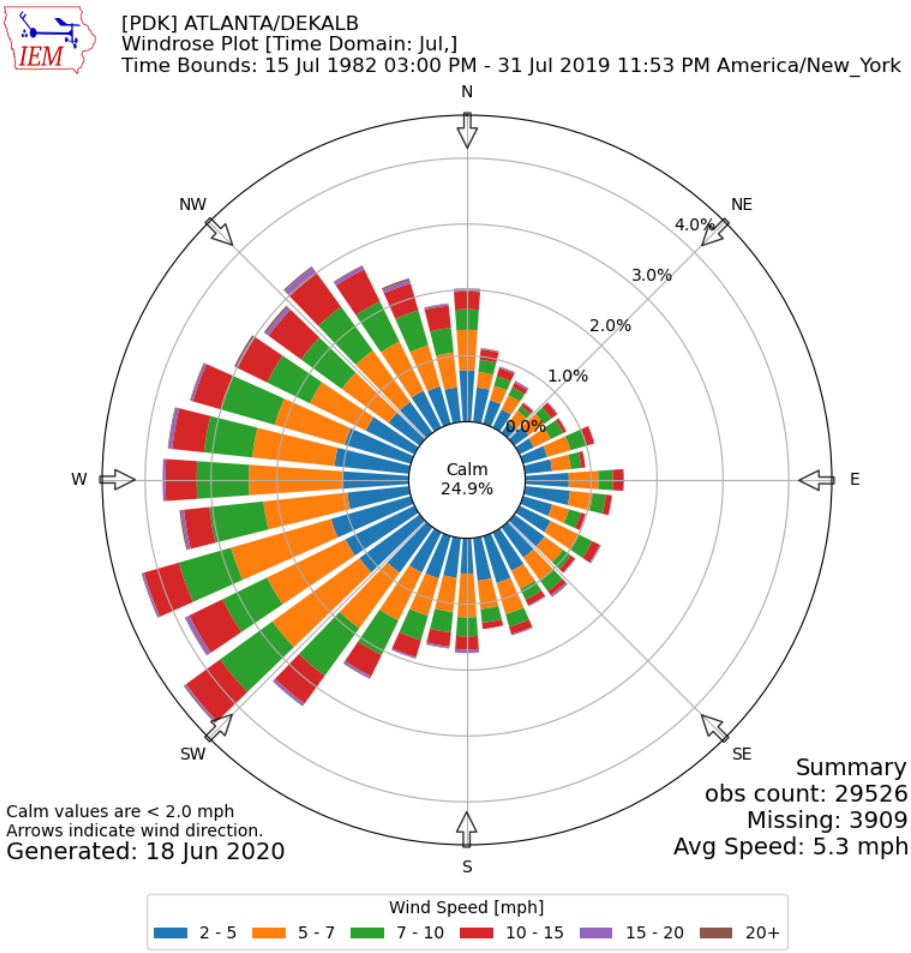

Figure 129. Wind rose for the July wind profile outside Atlanta (Iowa State University, Department of Agronomy, 2022)

Example fire spread analyses for the medium (3 tank) spill suburban fire scenarios are shown in Figure 130 (2-hour response shown). The 1-mph wind case remains primarily a fire around the original spill pool zone. The 10-mph wind analysis has spread somewhat downwind, but the fire spread is modest and would likely be controlled by the emergency response that would be employed in a suburban area. In contrast, the 20-mph high wind condition results in a rapid downwind fire spread that would be very difficult to contain in the initial emergency response and would likely result in an uncontrolled fire.

The comparison of the three scenarios shows that the high winds analyzed resulted in an orders-of-magnitude greater sized hazard area. As a result, it is an extreme outlier event and is significant for the overall consequence analysis severity.

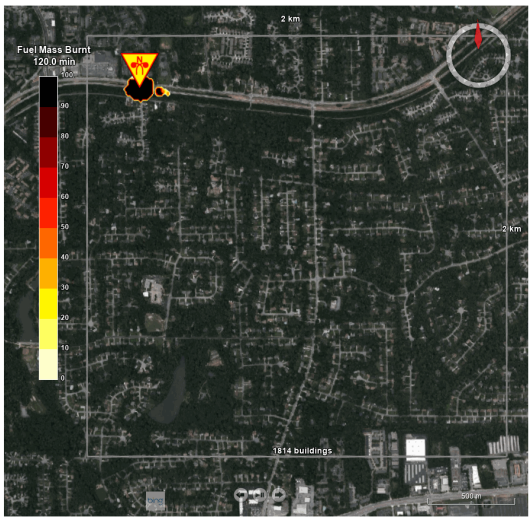

(a) 1-mph wind analysis

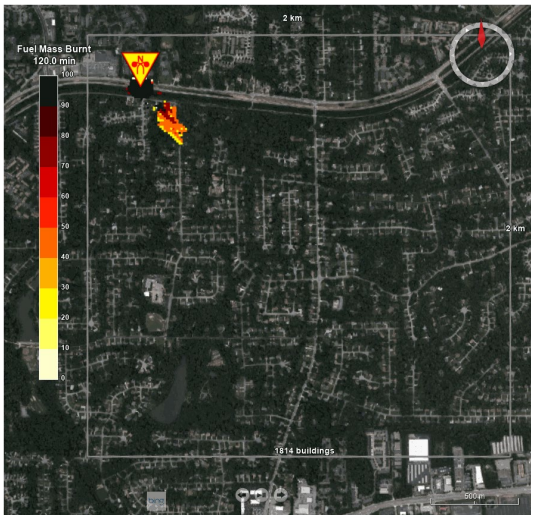

(b) 10-mph wind analysis

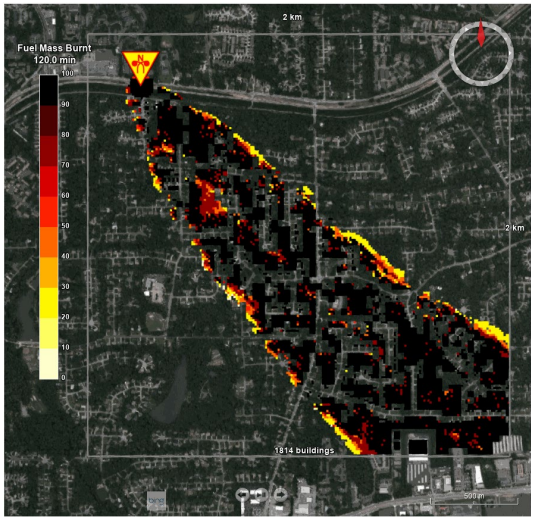

(c) 20-mph wind analysis

Figure 130. Effect of wind on the QUIC-FST fire spread analyses (suburban location)

One of the issues identified in the analysis was that the high wind scenarios (20 mph) had fires extending beyond the analysis boundary and thus required correction. The models for the sites were developed with a finite boundary indicated by the square in Figure 130. For the high wind scenarios, the fire zone clearly spreads outside this zone. However, the consequence measures are only calculated within the initial model boundary defined.

The ideal approach to correct this issue would be to redefine a larger model area and rerun the analyses. However, there were insufficient resources in this pilot study to rerun the analyses. As a result, an approach was developed to extrapolate the fire spread and associated consequence measures to correct for the limitations introduced by the model boundary.

The fire spread behavior for the suburban medium spill scenario with the 20-mph wind condition is shown in Figure 131. The earlier time response shown in Figure 131a shows that the fire in the high-wind case reaches the boundary of the model at approximately 40 minutes. The

corresponding raw burn area data output from the analyses is shown in Figure 132a. The burn area data shows that the area has an exponential growth in the early portion of the analysis contained within the model boundaries. However, beyond this point, at approximately 40 minutes, the growth flattens out as the fire zone extends primarily outside the model boundary.

To correct this issue in the analyses, the data beyond the time at which the fire zone reaches the model boundary was truncated. A polynomial curve was then fit to the early time fire spread. This polynomial curve was subsequently used to extrapolate the calculated early time fire spread response. These corrected fires spread curves are shown in Figure 132b. The other consequence measures (e.g., buildings affected, casualties) are also extrapolated proportionally with the burn area.

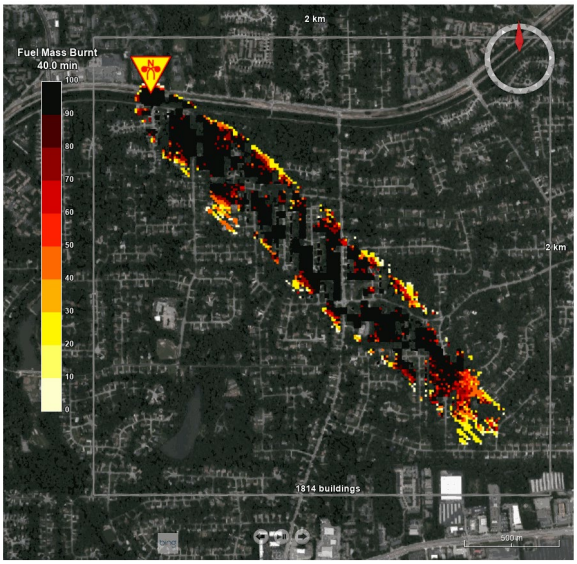

(a) 40-minute fire spread

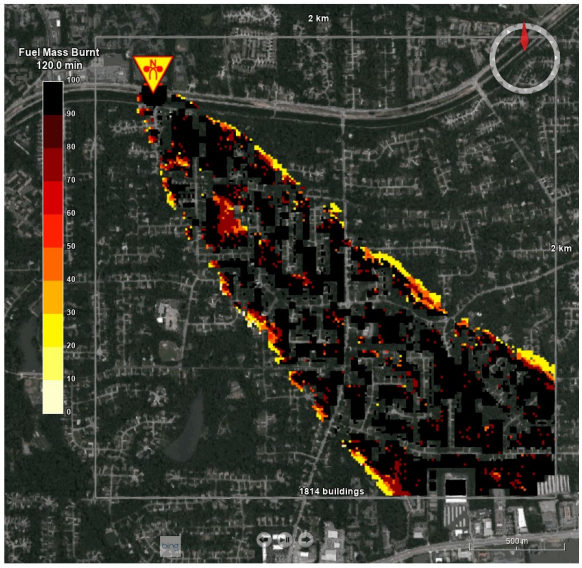

(b) 120-minute fire spread

Figure 131. Spread of the fire beyond the QUIC-FST analysis boundary

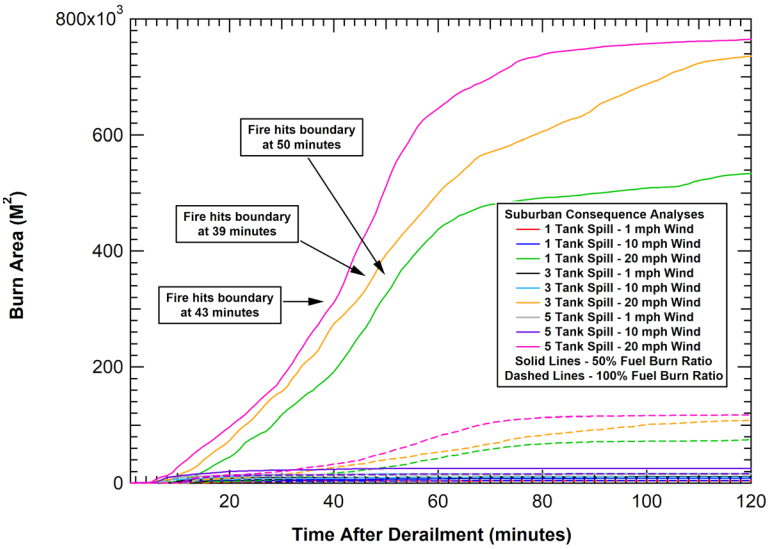

(a) Raw burn area data

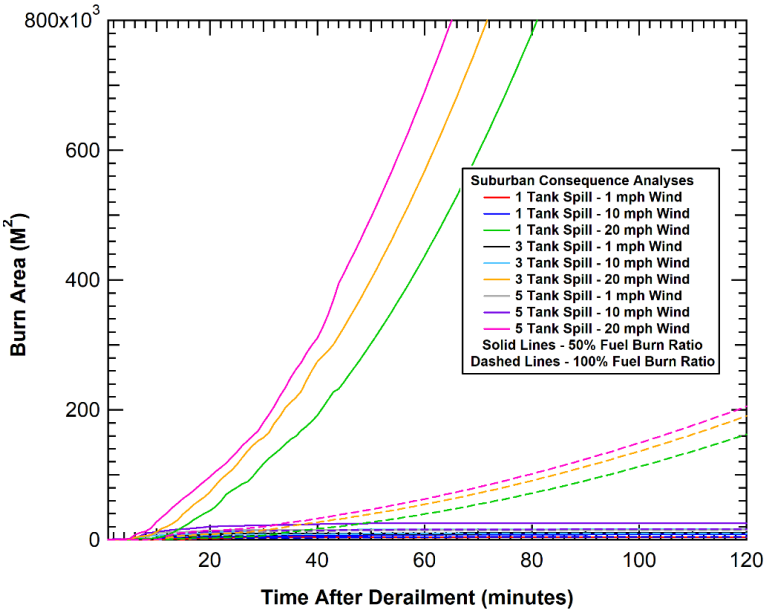

(b) Corrected burn area data with extrapolation

Figure 132. Raw and corrected fire spread data for the QUIC-FST analyses

Another issue identified by the analyses is that there are significant limitations imposed by the scope of this trial study. With only three locations and three wind conditions, the selection of those locations and wind directions will have a larger influence on the overall consequence than it would with a significantly larger distribution of sites and conditions. A demonstration of this effect is shown in Figure 133 where the medium spill/ high wind analyses for both the rural and suburban sites are compared. The rural site selected had a significant amount of farmland downwind with a low level of supplemental fuel for the fire spread. As a result, the fire has natural barriers that result in preventing the uncontrolled wildfire from spreading. This can be seen in the comparison of the burn areas for the high wind cases in Figure 134. The fire growth is uncontrolled in the urban and suburban scenarios. However, the rural fire spread has stopped after approximately 50 minutes and the fire has effectively burned itself out.

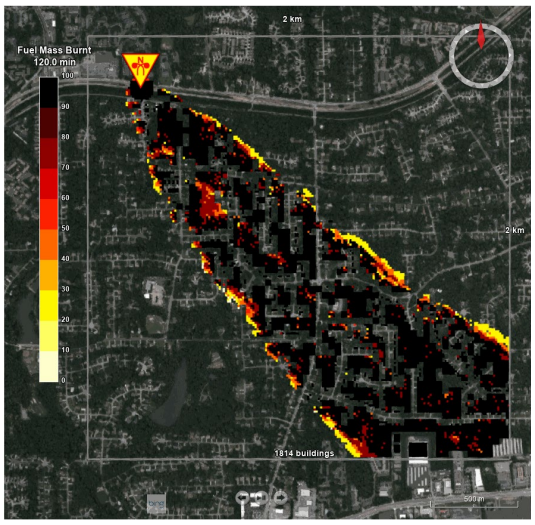

(a) 120-minute suburban fire spread

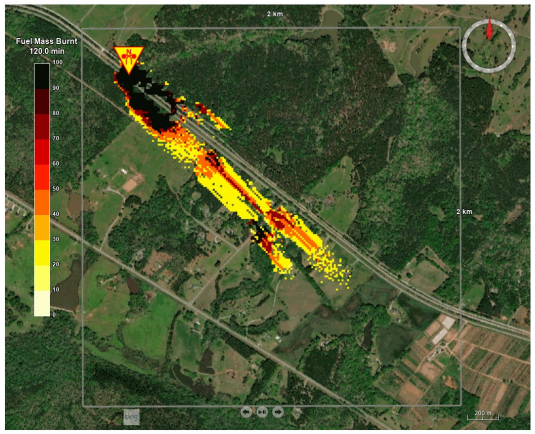

(b) 120-minute rural fire spread

Figure 133. Spread of the fire beyond the QUIC-FST analysis boundary

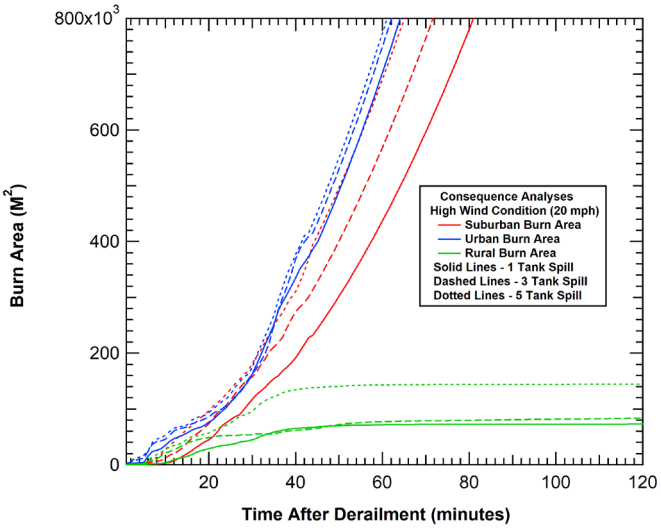

Figure 134. Comparison of the high wind burn areas for the three locations

In a more expanded study, sites with different characteristics should be added, such as differentiating rural farmland sites and rural forested locations. To demonstrate this effect, a supplemental analysis was performed for this location where the wind direction was modified to be in a slightly more easterly direction through a more highly vegetated region. The analysis is for the medium (3 tank) spill, and the comparison of this scenario with the corresponding baseline wind orientation is shown in Figure 135. With the altered wind direction, the fire spread again rapidly grows with more uncontrolled behavior and goes beyond the analysis boundary.

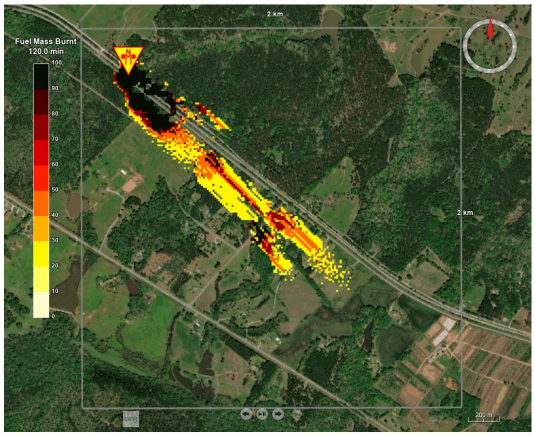

(a) 120-minute rural fire spread (baseline wind direction)

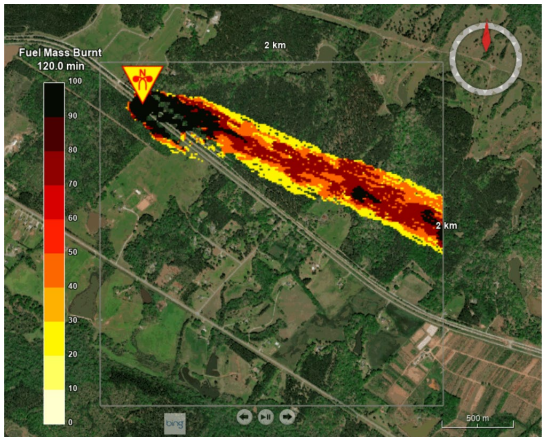

(b) 120-minute rural fire spread (modified wind direction)

Figure 135. Spread of the fire beyond the QUIC-FST analysis boundary

It should be noted that the baseline wind orientation results were used in this trial study and for the development of the consequence calculator. Since a large portion of a route is typically rural, this will have an influence on reducing the burn area consequence metric. However, the rural analyses do not result in any burned buildings or casualties. Thus, the rural site selection will not have an impact on the other consequence metrics.

The other consequence metrics obtained from the urban and suburban consequence analyses are shown in Figure 136 and Figure 137. The buildings at risk in the fire spread analyses are shown in Figure 136. Clearly, the wildfire spread in the 20-mph high wind scenarios are outliers compared to the other scenarios. The worst-case large spill analyses with 10-mph wind only result in 5 buildings at risk in the suburban analysis and 13 buildings at risk in the urban analysis.

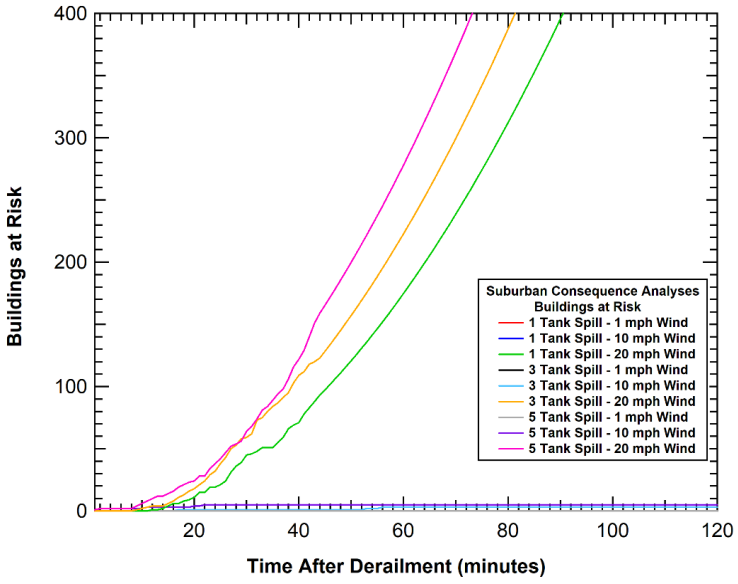

(a) Suburban analyses

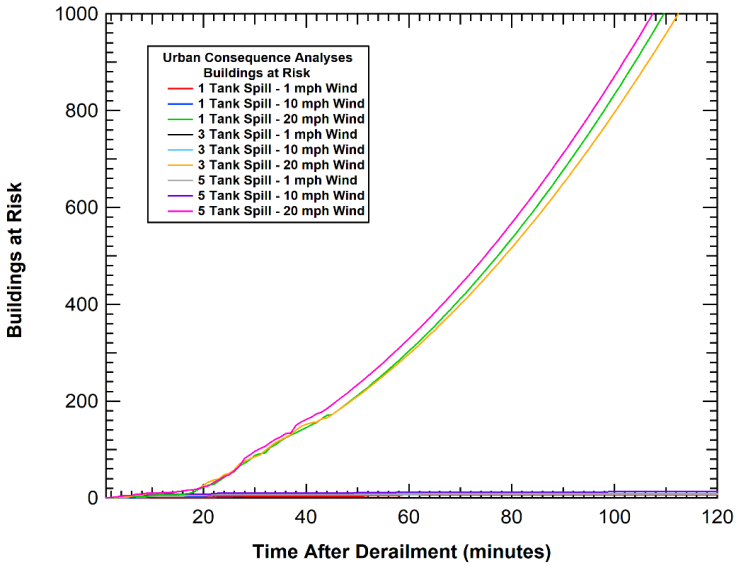

(b) Urban analyses

Figure 136. Buildings at risk from fire spread in the QUIC-FST analyses

The calculated smoke inhalation and fire (i.e., burn) casualties are summarized in Figure 137 and show similar trends. The raw casualty numbers are quite high for multiple reasons. The first is that these results reflect full occupancy rates without any adjustments for evacuations. Incorporating evacuation corrections would result in the prevention of most casualties. Note that the casualty numbers include both injuries and fatalities, and that 86 percent are injuries rather than fatalities. Note also that the 20-mph wind scenarios are driven by rapid expansion of the fire area caused by wind driven hotspot initiation events. This behavior is chaotic, and the magnitude of the consequences do not always remain in the same order of the initiation size (e.g., the smaller spill results in a slightly higher consequence level at later times). This may also have been exacerbated by the procedures applied to extrapolate the cues when the fire spread beyond

the calculation zone. Ideally, a much larger number of fires spread simulations would be analyzed, and on average, these effects would likely be eliminated.

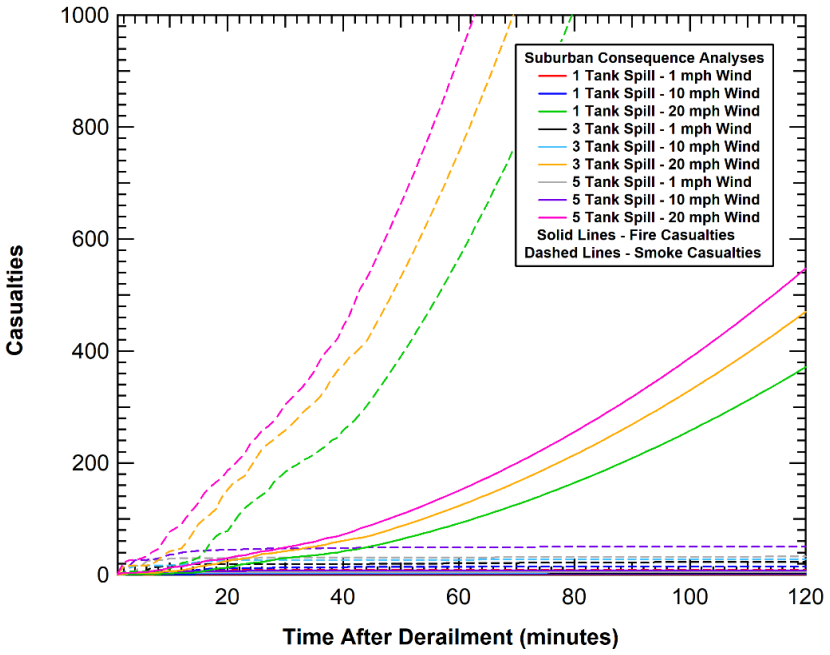

(a) Suburban analyses

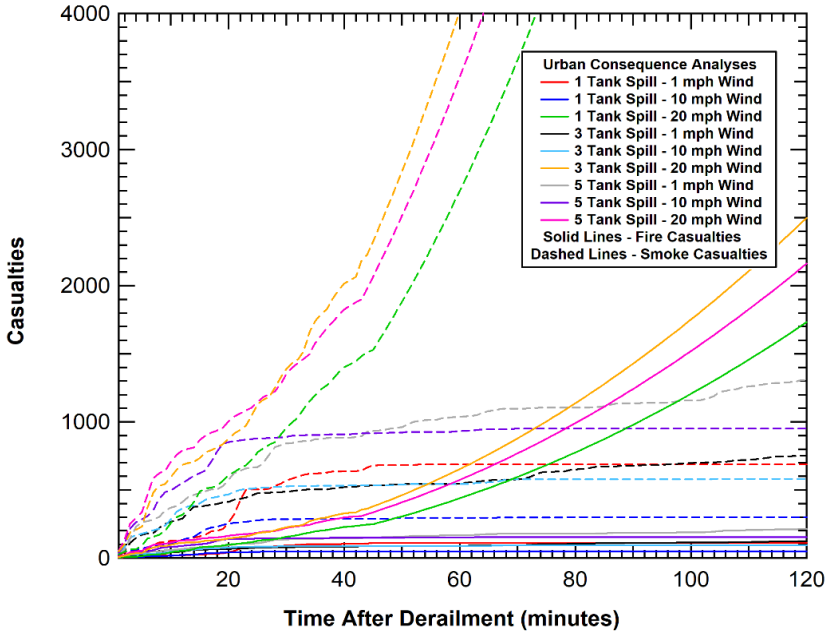

(b)

(c) Urban analyses

Figure 137. Raw casualties from fire spread in the QUIC-FST analyses

8.4 Corrected Consequence Curves

The consequence curves presented in the previous section are the raw results from the QUIC-FST analyses. To obtain a better measure of the true risk of a derailment and fire the team scaled

these results by the appropriate correction factors. These include factors like the annual fuel load moisture content correction (described in Section 8.2.5) and population evacuation corrections (described in Section 8.2.6).

An additional factor to be included in the assessment is a distribution of the route (i.e., network) that falls into the different population and building density zones. In this example, it was assumed that 95 percent of the route is rural, 4 percent is suburban, and 1 percent is urban.

As described in Section 8.3, the local wind data also was applied to develop the combined consequence curves. As stated in that section, an accurate incorporation of wind effects would require a more detailed assessment of weather at each location and how it varies throughout the year. A high wind in the middle of the fire season is much more hazardous than a high wind in winter. For the sake of the analyses in this section the team assumed a low wind condition 50 percent of the time, a medium wind condition 49 percent of the time, and a high wind condition 1 percent of the time.

Using these assumed characteristics for the route, corrections for evacuation, and seasonal corrections for dire spread, the team obtained the various consequence measures for different size spills. The buildings at risk per derailment that results in a fire for the different spill size initiating events are shown in Figure 138.

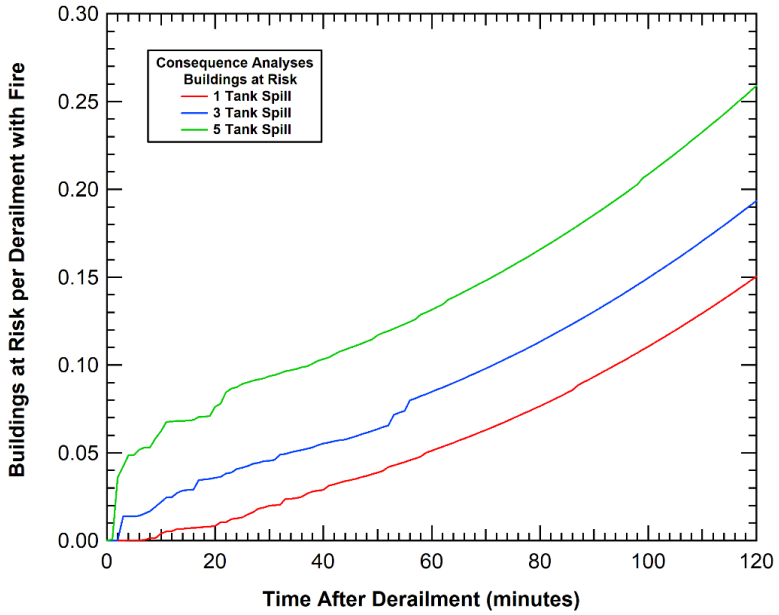

Figure 138. Corrected buildings at risk for a derailment and fire

The number of buildings at risk after 2 hours burn time range from 0.15 buildings per derailment resulting in a fire initiated by a 1-tank spill size up to 0.26 buildings for a derailment and fire initiated by a 3-car spill size. The corresponding curves for the area with a 50 percent and 100 percent fuel burn ratio are provided in Figure 139.

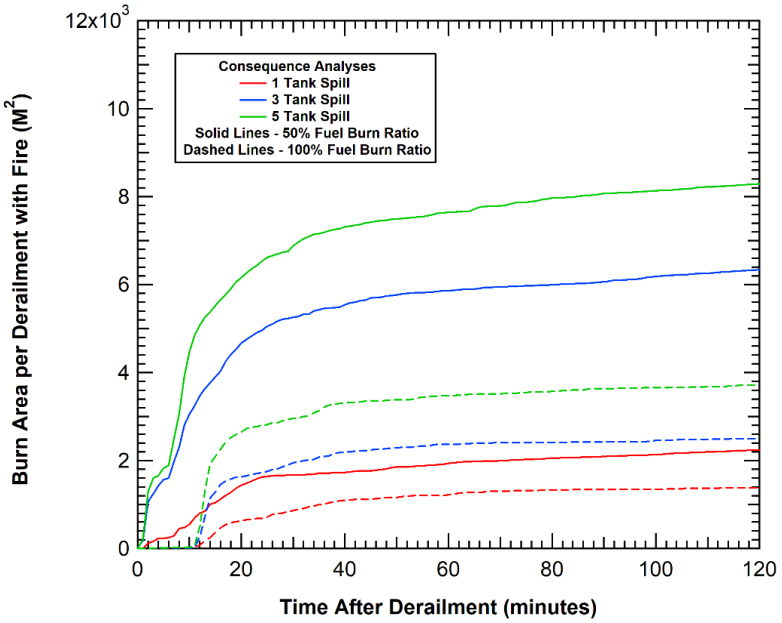

Figure 139. Corrected fuel burn areas for a derailment and fire

The consequence curves for smoke, burn and total casualties (defined as serious injuries plus fatalities) as well as the curves for total fatalities per derailment and fire with the different spill size initiating events are shown in Figure 140 and Figure 141.

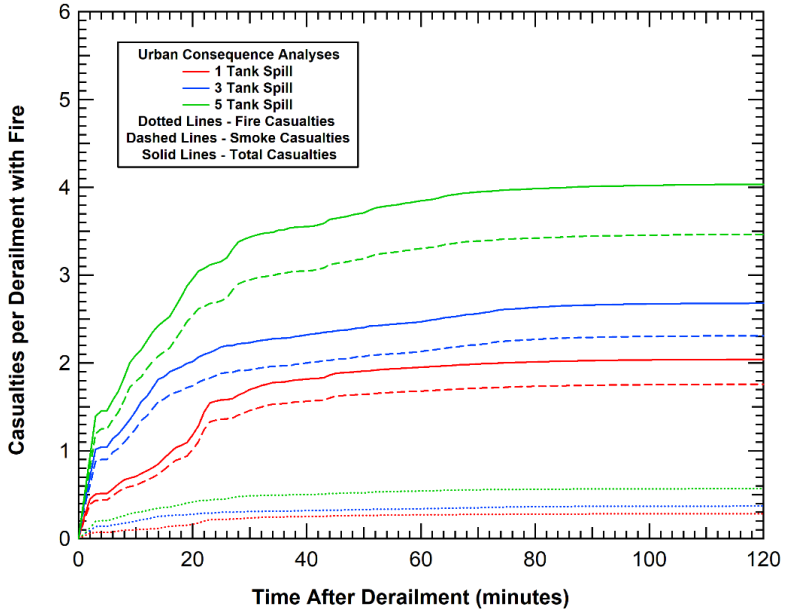

Figure 140. Corrected buildings at risk for a derailment and fire

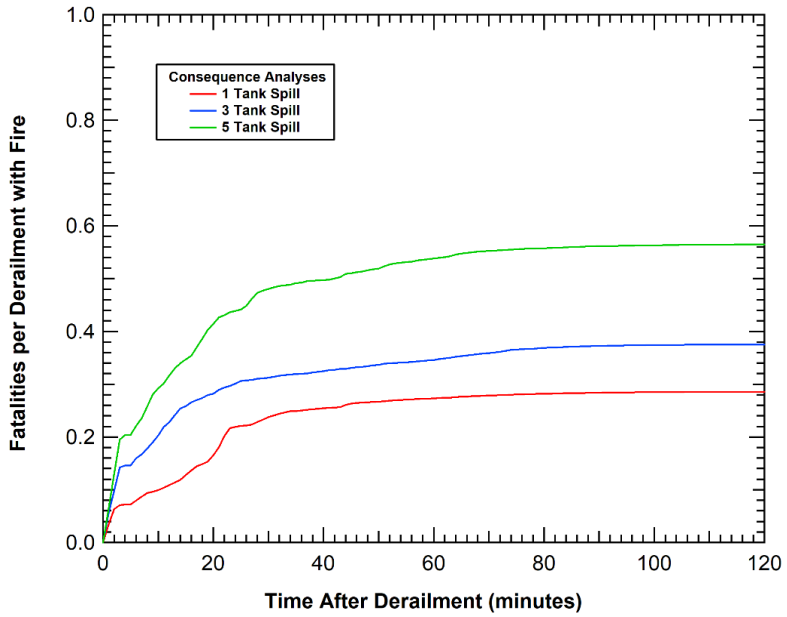

Figure 141. Corrected fuel burn areas for a derailment and fire

The total casualties per derailment with fire (2-hour time duration) ranges from approximately two for the 1-car spill to approximately four with the 3-car spill. Most of the casualties are serious injuries from smoke inhalation. The corresponding fatalities per derailment with fire (2-hour time duration) ranges from 0.28 for the 1-car spill to 0.56 for the 3-car spill.

8.5 Limitations of the Consequence Analyses

The consequence analyses performed here were part of a preliminary study to demonstrate an approach to analyze consequences resulting from changes in severity of flammable liquid releases in unit trains versus manifest trains. The scope was limited to assessing derailments resulting in fires at three locations, at three spill sizes, and under three wind conditions. Performing an assessment that would be representative of the US freight rail network would require analyses over a much wider range of locations and conditions.

Furthermore, the curves presented in Section 8.4 contain only preliminary estimates for wind conditions, fire fuel moisture content distributions, and network or route population density distributions.

Finally, the above assessment is for derailments that result in a spill and fire. Additional corrections should be applied to determine the percentage of derailments that result in fires for different severity derailments and different sized releases.

9. Railroad Hazmat Transportation Case Study

Section 3 summarizes the proposed methodology for a risk analysis comparison of unit and manifest trains, considering both the mainline and yard components of freight rail transportation. To demonstrate the application of this approach to an actual railway hazmat transportation scenario, this section presents a detailed step-by-step case study calculation and comparison using the methodology outlined in Section 3 and further detailed in subsequent sections. Eight scenarios were considered to compare the performance of unit trains and manifest trains carrying the same amount of hazmat from the same origin to the same destination under different conditions.

9.1 Case Study Overview

This case study was inspired by an actual hazmat unit train derailment and release incident. On November 7, 2013, a southbound Alabama & Gulf Coast Railway (AGR) train was traveling from Amory, Mississippi, toward Walnut Hill, Florida, with 88 loaded hazmat tank cars, two buffer cars, and three locomotives. The train derailed 26 railcars and one locomotive near Aliceville, Alabama, leading 26 tank cars to release a combined volume of approximately 720,000 gallons of crude oil.

The case study is designed to evaluate the relative risk of making a similar crude oil shipment in a single unit train as compared to multiple manifest trains. The team assumed that 100 high-hazard flammable tank cars were transported from Amory, Mississippi, to Walnut Hill, Florida (approximately 400 miles). Two options were proposed to transport the 100 tank cars to compare the risks related to each operating strategy:

- One unit train with five locomotives and 100 tank cars
- Five manifest trains, each including 80 non-tank cars and a block of 20 tank cars

Regardless of the train type, the following assumptions were made:

- Train speed is 25 mph
- Each train has five locomotives (each weighing 212.5 tons)
- Each railcar is loaded with a gross railcar weight of 143 tons (regardless of car type)
- All tank cars conform to DOT 117 specification standards
- The conditional probability of release for a DOT 117 tank car is 0.043 (Treichel et al., 2019a)
- Derailment rates and parameters used in various distributions are all estimated based on Class I railroad annual report financial data, Surface Transportation Board waybill sample data, and mainline and yard/terminal derailments from the FRA REA database for the years 1996-2018, as described in previous sections.
- The factor reflecting the percentage of release accidents involving fires is estimated based on historical derailment data from the TCAD from 1980 to 2018 (Treichel et al., 2019b). The TCAD data shows that 65 out of 1,863 release accidents involved fire events. Thus, for illustration, the factor f in Equation (3-16) is assumed to be 3.49 percent (65/1,863) in this case study.

9.2 Case Study Scenarios

Using the methodology outlined in previous sections, the team quantified and compared the risk associated with one 100-car unit train or five manifest trains (each containing a block of 20 tank cars and 80 non-tank cars) traveling 400 miles at a speed of 25 mph across multiple scenarios (Table 70).

The eight case study scenarios were designed to test the impact of five different factors, as follows:

- **Train Type** is the primary factor. Scenarios 1 and 2 use one unit train to transport all 100 tank cars. Scenarios 3-8 use five manifest trains (each containing a block of 20 tank cars and 80 non-tank cars) to transport a total of 100 tank cars.
- **Tank Car Positions in the Manifest Train** is the second factor. Scenarios 3, 5, and 6 place the block of 20 tank cars at the back of the train (i.e., the location with the lowest probability of derailment according to the probability distribution of position-based derailment on the mainline), while Scenarios 4, 7, and 8 place this block at the middle of the train (i.e., the highest probability of derailment according to the probability distribution of position-based derailment on the mainline).
- **Yard/Terminal Calculation Approach** is used to compare the relative risks resulting from using the *detailed approach* (described in Section 6.4.2) with a known number of yards and terminals, and the *generic approach* (described in Section 6.4.1) where the number of yards and terminals is not known. Scenario 1 applies the generic approach to the unit train. Using the generic approach for unit trains is presented for illustrative and comparative purposes only, since in practice, the detailed approach can always be applied to a unit train with its known operating pattern of one origin and one destination terminal. Scenarios 3 and 4 apply the generic approach to the manifest train, Scenario 2 applies the detailed approach to the unit train, and Scenarios 5-8 apply the detailed approach to the manifest train.
- **Yard Switching Approach** is considered to compare the relative effects of making different assumptions about how railcars are switched in the yard. Scenarios 3, 5, and 6 consider the block of 20 tank cars to be *switched alone*. Scenarios 4, 7, and 8 consider the block of 20 tank cars to be switched *en masse* with a similarly sized group of non-hazmat railcars. Note that in this experiment design, the position of the tank car block in the manifest train on the mainline is correlated with the switching approach: tank cars positioned at the middle of the manifest train are switched *en masse*, while tank cars positioned at the back of the train are switched alone. This correspondence reflects the practicalities of how a manifest train might be switched by backing it over a hump or switching lead upon arrival at a classification yard. This factor does not apply to unit train Scenarios 1 and 2.
- **Yard Type** is included to compare the relative risks of hump and flat switching yards. Scenarios 5 and 7 use flat yards, while Scenarios 6 and 8 use hump yards. Scenarios 3 and 4 use average rates and distributions calculated across both yard types to reflect unknown yard types. This factor does not apply to unit train Scenarios 1 and 2 since they both involve unit train terminals instead of classification yards.

Each of the eight scenarios was assigned a three- or five-character code to track the various factor levels associated with it. Each character designates the level of one of the five factors. For example, **MBDAH** corresponds to **M**anifest, **B**ack of train, **D**etailed approach, switched **A**lone, and **H**ump yard; **U-G-T** represents **U**nit, **G**eneric approach, and **T**erminal. Other character designations are defined below Table 70.

Table 70. Case study scenarios

Scenario and Code	Train type	Number of trains needed to transport 100 tank cars	Position of 20 tank car block in manifest train	Yard rate and switching approach	Number of terminals or classification yards	Yard type
1 U-G-T	Unit train	1	n/a	Generic, n/a	Unknown	Term.
2 U-D-T	Unit train	1	n/a	Detailed, n/a	1 origin 1 destination	Term.
3 MBGAL	Manifest train	5	Back of train	Generic, Alone	Unknown	All
4 MMGEL	Manifest train	5	Middle of train	Generic, En Masse	Unknown	All
5 MBDAF	Manifest train	5	Back of train	Detailed, Alone	1 origin 1 intermediate 1 destination	Flat
6 MBDAH	Manifest train	5	Back of train	Detailed, Alone	1 origin 1 intermediate 1 destination	Hump
7 MMDEF	Manifest train	5	Middle of train	Detailed, En Masse	1 origin 1 intermediate 1 destination	Flat
8 MMDEH	Manifest train	5	Middle of train	Detailed, En Masse	1 origin 1 intermediate 1 destination	Hump

All = Uses factors calculated across both yard types
Term.: unit train **term**inal
U-G-T: **U**nit train, **G**eneric yard rate, unit train **T**erminal
U-D-T: **U**nit train, **D**etailed yard rate, unit train **T**erminal
MBGAL: **M**anifest train, **B**ack of train, **G**eneric yard rate, switched **A**lone, a**L**l yard types
MMGEL: **M**anifest train, **M**iddle of train, **G**eneric yard rate, switched **E**n masse, a**L**l yard types
MBDAF: **M**anifest train, **B**ack of train, **D**etailed yard rate, switched **A**lone, **F**lat yard type
MBDAH: **M**anifest train, **B**ack of train, **D**etailed yard rate, switched **A**lone, **H**ump yard type
MMDEF: **M**anifest train, **M**iddle of train, **D**etailed yard rate, switched **E**n masse, **F**lat yard type
MMDEH: **M**anifest train, **M**iddle of train, **D**etailed yard rate, switched **E**n masse, **H**ump yard type

9.3 Risk Calculation

Due to the large number of scenarios, the team first calculated the risks related to mainline transportation and yard transportation separately, and then combined them for each scenario. Instead of calculating the total risk associated with each scenario one by one, calculating the risks based on mainline and yard separately could avoid unnecessary repetition for similar scenarios.

9.3.1 Risk Related to Mainline Transportation

Using the approach introduced in previous sections to generate Table 3, the team calculated the train derailment probability by cause and train type for the case study train configuration of five locomotives (each weighing 212.5 tons), 100 total railcars (each weighing 143 tons regardless of type), and a speed of 25 mph. The derailment probabilities per shipment on a 1-mile segment of the mainline route for a unit train and manifest train are 8.53E-07 and 9.54E-07, respectively. Table 71 shows a comparison between the two operating strategies using manifest trains to carry 100 tank cars over 400 miles.

Table 71. Comparison between two operating strategies

Train type	Number of trains needed to carry 100 tank cars	Number of tank cars per train	Derailment probability per shipment
Unit train	1	100	8.53E-07
Manifest train	5	20	9.54E-07

Applying Equations (3-6) to (3-10) with all the parameters discussed in Section 3.1, the team obtained the probability distribution of position-based derailment. The risk of derailment increases initially and then decreases with a long tail as the position on the train moves toward the end. Thus, the best-case scenario, which places the block of tank cars at the end of the manifest train (train configuration is shown in Figure 142a), has the lowest derailment probability (the probability distribution of position-based derailment is shown in Figure 143a). For the worst-case scenario, the block of 20 tank cars is located immediately after five locomotives, which has the highest risk of derailment compared to all other positions. The train configuration for the worst-case scenario is described in Figure 142b and the probability distribution of position-based derailment is shown in Figure 143b.

(a) Best-case scenario

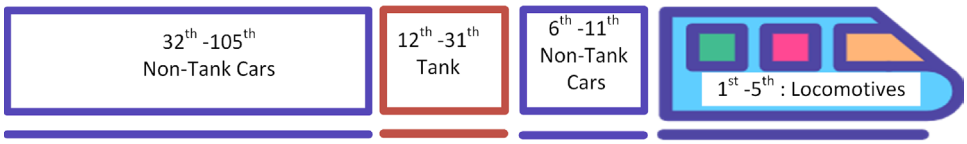

(b) Worst-case scenario

Figure 142. Train consist for the manifest train (a) best-case scenario, and (b) worst-case scenario

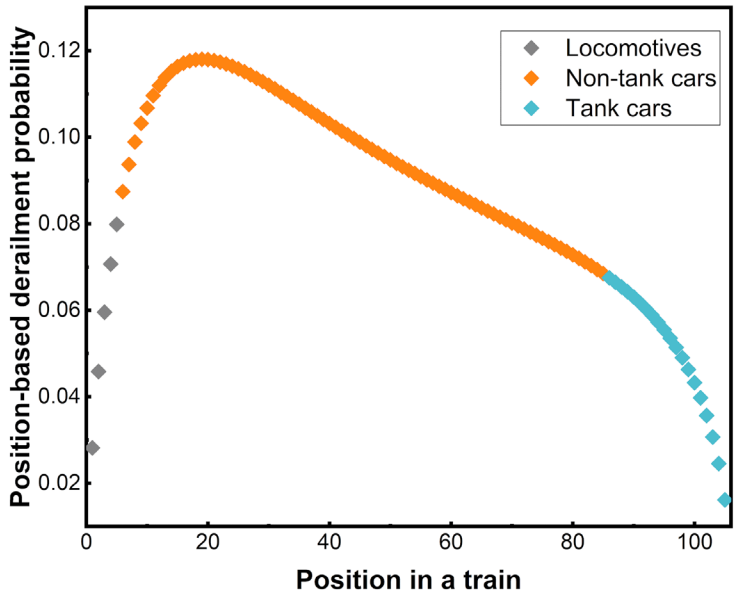

(a)

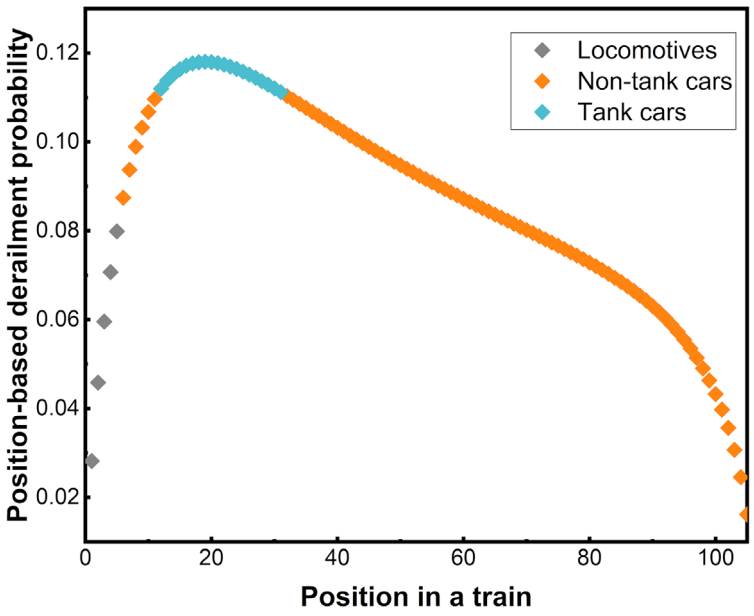

(b)

Figure 143. Position-based derailment probability distribution for the manifest train (a) best-case scenario, and (b) worst-case scenario on mainline

The lading capacity for DOT 117s varies according to detailed specifications, but generally ranges from 28,000 - 32,000 gallons. Therefore, the probability distribution of release quantity for one non-pressurized tank car developed from Section 3.1.8 is applicable. Using the same methodology as in Section 3.1.9, the team calculated the reverse cumulative distribution of release quantity per mile per train shipment for the unit train, the best-case scenario for the manifest train, and the worst-case scenario for the manifest train (Figure 144).

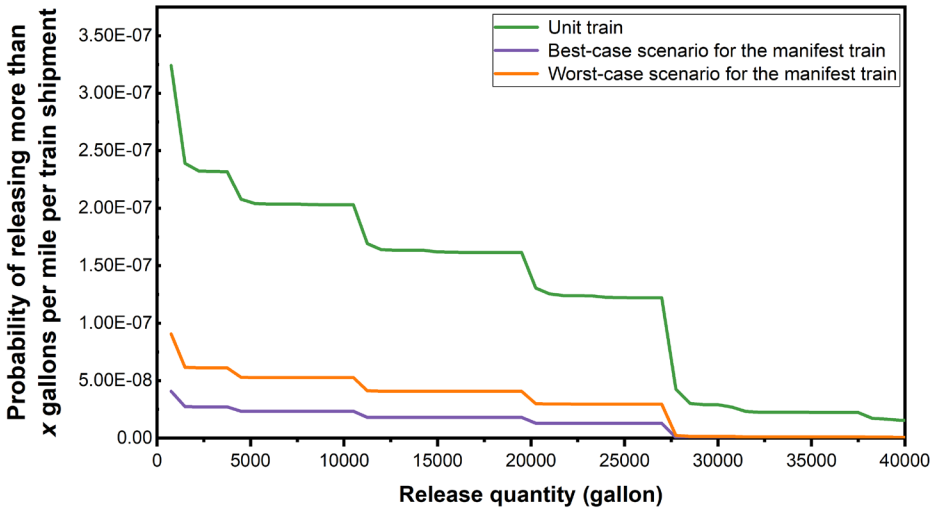

Figure 144. Reverse cumulative distribution of release quantity per train shipment per mile

The expected releasing quantities per shipment per mile are 5.23E-03 for the unit train, 5.35E-04 for the best-case scenario using the manifest train, and 1.22E-03 for the worst-case scenario using the manifest train. Since five manifest trains are needed to transport 100 tank cars, the expected releasing quantity for the strategies of using one unit train to transport all tank cars in one shipment, the best-case train configuration by five manifest trains, and the worst-case train configuration by five manifest trains (each shipment travels 400 miles) are calculated in Table 72. According to Table 72, from the perspective of the expected releasing quantity for all strategies on mainline, using five manifest trains and putting the hazmat cars at the lowest-risk position outperforms using one unit train to transport 100 hazmat cars. If the block of tank cars is placed at the highest-risk position, the resulting safety performance could be the worst amongst the three strategies.

Table 72. Summary of the expected releasing quantity for all strategies on mainline.

Scenarios	Total expected quantity of release on mainlines over 400 miles (gallons)
One unit train	2.09
The best-case train configuration by five manifest trains	1.07
The worst-case train configuration by five manifest trains	2.45

As outlined in Section 3.1.10, the consequence of release is defined as the expected casualties calculated by Equation (3-16). Table 73 lists the expected casualties for three strategies using different metrics: casualties per shipment per mile, casualties per traffic demand per mile, and casualties per traffic demand over 400 miles. A unit train has higher expected casualties per shipment per mile than a manifest train, regardless of the placement of the block of tank cars. However, the best-case train configuration by five manifest trains has fewer expected casualties than one unit train transporting 100 tank cars, while placing the block of tank cars at the highest-risk positions results in the largest expected casualties. The results of the comparison between strategies using unit trains or manifest trains (shown in Table 73) are similar, with the safest train operating plan being sensitive to the exact position of the hazmat cars in the manifest train. As

such, it is important to consider the risks in the yard (for manifest trains) and terminal (for unit trains) in addition to the risks on mainlines.

Table 73. Summary of expected casualties for all strategies on the mainline

Strategy	Casualties per shipment per mile	Casualties per traffic demand per mile	Casualties per traffic demand over 400 miles
One unit train	4.84E-07	4.84E-07	1.94E-04
The best-case train configuration by five manifest trains	5.20E-08	2.60E-07	1.04E-04
The worst-case train configuration by five manifest trains	1.18E-07	5.91E-07	2.36E-04

9.3.2 Risk Related to Yard and Terminal Operations

Compared to transporting the case study shipment in a single unit train shuttling between loading and unloading terminals, transporting 100 tank cars in multiple manifest trains introduces the additional probability of releasing hazardous materials due to derailments while being disassembled, sorted, and reassembled into new trains at classification yards. Both train service options also experience additional non-mainline risk when arriving at and departing from terminals (for unit trains) and classification yards (for manifest trains). This section calculates the case study yard and terminal derailment risks associated with each train service strategy previously described in Table 70. It is necessary to calculate the respective yard risks for manifest train shipments and terminal risks for unit train shipments separately, given the distinct risk composition of each type of train. In addition to train type, as explained in Section 9.2, the yard and terminal calculations must also consider the yard/terminal calculation approach, railcar position in the manifest train, yard switching approach, and yard type.

9.3.2.1 Yard and Terminal A/D Derailment Likelihood

6.1.1.1.1 Case Study with Unit Trains

For the case study with unit trains, there are two A/D scenarios to consider. If the specific number of terminals involved is unknown, the generic mileage-based approach is applied to calculate the expected likelihood of unit train A/D derailments at terminals (Scenario 1 U-G-T). This approach would not normally be applied in practice, since, by definition, a unit train operates between one origin terminal and one destination terminal, which is known and can be calculated by the detailed approach. However, it is presented here for completeness and to allow for fair comparisons with manifest train scenarios employing the generic approach. The second approach represents the practical condition where the number of terminals is known. This detailed, route-based approach considers that the unit train operates between two terminals (i.e., one origin and one destination) in calculating the number of A/D events and the corresponding likelihood of terminal A/D derailment (Table 74). In both cases, the calculation of overall unit train A/D derailment likelihood combines the train-mile and car-mile (or trains processed, and railcars processed) unit train A/D derailment rates introduced in Section 6 to reflect derailment causes linked to each respective metric.

For the case study shipment in a single unit train covering 400 miles between origin and destination terminals, the generic approach in Scenario 1 (U-G-T) yields a lower derailment

likelihood than the detailed approach in Scenario 2 (U-D-T), although both share approximately the same order of magnitude. For a relatively short unit train shipment of 400 miles, the generic approach is expected to underestimate the unit train A/D derailment likelihood because fewer mainline train-miles and car-miles are accumulated for each terminal A/D event. This difference in results highlights the benefit of applying the detailed approach that directly considers the number of train A/D events in calculating A/D derailment likelihood and not just the mainline travel distance as a proxy.

Table 74. Case study: likelihood of unit train terminal arrival and departure derailment

Metric Unit	Metric unit proportion	Unit Train Arrival/Departure	
Mainline train-miles	62.80%	(Unit Train A/D Derailments per Mainline Train-Mile) × (400 train-miles)	1.92E-04
Mainline car-miles	37.20%	(Unit Train A/D Derailments per Mainline Car-Mile) × (400 miles × 100 cars)	1.85E-04
Generic Approach	Combined	Scenario 1 (U-G-T)	**1.89E-04**
Trains processed	62.80%	(Unit Train A/D Derailments per Train A/D Event) × (2 A/D events)	2.53E-04
Cars processed	37.20%	(Unit Train A/D Derailments per Car A/D Event) × (2 A/D events × 100 cars)	2.44E-04
Detailed Approach	Combined	Scenario 2 (U-D-T)	**2.49E-04**

6.1.1.1.2 Case Study with Manifest Trains

Similarly, for the case study with manifest trains, if the number of intermediate classification yards is unknown, a generic mileage-based approach is considered when calculating the yard A/D derailment likelihood (Scenarios 3 and 4). Although the specific number of yards is known in the case study, the generic approach is presented here in the interest of completeness. Since the case study specifies that the manifest train shipments pass through one intermediate classification yard, the detailed event-based approach (Scenarios 5-8) was used to consider the exact number of intermediate yards when calculating A/D derailment likelihood (Table 75).

The case study calculation of manifest train A/D derailment likelihood combines the train-mile and car-mile (or trains processed, and railcars processed) manifest train A/D derailment rates introduced in Section 6 to reflect derailment causes linked to each respective metric. The detailed approach further distinguishes between yard type, with separate manifest train A/D likelihood assuming all three yards are hump classification yards (Scenarios 6 and 8) or flat switching yards (Scenarios 5 and 7). The generic approach makes no distinction between yard types and is calculated with the average A/D derailment rate taken across all yard types.

For the 400-mile case study shipment, the detailed approach produces a higher A/D derailment likelihood for flat yards compared to hump yards, while the generic approach calculated from mainline metrics averaged over all yard types yields a value falling between the two detailed results. Unlike the unit train case study, a 400-mile shipment is more representative of manifest train operations and the generic approach can better estimate the number of yard A/D events and corresponding derailment likelihoods. However, to avoid this sensitivity to mainline distance, the

detailed approach with the actual number of yard A/D events by yard type should be used, when possible, to provide the best results.

Table 75. Case study manifest train yard arrival and departure derailment likelihood

Metric Unit	Metric unit proportion	Manifest Train Arrival/Departure		
		Type of Yard	Hump	Flat
Trains processed	78.08%	5 Trains × (Manifest Train A/D Derailments per Train A/D Event) × (4 A/D events)	7.31E-04	2.38E-03
Cars processed	21.92%	5 Trains × (Manifest Train A/D Derailments per Car A/D event) × (4 A/D events × 100 cars)	1.24E-03	4.04E-03
Detailed Approach	Combined	Scenario 6 (MBDAH) and Scenario 8 (MMDEH)	**8.42E-04**	
		Scenario 5 (MBDAF) and Scenario 7 (MMDEF)		**2.74E-03**
Mainline train-miles	78.08%	5 Trains × (Manifest Train A/D Derailments per Mainline Train-Mile) × 400 train-miles	1.40E-03	
Mainline car-miles	21.92%	5 Trains × (Manifest Train A/D Derailments per Mainline Car-Mile) × (400 miles × 100 cars)	2.38E-03	
Generic Approach	Combined	Scenario 3 (MBGAL) and Scenario 4 (MMGEL)	**1.61E-03**	

In this analysis framework, the position of the tank cars at the middle or back of the manifest train does not influence the A/D derailment likelihood since the block of tank cars will traverse 400 miles no matter where they are placed. Therefore, Scenarios 3 and 4 have the same manifest train A/D derailment event likelihood even though they involve trains with tank cars at different positions in the train. Scenarios 5 through 8 yield equal results despite differing in hazmat railcar position. However, this factor of position in a manifest train will be important for later calculations of derailment severity.

9.3.2.2 Manifest Train Yard Switching Derailment Likelihood

A similar approach is applied to calculate the manifest train yard switching derailment likelihood for each scenario (Table 76). In addition to the yard derailment rate approach (e.g., generic versus detailed) and yard type (e.g., hump or flat for the detailed approach, and an average of all for the generic approach), the yard switching derailment likelihood calculation distinguishes between the two yard switching approaches. For this case study, the block of 20 tank cars can be analyzed as being switched alone as an independent group of 20 tank cars, or as being switched *en masse* as a block of 20 tank cars behind 19 other non-hazmat cars for a total switching cut of 39 railcars. The analysis considered 19 non-hazmat railcars in front of the 20 tank cars because the analysis of historical yard switching derailment data from 1996-2018 suggests that the probability of more than 20 railcars derailing in a yard switching derailment is effectively zero. Thus, within this framework, a yard switching derailment starting at a point of derailment more than 19 cars away from the block of 20 tank cars will have a negligible probability of derailing any tank cars and can be ignored. The total cut size of 20 railcars or 39 railcars was used for each

scenario as appropriate when calculating the number of railcars processed through classification yards for the detailed approach (Scenarios 5-8), or when calculating the number of mainline car-miles for the generic approach (Scenarios 3 and 4).

In the detailed approach, the case study scenarios with flat switching yards exhibit slightly lower yard switching derailment likelihoods than hump yards, and switched alone scenarios exhibit a lower yard switching derailment likelihood than switched together *en masse* scenarios (Table 76). The generic approach yields an overall higher yard switching derailment likelihood than the detailed approach. The explanation for this appears to be the larger weight placed on mainline train-miles compared to mainline car-miles. Since train-miles are independent of train length, the mainline train-miles portion of the generic approach calculation does not consider the relatively small proportion of the manifest train (20 percent) that consists of hazmat cars, but instead generates large yard switching derailment likelihood values that are more in line with full manifest train lengths. If the values calculated using mainline train-miles are proportionately scaled by a factor of 0.2 to reflect the portion of the manifest train with hazmat railcars of interest, and then added to the values calculated using mainline car-miles, the results are much more consistent with those calculated using the detailed approach.

Table 76. Case study manifest train yard switching derailment likelihood

Metric Unit	Metric unit proportion	Manifest Train				
		Yard Switching				
		Yard Type	Hump		Flat	
		Switching Approach	Alone	En Masse	Alone	En Masse
Cars processed	100%	5 Trains × 2 Yards × (20 for alone or 39 for en masse cars switched) × (Yard Switching Derailments per Car Processed)	1.30E-03	2.53E-03	1.28E-03	2.49E-03
Detailed Approach			**1.30E-03** Scenario 6 (MBDAH)	**2.53E-03** Scenario 8 (MMDEH)	**1.28E-03** Scenario 5 (MBDAF)	**2.49E-03** Scenario 7 (MMDEF)
Mainline train-miles	78.08%	5 Trains × (Yard Switching Derailments per Mainline Train-Mile) × 400 train-miles	3.14E-03	3.14E-03	3.14E-03	3.14E-03
Mainline car-miles	21.92%	5 Trains × (Yard Switching Derailments per Mainline Car-Mile) × 400 miles × (20 cars for alone or 39 cars for en masse)	1.07E-03	2.10E-03	1.07E-03	2.10E-03
Generic Approach	Combined		**2.69E-03** Scenario 3 (MBGAL)	**2.91E-03** Scenario 4 (MMGEL)	**2.69E-03** Scenario 3 (MBGAL)	**2.91E-03** Scenario 4 (MMGEL)

9.3.2.3 Combination of A/D and Yard Switching Derailment Likelihood

Comparing the A/D and yard switching derailment likelihoods across all unit and manifest train case study scenarios (Table 77), the unit train service option consistently exhibits lower yard/terminal derailment probabilities than manifest train service scenarios. In some cases, the unit train is approximately one order of magnitude less likely to derail in a terminal compared to a classification yard. Between the manifest train service options, the hump yard scenario tends to offer a lower combined derailment likelihood because of its lower A/D derailment probability compared to flat yards.

Table 77. Summary of derailment likelihood per traffic demand

Scenario and code	Train type	Total A/D derailment probability	Total yard switching derailment probability
1 U-G-T	Unit train	1.89E-04	-
2 U-D-T	Unit train	2.49E-04	-
3 MBGAL	Manifest train	1.61E-03	2.69E-03
4 MMGEL	Manifest train	1.61E-03	2.91E-03
5 MBDAF	Manifest train	2.74E-03	1.28E-03
6 MBDAH	Manifest train	8.42E-04	1.30E-03
7 MMDEF	Manifest train	2.74E-03	2.49E-03
8 MMDEH	Manifest train	8.42E-04	2.53E-03

U-G-T: **U**nit train, **G**eneric yard rate, unit train **T**erminal
U-D-T: **U**nit train, **D**etailed yard rate, unit train **T**erminal
MBGAL: **M**anifest train, **B**ack of train, **G**eneric yard rate, switched **A**lone, a**L**l yard types
MMGEL: **M**anifest train, **M**iddle of train, **G**eneric yard rate, switched **E**n masse, a**L**l yard types
MBDAF: **M**anifest train, **B**ack of train, **D**etailed yard rate, switched **A**lone, **F**lat yard type
MBDAH: **M**anifest train, **B**ack of train, **D**etailed yard rate, switched **A**lone, **H**ump yard type
MMDEF: **M**anifest train, **M**iddle of train, **D**etailed yard rate, switched **E**n masse, **F**lat yard type
MMDEH: **M**anifest train, **M**iddle of train, **D**etailed yard rate, switched **E**n masse, **H**ump yard type

9.3.2.4 Yard and Terminal A/D Derailment Severity

The yard derailment severity for different scenarios is calculated using yard and terminal A/D. As described in Section 6, the best-fit beta distributions for the empirical NPOD distributions for unit train and manifest train A/D derailments are beta (0.77, 0.90) and beta (0.53, 0.91), respectively, as depicted earlier in Figure 107. Applying the manifest train and unit train lengths for the example shipment, the conditional probability (given a yard A/D derailment occurs) of railcars at each position in the train being the POD for the two train types is calculated in Figure 145. The case study manifest train distribution exhibits a stronger skew toward the front of the train compared to the unit train. Note that the risk analysis in the yard does not include locomotives.

Applying Equations (3-28) through (3-32) to the calculated conditional probability of POD at each position (Figure 145) for the case study manifest trains and unit train yields the conditional

probability distribution (given an A/D derailment occurs) of a railcar derailing at each position in the train (Figure 146). As can be concluded from the figures, when the 20 hazmat cars are placed in the middle of the case study manifest train (Figure 146b), they have a larger chance of derailing during a yard A/D event compared to when they are placed at the end of the train (Figure 146a). Therefore, it is necessary to consider different placement options for the 20 tank cars in the case study scenario design. In comparison, the unit train exhibits a more uniform conditional position-based yard A/D derailment probability over the length of the train (Figure 146c). Since the unit train is composed only of tank cars, there are no alternative railcar arrangements to consider.

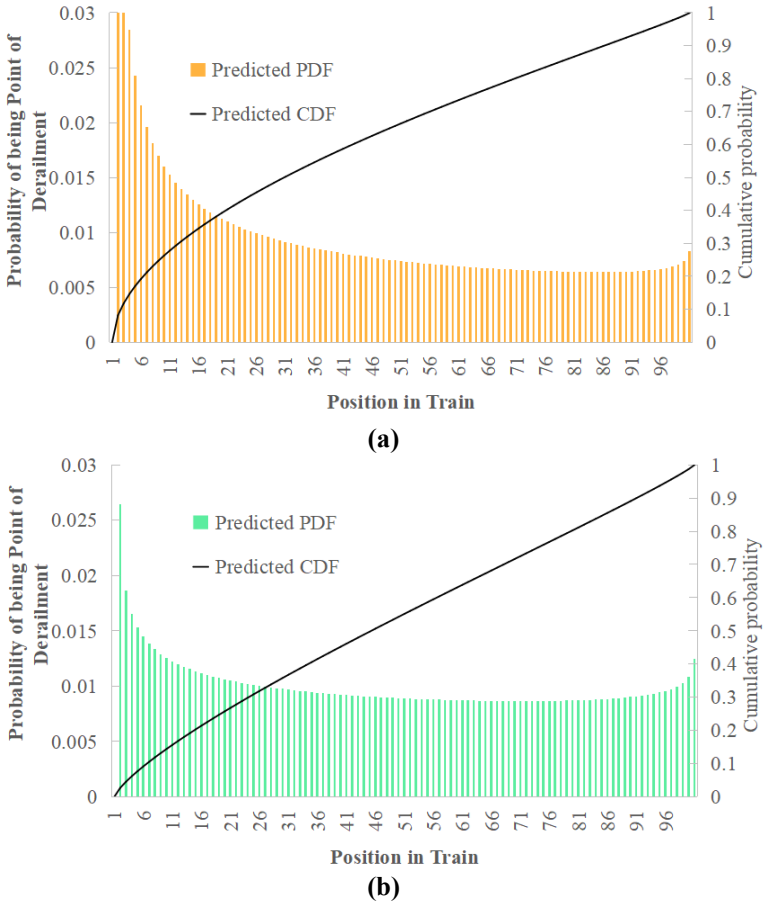

Figure 145. Probability of railcars at each position being point of derailment for (a) manifest train and (b) unit train in example shipment given a derailment during yard arrival and departure process

The probability of x tank cars derailing given a derailment occurs can be calculated based on the position of the block of tank cars in the train using Equations (3-28) and (3-29):

$$\mathrm{P}_{\mathrm{arr/dep}}\left(x_{tank}|\mathrm{derail}\right) = \sum_{\mathrm{k}} \sum_{\left[\forall \mathrm{x\ that\ } x_{tank} = \sum_{j=k}^{j=k+x} I_t(j)\right]} \mathrm{POD(k)} \times \mathrm{P}(x|k) \qquad (9\text{-}1)$$

where:

x_{tank} = the number of tank cars among all railcars derailed based on the layout of tank cars

$POD(k)$ = the probability that POD is at the k^{th} position of a train

$P_i(x|k)$= the probability of x vehicles derailing given the POD is at the k^{th} position of a train

$I_t(j)$= the 0-1 indicator, which is equal to 1 if the car at j^{th} position of a train is a tank car, and 0 otherwise

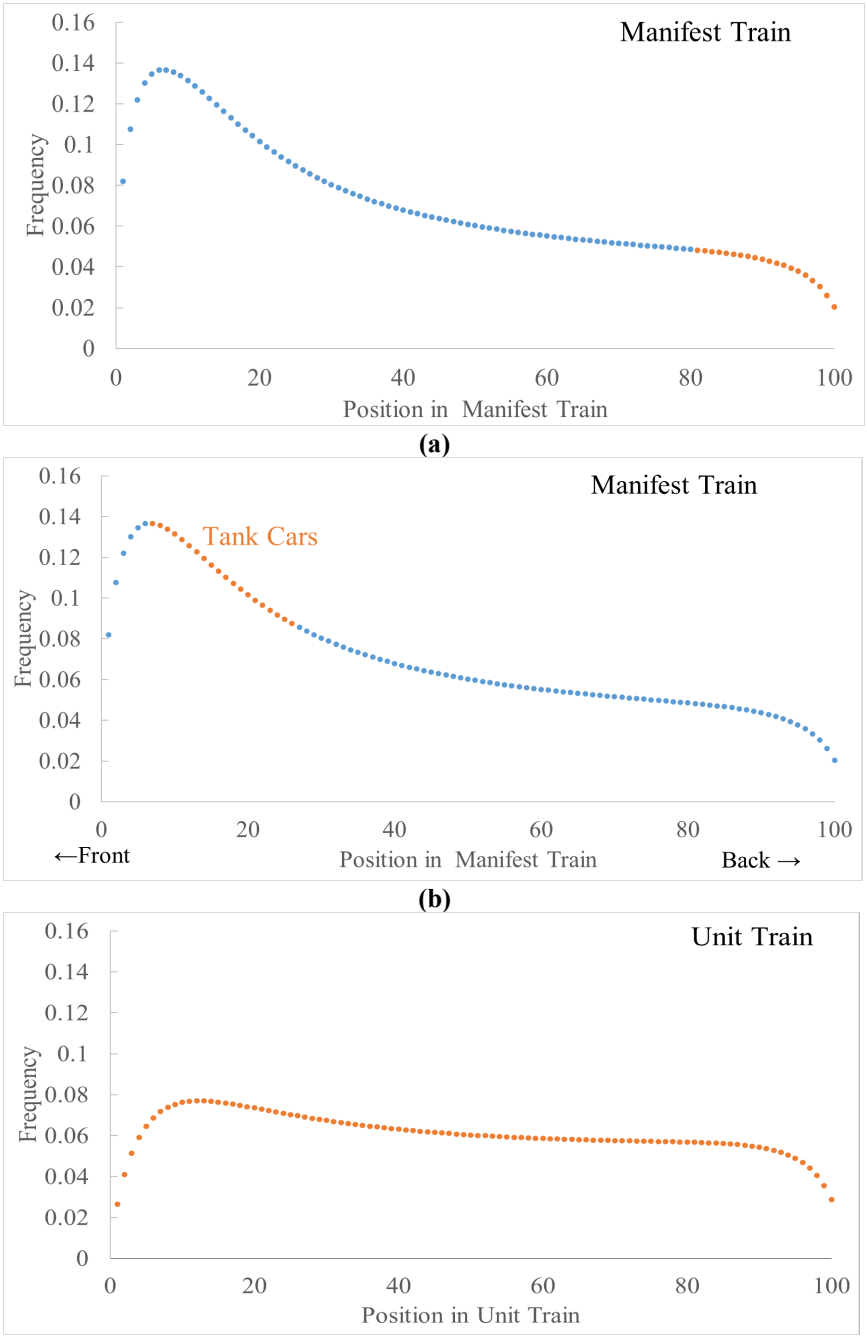

Figure 146. Position-based derailment probability distribution during yard arrival and departure process for (a) manifest train back of train placement, (b) manifest train middle of train placement, and (c) unit train given a yard arrival and departure derailment

Using this approach, the team calculated the conditional probability distribution of x tank cars derailing given a yard and terminal A/D derailment for the case study manifest train (Figure 147a) and unit train (Figure 147b). For the case study manifest train, the conditional probabilities associated with positioning the 20 tank cars at the middle or back of the train are indicated separately in Figure 147a.

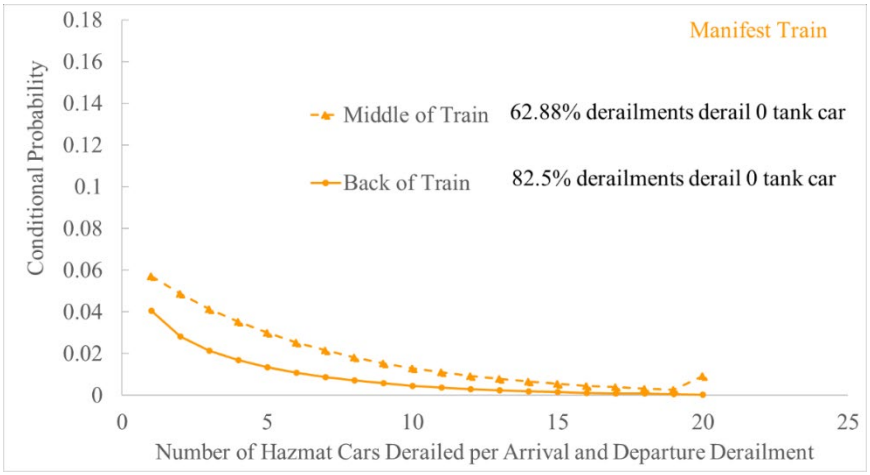

(a)

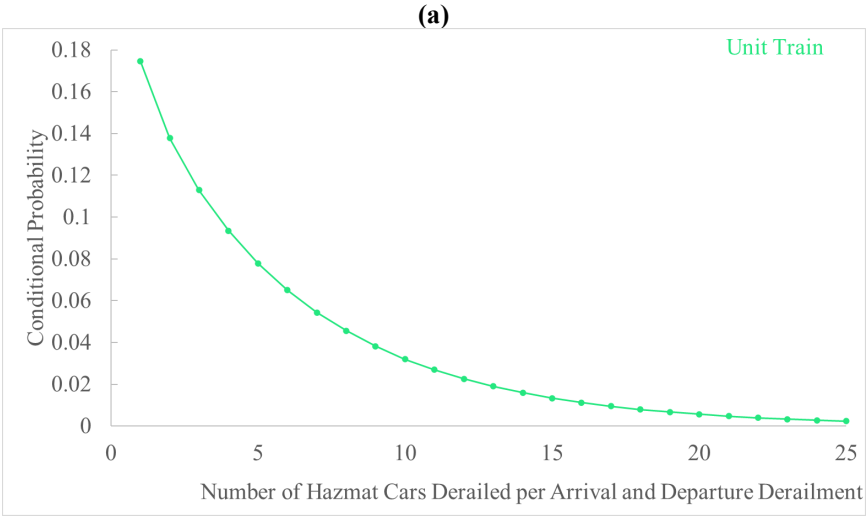

(b)

Figure 147. Conditional probability distribution of derailing x tank cars during arrival and departure process for (a) manifest train, and (b) unit train given a yard arrival and departure derailment

Notice that five locomotives are included for line-haul risk calculation since the mainline operations normally have high speeds and it is necessary to consider locomotives for a derailment incident. However, since train activities in yards/terminals proceed with reduced speeds and the mainline locomotives are not always included (e.g., the yard switching events are hauled by a switch engine), the risk calculation in yards/terminals does not include locomotives.

Since the manifest train is assumed to ship 20 tank cars along with 80 non-tank cars, even if a yard A/D derailment occurs, there is still a possibility that the derailed railcars are all non-tank cars. Therefore, the sum of conditional probabilities over each number of tank cars derailed in

Figure 147a is less than 1 for manifest trains since these higher probabilities of derailing zero tank cars are not plotted for clarity. For the back of train case study scenarios, 82.5 percent of the manifest train A/D derailments involve only non-tank cars (i.e., zero tank cars derailed). For the middle of train case study scenario, 62.88 percent of the manifest train A/D derailments involve only non-tank cars.

In comparison, since the unit train only contains tank cars, all unit train terminal A/D derailments involve derailing at least one tank car. Hence, the sum of conditional probability over each number of tank cars derailed per unit train A/D derailment is exactly one (Figure 147b), and the conditional probability of derailing zero tank cars, given a unit train A/D derailment occurs (defined as $P_{arr/dep}(derail)$), is equal to zero.

To determine the total probability distribution per arrival and departure derailment for the number of hazmat railcars derailed in yard and terminal A/D derailments for the case study conditions, the team multiplied each number of hazmat cars derailed given the arrival and departure derailment and the conditional probability (Figure 147) by the corresponding derailment likelihood (Table 77) for each example shipment case study scenario:

$$P_{arr/dep}\,(x_{tank}) = P_{arr/dep}\,(derail) \times P_{arr/dep}\,(x_{tank}|derail) \quad (9\text{-}2)$$

where:

$P_{arr/dep}(x_{tank})$= probability of x_{tank} hazmat railcars derailed in yard (for manifest trains) or terminal (for unit trains) A/D derailments per traffic demand

$P_{arr/dep}\,(derail)$= probability of a classification yard (for manifest trains) or terminal (for unit trains) derailment

$P_{arr/dep}\,(x_{tank}|derail)$= conditional probability of derailing x_{tank} tank cars during the A/D process given a yard or terminal A/D derailment

For the case study unit trains, the probability of derailing a given number of hazmat cars per traffic demand in terminals (Figure 148a) is larger when calculated using the detailed approach (Scenario 2) compared to the generic approach (Scenario 1). The probability of derailing 10 of the 100 hazmat cars in the unit train during an A/D derailment is an order of magnitude smaller than the probability of derailing only one hazmat car in the unit train.

For the case study manifest trains, the A/D probability of derailing a given number of hazmat cars per traffic demand in classification yards (Figure 148b) is generally higher than the same number of cars for unit trains when the number of railcars derailed is low. Some of the best-case manifest train A/D derailment size probability distributions approach that of the unit train, particularly the case with the tank cars at the back of the train and hump yards (Scenario 6). However, since the yard switching risk still must be calculated for manifest trains and incorporated with this A/D value, this does not represent a complete comparison between train service strategies for the case study shipment.

Comparing the different manifest train service scenarios analyzed using the *detailed approach*, the combination of flat yards and tank cars at the middle of the train (Scenario 7) produces the largest yard A/D derailment probability, followed by flat yards and tank cars at the back of the train (Scenario 5), hump yards and middle of train placement (Scenario 8), and finally hump yards and back of train placement (Scenario 6). The *generic approach* tends to produce results

that fall midway between the corresponding scenarios for a given tank car placement (i.e., back versus middle), reflecting the combination of hump and flat yard characteristics.

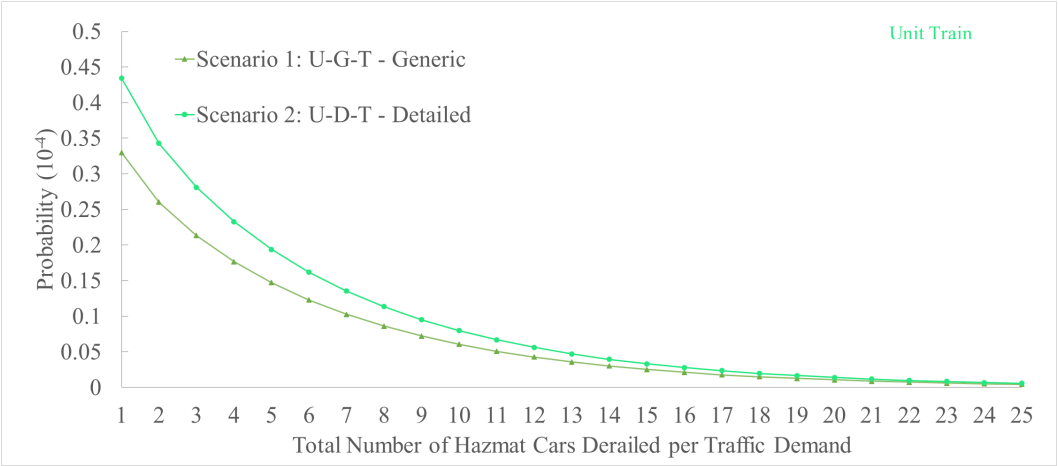

(a)

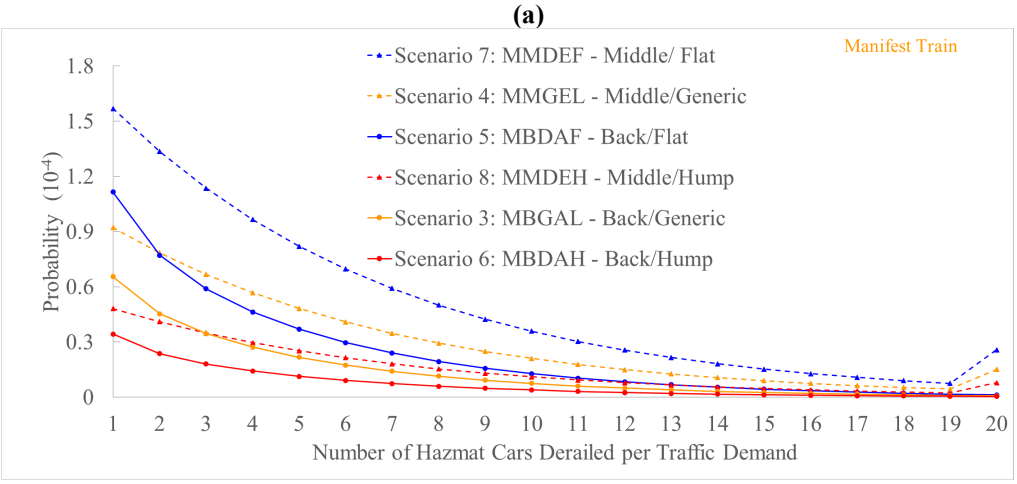

(b)

Figure 148. Total probability of derailing x tank cars during arrival and departure events per traffic demand for (a) unit train, and (b) manifest train

9.3.2.5 Manifest Train Yard Switching Derailment: The Probability Distribution of the Number of Tank Cars Derailed

For manifest train yard switching accident severity, the calculated conditional probability distribution of derailing x tank cars during manifest train yard switching events exhibits different characteristics depending on the yard switching approach, given that a yard switching derailment occurs (defined as $P_{switching}(x_{tank}|derail)$). When the 20 tank cars are assumed to remain in a group to be switched alone, there is no potential impact from any other non-hazmat railcars derailing in front of and spreading to the tank cars. Therefore, given a yard switching derailment when the tank cars are switched alone, there is at least one tank car derailed (Figure 149a).

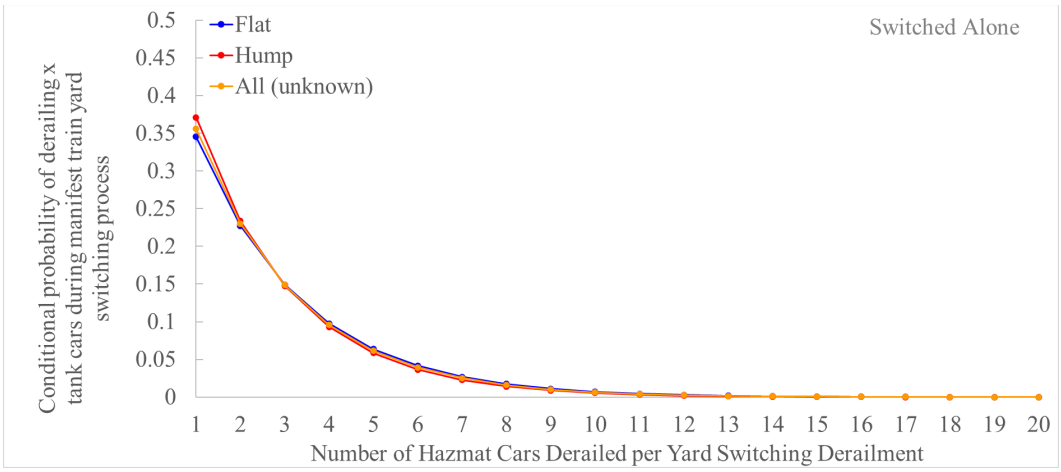

(a)

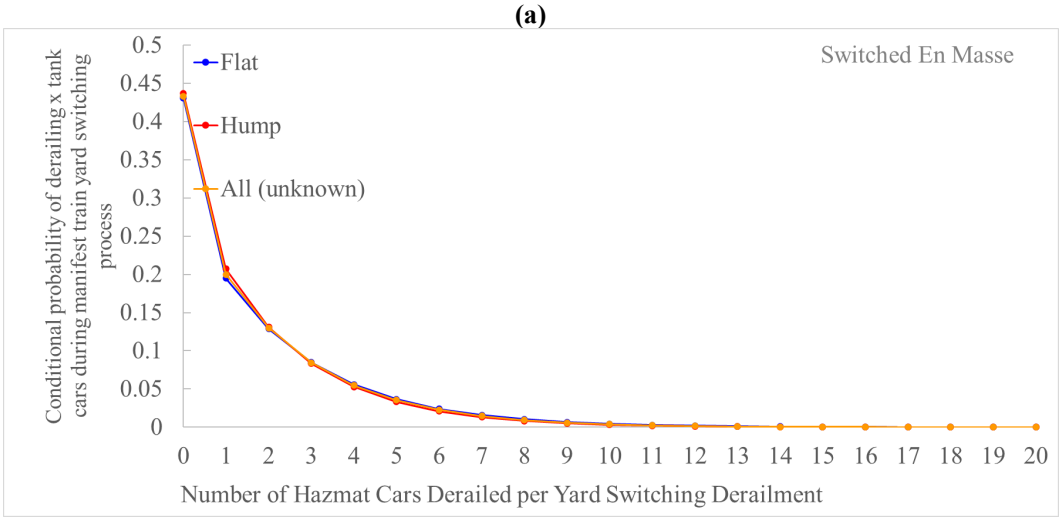

(b)

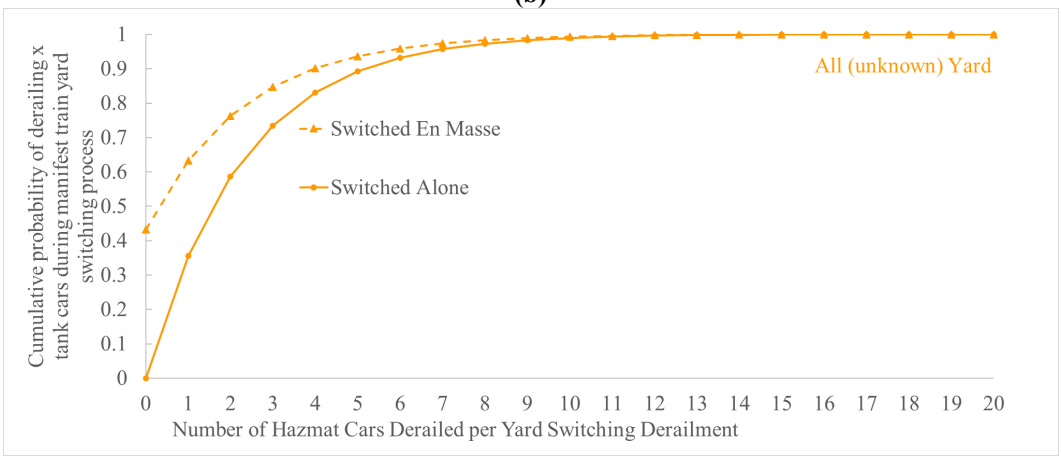

(c)

Figure 149. Conditional probability distribution of derailing x tank cars during manifest train yard switching process for (a) switched alone, (b) switched en masse, and (c) cumulative conditional probability distribution comparison between the two switching approaches given a yard switching derailment with all (unknown) yard types

In comparison, when the tank cars are switched *en masse* together with other non-hazmat railcars in front of them, they are exposed to additional risks created if any of the non-hazmat railcars in front of them derails and affects the tank cars. Recall the assumption that yard switching derailments derail a maximum of 20 railcars. Under this assumption, more than 19 non-tank cars grouped in front of the tank cars will not have any impact on the tank cars behind. To explain this, assume 20 non-tank cars followed by 20 tank cars are switched together. If the first railcar (i.e., non-tank car) of the group derails and the resulting derailment spreads back through the railcars to derail the maximum amount of 20 railcars, none of the 20 tank cars will be derailed since the final car to derail is the last non-tank car immediately in front of the first tank car in the group. For this reason, to analyze the yard switching derailment severity, the switched *en masse* scenario assumes 19 non-tank cars followed by 20 tank cars. In this case, if the point of derailment is the first of the 19 non-tank cars in the group and the derailment spreads back through the railcars to a maximum amount of 20 railcars, the final car to derail will be the first of the 20 tank cars. In this approach, there is a possibility that a small derailment starting in the 19 non-hazmat railcars will not be large enough to spread back to the 20 tank cars. For this reason, the probability of derailing zero tank cars given a yard switching derailment is not zero when the case study tank cars are switched *en masse* together with non-hazmat cars (Figure 149b).

Comparing the two yard switching approaches, given a larger group of cars is switched (39 railcars for switched *en masse* versus 20 railcars for switched alone), the base likelihood of having a yard switching derailment increases for the switched *en masse* scenario compared to switched alone. However, many of the yard-switching derailments that occur when switching all 39 cars (19 non-tank and 20 tank cars) together will involve mostly non-tank cars or relatively few tank cars. Therefore, Figure 149c is skewed toward lower severity (i.e., tank cars derailed) for the switched *en masse* scenario as compared to switched alone.

To determine the total probability distribution per traffic demand for the number of hazmat railcars derailed in yard switching derailments under the case study conditions, for each number of hazmat cars derailed given a yard switching derailment, multiply the conditional probability of derailing x_{tank} tank cars (Figure 147) by the yard switching derailment likelihood (Table 77) for each example shipment scenario:

$$P_{switching}(x_{tank}) = P_{switching}(derail) \times P_{switching}(x_{tank}|derail) \quad (9\text{-}3)$$

where:

$P_{switching}(derail)$= probability of a yard switching derailment

$P_{switching}(x_{tank}|derail)$= conditional probability of derailing x_{tank} tank cars given a yard switching derailment

$P_{switching}(x_{tank})$= probability of x_{tank} hazmat railcars derailed in a yard switching derailment per traffic demand

The overall manifest train yard switching derailment probability calculated per traffic demand reflects the differences in yard switching approach (Figure 150). Except for the scenario with all (unknown) yards using the generic approach, all other scenarios follow the pattern of the switched alone approach, exhibiting lower tank car yard switching derailment risks than the switched *en masse* scenario for the example manifest train shipment.

The substantial deviation for unknown yard type, especially for the switched alone scenario using the generic approach, is potentially due to the small number of railcars considered in the yard switching risk calculation (the risk of non-tank cars in the manifest train is ignored). Therefore, as mentioned previously, the detailed event-based approach is preferred.

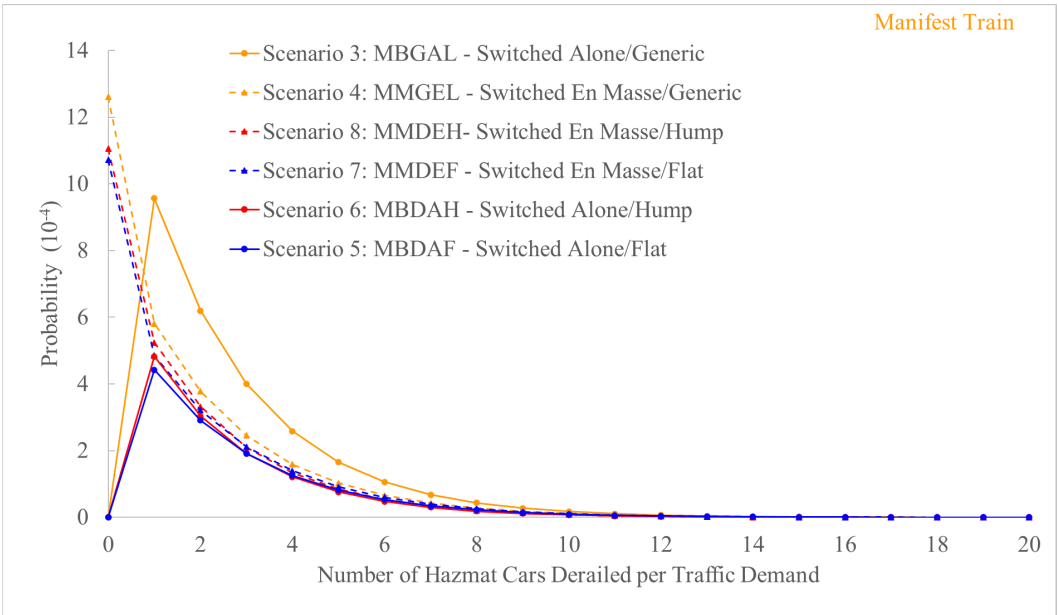

Figure 150. Total probability of derailing x tank cars during yard switching events for the example shipment using manifest train

9.3.2.6 A/D and Yard Switching Derailment: Probability Distribution of the Total Number of Tank Cars Derailed

Combining the yard arrival and departure risk (Figure 148) and yard switching risk (Figure 149) for the manifest train, the probability distribution for the number of tank cars derailed is calculated by:

$$P_{total}(x_{tank}) = P_{arr/dep}(x_{tank}) + P_{switching}(x_{tank}) \quad (9\text{-}4)$$

where:

$P_{total}(x_{tank})$= the total probability of derailing x_{tank} hazmat railcars (considering both A/D risk and switching risk) in a yard for a manifest train per traffic demand

$P_{switching}(x_{tank})$= probability of x_{tank} hazmat railcars derailed in yard switching derailment per traffic demand

$P_{arr/dep}(x_{tank})$= probability of x_{tank} hazmat railcars derailed in yard (for manifest trains) A/D derailments per traffic demand

The resulting total manifest train yard derailment probability distribution of the number of tank cars derailed combining the two (i.e., A/D and yard switching) risks (Figure 151b) can be compared to the unit train terminal derailment probability distribution of the number of tank cars derailed based on terminal A/D risk (Figure 151a). For low-severity yard derailments (i.e., low number of cars derailed), all the case study manifest train service options exhibit higher

derailment probabilities than the unit trains. To compare the large-scale accidents of greatest interest in hazmat transportation risk analysis, the total probability distribution of the number of tank cars derailed is overlaid for unit trains at terminals and manifest trains at classification yards with a focus on the range of 10 to 20 cars derailed (Figure 151c).

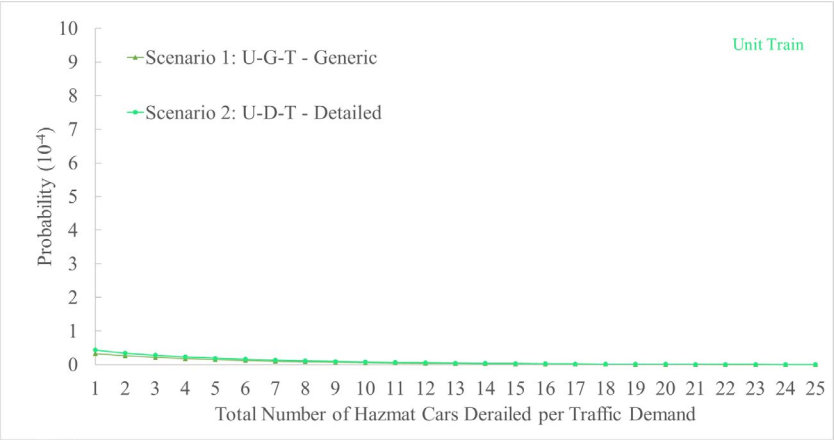

(a)

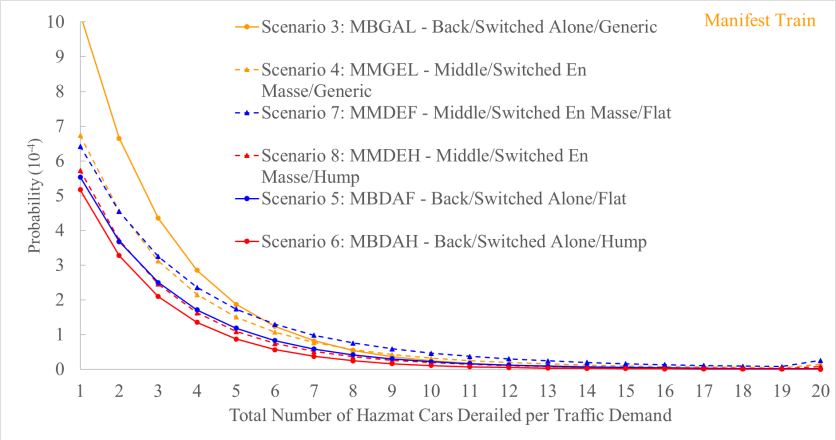

(b)

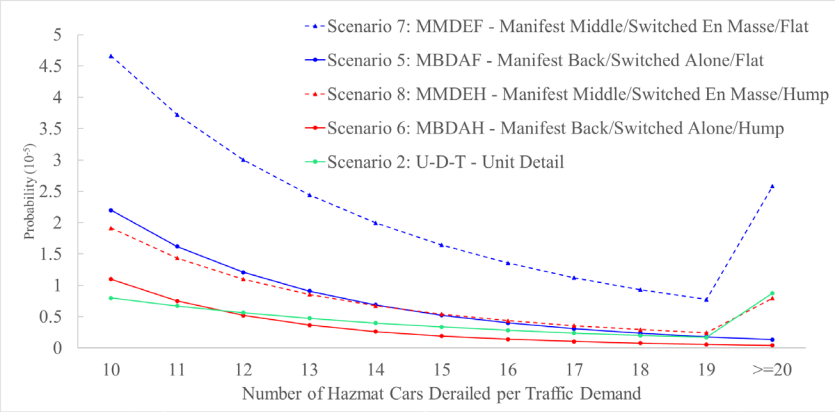

(c)

Figure 151. Overall yard and terminal probability distribution of tank car derailment per traffic demand for (a) unit train, (b) manifest train with various scenarios, and (c) comparison for severe tank car derailments

Overall, for the case study scenarios, manifest trains with tank cars at the middle of the train and switching the tank cars *en masse* with other railcars in flat yards shows the largest likelihood of large-scale tank car yard derailments (i.e., greater than 10 tank cars derailed), followed by hump yards with tank cars at the middle, and flat yards with tank cars at the back. The case study unit trains tend to have higher likelihoods of severe tank car derailments than manifest trains at hump yards with tank cars at the back of the train. Although the probability decreases as severity increases for all scenarios, the unit train has the flattest distribution with more consistent likelihood of large yard derailments due to the larger number of tank cars (100) on the case study unit train compared to the manifest train (20 tank cars).

For the case study conditions, shipping the same number of tank cars by unit trains will, on average, derail fewer hazmat cars in terminals compared to options using smaller blocks of tank cars in multiple manifest trains in yards (Table 78). Comparing manifest train service options, routing the case study train through flat yards will exhibit a higher probability of derailing more tank cars than routing the case study train through hump yards. Changing the position of tank cars in manifest trains and yard switching strategy can reduce the risk of derailing tank cars in yards by 30 to 40 percent, depending on the yard type. The risk estimation with unknown yard types using the generic approach only yields an approximate risk prediction and is less accurate than the detailed approach with known yard numbers and characteristics.

Table 78. Summary of case study yard and terminal tank car derailment risk

Shipping 100 tank cars over 400 miles		Scenario	Average tank cars derailed	Probability of derailing zero tank cars
Unit Train	Detailed	1 U-G-T	1.52E-03	99.98%
	Generic	2 U-D-T	1.15E-03	99.98%
Manifest Train	All (unknown)	3 MBGAL	8.79E-03	98.82%
		4 MMGEL	8.25E-03	98.95%
	Flat Yard	5 MBDAF	5.88E-03	99.24%
		7 MMDEF	1.03E-02	98.73%
	Hump Yard	6 MBDAH	4.16E-03	99.44%
		8 MMDEH	5.74E-03	99.25%

U-G-T: **U**nit train, **G**eneric yard rate, unit train **T**erminal
U-D-T: **U**nit train, **D**etailed yard rate, unit train **T**erminal
MBGAL: **M**anifest train, **B**ack of train, **G**eneric yard rate, switched **A**lone, a**L**l yard types
MMGEL: **M**anifest train, **M**iddle of train, **G**eneric yard rate, switched **E**n masse, a**L**l yard types
MBDAF: **M**anifest train, **B**ack of train, **D**etailed yard rate, switched **A**lone, **F**lat yard type
MBDAH: **M**anifest train, **B**ack of train, **D**etailed yard rate, switched **A**lone, **H**ump yard type
MMDEF: **M**anifest train, **M**iddle of train, **D**etailed yard rate, switched **E**n masse, **F**lat yard type
MMDEH: **M**anifest train, **M**iddle of train, **D**etailed yard rate, switched **E**n masse, **H**ump yard type

The conditional probability of release for a DOT 117 tank car on the mainline is 0.043 (Treichel et al., 2019), which is multiplied by a factor of 0.35, as discussed in Section 3.2.4. Applying these numbers to Equation (6-26), the probability distribution of the number of hazmat railcars released in yard per traffic demand using unit trains and manifest trains can be obtained. Then, using the methodology explained in Section 3.1.8 and Section 3.1.10, the probability distribution of releasing quantity and consequence of release (i.e., casualties) per traffic demand in yards considering both A/D risk and switching risk can be calculated.

9.3.3 Total Risk Combining Potential Risk on the Mainlines and in the Yard

Table 79 shows the total expected casualties when combining risks on the mainline and in yards.

Table 79. Summary of total expected casualties considering risk on the mainline and in the yard per example strategy

Scenario	Expected casualties on mainline	Expected casualties in yard	Expected casualties in total	Rank (expected casualties low to high)
6 MBDAH	3.63E-06	2.72E-06	6.35E-06	1
5 MBDAF	3.63E-06	3.85E-06	7.48E-06	2
1 U-G-T	6.76E-06	7.45E-07	7.51E-06	3
2 U-D-T	6.76E-06	9.82E-07	7.74E-06	4
3 MBGAL	3.63E-06	5.75E-06	9.38E-06	5
8 MMDEH	8.24E-06	3.75E-06	1.20E-05	6
4 MMGEL	8.24E-06	5.39E-06	1.36E-05	7
7 MMDEF	8.24E-06	6.68E-06	1.49E-05	8

U-G-T: **U**nit train, **G**eneric yard rate, unit train **T**erminal
U-D-T: **U**nit train, **D**etailed yard rate, unit train **T**erminal
MBGAL: **M**anifest train, **B**ack of train, **G**eneric yard rate, switched **A**lone, a**L**l yard types
MMGEL: **M**anifest train, **M**iddle of train, **G**eneric yard rate, switched **E**n masse, a**L**l yard types
MBDAF: **M**anifest train, **B**ack of train, **D**etailed yard rate, switched **A**lone, **F**lat yard type
MBDAH: **M**anifest train, **B**ack of train, **D**etailed yard rate, switched **A**lone, **H**ump yard type
MMDEF: **M**anifest train, **M**iddle of train, **D**etailed yard rate, switched **E**n masse, **F**lat yard type
MMDEH: **M**anifest train, **M**iddle of train, **D**etailed yard rate, switched **E**n masse, **H**ump yard type

All scenarios are ranked according to the total expected casualties from low to high. The results demonstrate that using five manifest trains (Scenarios 6 and 5) and placing the block of tank cars at the lowest-risk position (i.e., back of the manifest train) corresponds to the lowest total risk in expected casualties for known yard type (i.e., flat or hump). It is followed by strategies (Scenarios 1 and 2) using one unit train carrying 100 tank cars over 400 miles. The comparison between Scenarios 6 and 5, and Scenarios 1 and 2 indicates that although manifest trains experience additional risk from the switching process at intermediate classification yards, placing hazmat cars at the lowest-risk positions in manifest trains outperforms transporting all tank cars in one unit train. Scenario 3 ranks fifth, using five manifest trains and placing the block of tank

cars at the end of manifest trains using generic yard rates. Although Scenario 3 places the block of tank cars at the lowest-risk position (like Scenarios 6 and 5), it still has a higher risk than Scenarios 1 and 2 due to the different calculation approaches used. Figure 151b shows that Scenario 3 has the highest yard switching derailment severity, which results in a higher risk than strategies involving the unit train. Positioning the block of tank cars at relatively high-risk positions, such as in Scenarios 8, 4, and 7, generates the highest expected casualties.

9.4 Sensitivity Analysis

The case study described and calculated above compares the operating strategies using one unit train or multiple manifest trains transporting 100 hazmat cars over 400 miles. The five factors considered include train type (unit train or manifest train), position in manifest train (at the middle or back of a manifest train), yard switching approach (switched alone or switched en masse), and yard type (all yards, flat yard, or hump yard). All eight scenarios are designed with the assumption that the train derailment speed is 25 mph on mainlines. As described in Chapter 6.1, the fundamental operations in the yard proceed with a reduced speed on non-mainline track and yards/terminals. However, speeds typically vary from 25 mph to 50 mph for mainline operations. Thus, in this chapter, we test the sensitivity of the overall risk on speed using scenarios with detailed yard rate. The operating speeds on the mainline are set to 25 mph, 40 mph, and 50 mph for comparative purposes. All other factors remain the same as in Chapter 9.1. The operation speed for yard and terminal risks is assumed to be 15 mph, due to the operating characteristics of railroad yards and terminals. Table 80 compares expected casualties on the mainline for different derailment speeds. The expected casualties increase with increased derailment speeds.

Table 80. Expected casualties on mainline for different derailment speeds

Strategies	Derailment speed on the mainline		
	25 mph	40 mph	50 mph
One unit train	6.76E-06	1.38E-05	2.37E-05
The best-case train configuration by five manifest trains	3.63E-06	7.89E-06	1.53E-05
The worst-case train configuration by five manifest trains	8.24E-06	1.72E-05	3.13E-05

Error! Not a valid bookmark self-reference. presents the total expected casualties considering mainline risk and yard risk with various operating speeds on the mainline. The operating speed in the yard is assumed to be 15 mph for all cases. The results from **Error! Not a valid bookmark self-reference.** show that the total expected casualties increase as operating speed increases, but changing the operating speed does not change the rank of each scenario as expected. However, a higher speed for the low-rank scenario (e.g., Scenario 6 at 50 mph) may have higher expected casualties than a high-rank scenario with a lower speed (e.g., Scenario 2 at 25 mph). This indicates that speed plays a vital role in increasing or reducing expected casualties. At a higher speed, the probability of derailment at each position increases. Once a derailment occurs, it tends to derail more tank cars than scenarios at lower speeds.

Table 81. Total expected casualties combining mainline risk and yard risk with various operating speeds on the mainline

Scenario and code	Derailment Speed on Mainline			Rank (expected casualties low to high)
	25 mph	40 mph	50 mph	
6 MBDAH	6.35E-06	1.06E-05	1.80E-05	1
5 MBDAF	7.48E-06	1.17E-05	1.91E-05	2
2 U-D-T	7.74E-06	1.48E-05	2.47E-05	3
8 MMDEH	1.20E-05	2.10E-05	3.52E-05	4
7 MMDEF	1.49E-05	2.39E-05	3.80E-05	5

U-D-T: **U**nit train, **D**etailed yard rate, unit train **T**erminal
MBDAF: **M**anifest train, **B**ack of train, **D**etailed yard rate, switched **A**lone, **F**lat yard type
MBDAH: **M**anifest train, **B**ack of train, **D**etailed yard rate, switched **A**lone, **H**ump yard type
MMDEF: **M**anifest train, **M**iddle of train, **D**etailed yard rate, switched **E**n masse, **F**lat yard type
MMDEH: **M**anifest train, **M**iddle of train, **D**etailed yard rate, switched **E**n masse, **H**ump yard type

10. Conclusion

The research team developed a risk analysis methodology to analyze the risk associated with railroad hazardous materials transportation given a specific train configuration, train length, the placement of the block of hazmat cars in a train, speed, yard type, yard switching approach, traffic exposure, and other operational factors. The methodology accounts for transportation risks on both mainlines and yards/terminals. The methodology integrates train derailment probability, derailment severity, probability of a hazmat car derailing and releasing, amount of hazmat releasing quantity, and the release consequence (in terms of casualties). For each risk component, the team developed analytical approaches for estimation, based on the data available and necessary assumptions.

For an illustrative example, to transport 100 tank cars over 400 miles, the results (based on the data, parameters, and assumptions specific to the illustrative case study in this report) show that using five manifest trains and placing the block of tank cars at the positions with the lowest probabilities of derailing on mainlines might result in the lowest total risk (measured by expected casualties), compared to using one unit train carrying 100 tank cars over the same distance. This is probably because although manifest trains may have additional hazmat release risk due to switching activities at intermediate classification yards, placing hazmat cars at certain positions in the train consist could result in lower risk on mainlines, which may offset the additional risk in yards. By contrast, placing the block of tank cars at the positions with the highest probabilities of derailing in a manifest train can result in the highest total transportation risk, more so than using unit trains to transport the same demand. The risk analysis methodology can be used to quantify the overall transportation risk (including mainline and yard/terminal) given any specific train configurations and operational characteristics, thereby providing a comparative risk evaluation of alternative service options.

11. References

AAR (2014). Preliminary Distributions of Quantities Lost from Tank Cars Releasing Lading in Accidents – RSI-AAR Railroad Tank Car Safety Research and Test Project (Report No. WP-14-02). Association of American Railroads.

AAR (2019a). AAR Data Center. Association of American Railroads.

AAR (2019b). Annual Report of Hazardous Materials Transported by Rail: Calendar Year 2018.

Aberdeen Carolina & Western Railway (2022). Benefits of a Unit Train. ACW Railway Company.

Adams, G., Mintz, T., Necsolu, M., & Mancillas, J. (2011). Analysis of Severe Railway Accidents Involving Long Duration Fires (Report No. NUREG/CR-7034). Center for Nuclear Waste Regulatory Analyses.

ADL (1996). Risk assessment for the transportation of hazardous materials by rail. Supplementary report: Railroad accident rate and risk reduction option effectiveness analysis and data.

Agresti, A., & Kateri, M. (2011). Categorical Data Analysis. In M. Lovric (Ed.), International Encyclopedia of Statistical Science. Springer, Berlin, Heidelberg (pp. 206-208).

American Institute of Chemical Engineers (AIChE) (1995). Guidelines for Chemical Transportation Risk Analysis (Report No. AICHE G-28).

An, M., Huang, S., & Baker, C. J. (2007). Railway risk assessment - the fuzzy reasoning approach and fuzzy analytic hierarchy process approaches: A case study of shunting at Waterloo depot. *Proceedings of the Institution of Mechanical Engineers, Part F: Journal of Rail and Rapid Transit, 221*(3), 365-383.

Andersen, D. R., Booth, G. F., Vithani, A. R., Singh, S. P., Prabhakaran, A., Stewart, M. F., & Punwani, S. K. (John) (2012). Train Energy and Dynamics Simulator (TEDS): A State-of-the-Art Longitudinal Train Dynamics Simulator (Report No. RTDF2012-9418), 57-63.

Andersen, D. R., Mattoon, D. W., & Singh, S. P. (1991). Revenue Service Validation of Train Operations and Energy Simulator (TOES) Version 1.5: Part I: Conventional Unit Coal Train. AAR Technical Center.

Andersen, D. R., Mattoon, D. W., & Singh, S. P. (1992). Revenue Service Validation of Train Operations and Energy Simulator (TOES) Version 2.0: Part II: Intermodal Train. AAR Technical Center.

Anderson, R. T. (2005). Quantitative Analysis of Factors Affecting Railroad Accident Probability and Severity. Master's Thesis, University of Illinois at Urbana-Champaign.

Anderson, R. T., & Barkan, C. P. L. (2004). Railroad Accident Rates for Use in Transportation Risk Analysis. *Transportation Research Record, 1863*(1), 88-98.

Anderson, R. T., & Barkan, C. P. L. (2005). Derailment Probability Analyses and Modeling of Mainline Freight Trains. *Proceedings of the 8th International Heavy Haul Railway Conference, 7*.

Anonymous (2015). Train Symbols. *Accessed on Google.com*.

Atanassov, I., & Dick, C. T. (2015). Capacity of Single-Track Railway Lines with Short Sidings to Support Operation of Long Freight Trains. *Transportation Research Record, 2475*(1), 95-101.

Azad, N., Hassini, E., & Verma, M. (2016). Disruption risk management in railroad networks: An optimization-based methodology and a case study. *Transportation Research Part B: Methodological, 85*, 70-88.

Bagheri, M. (2010). Risk-Based Model for Effective Marshalling of Dangerous Goods Railway Cars. Doctoral Dissertation, University of Waterloo.

Bagheri, M., Saccomanno, F., Chenouri, S., & Fu, L. (2011). Reducing the threat of in-transit derailments involving dangerous goods through effective placement along the train consist. *Accident Analysis & Prevention, 43*(3), 613-620.

Bagheri, M., Saccomanno, F. F., & Fu, L. (2010). Effective placement of dangerous goods cars in rail yard marshaling operation. *Canadian Journal of Civil Engineering, 37*(5), 753-762.

Bagheri, M., Saccomanno, F., & Fu, L. (2012). Modeling hazardous materials risks for different train make-up plans. *Transportation Research Part E: Logistics and Transportation Review, 48*(5), 907-918.

Bagheri, M., Verma, M., & Verter, V. (2014). Transport Mode Selection for Toxic Gases: Rail or Road? *Risk Analysis, 34*(1), 168-186.

Barkan, C. P. L. (2008). Improving the design of higher-capacity railway tank cars for hazardous materials transport: Optimizing the trade-off between weight and safety. *Journal of Hazardous Materials, 160*(1), 122-134.

Barkan, C. P. L., Dick, C. T., & Anderson, R. (2003). Railroad Derailment Factors Affecting Hazardous Materials Transportation Risk. *Transportation Research Record, 1825*(1), 64-74.

Barrington, B., & Peltz, D. (2009). 10,000 ft Distributed Power Intermodal Trains. *Proceedings of the 9th International Heavy Haul Conference – Heavy Haul Innovation and Development*, 673-681.

Barrow, K. (2019). Precision Scheduled Railroading – Evolution or Revolution. *International Railway Journal, 59*(9), 24-28.

Barton, R., & McWha, T. (2012). Reducing Emissions in the Rail Sector: Technology and Infrastructure Scan and Analysis. Transport Canada Transportation Development Centre Report ST.

Beck, R., Connell, D., & Iden, M. (2003). Western Coal Service on Union Pacific Railroad: Operations and Maintenance Update. *Proceedings of the International Heavy Haul Association Specialist Technical Session*.

Bell, S. (2013). Driving efficiency, preserving infrastructure and creating capacity with long trains. *Proceedings of the 10th International Heavy Haul Association Conference*, 789-795.

Bing, A., Dizon, A., Brickett, J., Papson, A., O'Rourke, L., ICF International (Firm), & Booz Allen Hamilton (2015). Risk evaluation framework and selected metrics for tank cars carrying hazardous materials (Report No. DOT/FRA/ORD-15/07). FRA.

Birk, A. M. (2000). Review of AFFTAC Thermal Model. Transport Canada, Transportation Development Centre.

Blaine, D. G., Hengel, M. F., & Peterson, J. H. (1981). Train Brake and Track Capacity Requirements for the '80s. *Journal of Engineering for Industry, 103*(4), 392-401.

Blaszak, M. (1992). Illinois Central: A Railroad for the Nineties. Trains Magazine.

Branscomb, L., Fagan, M., Auerswald, P. E., Ellis, R., & Barcham, R. (2010). Rail Transportation of Toxic Inhalation Hazards: Policy Responses to the Safety and Security Externality (Report No. RPP-2010-01). SSRN.

Britton, M. A., Asnaashari, S., & Read, G. J. M. (2017). Analysis of train derailment cause and outcome in Victoria, Australia, between 2007 and 2013: Implications for regulation. *Journal of Transportation Safety & Security, 9*(1), 45-63.

Brokaw, J. (2021). E-SIM: Computerized Event Simulation Modeling for Egress/Ingress. ARA. Accessed October 2021.

Brosseau, J. (2014). Analysis and Modeling of Benefits of Alternative Braking Systems in Tank Car Derailments (Report No. R-1007). Transportation Technology Center, Inc.

Canadian National Railway (2019). Railroad Emergency Preparedness Guide (Dangerous Goods Awareness Level).

"Canadian Traindude" (2019). CN Train Derailment North of Saskatoon.

Chen, S. X., & Liu, J. S. (1997). Statistical Applications of the Poisson-binomial and Conditional Bernoulli Distributions. *Statistica Sinica, 7*(4), 875-892.

Cheng, J., Verma, M., & Verter, V. (2017). Impact of train makeup on hazmat risk in a transport corridor. *Journal of Transportation Safety & Security, 9*(2), 167-194.

Chowdhury, B. (2016). FluxCalc Technical Notes.

Christou, M. D. (1999). Analysis and control of major accidents from the intermediate temporary storage of dangerous substances in marshalling yards and port areas. *Journal of Loss Prevention in the Process Industries, 12*(1), 109-119.

Cook, P. (2015). Insights Into The Largest Frac Sand Unit Train On Record. Petroleum Connection.

Cozzani, V., Bonvicini, S., Spadoni, G., & Zanelli, S. (2007). Hazmat Transport: A Methodological Framework for the Risk Analysis of Marshalling Yards. *Journal of Hazardous Materials, 147*(1-2), 412-423.

Crepeau, J., & Etheridge, M. (2019). Nuclear Capability Services, Quic-FST Verification and Validation (V&V) Report. Defense Threat Reduction Agency (DTRA) Technical Report, Version 1.

Croft, B., & Johnson, A. F. (2013). Oil Pollution Act (OPA) Emergency Response Action Letter Report: Aliceville Train Derailment – Correspondence to Jordan Garrard, Environmental Protection Agency. TetraTech.

Davis, W. J. (1926). The tractive resistance of electric locomotives and cars. General Electric.

DHS (2004). Characteristics and Common Vulnerabilities – Infrastructure Category: Railroad Yards. Department of Homeland Security Protective Security Division.

Diaz de Rivera, A., Dick, C. T., & Evans, L. E. (2020). Potential for Moving Blocks and Train Fleets to Enable Faster Train Meets on Single-Track Rail Corridors. *Journal of Transportation Engineering, Part A: Systems, 146*(8), 04020077.

Dick, C. T. (2019). Influence of traffic complexity and schedule flexibility on railway classification yard capacity and mainline performance. Doctoral Dissertation, University of Illinois at Urbana-Champaign.

Dick, C. T., Atanassov, I., Kippen, F. B., & Mussanov, D. (2019). Relative train length and the infrastructure required to mitigate delays from operating combinations of normal and over-length freight trains on single-track railway lines in North America. *Proceedings of the Institution of Mechanical Engineers, Part F: Journal of Rail and Rapid Transit, 233*(7), 731-742.

Dick, C. T., & Brown, L. E. (2014). Design of Bulk Railway Terminals for the Shale Oil and Gas Industry. *Proceedings of the 2014 ASCE Shale Energy Engineering Conference*, 704-714.

Dick, C. T., & Clayton, A. M. (2001). Impact of New Railway Technology on Grain Transportation in Western Canada. *Transportation Research Record, 1742*(1), 45-53.

Dick, C. T., Zhao, J., Liu, X., & Kirkpatrick, S. W. (2021). Quantifying Recent Trends in Class 1 Freight Railroad Train Length and Weight by Train Type. *Transportation Research Record, 2675*(12), 890-903.

Dong, Y. (1997). Modeling rail freight operations under different operating strategies. PhD Thesis, Massachusetts Institute of Technology.

Etheridge, M. (2020a). Nuclear Capability Services, NuCS Fire Injury Model Methodology Report. Defense Threat Reduction Agency (DTRA) Technical Report, Version 2. February 2020.

Etheridge, M. (2020b). Nuclear Capability Services, Quick Urban and Industrial Complex (QUIC) – Fire Smoke Thermal (FST) Methodology Report. Defense Threat Reduction Agency (DTRA) Technical Report, Version 4. June 2020.

Evans, A. W. (2011). Fatal train accidents on Europe's railways: 1980-2009. *Accident Analysis & Prevention, 43*(1), 391-401.

Fahy, R. F. (2006). EXIT89: An evacuation model for high-rise buildings. *Fire Safety Science – Proceedings of the Third International Symposium*, 815–823.

Fang, K., Ke, G. Y., & Verma, M. (2017). A routing and scheduling approach to rail transportation of hazardous materials with demand due dates. *European Journal of Operational Research, 261*(1), 154-168.

FRA (2005). Safe Placement of Train Cars: A Report.

FRA (2011). FRA Guide for Preparing Accident/Incident Reports.

FRA. (2012). Railroad Equipment Accident/Incident Reporting Threshold.

FRA (2013). Railroad Safety Statistics 2011 Preliminary Annual Report.

FRA (2015, April 27). Emergency Order Establishing a Maximum Operating Speed of 40 mph in High-Threat Urban Areas for Certain Trains Transporting Large Quantities of Class 3 Flammable Liquids. Federal Register, National Archives.

FRA (2019). 6180.54 – Rail Equipment Accident/Incident.

FRA (2021). Monetary Threshold Notice.

Fullerton, G. A., DiDomenico, G. C., & Dick, C. T. (2015). Sensitivity of Freight and Passenger Rail Fuel Efficiency to Infrastructure, Equipment, and Operating Factors. *Transportation Research Record, 2476*(1), 59-66.

General Electric (2004). LOCOTROL Distributed Power System.

Glickman, T. S., & Erkut, E. (2007). Assessment of hazardous material risks for rail yard safety. *Safety Science, 45*(7), 813-822.

Glickman, T. S., Erkut, E., & Zschocke, M. S. (2007). The cost and risk impacts of rerouting railroad shipments of hazardous materials. *Accident Analysis & Prevention, 39*(5), 1015-1025.

Government Accountability Office (GAO) (2019). Rail Safety: Freight Trains Are Getting Longer, and Additional Information Is Needed to Assess Their Impact (Report No. GAO-19-443). Government Accountability Office.

Grimes, G. A. (1981). Planning for Unitrain Operations on Missouri Pacific. *Proceedings of the Transportation Research Forum, 22*, 121-126.

Hans, J. M. (1974). Evacuation risks: An evaluation. US Environmental Protection Agency, Office of Radiation Programs, National Environmental Research Center.

Harrison, E. H. (2005). CN: How We Work and why: Running a Precision Railroad. Canadian National Railway Company.

Hay, W. W. (1982). Railroad Engineering. John Wiley & Sons, NY.

Hazrati Ashtiani, I., Rakheja, S., Ahmed, A. K. W., & Zhang, J. (2015). Hunting Analysis of a Partially-Filled Railway Tank Car. *Proceedings of the 2015 Joint Rail Conference*. ASME.

Hosseini, S. D., & Verma, M. (2017). A Value-at-Risk (VAR) approach to routing rail hazmat shipments. *Transportation Research Part D: Transport and Environment, 54*, 191-211.

Hosseini, S. D., & Verma, M. (2018). Conditional value-at-risk (CVaR) methodology to optimal train configuration and routing of rail hazmat shipments. *Transportation Research Part B: Methodological, 110*, 79-103.

IAFC (2015, March). Unit Train Derailment Site Case Study: Emergency Response Tactics. International Association of Fire Chiefs.

Iowa State University, Department of Agronomy (2022). Iowa Environmental Mesonet (IEM).

Iranitalab, A., Khattak, A., & Thompson, E. (2019). Statistical modeling of types and consequences of rail-based crude oil release incidents in the United States. *Reliability Engineering & System Safety, 185*, 232-239.

Jeong, D. Y., Lyons, M. L., Orringer, O., & Perlman, A. B. (2007). Equations of Motion for Train Derailment Dynamics (Report No. RTDF2007-46009). *Proceedings of the ASME Rail Transportation Division Conference*, 21-27.

Kang, D., Zhao, J., Dick, C. T., Liu, X., Bian, Z., Kirkpatrick, S. W., & Lin, C.-Y. (2022a). Comparing Unit Trains versus Manifest Trains for the Risk of Rail Transport of Hazardous Materials – Part I: Risk Analysis Methodology. *Accident Analysis & Prevention* (Paper under Review).

Kang, D., Zhao, J., Dick, C. T., Liu, X., Bian, Z., Kirkpatrick, S. W., & Lin, C.-Y. (2022b). Comparing Unit Trains versus Manifest Trains for the Risk of Rail Transport of Hazardous Materials – Part II: Application and Case Study. *Accident Analysis & Prevention* (Paper under Review).

Kawprasert, A., & Barkan, C. P. (2008). Effects of Route Rationalization on Hazardous Materials Transportation Risk. *Transportation Research Record, 2043*(1), 65-72.

Kawprasert, A., & Barkan, C. P. (2010). Effect of Train Seed on Risk Analysis of Transporting Hazardous Materials by Rail. *Transportation Research Record, 2159*(1), 59-68.

Keaton, M. H. (1991). Service-cost tradeoffs for carload freight traffic in the U.S. rail industry. *Transportation Research Part A: General, 25*(6), 363-374.

Kendall, M. G. (1975). Rank Correlation Measures (202, 15). Charles Griffin and Company.

Kenkel, P. L., Henneberry, S. R., & Agustini, H. N. (Eds.) (2004). An Economic Analysis of Unit-Train Facility Investment.

Kirkpatrick, S. W. (2005). Analysis of the Tank Car Response in the Minot ND Derailment (ARA Technical Report). ARA.

Kirkpatrick, S. W., Peterson, B. D., & MacNeill, R. A. (2006). Finite Element Analysis of Train Derailments. *Proceedings of the International Crashworthiness Conference*.

Kumar, S. (2011). Improvement of Rail Yard Operations. In M. Kutz (Ed.), Handbook of Transportation Engineering, Volume II: Applications and Technologies, Second Edition. McGraw-Hill Education.

Lai, Y.-C., Kawprasert, A., Lin, C.-Y., Saat, M. R., Liang, C.-H., & Barkan, C. P. L. (2011). Integrated Optimization Model to Manage Risk of Transporting Hazardous Materials on Railroad Networks. *Transportation Research Record, 2261*(1), 115-123.

Lam, C., Edwards, D., & Lougheed, G. (2015). Rail tank cars exposed to fire: Literature review of crude oil, condensate and ethanol behaviour (Report No. NR16-140/2015E-PDF). National Research Council Canada.

Li, W., Roscoe, G. S., Zhang, Z., Saat, M. R., & Barkan, C. P. L. (2018). Quantitative Analysis of the Derailment Characteristics of Loaded and Empty Unit Trains. *Transportation Research Record, 2672*(10), 156-165.

Lin, C.-Y., Rapik Saat, M., & Barkan, C. P. (2020). Quantitative causal analysis of mainline passenger train accidents in the United States. *Proceedings of the Institution of Mechanical Engineers, Part F: Journal of Rail and Rapid Transit, 234*(8), 869-884.

Ling, L., Dhanasekar, M., & Thambiratnam, D. P. (2017). A passive road-rail crossing design to minimise wheel-rail contact failure risk under frontal collision of trains onto stuck trucks. *Engineering Failure Analysis, 80*, 403-415.

Linn, R. R., Goodrick, S. L., Brambilla, S., Brown, M. J., Middleton, R. S., O'Brien, J. J., & Hiers, J. K. (2020). QUIC-fire: A fast-running simulation tool for prescribed fire planning. *Environmental Modelling & Software, 125*, 104616.

Liu, X. (2015). Statistical Temporal Analysis of Freight Train Derailment Rates in the United States: 2000 to 2012. *Transportation Research Record, 2476*(1), 119-125.

Liu, X. (2016a). Analysis of Collision Risk for Freight Trains in the United States. *Transportation Research Record, 2546*(1), 121-128.

Liu, X. (2016b). Risk Analysis of Transporting Crude Oil by Rail: Methodology and Decision Support System. *Transportation Research Record, 2547*(1), 57-65.

Liu, X. (2017a). Risk Comparison of Transporting Hazardous Materials in Unit Trains versus Mixed Trains. *Transportation Research Record, 2608*(1), 134-142.

Liu, X. (2017b). Statistical Causal Analysis of Freight-Train Derailments in the United States. *Journal of Transportation Engineering, Part A: Systems, 143*(2).

Liu, X. (2017c). Optimizing rail defect inspection frequency to reduce the risk of hazardous materials transportation by rail. *Journal of Loss Prevention in the Process Industries, 48*, 151-161.

Liu, X., Barkan, C. P. L., & Saat, M. R. (2011). Analysis of Derailments by Accident Cause: Evaluating Railroad Track Upgrades to Reduce Transportation Risk. *Transportation Research Record, 2261*(1), 178-185.

Liu, X., Rapik Saat, M., & Barkan, C. P. L. (2017). Freight-train derailment rates for railroad safety and risk analysis. *Accident Analysis & Prevention, 98*, 1-9.

Liu, X., Saat, M. R., & Barkan, C. P. (2014a). Probability analysis of multiple-tank-car release incidents in railway hazardous materials transportation. *Journal of Hazardous Materials, 276*, 442-451.

Liu, X., Saat, M. R., & Barkan, C. P. L. (2012). Analysis of Causes of Major Train Derailment and Their Effect on Accident Rates. *Transportation Research Record, 2289*(1), 154-163.

Liu, X., Saat, M. R., & Barkan, C. P. L. (2013a). Safety Effectiveness of Integrated Risk Reduction Strategies for Rail Transport of Hazardous Materials. *Transportation Research Record, 2374*(1), 102-110.

Liu, X., Saat, M. R., & Barkan, C. P. L. (2013b). Integrated risk reduction framework to improve railway hazardous materials transportation safety. *Journal of Hazardous Materials, 260*, 131-140.

Liu, X., Saat, M. R., & Barkan, C. P. L. (2014b). Probability analysis of multiple-tank-car release incidents in railway hazardous materials transportation. *Journal of Hazardous Materials, 276*, 442-451.

Liu, X., Saat, M. R., Qin, X., & Barkan, C. P. L. (2013). Analysis of U.S. freight-train derailment severity using zero-truncated negative binomial regression and quantile regression. *Accident Analysis & Prevention, 59*, 87-93.

Liu, X., & Schlake, B. W. (2016). Probabilistic analysis of the release of liquefied natural gas (LNG) tenders due to freight-train derailments. *Transportation Research Part C: Emerging Technologies, 72*, 77-92.

Liu, X., Turla, T., & Zhang, Z. (2018). Accident-Cause-Specific Risk Analysis of Rail Transport of Hazardous Materials. *Transportation Research Record, 2672*(10), 176-187.

Lovett, A. H., Dick, C. T., & Barkan, C. P. (2015). Determining freight train delay costs on railroad lines in North America. *Proceedings of RailTokyo, 2015*.

Lovette, P. M., & Thivierge, J. (1992). Train make-up manual. AAR.

Martey, E. N., & Attoh-Okine, N. (2018). Bivariate severity analysis of train derailments using copula-based regression models. *ASCE-ASME Journal of Risk and Uncertainty in Engineering Systems, Part A: Civil Engineering, 4*(4), 04018034.

Martey, E. N., & Attoh-Okine, N. (2019a). Analysis of Train Derailment Severity Using Vine Copula Quantile Regression Modeling. *Transportation Research Part C: Emerging Technologies, 105*, 485-503.

Martey, E. N., & Attoh-Okine, N. (2019b). Analysis of train derailment severity using vine copula quantile regression modeling. *Transportation Research Part C: Emerging Technologies, 105*, 485-503.

Martland, C. D. (2008). Railroad train delay and network reliability. Transportation Technology Center, Inc.

Martland, C. D. (2013). Introduction of heavy axle loads by the North American rail industry, 1990 to 2012.

Martland, C. D., Zhu, Y., Lahrech, Y., & Sussman, J. M. (2001). Risk and Train Control: A Framework for Analysis. *Transportation Research Record, 1742*(1), 25-33.

McClanachan, M., & Cole, C. (2012). Current Train Control Optimization Methods With a View for Application in Heavy Haul Railways. *Proceedings of the Institution of Mechanical Engineers, Part F: Journal of Rail and Rapid Transit, 226*(1), 36-47.

Meng, Q., & Qu, X. (2012). Estimation of rear-end vehicle crash frequencies in urban road tunnels. *Accident Analysis & Prevention, 48*, 254-263.

Mokkapati, C., Pascoe, R. D., & Ansaldo, S. (2011). A Simple and Efficient Train Braking Algorithm for PTC Systems. *AREMA Annual Conference*.

Moore Ede, W., Polivka, A., & Tunna, J. (2007). Optimizing capacity by trade-offs among train control, infrastructure, mechanical, and engineering considerations. *Proceedings of the 2007 IHHA Specialist Technical Session*, 413-421.

Morales-Ivorra, S., Real, J. I., Hernández, C., & Montalbán, L. (2016). Derailment risk and dynamics of railway vehicles in curved tracks: Analysis of the effect of failed fasteners. *Journal of Modern Transportation, 24*(1), 38-47.

MTBS (Monitoring Trends in Burn Severity) (2019). Direct Download. Accessed November 2019.

Nathan Zeller. (2019, January 24). Warman crazy train Derailment near Saskatoon, Saskatchewan on my way to work. Hilarious commentary.

National Academies of Sciences, Engineering, and Medicine (1994). Ensuring Railroad Tank Car Safety (Special Report 243). Washington, DC: The National Academies Press.

Nayak, P. R., Palmer, D. W., & Little, A. D. (1980). Issues and Dimensions of Freight Car Size: A Compendium (Report No. FRA/ORD-79/56). Federal Railroad Administration.

Nayak, P. R., Rosenfield, D. B., & Hagopian, J. H. (1983). Event Probabilities and Impact Zones for Hazardous Materials Accidents on Railroads (Report No. DOT/FRA/ORD-83/20). Federal Railroad Administration.

Newman, R. R., Zarembski, A. M., & Resor, R. R. (1991). Economic Implications of Heavy Axle Loads on Equipment Design Operations and Maintenance. *American Society of Mechanical Engineering, WAM, RTD-Volume 4, Rail Transportation*.

NIFC (National Interagency Fire Center) (2021). Total wildland fires and acres (1983-2020). Accessed March 2021.

NTSB (2004). Derailment of Canadian Pacific Railway Freight Train 292-16 and Subsequent Release of Anhydrous Ammonia Near Minot, North Dakota, January 18, 2002 (NTSB Railroad Accident Report No. NTSB/RAR-04/01). National Transportation Safety Board.

NTSB (2005). Collision of Norfolk Southern Freight Train 192 With Standing Norfolk Southern Local Train P22 With Subsequent Hazardous Materials Release at Graniteville, South Carolina January 6, 2005 (Report No. RAR-05/04; p. 68). National Transportation Safety Board.

NTSB (2015). CSX crude oil train derailment (Report No. DCA15FR005). National Transportation Safety Board.

O'Sullivan, S., & Jagger, S. (2004). Human vulnerability to thermal radiation offshore. Health & Safety Laboratory.

Paetsch, C. R., Perlman, A. B., & Jeong, D. Y. (2006). Dynamic Simulation of Train Derailments. Paper No. IMECE2006-14607, 105-114.

Personal Communication on Video Analysis of the Saskatoon Derailment. (2019). Personal communication.

PHMSA (2015). Hazardous Materials: Enhanced Tank Car Standards and Operational Controls for High-hazard Flammable Trains: Final Rule (Report No. PHMSA-2012-0082). Federal Railroad Administration.

Prabhakaran, A., & Booth, G. (2018). Objective Evaluation of Risk Reduction from Tank Car Design and Operations Improvements – Extended Study (Report No. DOT/FRA/ORD-18/36). Federal Railroad Administration.

Prater, M., & O'Neil Jr, D. (2013). The Shift to Larger Railcars for the Shipment of Grain.

Purdy, G., Campbell, H. S., Grint, G.C., & Smith, L. M. (1988). An analysis of the risks arising from the transport of liquefied gases in Great Britain. *Journal of Hazardous Materials, 20*, 335-355.

Purser, D. (2010). Dependence of modelled evacuation times on key parameters and interactions. In Pedestrian and Evacuation Dynamics 2008 (667-675). Springer.

QStation. (2022). BNSF Symbol Guide.

Raj, P. K. (1988). A Risk Assessment Study on the Transportation of Hazardous Materials Over the U.S. Railroads (Report No. DOT/FRA/ORD-88/14). Federal Railroad Administration.

Raj, P. K. (1995). Hazardous Materials Transportation in Tank Cars: Analysis of Risks Part II (Report No. DOT/FRA/ORD-95/03). Federal Railroad Administration.

Raj, P. K., & Turner, C. K. (1993). Hazardous Materials Transportation in Tank Cars: Analysis of Risks, Part I (Report No. FRA-ORD-93/34). Federal Railroad Administration.

Richards, C. W. (2006). Map of the Month: Multiple-track Main Lines. 66(1).

Runnels, S. R. (2016). User Manual For AFFTAC 4.00. Prepared for The RSI-AAR Railroad Tank Car Safety Research & Test Project (RA-16-02). The RSI-AAR Railroad Tank Car Safety Research & Test Project.

Saat, M. R., & Barkan, C. P. (2011). Generalized Railway Tank Car Safety Design Optimization for Hazardous Materials Transport: Addressing the Trade-off Between Transportation Efficiency and Safety. *Journal of Hazardous Materials, 189*(1-2), 62-68.

Saat, M. R., Werth, C. J., Schaeffer, D., Yoon, H., & Barkan, C. P. L. (2014). Environmental risk analysis of hazardous material rail transportation. *Journal of Hazardous Materials, 264*, 560-569.

Saccomanno, F. F., & El-Hage, S. (1989a). Minimizing derailments of railcars carrying dangerous commodities through effective marshaling strategies. *Transportation Research Record, 1245*(34-51), 39-41.

Saccomanno, F. F., & El-Hage, S. M. (1989b). Minimizing Derailments of Railcars Carrying Dangerous Commodities Through Effective Marshaling Strategies. *Transportation Research Record, 18*.

Saccomanno, F. F., & El-Hage, S. M. (1991a). Establishing derailment profiles by position for corridor shipments of dangerous goods. *Canadian Journal of Civil Engineering, 18*(1), 67-75.

Saccomanno, F. F., & El-Hage, S. M. (1991b). Establishing derailment profiles by position for corridor shipments of dangerous goods. *Canadian Journal of Civil Engineering, 18*(1), 67-75.

Saccomonno, F. F., & El-Hage, S. M. (1989). Establishing Derailment Profile by Railcars Carrying Dangerous Commodities through Effective Marshalling Strategies. *Transportation Research Record: Journal of the Transportation Research Board, 1245,* 34-51.

Sadeghi, J., & Shoja, S. (2016). Influences of Track and Rolling Stock Parameters on the Railway Load Amplification Factor. *Proceedings of the Institution of Mechanical Engineers, Part F: Journal of Rail and Rapid Transit, 230*(4), 1202-1212.

Schafer, D. H., & Barkan, C. P. L. (2008). Relationship between Train Length and Accident Causes and Rates. *Transportation Research Record, 2043*(1), 73-82.

Schlake, B. W., Barkan, C. P. L., & Edwards, J. R. (2011). Train Delay and Economic Impact of In-Service Failures of Railroad Rolling Stock. *Transportation Research Record, 2261*(1), 124-133.

Serrano, J. A., & Saat, M. R. (2014). Flammable Liquid Fire Consequence Modeling. *Proceedings of the ASME/IEEE Joint Rail Conference* (Vol. 45356, p. V001T06A014). American Society of Mechanical Engineers.

Sharma & Associates, Inc. (2015). Validation of the Train Energy and Dynamics Simulator (TEDS) (Report No. DOT/FRA/ORD-15/01). Federal Railroad Administration.

Short, K. C. (2015). Sources and implications of bias and uncertainty in a century of US wildfire activity data. *International Journal of Wildland Fire, 24*(7), 883-891.

Stagl, J. (2018, July). Class I Railroads Continue the Longer-Train Trend. *Progressive Railroading*.

Starr, J. T. (1976). The evolution of the unit train, 1960-1969. University of Chicago, Dept. of Geography.

STB (2020a). Public Use Carload Waybill Sample Data. Surface Transportation Board.

STB (2020b). R-1 Annual Report Financial Data. Surface Transportation Board.

Thompson, S. A. (2015). Consequence modelling of the population risk exposure resulting from airborne toxic material released from rail cars within Toronto, Ontario. *International Journal of Critical Infrastructures, 11*(3), 243-264.

Toma, E. E. (1998). A Computer Model of a Train Derailment. Ph.D. Thesis, M.E. Dept., Queens University, Ontario, Canada.

Transportation Safety Board of Canada (2014a). Derailment Speed Calculation: Montreal, Maine & Atlantic Railway, Train MMA-002 | Date of Occurrence: 06-Jul-2013 (Report No. LP039/2014). Operational Services Branch.

Transportation Safety Board of Canada (2014b). Runaway and Main-Track Derailment—Montreal, Maine & Atlantic Railway Freight Train MMA-002 Mile 0.23, Sherbrooke Subdivision Lac-Mégantic, Quebec (Report No. R13D0054). Operational Services Branch.

Treichel, T., Ghosh, L., Saat, M. R., Barkan, C. P. L., Liu, X., Kirkpatrick, S., Song, J., & Zhou, X. (2019a). Conditional Probability of Release (CPR) Estimates for Railroad Tank Cars in Accidents (p. 108).

Treichel, T., Ghosh, L., Saat, M. R., Barkan, C. P., Liu, X., Kirkpatrick, S., Song, J., & Zhou, X. (2019b). Conditional probability of release (CPR) estimates for railroad tank cars in accidents (Report No. RA-19-01). RSI-AAR Railroad Tank Car Safety Research and Test Project.

Union Pacific Historical Society (2021). UPRR Train Symbols.

Union Pacific Railroad Company (2020). How Manifest Service Works.

U.S. DOT, Transport Canada, & Secretaría de Infraestructura, Comunicaciones y Transportes, (SCT) (2016). 2016 Emergency Response Guidebook.

US EPA (2021). Climate Change Indicators: Wildfires. Accessed October 2021.

Vera, C., Paulin, J., Suárez, B., & Gutiérrez, M. (2005). Simulation of Freight Trains Equipped with Partially Filled Tank Containers and Related Resonance Phenomenon. *Proceedings of the Institution of Mechanical Engineers, Part F: Journal of Rail and Rapid Transit, 219*(4), 245-259.

Verma, M. (2009). A cost and expected consequence approach to planning and managing railroad transportation of hazardous materials. *Transportation Research Part D: Transport and Environment, 14*(5), 300-308.

Verma, M. (2011). Railroad transportation of dangerous goods: A conditional exposure approach to minimize transport risk. *Transportation Research Part C: Emerging Technologies, 19*(5), 790-802.

Verma, M., & Verter, V. (2007). Railroad Transportation of Dangerous Goods: Population Exposure to Airborne Toxins. *Computers & Operations Research, 34*(5), Article 5.

Wang, B. Z. (2019). Quantitative analyses of freight train derailments. Doctoral Dissertation, University of Illinois at Urbana-Champaign.

Wang, B. Z., Barkan, C. P. L., & Rapik Saat, M. (2020). Quantitative Analysis of Changes in Freight Train Derailment Causes and Rates. *Journal of Transportation Engineering, Part A: Systems, 146*(11).

Welch, N., & Gussow, J. (1986). Expansion of Canadian National Railway's Line Capacity. *Interfaces, 16*(1), 51-64.

Wu, Q., Luo, S., & Cole, C. (2014). Longitudinal Dynamics and Energy Analysis for Heavy Haul Trains. *Journal of Modern Transportation, 22*(3), 127-136.

Xiao, X., Jin, X., Deng, Y., & Zhou, Z. (2008). Effect of curved track support failure on vehicle derailment. *Vehicle System Dynamics, 46*(11), 1029-1059.

Yee, T. W. (2020). VGAM: Vector generalized linear and additive models. R package version 1.1-1.

Yoon, H., Werth, C. J., Barkan, C. P. L., Schaeffer, D. J., & Anand, P. (2009). An environmental screening model to assess the consequences to soil and groundwater from railroad-tank-car spills of light non-aqueous phase liquids. *Journal of Hazardous Materials, 165*(1), 332-344.

Zhang, Z., Lin, C.-Y., Liu, X., Bian, Z., Dick, C. T., Zhao, J., & Kirkpatrick, S. (2022). An Empirical Analysis of Freight Train Derailment Rates for Unit Trains and Manifest Trains. *Journal of Rail and Rapid Transit*.

Zhang, Z., & Liu, X. (2020). Safety risk analysis of restricted-speed train accidents in the United States. *Journal of Risk Research, 23*(9), 1158-1176.

Zhang, Z., Turla, T., & Liu, X. (2021). Analysis of human-factor-caused freight train accidents in the United States. *Journal of Transportation Safety & Security, 13*(10), 1157-1186.

Zhao, J., & Dick, C. T. (2022). Quantitative Derailment Rate Comparison of Unit Trains at Transload Terminals and Manifest Trains at Railroad Switching and Hump Classification Yards. *Transportation Research Record*.

12. Abbreviations and Acronyms

ACRONYM	DEFINITION
A&S	Alton & Southern
AAR	American Association of Railroads
ADAMS	Automatic Dynamic Analysis of Mechanical Systems
ADL	Arthur D. Little, Inc
AFFF	Alcohol Resistant Aqueous Film-Forming Foam
AFFTAC	Analysis of Fire Effects on Tank Cars
AGR	Alabama & Gulf Coast Railway
AICE/AIChE	American Institute of Chemical Engineers
ANSI	American National Standards Institute
AR	Alcohol Resistant
ARA	American Railway Association
AREMA	American Railway Engineering and Maintenance-of-Way Association
ASCE	American Society of Civil Engineers
ASME	American Society of Mechanical Engineers
ATCCRP	Advance Tank Car Cooperative Research Project
BLEVE	Boiling Liquid Expanding Vapor Explosion
BNSF	BNSF Railway
BOE	Bureau of Explosives
BRC	Belt Railway Company of Chicago
CDF	Cumulative Density Function
CEO	Chief Executive Officer
CN	Canadian National Railway
CNGT	Canadian National Railway Grand Trunk Corporation
COFC	Container on Flatcar
CP	Canadian Pacific Railway
CPR	Conditional Probability of Releasing
CR	Consolidated Rail Corporation (Conrail)
CSX/CSXT	CSX Transportation
DHS	Department of Homeland Security
DMU	Diesel Multiple Unit
DOT	Department of Transportation
DP	Distributed Power
ECP	Electronically Controlled Pneumatic
EG&G	Edgerton, Germeshausen, and Grier, Inc.

ACRONYM	DEFINITION
EJ&E	Elgin Joliet & Eastern
EMU	Electric Multiple Unit
EPA	U.S. Environmental Protection Agency
EQR	Expected Quantity of Release
ERG	Emergency Response Guidelines
FDV	First Derailed Vehicle
FIRETEC	A physics-based, 3-D computer code designed to simulate the constantly changing, interactive relationship between fire and its environment. Mountain Research Station (RMRS)
FRA	Federal Railroad Administration
GAO	Government Accountability Office
GE	General Electric Company
GENSYS	A software tool for modeling vehicles running on rails.
GIS	Geographical Information Systems
GRL	Gross Rail Load
GTM	Gross Ton-Miles
gMCP	Group minimax concave penalty approach
HPAC	Hazard Prediction and Assessment Capability
HSSM	Hydrocarbon Spill Screening Model
IAFC	International Association of Fire Chiefs
IEEE	Institute of Electrical and Electronics Engineers
IEM	Iowa Environmental Mesonet
IHB	Indiana Harbor Belt
KCS	Kansas City Southern
LNG	Liquefied Natural Gas
LOCOTROL	A product of GE Transportation that permits railway locomotives to be distributed throughout the length of a train (distributed power).
LPG	Liquefied Petroleum Gas
LS-DYNA	An advanced general-purpose multiphysics simulation software package developed by the former Livermore Software Technology Corporation (LSTC).
MAE	Mean Absolute Error
MBDAF	Manifest train, Back of train, Detailed yard rate, switched Alone, Flat yard type
MBDAH	Manifest train, Back of train, Detailed yard rate, switched Alone, Hump yard type
MBGAL	Manifest train, Back of train, Generic yard rate, switched Alone, aLl yard types

ACRONYM	DEFINITION
MBS	Multi-Body Simulation
MMDEF	Manifest train, Middle of train, Detailed yard rate, switched En masse, Flat yard type
MMDEH	Manifest train, Middle of train, Detailed yard rate, switched En masse, Hump yard type
MMGEL	Manifest train, Middle of train, Generic yard rate, switched En masse, aLl yard types
MPH	Miles per Hour
MSE	Mean Squared Error
MTBS	Monitoring Trends in Burn Severity
NAR	Non-Accident Releases
NIFC	National Interagency Fire Center
NIST	National Institute of Standards and Technology
NPOD	Normalized position of the first car derailed in a train
NRC	U.S. Nuclear Regulatory Commission
NS	Norfolk Southern Railway
NSTB	National Transportation Safety Board
NT	Non-Tank car
NUCARS	A dynamic and adaptable multi-body dynamics software.
NuCS	Nuclear Capabilities Services
OILMAP	An oil spill model system suitable for use in oil spill response and contingency planning.
OILSPILL	A model that predicts the area and volume of contained and uncontained crude oil spills.
OPA	Oil Pollution Act
ORER	Official Railway Equipment Registers
PD	Position of the train derails at.
PHMSA	Pipeline and Hazardous Materials Safety Administration
PIH	Poison-by-Inhalation
POD	Position of the first car derailed in a train
PSR	Precision Scheduled Railroading
PTC	Positive Train Control
QR	Quantile Regression
QRR	Quadratic Reduced Rank
QUIC-FST	Quick Urban & Industrial Complex FST Model
REA	Rail Equipment Accident
RFA	Renewable Fuels Association

ACRONYM	DEFINITION
RR	Reduced Rank
RSAC	Railroad Safety Advisory Committee
RSI	Railway Supply Institute
SNF	Spent Nuclear Fuel
SOO	Soo Line Railroad
SSE	Sum of Squared Errors
STB	Surface Transportation Board
STCC	Standard Transportation Commodity Code
TC	Tank Car
TCAD	Tank Car Accident Database
TDU	Thermal Dose Units
TEDS	Train Energy and Dynamics Simulator
TG	Truncated Geometric
TIH	Toxic Inhalation Hazard
TOES	Train Operations and Energy Simulator
TOFC	Trailer on Flatcar
TRB	Transportation Research Board
TRRA	Terminal Railroad Association of St. Louis
TSB	Transportation Safety Board
TTCI	Transportation Technology Center, Inc.
UDE	Undesired Emergency Brake Application
UIUC	University of Illinois at Urbana-Champaign
UP	Union Pacific
UPHS	Union Pacific Historical Society
VAMPIRE	A railway dynamics simulation package providing analysis of rail vehicle performance and safety through simulation
VAR	Value-at-Risk
VGAM	Vector Generalized Additive Models
VGLM	Vector Generalized Linear Models
YS	Yard Switching
ZTNB	Zero-Truncated Negative Binomial